

Diatom Metabolomics

Dissertation

zur Erlangung des akademischen Grades
doctor rerum naturalium (Dr. rer. nat.)

vorgelegt dem Rat der Chemisch-Geowissenschaftlichen
Fakultät der Friedrich-Schiller-Universität Jena

von

Diplom Biologe Charles Vidoudez

geboren am 22.01.1982 in Lausanne (Schweiz)

Gutachter:

1. Prof. Dr. Pohnert

Institut für Anorganische und Analytische Chemie
Friedrich Schiller Universität, 07743 Jena

2. Prof. Dr. Hertweck

Departement of Molecular and Applied Microbiology
HKI, Beutenbergstr. 11a, 07745 Jena

3. Prof. Dr. Kroth

Plant Ecophysiology Group
Universität Konstanz, 78457 Konstanz

Tag der öffentlichen Verteidigung:

28.04.2010

*Une herbe marine, qui flotte en ondulant, un bout de planche, dont on voudrait deviner l'histoire,
un brin de sargasses, dont le léger sillage zèbre la surface des flots, il n'en faut pas davantage.*

Un Capitaine de 15 ans, Jules Verne

To my family

Acknowledgements

Four years ago I started this thesis work as a biologist in an, at that time, essentially chemist's lab. Many people helped me to adapt to this environment, and I also adapted this environment to me. These interdisciplinary interactions, though sometimes difficult for both sides, have been a source of an invaluable enrichment. These interactions, in conjunction with the hurdles of working on a thesis, have taught me a lot about science and have hopefully made me a better scientist. There are many people that I would like to thank for their help during these four years, and I hope that the persons I omit will understand.

First I would like to express all my gratitude to Prof. Dr. Pohnert, for accepting me in his research group. He granted me the opportunity to fulfil my dream of researching algae. His support, help, and advices throughout these years made the accomplishment of this thesis possible.

Completing this thesis would not have been possible without the unflagging support of my parents, Pierre and Christine Vidoudez, and my brother Philippe. Even though geographically separated for the past three years, their support and frequent visits helped me get through the difficulties inherent to the PhD student life.

I am extremely grateful to the entire Pohnert group for their help in the laboratory. First I want to thank Dr. Alexandra Barofsky, with whom I have been working for three years on diatoms. We have shared many frustrations and successes; she has taught me to be a bit more of a chemist, and I hope I taught her to be a bit more of a biologist. I give a great thanks to Dr. Emily Prince and Jennifer Sneed. Not only they have been an invaluable source of advice and thoughtful discussion, but they have also supported me during the numerous frustrations that occur when working on biological systems. In addition, I thank them for accomplishing the tedious task of correcting my English in all my publications, including this thesis. Thanks to Carsten Paul for his help, his insatiable curiosity, and the many discussions about experiments and results, which have helped me to keep a critical view. I thank also Dr. Matthew Welling for his friendliness and helpfulness during the four years in which he was my lab mate. Thanks to Dr. Wichard, for introducing me to the PUA world and for the hour-long discussions on this subject. Finally thanks to Jan Grüneberg, Martin Rempt, Astrid Spielmeier, Jerrit Weissflog, and Theresa Wiesemeyer for their help with chemistry and GC-MS, and to Andrea Bauer, Katharina Grosser, Hannes Richter, and Caroline Kurth for their help in the lab and discussions.

I would like to acknowledge the many people who helped me collect samples and conduct

experiments in the field. Thanks to Dr. Raffaella Casotti and Dr. François Ribalet from the Stazione Anton Dorhn for inviting me on the two research cruises on the north Adriatic Sea and for the long successful cooperation. I would also like to thank Dr. Mauro Bastianini from the Istituto di Scienze Marine-Venezia for the help and phytoplankton species and density determination during these cruises, and to the captains and crew of the RSV Dellaporta and Urania who made these cruises possible.

Many thanks to Dr. Jens Nejstgaard from the Bergen University in Norway, for giving us the opportunity to conduct mesocosm experiments, and for the help and support during this cooperation; to Dr. Hans H. Jackobsen of the National Institute for Aquatic Resources in Denmark for the cell counts of the mesocosms; and to all the other participants of these experiments.

Table of content

Acknowledgements	1
Table of content	3
List of figures	5
List of tables	6
Zusammenfassung/ abstract	7
Abbreviations	11
1. Introduction	13
2. Results and Discussion	29
2.1 Polyunsaturated aldehydes	29
2.1.1 Occurrence of PUA in the natural environment.....	30
2.1.2 Laboratory studies	36
2.1.3 Discussion	42
2.2 Development of a metabolomic method for diatoms	49
2.3 Metabolic survey of a <i>S. marinoi</i> culture	59
2.3.1 Experiment design.....	60
2.3.2 Overview of the cultures	61
2.3.3 Polyunsaturated aldehydes and fatty acids.....	63
2.3.4 Cell metabolites.....	67
2.3.5 Metabolites released in the medium.....	82
2.3.6 Discussion	88
2.4 Mesocosms	101
Experiment design	102
2.4.1 Bloom development	103
2.4.2 PUA.....	104
2.4.3 Dissolved metabolites	107
2.4.4 Discussion	110
2.5 Decadial treatment on <i>Phaeodactylum tricorutum</i>	113
2.5.1 ESTs preliminary analysis.....	114
2.5.2 Metabolomic profiling.....	115
2.5.3 Discussion	117
3. Conclusion	119
4. Materials and Methods	123
4.1 Culturing.....	124
4.1.1 Strains.....	124
4.1.2 Media.....	124
4.1.3 Culture conditions	124
4.1.4 Microscopy	125
4.1.5 Large volume cultures (10 L and 25 L).....	125

4.2	GC-MS specification	127
4.3	PUA, general methods	128
4.3.1	Preparation of PUA production potential samples	128
4.3.2	Preparation of dissolved PUA samples.....	129
4.3.3	Analysis and quantification of PUA samples	130
4.4	Fatty acids, general method	132
4.4.1	Sample preparation	132
4.4.2	Fatty acids samples analysis and quantification	132
4.5	Metabolomic samples, general method	133
4.5.1	GC-MS.....	133
4.5.2	Data processing.....	134
4.6	PUA experiments (chapter 2.1)	136
4.6.1	North Adriatic Sea sampling (chapter 2.1.1).....	136
4.6.2	Culture survey for dissolved PUA (first part of the chapter 2.1.2).....	137
4.6.3	PUA addition to cultures (middle part of the chapter 2.1.2)	138
4.6.4	Nutrient effects on PUA production potential (last part of the chapter 2.1.2).....	139
4.7	Metabolomic methods development (chapter 2.2)	140
4.7.1	Procedures to optimise the extraction mix.....	140
4.7.2	Procedures to optimise the volume of extraction	142
4.7.3	Procedures to test the different cartridges for solid phase extraction (SPE)	142
4.7.4	Procedures to optimise the derivatisation time	143
4.7.5	Procedure for tests of the GC liner	144
4.8	Metabolic survey of a <i>S. marinoi</i> culture (chapter 2.3).....	144
4.8.1	Culture preparation	144
4.8.2	Sampling	144
4.8.3	pH measurements.....	146
4.8.4	Nutrients	146
4.8.5	Chlorophyll a fluorescence	146
4.8.6	Photosystem II efficiency	146
4.8.7	Bacterial CFU determination.....	147
4.8.8	Diatom lag time for regrowth	147
4.9	Mesocosms (chapter 2.4).....	147
4.10	Decadial treatment of <i>P. tricorutum</i> (chapter 2.5).....	148
4.10.1	Culture preparation	148
4.10.2	Decadial treatment	148
4.11	Statistical analysis.....	149
	Appendices	151
	Bibliography.....	168
	Curriculum Vitae	177
	Selbständigkeitserklärung	179

List of figures

Figure 1: <i>S. marinoi</i> RCC75, in phase contrast microscopy.	15
Figure 2: Biosynthesis of PUA in diatoms.	17
Figure 3: Fatty acid composition of <i>S. costatum</i>	21
Figure 4: Surface distribution of PUA in the Adriatic Sea during the March 2006 cruise.	31
Figure 5: Surface distribution of PUA in the Adriatic Sea during the February 2008 cruise.	32
Figure 6: Production of PUA by cells from 1 litre of seawater at different depths.	33
Figure 7: PUA at the site of a natural bloom of <i>S. marinoi</i>	34
Figure 8: PUA (bars) and cell counts (dots) in a <i>S. marinoi</i> culture.	37
Figure 9: Cell densities of cultures after addition of heptadienal and octadienal.	39
Figure 10: Cell density of naive cultures after addition of heptadienal and octadienal.	40
Figure 11: PUA production potential (A, C, E) and PUA precursor PUFA (B, D, F) in <i>S. marinoi</i> cells grown under nutrient limited conditions.	41
Figure 12: Diatom metabolomics work plan.	50
Figure 13: Reproducibility of the extraction capacity of different solvent mixes.	52
Figure 14: Relative recovery of 9 sugars, 9 amino acids (AA), 6 fatty acids (FA) and 3 sterols when cells were extracted with the different solvent mixes.	52
Figure 15: Effects of extraction volume on recovery.	53
Figure 16: The influence of silylation time (at 40°C) on the recovery and variability of recovery of sugars, amino acids (AA), fatty acids (FA) and sterols.	55
Figure 17: Signal intensity in repeated injections with the same liner.	57
Figure 18: Normalization efficiency in repeated injections.	58
Figure 19: Experiment design for monitoring a <i>S. marinoi</i> G4 culture.	61
Figure 20: Polyunsaturated aldehydes production potential in <i>S. marinoi</i> G4.	64
Figure 21: Fatty acid composition of <i>S. marinoi</i> G4 cells.	66
Figure 22: Interphasic separation of <i>S. marinoi</i> G4 cell metabolites.	69
Figure 23: Intraphasic separation based on <i>S. marinoi</i> G4 cell metabolites in exponential phase.	75
Figure 24: Intraphasic separation based on <i>S. marinoi</i> G4 cell metabolites in stationary phase.	78
Figure 25: Intraphasic separation based on <i>S. marinoi</i> G4 cell metabolites in the declining phase.	79
Figure 26: Total ion count chromatograms of Easy extracts in exponential phase.	82
Figure 27: Interphasic separation of <i>S. marinoi</i> G4 metabolites found in the culture medium.	84
Figure 28: Intraphasic separation of <i>S. marinoi</i> G4 metabolites found in the culture medium.	87
Figure 29: Mesocosm design.	102
Figure 30: PUA production potential by the cells of one litre of mesocosms water, <i>S. marinoi</i> and <i>Phaeocystis</i> sp. densities.	105
Figure 31: Dissolved PUA, <i>S. marinoi</i> and <i>Phaeocystis</i> sp. in mesocosms.	106
Figure 32: A, <i>P. tricornutum</i> cell density.	115
Figure 33: CAPs grouping of <i>P. tricornutum</i> based on cell metabolites (left) or on medium metabolites (right).	116
Figure 34: Scheme of the <i>S. marinoi</i> metabolism in different growth phases and factors influencing transitions between phases.	121
Figure 35: Scheme of the large volume culture vessel.	126

List of tables

Table 1: Production of PUA by different strains of <i>S. marinoi</i>	20
Table 2: Relative solvent composition of the 11 different extraction mixes.	51
Table 3: Eigenvalues (λ), correlation (Δ^2) and diagnostics statistics of the Interphasic CAP on cell metabolites diagnostics	68
Table 4: Interphasic intensities of metabolites significant for phase separation of <i>S. marinoi</i> G4 cells in culture, identified by CAP.....	71
Table 5: Eigenvalues (λ), correlation (Δ^2) and diagnostics statistics of the CAP analysis of the exponential phase.....	74
Table 6: Intensities of metabolites in <i>S. marinoi</i> G4 cells, over 24 hours in the exponential phase.	76
Table 7: Eigenvalues (λ), correlation (Δ^2) and diagnostics statistics of the CAP analysis of the declining phase.	78
Table 8: Intensity of metabolites in <i>S. marinoi</i> G4 cells, over 20 hours in the declining phase..	81
Table 9: Summary of MET-IDEA peak detection and blank subtraction	83
Table 10: Eigenvalues (λ), correlation (Δ^2) and diagnostics statistics of the CAP analysis of the culture medium metabolites in between growth phases.	83
Table 11: Intensity of metabolites in <i>S. marinoi</i> G4 culture medium, in exponential, stationary and declining phase.	85
Table 12: Eigenvalues (λ), correlation (Δ^2) and diagnostics statistics of the CAP analysis of the exponential (E), stationary (S) and declining (D) phase.....	86
Table 13: Intensities of metabolite in <i>S. marinoi</i> G4 culture media, over 24 hours in the exponential phase.	88
Table 14: Dissolved metabolite intensities in the 6 mesocosms and in the sea.....	108
Table 15: Gene classes up-regulated in the low decadienal treatment.	114
Table 16: Eigenvalues (λ), correlation (Δ^2) and diagnostics statistics of the CAP analyses on the cells and medium metabolites, before (T = 0) and after 6, 24 and 48 hours (T = 6, T = 24 and T = 48) decadienal treatment.	116
Table 17: Constant parameters for GC-EI-MS analysis	128
Table 18: GC-MS parameters for PUA analysis	131
Table 19: GC-MS parameters for fatty acid analysis	133
Table 20: GC-MS parameters for metabolomic analyses.....	134
Table 21: AMDIS parameters.....	134
Table 22: MET-IDEA parameters	135
Table 23: MS spectra libraries	136
Table 24: Filtration volumes for metabolomic samples	145

Zusammenfassung/ abstract

Zusammenfassung

Diatomeen sind ein essentieller Bestandteil des eukaryotischen Phytoplanktons und haben einen signifikanten Anteil an der ozeanischen Kohlenstofffixierung. Sie sind auch die Grundlage vieler aquatischer Nahrungsnetze. Da sie das Potenzial haben pelagische Nahrungsnetze zu beeinflussen, besteht erhöhtes Interesse an inter- und intraspezifischen Interaktionen von Diatomeen.

Von Diatomeen freigesetzte polyungesättigte Aldehyde (PUA) wurden als Metaboliten, die in solchen Interaktionen eine potenzielle Rolle spielen intensiv erforscht. Zunächst wurden sie exklusiv als Verteidigungsmetaboliten gegen Fraßfeinde diskutiert, jüngst aber auch als mögliche Infochemikalien. Ich liefere hier den ersten Beweis für die Präsenz von PUA im Meer, gelöst in Seewasser. Dieses Ergebnis wird von Laborstudien bestätigt, in denen intakte Zellen der Diatomee *Skeletonema marinoi* PUA freisetzen. Die Freisetzung erfolgt während weniger Tage kurz vor dem Übergang der Kultur in die rückläufige Wachstumsphase. Freigesetzte PUA stellen somit ein potenzielles, zeitlich limitiertes Signal dar. Mesokosmos Experimente bestätigten, dass die Dynamik der PUA Freisetzung stark von regulativen Prozessen, die auf die entsprechenden Biosynthesewege einwirken abhängig ist. Der Verdacht auf einen potenziellen Signalcharakter der Verbindungen wird durch Bioassays an *S. marinoi* Kulturen gezeigt. Wenn Kulturen in der späten stationären Wachstumsphase mit biologisch relevanten PUA Konzentrationen behandelt werden, wird die Zellkonzentration direkt beeinflusst. Die Ergebnisse meiner Labor- und meiner Feldversuche unterstützen die Annahme, dass PUA als Infochemikalien Planktoninteraktionen steuern. Besonders ihre Beteiligung an der konzertierten Beendigung einer Planktonblüte liegt nahe.

Eine einzelne Substanzklasse kann jedoch nicht für alle beobachteten Interaktionen von Diatomeen verantwortlich sein. Unser Wissen über Infochemikalien und Interaktionen von Plankton Gemeinschaften wird oft dadurch limitiert, dass es keine umfangreichen Studien zu metabolischen Prozessen in Stresssituationen oder während der Zellalterung gibt. Deshalb entwickelte ich zusätzlich einen globaleren Ansatz, um einen Überblick über die metabolischen Prozesse und die freigesetzten Metaboliten von Planktonblüten zu erhalten. Dafür wurden Methoden zur metabolischen Untersuchung von Diatomeen entwickelt und sorgfältig optimiert. Hierzu wurden die Lösungsmittel zur Extraktion, die Extraktions- und Derivatisierungsmethode sowie die GC-MS Methode optimiert. Massgeblich dafür waren die Parameter der Reproduzierbarkeit, der Wiederfindungsrate und der erhaltenen Anzahl von Signalen. Es konnten so ca. 300 intrazellulären Substanzen quantifiziert und teilweise auch identifiziert werden. Von kleinen organischen Säuren, über Aminosäuren, Zucker, und Fettsäuren bis hin zu Sterole und Terpene konnten Metaboliten

unterschiedlichster polaritäten und chromatographischer Eigenschaften erfasst werden. Die Struktur eines Viertels der Substanzen wurde dabei aufgeklärt. Zusätzlich habe ich eine Methode für metabolische Studien entwickelt, mit der es möglich ist, die im Meerwasser gelösten Metaboliten zu analysieren. Vierzig bis 80 der vom Phytoplankton produzierten Verbindungen konnten quantifiziert werden, die Struktur der Hälfte dieser Substanzen konnte aufgeklärt werden. Mit Hilfe dieser Methoden konnte ich die intra- und extrazellulären Veränderungen während des Wachstums einer Laborkultur erfassen. Aber auch eine natürliche Algenblüte wurde verfolgt. Neben den zahlreichen Schlussfolgerungen zu einzelnen Metaboliten ergibt sich das Bild, dass während des exponentiellen Wachstums der Aminosäure- und der Zuckermetabolismus sehr aktiv sind. Der Fettsäuremetabolismus hingegen ist während des stationären Wachstums aktiver. Ein hoher Katabolismus und Auswirkungen einer potentiellen Eisenlimitierung wurden in der rückläufigen Wachstumsphase beobachtet.

Zusammengenommen zeigen diese Ergebnisse die Komplexität des Diatomeen Metabolismus und bringen Licht in die regulativen Prozesse während der verschiedenen Wachstumsphasen. Die Ergebnisse belegen die Regulation des Übergangs von Wachstumsphasen durch von einzelligen Algen des Planktons freigesetzte, gelöste Substanzen.

Abstract

Diatoms are an essential group of eukaryotic phytoplankton and contribute greatly to carbon fixation in the oceans. They are therefore the base of major aquatic food webs. The inter- and intra-specific interactions of diatoms have received an increasing interest, due to their potential to be major factors in the shaping of the pelagic food webs.

Polyunsaturated aldehydes (PUA) released by diatoms have been extensively studied for their potential in such interactions, first as defence against grazers, but also more recently as potential infochemicals. I provide here the first evidence that PUA are present in the sea, dissolved in the water. This presence is corroborated by results in culture, where the diatom *Skeletonema marinoi* released PUA from intact cells. This release occurred transiently before the culture changes to the declining phase, providing a time limited potential signal. Mesocosm studies confirmed that the dynamics of the PUA release were associated with strong regulations of the biosynthetic pathways. Additionally, when cultures in late stationary phase are challenged with biologically relevant concentrations of PUA, an effect on the cell concentration was observed. My results from culture and field studies support for the first time that PUA can play a role as infochemical in mediating plankton interactions and plankton bloom termination.

Because a single class of compounds cannot explain the complex dynamic of diatom interactions, a broader approach was needed. The lack of comprehensive detailed studies on diatom metabolic responses to aging and stress has slowed the advances in the understanding of plankton communities. I therefore developed and carefully optimised methods for metabolomic investigation of diatoms. Extraction mix, extraction methods and GC-MS procedures were optimised based on parameters of reproducibility, recovered peak numbers, and recovery rate,. A metabolomic space of ~300 compounds, with a polarity range spanning over small organic acids, amino acids, sugars, fatty acids, sterol, and terpens, was covered for the intracellular metabolites. The structures of a quarter of these compounds were tentatively elucidated. I also developed a metabolomic method to analyse the metabolites present in the water surrounding cells in culture and in the field. Forty to 80 compounds produced by the phytoplankton could be quantified, the structure of which one half could be tentatively elucidated. These methods allowed me to draw a picture of the intra- and extra-cellular changes occurring in diatom cells between the different growth phases of a culture or of a phytoplankton bloom. Besides many other conclusion on specific metabolites, the general picture arose that amino acid and sugar metabolisms are highly active in the exponential phase, and that fatty acid metabolism is more active in the stationary phase. High catabolism and potential iron limitation is detected in the declining phase.

Taken together all these results show the complexity of the diatom metabolism, and shed light on the processes changing in the different phases of growth. The results provide evidence of the regulation of the phase transitions by diffusible chemical compounds.

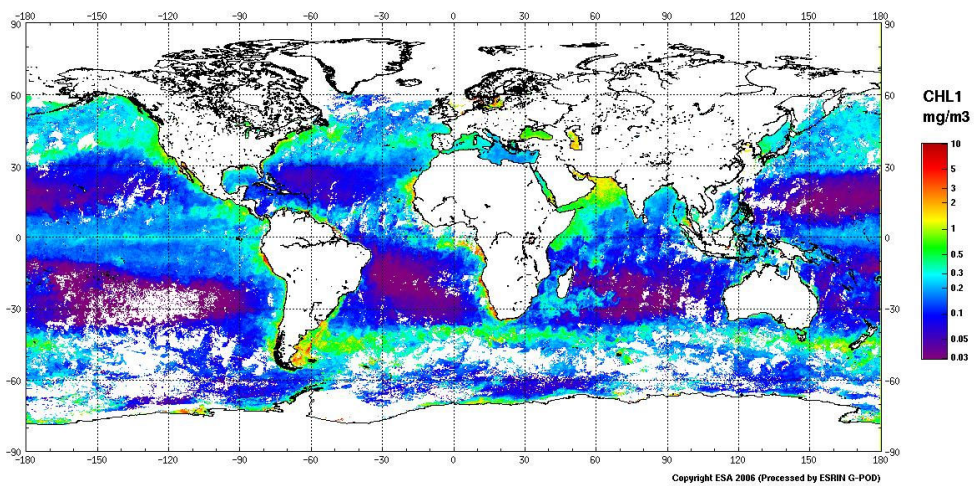
Abbreviations

AA	amino acid
AMDIS	automated mass spectral deconvolution and identification system
ANOVA	analysis of variance
BSTFA	2,2,2-trifluoro-N-trimethylsilyl-1-trimethylsilyloxy-ethanimine
CAP	canonical analysis of principal coordinates
CCMP	Provasoli-Guillard national center for culture of marine phytoplankton
CFU	colony forming unit
CODA	component detection algorithm
Decl.	declining
DRE	dynamic range extension
EC	enzyme commission
EI	electron impact
EPA	eicosapentaenoic acid
EST	expressed sequence tag
Exp.	exponential
FA	fatty acid
FT-IR	Fourier transformation infrared spectroscopy
GC	gas chromatograph/ gas chromatography
HDTETRA	hexadecatetraenoic acid
HDTRI	hexadecatrienoic acid
HEPES	4-(2-hydroxyethyl)-1-piperazineethanesulfonic acid
HPL	hydroxyperoxide lyase
Lim.	limiting
LOX	lipoxygenase
Met.	metabolite
MET-IDEA	metabolomics ion-based data extraction algorithm
MS	mass spectrometer / mass spectrometry
MSTFA	2,2,2-trifluoro-N-methyl-N-trimethylsilyl-acetamide
MUFA	monounsaturated fatty acid
NIST	national institute of standards and technology
NO	nitrite oxide
O/N	over night

Abbreviations

oTOF	orthogonal time-of-flight
PAR	photosynthetic active radiation
PC	polycarbonate
PCA	principal component analysis / principal coordinate analysis
PCD	programmed cell death
PES	polyethersulfone
PFBHA	O-(2,3,4,5,6-pentafluorobenzyl)hydroxylamine hydrochloride
PLS	partial least square
PP	polypropylene
PSII	photosystem II
PTFE	polytetrafluoroethylene
PUA	polyunsaturated aldehyde
PUFA	polyunsaturated fatty acid
RCC	Roscoff culture collection
Rel. Std.	relative standard deviation
ROS	reactive oxygen species
RT	room temperature
SDB	polystyrene-divinylbenzene
SNK	Student-Newman-Keuls
SOP	standard operating procedure
SPE	solid phase extraction
Stat.	stationary
TCA	tricarboxylic acid
Temp.	temperature
THF	tetrahydrofuran
Tris	tris(hydroxymethyl)aminomethane
UPLC	ultra performance liquid chromatography
UTEX	culture collection of algae at the University of Texas in Austin
λ	eigenvalue

1. Introduction



Spring blooms in the oceans (ENVISTAT February 2006, credits: ESA)

Diatoms, a successful group in a competitive environment

More than 2.8 billion years ago the establishment of phytoplankton marked the beginning of the oxygenated era on earth (Bekker *et al.*, 2004). The primary producers, using photosynthesis to gather their energy, have fuelled the major food webs on earth since that time. Currently, phytoplankton, which consists of less than 1% of the Earth's biomass, are responsible for nearly 50% of the global primary productivity (Field *et al.*, 1998). In order to maintain such a high rate of production, on average each planktonic organism must grow, die, and be replaced in a single week (Bidle and Falkowski, 2004). Although photosynthetic prokaryotes still dominate the phytoplankton (Moore *et al.*, 1998), since the Mesozoic (~250 million years) diatoms (Bacilliarophyceae, Haeckel 1878) have made their way in the marine ecosystems (Sims *et al.*, 2006). They represent the most successful and diversified group of eukaryotic phytoplankter in the modern ocean (Kooistra *et al.*, 2007). Diatoms are responsible for ~40% of the carbon fixation in the marine ecosystem, about one fifth of the photosynthesis on Earth (Nelson *et al.*, 1995), a contribution that equals to the one of the totality of the tropical rain forests (Field *et al.*, 1998).

Planktonic diatoms have colonised all the well mixed coastal and upwelling regions, as well as the photic zone of the open ocean. They also dominate the sea-ice edge, resulting in the dependence of food webs in the arctic and southern ocean on this group of microalgae (Armbrust, 2009). In addition to supporting the higher trophic levels, diatoms are also a major driver of the carbon pump that provides energy and carbon to the deep sea (Bowler *et al.*, 2010). Indeed, due to their heavy siliceous walls, dead and dying diatoms sink, thereby transferring the necessary energy for the organisms under the photic zone (Sarhou *et al.*, 2005).

When the light and temperature increase at the beginning of spring and the water stratifies after the winter mixing, phytoplankton initiate exponential growth. In a succession of bloom events, different groups proliferate and disappear rapidly. The succession is driven by the depletion of specific nutrients, the pressure of grazers, the infections by pathogens and the influence of other phytoplankter (Smetacek and Cloern, 2008). Diatoms typically bloom first and once the available silicate is depleted, die and form a resting stage that will seed the next blooms (Kooistra *et al.*, 2007).

To insure their success and survival in such a competitive environment, diatoms must have developed efficient methods to monitor their environment, deal with predators and competitors, regulate the formation and germination of resting cells, sinking, and cope with infections (Smetacek and Cloern, 2008).

Evidence is accumulating that allelopathy¹ plays a role in the regulation and control of phytoplankton communities (Gross, 2003; Legrand *et al.*, 2003). Allelochemicals have the potential to affect species succession (Subba Rao *et al.*, 1995; Long and Azam, 2001; Yamasaki *et al.*, 2007), and multiple reports of allelochemical interactions between phytoplankton have been reported (e.g. (Prince *et al.*, 2008)). Infochemical² mediated communication is also likely to be an important part in shaping pelagic interactions (Ianora *et al.*, 2006; Pohnert *et al.*, 2007; Pohnert, 2010).

Understanding the dynamics and interactions of diatoms is of major importance in order to comprehend the marine ecosystem. Therefore the basic processes during phases of growth need to be assessed and described in more detail. Although following diatom cultures can shed valuable light on diatom physiology, observing and measuring diatoms in the field is crucial in order to ground results with a realistic assessment of events in marine ecosystem. To this purpose, I conducted culture (*cf.* 2.1.2, 2.3) and field (*cf.* 2.1.1, 2.4) studies.

***Skeletonema marinoi* as model organism**

The centric diatom *Skeletonema costatum* (Greville) Cleve 1873 (**Figure 1**) was chosen as a primary model organism for the basic diatom physiology and interaction studies.

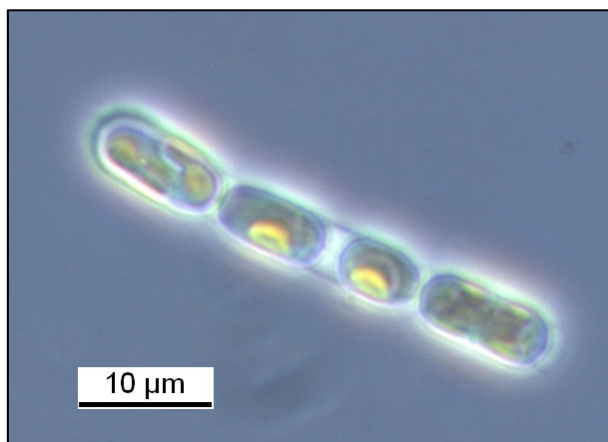


Figure 1: *S. marinoi* RCC75, in phase contrast microscopy.

The cosmopolitan diatom *S. costatum* forms dense coastal and oceanic blooms (Cloern *et al.*, 1985; Ianora *et al.*, 2004; Kooistra *et al.*, 2008). It is abundant in spring blooms, and can contribute to a large part of the diet of the higher trophic level organisms, like copepods. Its physiology and carbon fixation pathways have been studied (Beardall *et al.*, 1976; Mortainbertrand *et al.*, 1987a; 1987b; Puskaric and Mortain-Bertrand, 2003). It

also has been recently studied in respect to possible allelopathic effects. Filtrates from dense *S. costatum* culture inhibit the growth of *Heterosigma akashiwo* (Hada) Hada 1967 and *Chaetoceros mulleri* Lemmermman 1898 (Yamasaki *et al.*, 2007). Likewise, *S. costatum* cells strongly inhibited the growth of *Akashiwo sanguinea* (Hirasaka) Hansen 2000, a co-occurring species, while

¹ Allelopathy is meant here as defined by Rice in 1979 :”any direct or indirect effect (commonly negative) of one plant on another through the production of chemical compounds that escape into the environment (Rice, 1979).

² An infochemical is a compound involved in chemical communication between intra- or interspecific organisms.

Asterionella japonica Cleve 1878 had only a slight inhibition effect on *A. sanguinea*. The decline of a *S. costatum* bloom allowed a subsequent bloom of *A. sanguinea* (Matsubara *et al.*, 2008). Finally, *S. costatum* has been shown to have a stimulatory effect on *Thalassiosira weissflogii* (Grunow) Fryxell 1977 in a co-culture experiment (Paul *et al.*, 2009).

In 2005, Sarno *et al.* (Sarno *et al.*, 2005) revealed that strains reported to be *S. costatum*, consisted in fact of several species. *Skeletonema marinoi* (Greville) Sarno 2005 is the species corresponding to the majority of formerly *S. costatum* from the north east Atlantic and the Adriatic Sea (Sarno *et al.*, 2005; Kooistra *et al.*, 2008). I therefore chose *S. marinoi* as the equivalent for *S. costatum* in my experiments.

A double approach on diatom dynamics

To tackle dynamics of diatoms, I considered two approaches. First I chose to focus on a narrow class of compounds, polyunsaturated aldehydes (PUA), because they may play a role in diatom chemical signalling (*cf.* next section).

But because the interactions in diatom blooms are complex and cannot be explained by a single class of compounds, I also chose a metabolic profiling approach to monitor as many compounds as possible, both in the diatom cells and in the surrounding seawater. Since metabolic profiles of diatoms were nearly unstudied, I based my methods on those designed for metabolomic profiling of plants using GC-MS (*cf.* below).

Polyunsaturated aldehydes, a potential role in chemical communication

In 1996, T. Wendel and F. Jüttner investigated different freshwater diatoms for the production of volatile compounds (Wendel and Juttner, 1996). Using osmotic stress, they induced disintegration of the cells and analysed the compounds produced by the lipoxygenases activated in the process. Two diatom species, *Fragilaria* sp. Lyngbye 1819 and *Melosira varians* Agardh 1827 produced, as major volatiles, 2*E*,4*Z*-heptadienal (in the following heptadienal), 2*E*,4*Z*-octadienal (octadienal), 2*E*,4*Z*-decadienal (decadienal) and 2*E*,4*E*/*Z*,7*Z*-decatrienal (decatrienal).

Three years later, Miralto *et al.* observed that the hatching success of the eggs of copepods feeding on a *S. costatum* dominated bloom in the Adriatic Sea was seriously impaired (Miralto *et al.*, 1999). By analysing the reactive compounds produced by this diatom and by *Thalassiosira rotula* Meunier 1910, another marine diatom, they rediscovered these PUA. The correlation between the production of PUA and the “insidious effect” of these diatoms on copepod reproduction initiated a copious research effort.

The precursors of decadienal and decatrienal in *T. rotula* were identified in 2000 as arachidonic acid and eicosapentaenoic acid (EPA), respectively (Pohnert, 2000) (**Figure 2**). Later, eicosapentaenoic acid was confirmed as the precursor of heptadienal in *S. costatum* (d'Ippolito *et al.*, 2004). Octadienal proved to be produced from hexadecatrienoic acid (HDTRI) in *S. costatum* (d'Ippolito *et al.*, 2003) and in *T. rotula* (d'Ippolito *et al.*, 2006), and octatrienal from hexadecatetraenoic acid (HDTETRA) in *T. rotula* (Pohnert *et al.*, 2004).

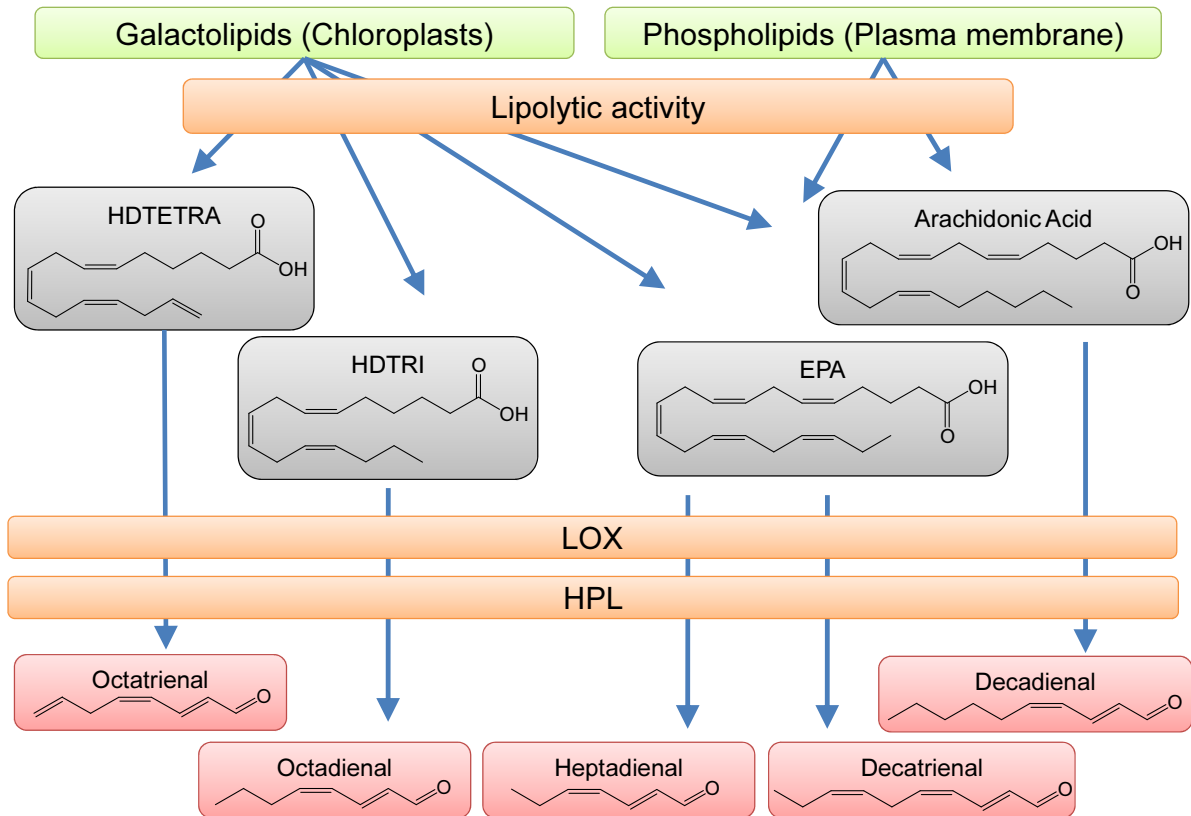


Figure 2 Biosynthesis of PUA in diatoms. In green, cellular components. In orange, enzyme activities: HPL HydroPeroxide Lyase, LOX, LipOXYgenase. In grey, free fatty acids. In red, PUA.

These precursor polyunsaturated fatty acids (PUFA) are released from lipids upon cell wounding. Arachidonic acid and EPA originate from the hydrolysis of the plasmalemmic phospholipids via a phospholipase 2 activity (EC 3.1.1.4) (Pohnert, 2002). In contrast, HDTRI and HDTETRA are released almost exclusively from the chloroplastic galactolipids by galactolipase activity (EC 3.1.1.26) (d'Ippolito *et al.*, 2004; Cutignano *et al.*, 2006). The PUFA are then converted into the corresponding PUA via the sequential action of a lipoxygenase (EC 1.13.11.12) and hydroperoxide lyase (EC 4.2.1.92) (**Figure 2**). The reaction mechanisms in *T. rotula* have been shown by (Barofsky and Pohnert, 2007). For a review on the oxylipin pathways in diatoms, see (Fontana *et al.*, 2007).

The role of PUA in plankton ecology has been the subject of a controversial discussion for more

than a decade. It was first proposed that PUA play a defensive role against grazers by directly impairing the hatching success of copepod eggs (Miralto *et al.*, 1999; Ianora *et al.*, 2004). The release of these compounds upon cell wounding/breakage fits well with a wound-activated defence which would be triggered when diatoms are eaten by a copepod. Although it is well established that a diatom diet can induce reproductive failure (e.g. (Ianora *et al.*, 2004; Poulet *et al.*, 2006; Vargas *et al.*, 2006; Poulet *et al.*, 2007; Ianora *et al.*, 2008)), the direct role of PUA is uncertain. In some cases, a direct correlation between production of PUA and reproductive failure has been found (Halsband-Lenk *et al.*, 2005; Horner *et al.*, 2005), but recent studies in the lab (Dutz *et al.*, 2008) and in the field (Poulet *et al.*, 2006; Poulet *et al.*, 2007; Wichard *et al.*, 2008) failed to correlate the PUA to the detrimental effects of diatoms. The “insidious” effects of the PUA are therefore contested. Additionally, the selective advantages of sacrificing a life in order to impair the next generation of grazers are not clear (Flynn and Irigoien, 2009).

A recently growing body of literature investigates the effects of PUA as infochemicals and/or allelopathic agents. Since the suggestion that these compounds may have cell-cell communication potential (Watson, 2003), the effects of PUA treatment on a variety of planktonic organisms with PUA have been studied. Decadienal is the most potent diatom growth inhibitor among the PUA. At concentrations of $\geq 2 \mu\text{M}$, it reduces the growth of the diatom *T. weissflogii* (Casotti *et al.*, 2005), the chlorophyte *Dunaliella tertiolecta* Butcher 1959 (Ribalet *et al.*, 2007a), and the dinoflagellate *Amphidinium carterae* Hulburt 1957 (Ribalet *et al.*, 2007a) by 50%. Octadienal and heptadienal also inhibited the growth of *D. tertiolecta* and *A. carterae*, at higher concentrations (5.6 μM and 10.7 μM) than decadienal (Ribalet *et al.*, 2007a). The growth of several bacteria species and fungi is as well inhibited by decadienal (Bisignano *et al.*, 2001; Adolph *et al.*, 2004), but all PUA proved inactive against, or stimulating to, several other bacteria species isolated from a diatom bloom producing PUA (Ribalet *et al.*, 2008). At higher concentrations, all these dienals either interfered with the cell cycle progression (Casotti *et al.*, 2005) or initiated DNA degradation and chromatin fragmentation (Ribalet *et al.*, 2007a). These processes of DNA degradation and affects on the cell cycle bear the hallmark of programmed cell death (PCD) (Casotti *et al.*, 2005). This implies a lethal effect resulting not only from the direct toxicity of the compounds, but from a genetically controlled PCD process. Decadienal effects on other diatoms have been therefore studied in details. When submitted to a high concentration (33 μM) of this PUA, *T. weissflogii* and *Phaeodactylum tricorutum* Bohlin 1897 initiate a nitric oxide (NO) burst (Vardi *et al.*, 2006). Low concentration of decadienal also arrested the cell cycle of *P. tricorutum*, without further PCD initiation. The NO generation in *P. tricorutum* was shown to result from a Ca^{2+} transduction pathway. A. Vardi *et al.* also showed that a pretreatment with a non-lethal concentration of the PUA induced resistance to a

subsequent treatment with a higher and otherwise lethal concentration of this compound. The second treatment induced a higher Ca^{2+} and subsequent NO response in the pretreated cells that in naive cells. Even more interesting was that the information of a decadienal treatment was transmitted to naive cells: when a treated population was mixed with an untreated population, the cells of the later apparently perceived a signal originating from the treated cells. When a new PUA treatment was applied, the naive cells mixed with pretreated cells exhibited reaction levels similar to the pretreated cells and higher than exposed naive cells (Vardi *et al.*, 2006).

Even if PUA are not the cell-cell signals responsible for this transmission of stress conditions in this case, it is clear that PUA are quantitatively detected by at least some diatoms and induce a response. Furthermore, this experiment showed convincing evidence that transmission of information can occur within the phytoplankton, and that it provides increased resistance to stress conditions (in this case a decadienal treatment).

Clues are therefore accumulating that PUA may play infochemical or allelopathic roles (for a review, see (Leflaive and Ten-Hage, 2009)), yet almost nothing is known about their presence dissolved in the seawater. The first part of this thesis aims therefore to get more information on the dynamics of PUA in the seawater and in diatom cells, the factors influencing the release and the potential production of PUA (*cf.* 2.1).

PUA and S. marinoi

S. marinoi (and possibly other species from the former *S. costatum*) is a major producer of heptadienal, octadienal, and octatrienal in the marine phytoplankton (**Table 1**). Several studies have investigated the production of PUA after wounding (referred as PUA production potential) in *S. marinoi*, at different time points of the growth phase. For some strains, the potential increases in stationary or declining phases as compared to the exponential phase (Ribalet *et al.*, 2007b ; Taylor *et al.*, 2009); while for others, the potential did not significantly change between phases (Taylor *et al.*, 2009) (**Table 1**). Also one preliminary study seems to indicate that the nutrient level (N and P) also influences PUA production potential (Ribalet *et al.*, 2007b). The production potential of different strains also is very different, and the factors regulating this potential are unclear. It is clear from **Table 1** that measuring the PUA at only one time point is not enough to tackle their complex dynamics. A closer study of the production potential of *S. marinoi* could shed some new light on the PUA story.

In addition to the PUA production potential, the dynamics of the precursor fatty acids, the PUFA, are also important. The fatty acid composition of *S. marinoi* has been studied several times (Volkman *et al.*, 1989; Berge *et al.*, 1995; Blanchemain and Grizeau, 1996). The majority of the

fatty acids are PUFA (**Figure 3**), with EPA counting for a third of the total fatty acid content. HDTRI and HDTETRA account for another ~25%. Berge *et al.* (Berge *et al.*, 1995) also determined that the concentration of EPA is similar in the phospholipids and in the glycolipids, while HDTRI and HDTETRA are mainly in the glycolipids. These data were collected from cells in exponential phase. Other studies examined the variation of fatty acid content in correlation with growth phases.

Table 1: Production of PUA by different strains of *S. marinoi*

Strain (origin)	Growth Phase	PUA fmol cell ⁻¹ (% of total PUA)				Reference
		Total	Heptadienal	Octadienal	Octatrienal	
RCC75 (-)	Stat.	0.13±0.16	0.075 [†] (58%)	0.029 [†] (38%)	0.00086 [†] (3%)	(Wichard <i>et al.</i> , 2005a)
CCMP2092 (Adriatic sea)	Exp.	1.23±0.37	0.66 [†] (53.7%)	0.26 [†] (39.5%)	0.017 [†] (6.8%)	(Ribalet <i>et al.</i> , 2007b)
	Stat.	4.21±0.99	2.39 [†] (56.8%)	0.95 [†] (39.6%)	0.035 [†] (3.7%)	
	Decl.	4.39±0.69	3.02 [†] (68.8%)	0.98 [†] (32.3%)	0.025 [†] (2.6%)	
	N-lim. Stat.	5.9±0.94	3.8±0.7		Trace	
	P-lim. Stat.	7.49±0.08	4.2±0.15	3.3±0.1	Trace	
FE6 (Adriatic sea)	Stat.	1.47	1.12±0.031	0.35±0.009		(Taylor <i>et al.</i> , 2007)
GUMACC (Gullmar Fjord, Sweden)						(Taylor <i>et al.</i> , 2009)
GF04-1F, GF04-1G, GF04-1J (Spring bloom)	Exp.	0.33 [‡]				
	Stat.	1.33 [‡]				
GF04-7C, GF04-7F, GF04-7J (Summer bloom)	Exp.	1.04 [‡]				
	Stat.	1.46 [‡]				
GF04-9A, GF04-9B, GF04-9D (Autumn bloom)	Exp.	0.55 [‡]				
	Stat.	0.55 [‡]				

[†], calculated from the %. [‡], estimation from graphs. RCC, Roscoff Culture Collection. CCMP, Provasoli-Guillard National Centre for Culture of Marine Phytoplankton. GUMACC, Göteborg University Marine Algal Culture Collection

Contradictory results were obtained: in some study, the EPA concentration was higher in exponential phase (e.g. (Ackman *et al.*, 1964)), while in other the EPA concentrations did not significantly change (Blanchemain and Grizeau, 1996). In addition to the possible variation due to the different cryptic species labelled *S. costatum* used at that time, variation among strains of the same species are likely as for the PUA potential. The generalisation of these studies is limited, because they often focus on only one growth phase or time point. In order to get more details about diatom physiology, it would be important to survey the fatty acid content with a higher temporal definition. This is partially achieved in chapter 2.3.

Extension of the search, the metabolomic approach

More than a decade ago, in the bloom of the genomic era, Oliver *et al.* suggested developing methods to measure metabolome variation in yeast in order to link genomic variation with phenotypic variation on the metabolome level (Oliver *et al.*, 1998). This is considered by O. Fiehn

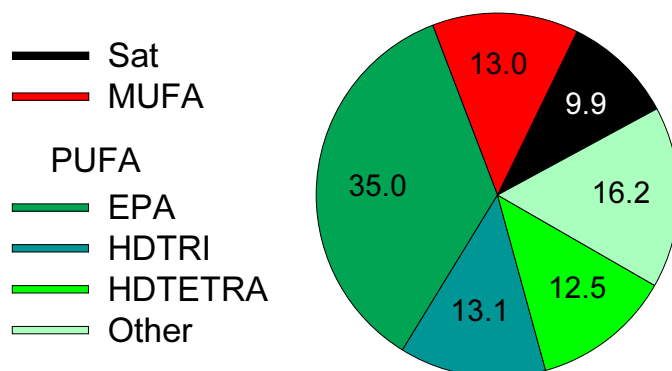


Figure 3: Fatty acid composition of *S. costatum*. Sat, saturated fatty acids. MUFA, monounsaturated fatty acids. PUFA, polyunsaturated fatty acids. The numbers in the chart represent the % of the total fatty acids. Data from (Berge *et al.*, 1995).

of how an organism reacts to any stimuli could be drawn, greatly improving our understanding of some biological processes. However, this goal is currently unreachable in practice, particularly due to technical limitations. Other “omics” fields deal with a single class of compound, such as DNA, RNA, or protein. The analytical and chemometric steps can therefore be extremely specialised and therefore very sensitive and reproducible. However, for metabolomics, one has to cope with a tremendous variety of compound classes, and at present no single analytical method is able to precisely analyse all of them. A realistic application of metabolomics requires that a compromise between precision, reproducibility, range of metabolites analysed, level of information (metabolite identified, quantified), and time of analysis is found. Such compromise has allowed for the successful application of metabolomics and metabolic profiling to plant science, among others. (e.g. (Fiehn *et al.*, 2000; Roessner *et al.*, 2001; Kopka *et al.*, 2004; Fiehn, 2008)).

Very recently, studies started to apply this broader approach to decipher diatom physiology and interactions. Metabolomic methods have been tentatively applied to diatoms. First, Allen *et al.* used metabolomic methods to identify 76 compounds which varied in *P. tricornutum* in response to iron starvation. They observed a reduction in the metabolism related to photosynthesis when iron was depleted (Allen *et al.*, 2008).

The intracellular metabolism is of major interest, but it has been known for a long time that diatoms can excrete a significant amount of their photosynthetic production (e.g. (Myklestad and Haug, 1972; Myklestad *et al.*, 1972; Sharp, 1977)). As early as 1989, Myklestad *et al.* studied the release rate of amino acids and sugars by the diatom *Chaetoceros affinis* Lauder 1894. They

to be the beginning of a new “omics”, metabolomics (Fiehn, 2008). In essence, metabolomics is aimed to be the broadest approach possible to characterise the state of a biological entity. Taking a series of snapshots of the concentration of every metabolite present at a certain point would allow an in depth understanding of the dynamics of the metabolic processes that are occurring in an organism. From this information, a clear picture

reported that up to 10% of the total photosynthesis production was excreted in exponential phase, and up to 58% in stationary phase. Aspartic acid, glutamic acid, serine, glutamine, glycine, alanine, valine and leucine were detected in exponential phase exudates, while arginine, asparagine, tyrosine and isoleucine were also excreted in stationary phase. Sugars were the most abundant extracellular compounds released, and more than 80% were polysaccharides (Myklestad *et al.*, 1989). However, these measurements were tedious, requiring a specific method for each class of compounds. In an attempt to observe all exo-metabolites in one method, Puskaric *et al.* used radiotracers and 2D electrophoresis to show that *S. costatum* actively excretes amino acids, sucrose, sugar alcohols and some organic acid intermediates of the tricarboxylic acid (TCA) cycle (Puskaric and Mortain-Bertrand, 2003).

More recently, Barofsky *et al.* applied metabolomic methods to investigate the metabolites exuded by *S. marinoi* strain G4 and *Thalassiosira pseudonana* Hasle 1977 (Barofsky *et al.*, 2009). Very different patterns in the release of many metabolites were observed for each species. Some metabolites decreased in the exponential phase and stayed at low levels, some others increased continuously throughout the growth phases, some increased only in a specific phase. Furthermore the majority of the patterns suggested that the stationary phase is, on the level of the exuded metabolites, only a transition phase between the exponential and declining phase. The method used (ultra performance liquid chromatography-mass spectrometry, UPLC-MS) unfortunately did not allow direct identification of these metabolites. In a subsequent study, analysing intra- and extracellular metabolite profiles by UPLC-MS, Barofsky *et al.* observed very different metabolic profiles depending on the growth phases in *S. marinoi* strain G4. When offered to copepods, *S. marinoi* G4 in the late stationary phase was preferred, suggesting that the grazers can choose their prey based on the metabolite content and/or on the released metabolite profile of diatom cells (Barofsky *et al.*, 2010).

In an experiment involving the co-culture of two competing diatoms, Paul *et al.* found stimulation by dissolved diffusible compounds from *S. marinoi* on *T. weissflogii* (Paul *et al.*, 2009). The analysis of the cells revealed a change of the intracellular metabolic profile when both competitors were in the same culture, though separated by a permeable membrane, suggesting that diatoms can sense clues, or exploit exudates, from another species and react to it.

To address the questions of diatom dynamics in their natural ecosystems, a finer understanding of their intracellular and extracellular metabolism, is indispensable. I therefore chose to examine the intra and extra cellular metabolic profile of *S. marinoi* in different growth phases in culture with gas chromatography-mass spectrometry (GC-MS), in order to characterize the basic metabolism dynamics of this diatom and to evaluate the efficiency of the metabolic profiling.

Several analytical approaches to analyse the metabolic profile are possible. As mentioned before, UPLC-MS analysis of diatom metabolites has already successfully been applied, but does not allow the identification of the compounds. Fourier transformation infrared spectroscopy (FT-IR) has also been used for plant metabolomics (Goodacre *et al.*, 2007b). Although FT-IR is not biased towards any particular chemical species, it only creates a metabolic fingerprint but does not allow the identification of any metabolites. The use of GC-MS with electron impact ionisation (EI) is promising because it combines a chromatographic method with an analytic technique (EI-MS) that allows database comparison and identification of at least some of the compounds (Fiehn *et al.*, 2000; Roessner *et al.*, 2001; Fiehn, 2008). Complex samples can therefore be analysed in detail and, to some extent, the metabolites can be identified and quantified.

Nevertheless, the analysis of intra- and extra-cellular metabolites of organisms living in seawater poses numerous challenges. Seawater is a difficult matrix when it comes to analysing dissolved compounds. The plant GC-MS metabolomic techniques, although already applied to diatoms (Allen *et al.*, 2008), have not yet been optimised. Optimisation and test of the metabolomic methods is nevertheless essential to produce reliable data (Fiehn, 2007).

The metabolomics development requirements

The current standard method for preparing plant extracts to be analysed by GC-MS is based on: i) the extraction of as many compounds as possible in a suitable solvent or solvent mix, including the addition of an internal standard ii) the evaporation of the extraction solvent and the derivatisation of aldehydes and ketones by methoxymation and of acidic protons by silylation.

Several optimisations of these steps are to be considered:

i) Two extraction procedures for plant metabolomics are commonly used, with some variations. The first is a modified Bligh and Dyer method (Fiehn *et al.*, 2000) in which two fractions (usually chloroform/methanol and a methanol/water) are produced and either both or only one is analysed. The second procedure consists only of extraction of samples with methanol (Lisec *et al.*, 2006). The first method potentially results in a broader range of metabolites extracted, but doubles the number of samples. The second is easier because it generate only one fraction to be analysed, but is more restrictive in the range of polarity of extracted metabolites. This results in a smaller number of metabolites extracted and a less reliable extraction of some compounds.

Several studies on different biological samples show that an optimisation of the extraction solvent can increase the quality of the metabolomic analysis. For example, after testing solvent mixes, including different combinations of methanol, ethanol, acetonitrile and chloroform, blood plasma

was found to be best extracted with methanol:water (8:1) (Jiye *et al.*, 2005). In case of yeast, pure methanol resulted in the best recoveries, except for sugars (Villas-Boas *et al.*, 2005). In this latter study, three parameters to measure extraction efficiency were introduced: the total number of peaks detected, the recovery potential for different classes of compounds, and the reproducibility of the extraction (measured as the average relative standard deviation of the peak integrations).

An extraction using one single solvent is more likely to be highly reproducible, as long as the sample itself does not contain a significant volume of water, but results in a lower polarity range of extraction. On the other hand, complex mixtures can achieve a better extraction, but small variations in the solvent mix preparation can result in different extraction efficiencies.

It is therefore clear that different extraction solutions should be tested when analysing a new type of biological sample, as in the case of diatoms. This is achieved in chapter 2.2.

Metabolic processes are fast. To take a biological sample with an unaltered metabolome, it is crucial to quench the metabolism as quickly and as efficiently as possible (Winder *et al.*, 2008). For plant material, shock freezing in liquid nitrogen is the most convenient and efficient method (Lisec *et al.*, 2006). However, when it comes to microorganisms suspended in a culture medium, shock freezing is not an option. Separation and concentration of the cells from the culture medium is necessary. Some studies have tried to solve this problem. The resulting method is to “shock cool” the culture by the addition of a cold methanol solution (60-70% methanol at -70°C to -40°C). The temperature of the culture drops very quickly below 0°C, and the metabolism is dramatically slowed. The goal is to reach a methanol concentration in the medium that prevents the freezing of the solution without impairing the cell wall integrity. This has proved to be achievable for *Escherichia coli* Escherich 1885 (Winder *et al.*, 2008) and *Chlamydomonas reinhardtii* Dangeard 1888 (Lee and Fiehn, 2008). Once cooled, the culture can be centrifuged to collect the cells for extraction, while the cells remain at subzero temperatures. Unfortunately this elegant method is inapplicable when the cell density is low, as in field plankton samples. In such cases, it is indeed often necessary to filter 5-10 litres of water to collect enough cells for metabolite analysis, and “shock-cooling” such volumes would require a prohibitive volume of cold methanol. The quenching of phytoplankton cultures or field samples is a tricky problem that remains unsolved. Filtration remains the preferred method for field sample concentration. Care has to be taken to balance filtration time and speed to achieve the quickest concentration without damaging cells. But one should always be aware that the metabolomic results from such studies will probably include a partly altered metabolic profile due to this stressful concentration method. Although the cold methanol quenching could be applied to dense diatoms cultures, I decided to not apply this method in my experiments, in order to have a similar concentration method between culture and field

samples.

A suitable internal standard is also important to take in account the extraction and derivatisation effects. Ribitol, a pentose alcohol, is used for most plant metabolomic studies (Lisec *et al.*, 2006). It has several advantages: i) it is derivatised by the silylation step, therefore providing the possibility of correcting for variations occurring at this step; ii) it is polar and therefore can provide correction for the extraction of polar compounds; iii) it elutes in the middle of the chromatogram, providing a reference for retention time and chromatography conditions that can be used for almost the entire chromatogram. However, ribitol also has some disadvantages: i) it does not provide a standard for the methoxymation step; ii) it is not a representative extraction standard for non-polar compounds.

It is clear that due to the complexity of the mix of metabolites analysed in metabolomics, a single standard cannot be representative for all compounds. The best internal standard strategy would be to use a wide range of isotopically marked compounds covering all major compound classes (Fiehn *et al.*, 2008). However, if the normalisation strategy is carefully examined, ribitol can provide an inexpensive compromise. ii) Once the biological material has been extracted, polar moieties must be derivatised to allow analysis by GC-MS. The common technique employed in metabolomics (Lisec *et al.*, 2006) consists of two steps. First the aldehydes and ketones are protected by methoxymation, usually in pyridine (methoxyamine 20 mg mL⁻¹ at 40-42°C for 60-90 min). The next steps consists of silylation with 2,2,2-trifluoro-N-methyl-N-trimethylsilyl-acetamide (MSTFA) or 2,2,2-trifluoro-N-trimethylsilyl-1-trimethylsilyloxy-ethanimine (BSTFA) to replace acidic protons (from alcohols, amines, carboxylic acids, thiols and phosphate groups) by an alkylsilyl group (trimethylsilyl in case of MSTFA), usually at 37°C for 30 min. This usually results in less polar, more volatile and more thermally stable compounds that can be separated in the GC. The optimisation of the two derivatisation steps has been extensively studied by Gullberg *et al.* (Gullberg *et al.*, 2004). The methoxymation step necessitated a compromise. Disaccharides, like sucrose, are efficiently derivatised after 2 hours at room temperature (RT), but the resulting compounds degraded if high temperature are maintained too long (>3 hours). Some compounds, like glucosamine, required long derivatisation times at high temperature (16 hours at 60°C) to achieve good derivatisation, while other, e.g. α -ketoglutarate, required long derivatisation time but at room temperature (RT), being otherwise degraded. Gullberg *et al.* therefore proposed to adopt a derivatisation carried at 60°C for one hour, followed by 16 hours at RT. I applied a modified version of this protocol for my derivatisation (*cf.* 2.2). The silylation step also poses some challenges. While the derivatisation of an alcohol group is straightforward, that is not the case for the primary amines, such as amino acids. Both protons can be derivatised, one after the other, but the kinetics of these sequential reactions can be very different among different compounds. This

results in several problems: at any time before the complete derivatisation, two or three derivatives, corresponding to one compound in the original sample, will be present. The ratio between these derivatives will change with derivatisation time and the starting concentration of the original compound (Kanani and Klapa, 2007). This will lead to the presence of interdependent peaks in the chromatogram that could have changing ratios, the response factor of each derivative being different. This complication must be considered during the multivariable analysis of the data. In practice, the time and temperature necessary for complete derivatisation is often very long (> 5 hours), and other compounds could degrade during this time. The silylation time should then be a compromise between a reasonable derivatisation of amines and a degradation of other compounds. Additionally, the amine-containing compounds should be treated with care during the multivariate analysis. Some methods have been proposed to correct for this problem (Kanani and Klapa, 2007), but they are difficult to implement and require the identification of all peaks originating from a single amine-compound. Unfortunately, no algorithm exists yet that could identify all these peaks, and the methods can therefore only be applied in case of manual identification. A promising technique, based on fragmentation pattern annotation, could theoretically identify all the peaks having a similar fragmentation pattern even if derivatised several times (Böcker *et al.*, 2009). All the peaks originating from the same compound could thereby be identified and the correction method from Kanani *et al.* (Kanani and Klapa, 2007) could then be applied. Unfortunately, this method requires mass spectra with very high resolution and very low background noise. The generation of mass spectra with reliably high resolution across the entire chromatogram of a metabolomics sample that includes peaks that differ by several orders of magnitude in intensity is still difficult. Therefore, the silylation step has also to be adapted to the samples type (*cf.* 2.2).

Then a data set containing peak intensity and retention time pairs has to be generated. Several software solutions are currently available (Fiehn *et al.*, 2005; Lisec *et al.*, 2006). Most of them are commercial and linked to a particular instrument, e.g. Markerlynx (delivered with Waters instruments). Markerlynx proved to be useful in the analysis of chromatograms generated by UPLC-MS (Barofsky *et al.*, 2009; Barofsky *et al.*, 2010). However, in case of GC-MS data, the usefulness of Markerlynx was limited, because the numerous fragments from one analyte are considered by this software as independent compounds. This software is still useful for evaluation of chromatogram data, but further analysis requires to manually grouping all mass-retention time pairs generated from one compound and selecting one to be used in the multivariate analysis. As a replacement, a combination of two freeware programs is often used (Lisec *et al.*, 2006). The Automated Mass Spectral Deconvolution and Identification System (AMDIS) (Stein, 1999) deconvolutes chromatograms and generates lists of spectra. These lists are then fed to the Metabolomics Ion-based Data Extraction Algorithm (MET-IDEA) (Broeckling *et al.*, 2006). This

second software selects in each spectrum a model ion for every compound and integrates the area of the peak in the corresponding trace. Finally it generates a table with intensities of all peaks in all submitted chromatograms. This data set can then be analysed by multivariate statistics. I chose these two softwares to analysing my samples.

Once a data set has been produced, multivariate statistical analysis can be used to extract patterns or to visualise changes of metabolite profiles (Eriksson *et al.*, 2006). Several multivariate projection methods can be used, including non-supervised methods like principal component analysis (PCA), principal coordinate analysis (PCA), or supervised methods, e.g. partial least squares (PLS). All these methods can be used to display the data set in a two or three dimensional plot that emphasises the difference between groups of samples. Every sample can indeed be represented as a point in an n-dimensional space, where n is the number of variables (in this case the number of compounds quantified from the chromatogram). Some grouping may occur in this multidimensional space. The multivariate projection methods are then used to identify the groups and create a set of new variables (linear combinations of the original variables) that maximise the differences between them. The samples are then projected from the n-dimension space onto the two or three dimensional space defined by the most explicative new variables. Non-supervised methods create new variables, corresponding to new axes, which maximise the highest differences present in the data set. Supervised methods, on the other hand, create new variables that maximise the differences between predefined groups of samples (Eriksson *et al.*, 2006) (for a review on metabolomics multivariate data analyses, see (Jansen *et al.*, 2009)). I chose this latter strategy and used Canonical Analysis of Principal coordinates (CAP).

Canonical analysis of principal coordinates (CAP)

CAP is a supervised projection method (Anderson and Willis, 2003). The data set is submitted to a program that creates a distance matrix of the samples, and then performs the CAP. This method requires two steps: i) a principal coordinate analysis, followed by ii) a canonical correlation analysis. This provides a flexible and meaningful constrained ordination (Anderson and Willis, 2003). This method has the advantage of being not very sensitive to hidden correlations in the dataset, as expected with metabolic samples containing amine-derivatives.

First the canonical constrained axes eigenvalue and Δ^2 are calculated. There is one axis less than predefined groups. Each axis eigenvalue and Δ^2 provides information about the separation efficiency of the axis. A high eigenvalue (>0.9) indicates that the axis separates the groups well, and a high Δ^2 means that groups correlate with this axis well. Then, the projected coordinates of every sample on the created axis are calculated. Three statistic tests allow an evaluation of the separation achieved by the CAP.

The first test is a “leave one-out test”, estimating the goodness of fit. By doing the CAP analysis with one sample less, and then predicting from the generated model to which group this left-out sample belongs to, and comparing the results with real grouping, it is possible to evaluate nearly without bias and reasonably well how distinct the groups are in the multivariate space (Seber, 1984). The results can be expressed as percentage of miss-classification: if low, then the groups are very distinct; if high, they are overlapping.

A second test evaluates if there is a significant difference of the multivariate location among the groups. The statistic is the sum of the canonical correlations and a p-value is calculated by permutation (Anderson, 2001).

Finally a correlation test determines if the correlation Δ^2 of the first constrained axis is significant.

One major parameter in this method is the type of distance matrix created. I choose the Bray-Curtis dissimilarity, because, compared to Euclidian distances, it retains sensitivity in more heterogeneous data sets and gives less weight to outliers (McCune B. *et al.*, 2002).

On metadata

The success of omics methods relies partly on the comparison between other experiments performed by other labs. Indeed, omics experiments often require high amounts of samples, and huge data set are produced and analysed. Comparison with previous experiments can greatly improve the meaning derived from a particular experiment. However, biological systems are very complex, and a lot of parameters can influence the final data set. It is therefore of major importance to record as many parameters (metadata) as possible (Fiehn *et al.*, 2007a; Fiehn *et al.*, 2007b; Goodacre *et al.*, 2007a; Morrison *et al.*, 2007; Sumner *et al.*, 2007; van der Werf *et al.*, 2007). Standards for reporting metabolomic data have been proposed, but so far, the community has not adopted a general template.

I therefore chose to gather all the possibly relevant metadata during my experiments and report them in the appendix.

2. Results and Discussion

2.1 Polyunsaturated aldehydes¹



S. marinoi bloom in the north Adriatic Sea

¹ Parts of this chapter are based on: Vidoudez, C. and Pohnert, G. (2008) Growth phase-specific release of polyunsaturated aldehydes by the diatom *Skeletonema marinoi*. *Journal of Plankton Research*, **30**, 1305-1313.
Ribalet, F., Vidoudez, C., Cassin, D., Pohnert, G., Ianora, A., Miralto, A. and Casotti, R. (2009) High plasticity in the production of diatom-derived polyunsaturated aldehydes under nutrient limitation: physiological and ecological implications. *Protist*, **160**, 444-451.

The first prerequisite for an infochemical/allelopathic role of the PUA would be that they are released into the environment of the producing diatoms so that they could be perceived by or act on conspecific cells, predators or competitors. PUA were only found to be released upon cell breakage, mainly supposed to happen while eaten by a grazer. I therefore wanted to investigate the presence or absence of PUA in the water during culturing, and diatom blooms in the sea.

2.1.1 Occurrence of PUA in the natural environment

We participated in two cruises on the north Adriatic Sea, in March 2006 and February 2008. Several stations were sampled for dissolved PUA, post-wounding production of PUA by the cells (referred as PUA production potential), as well as for cell counts and species determination.

In 2006, we sampled only the upper region of the Adriatic Sea, close to Venice (north of station C01, **Figure 4**) and the Po river estuary. A bloom of *S. marinoi* ($>12 \cdot 10^6$ cells L⁻¹) was present at station 2E01, probably due to the high nutrients brought by the river waters (**Figure 4A**). At the other stations where species and cell concentrations were determined, samples from the N6 station contained $0.6 \cdot 10^6$ *S. marinoi* cells L⁻¹ while all the other showed less than $20 \cdot 10^3$ cells L⁻¹ of this species. With these cell densities, *S. marinoi* represented more than 90% of the diatoms present at station 2E01 and N6, but only ~60% of the diatoms on the other stations. At the bloom location also the highest PUA production potential was found. The cells present in one litre of seawater could produce more than 4 nmol of heptadienal and more than 1.6 nmol of octadienal (**Figure 4 B & C**), representing 0.3 and 0.1 fmol cell⁻¹ respectively, if normalised to the *S. marinoi* density. At the N6 station, only 0.3 and 0.06 nmol of heptadienal and octadienal were produced by the cells from one litre of seawater, but this correspond to 0.6 and 0.1 fmol *S. marinoi* cell⁻¹ respectively. The results indicate that the PUA production potential was tightly correlated with the density of *S. marinoi* at these two stations, suggesting that *S. marinoi* was the main PUA producer. Cells at station C01 also had a small PUA production potential (0.16 nmol heptadienal and 0.05 nmol octadienal per cells from 1 L), but cell density and species composition was not determined for this station.

PUA were also present dissolved in the seawater (**Figure 4 D & E**). I measured the highest concentration of heptadienal (0.15 nM) at the station where *S. marinoi* was blooming (2E01). Heptadienal was also present at the N6 station (0.06 nM) and at the only station sampled in the C transect (0.1 nM). Octadienal concentration was the highest at the second station of the N transect, with 0.4 nM, while this compound was only found at 0.02 nM at the bloom.

In 2008 we sampled stations more widely distributed in the north Adriatic Sea. The highest *S. marinoi* density was found at station V13, in the same costal region as the bloom observed in 2006 (**Figure 5A**). Although the cell concentration ($0.8 \cdot 10^6$ cells L⁻¹) was ~10x lower than in 2006, *S.*

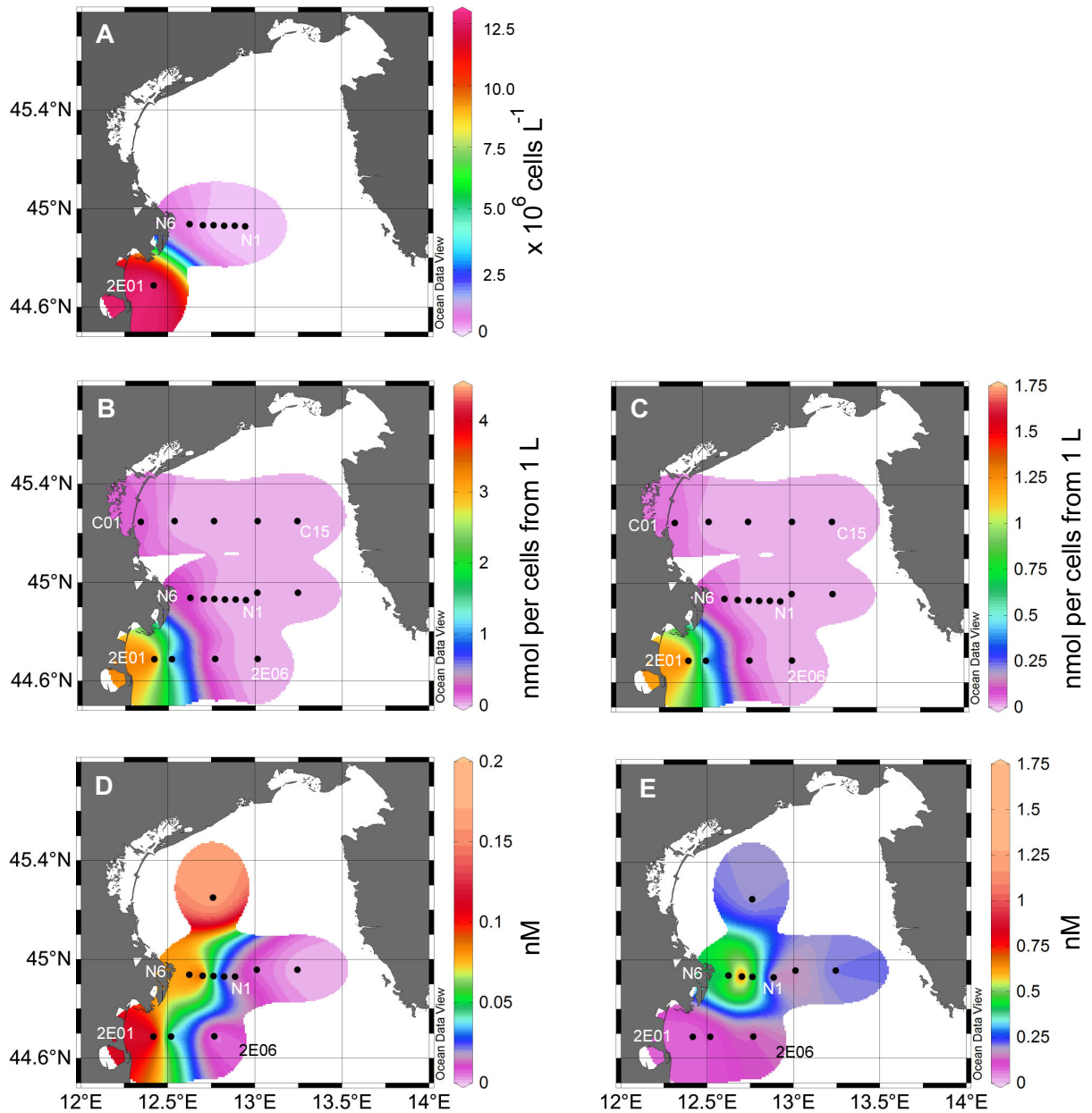


Figure 4: Surface distribution (0-1 m) of PUA in the Adriatic Sea during the March 2006 cruise. **A**, *S. marinoi* cell density. **B**, heptadienal and **C**, octadienal produced by the $>1.2 \mu\text{m}$ fraction from 1 L of seawater, after wounding. **D**, heptadienal and **E**, octadienal dissolved in the seawater. The closed circles indicate the sampling stations. Please notice the different scaling. The colour shade is extrapolated from the station values and is shown to simplify the comparison of the stations.

marinoi still represented $>95\%$ of the diatoms present at this station. Despite the lower cell density, the cells present in one litre of seawater showed a very high PUA production potential, with 18 nmol per cells from 1 L ($22 \text{ fmol } S. \text{ marinoi } \text{cell}^{-1}$) heptadienal and 10 nmol per cells from 1 L ($13 \text{ fmol } S. \text{ marinoi } \text{cell}^{-1}$) octadienal (**Figure 5 C & D**). At station V21, no *S. marinoi* was detected, but 3.6 nmol of heptadienal and 1.6 nmol octadienal were produced by the cells collected from one litre of seawater. We identified a large number of undetermined cryptophytes at that station ($4 \cdot 10^4 \text{ cells L}^{-1}$), as well as at the V13 station ($2.5 \cdot 10^5 \text{ cells L}^{-1}$). Other stations showed a low background

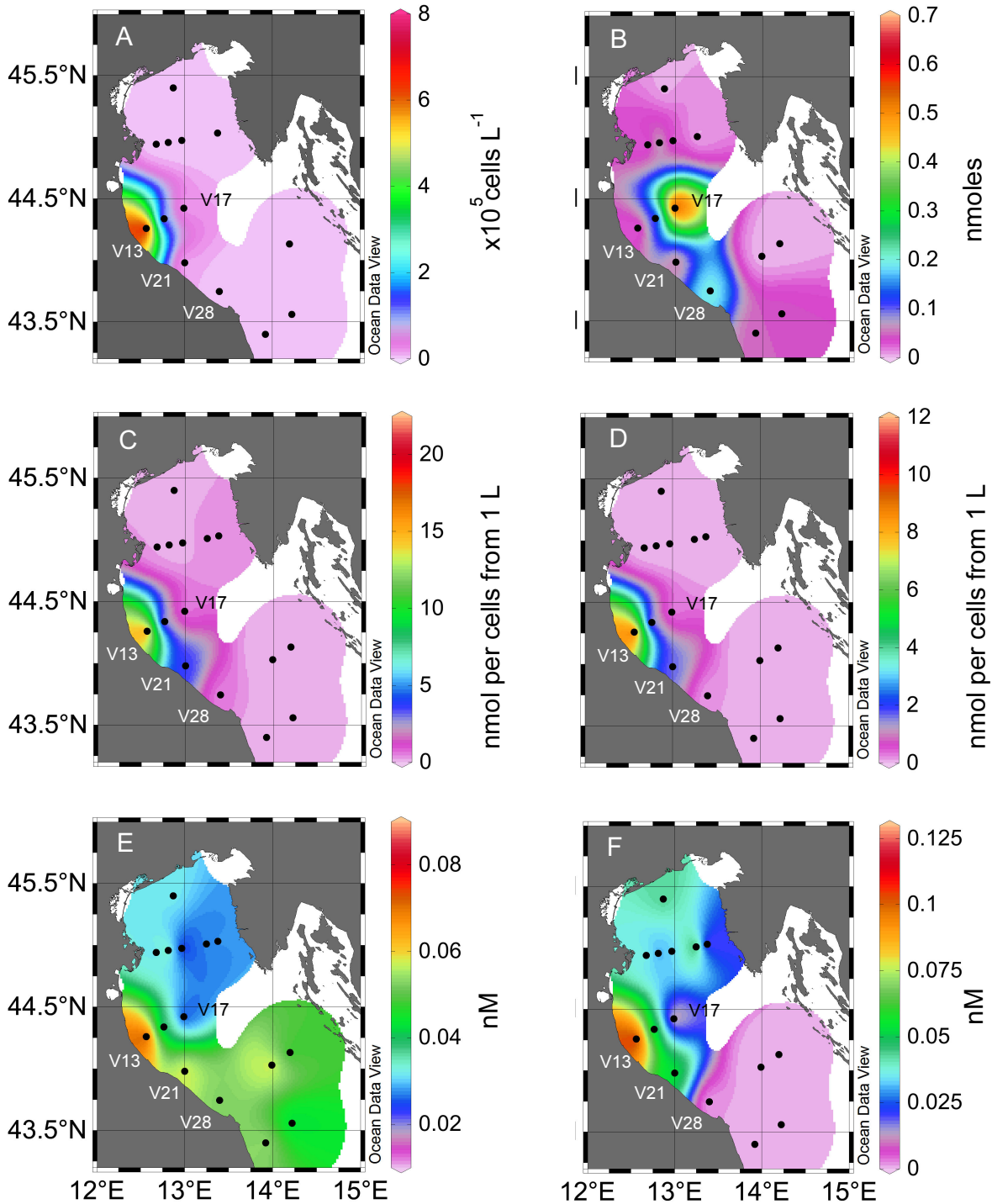


Figure 5: Surface distribution (0-1 m) of PUA in the Adriatic Sea during the February 2008 cruise. **A**, *S. marinoi* cell density. **B**, heptadienal produced by the $1.2 \mu\text{m} > x > 0.2 \mu\text{m}$ fraction from 1 L of seawater, after wounding. **C**, heptadienal and **D**, octadienal produced by the $>1.2 \mu\text{m}$ fraction from 1 L of seawater, after wounding. **E**, heptadienal and **F**, octadienal dissolved in the seawater. The closed circles indicate the sampling stations. Note the different scaling. The colour shade is extrapolated from the station values and is shown to simplify the comparison of the stations.

production potential of heptadienal (0.0-0.4 nmol per cells from 1 L) and octadienal (0.0-0.09 nmol per cells from 1 L), decreasing with the distance from the bloom. In addition to the cell sample types (cells $>1.2 \mu\text{m}$) that were collected in 2006, I also measured the production of PUA of cells

smaller than 1.2 μm . This picoplankton (range from 1.2 to 0.2 μm) fraction produced only heptadienal with a distinctive peak at station V17, with 0.6 nmol per cells from 1 L production potential (**Figure 5B**), 10 fold more than the heptadienal produced by the cells from the $>1.2 \mu\text{m}$ (0.05 nmol per cells from 1 L) at that station.

As observed in 2006, PUA were also present dissolved in the seawater. The highest concentrations were measured at the V13 station; reaching 0.08 nM heptadienal and 0.1 nM octadienal (**Figure 5 E & F**). The concentration followed the trend found for the PUA production potential, decreasing with the distance from the bloom.

During the 2008 cruise, the PUA production potential of the $>1.2 \mu\text{m}$ fraction and the picoplankton was also measured for different depths at three different stations (V13, V21 & V28) (**Figure 6**). At the bloom station (V13), the production potential was halved at 13 m depth related to the surface (heptadienal: surface 18 nmol per cells from 1 L, 13 m 8 nmol per cells from 1 L; Octadienal: surface 10 nmol per cells from 1 L, 13 m 4.5 nmol per cells from 1 L) while the *S. marinoi* density

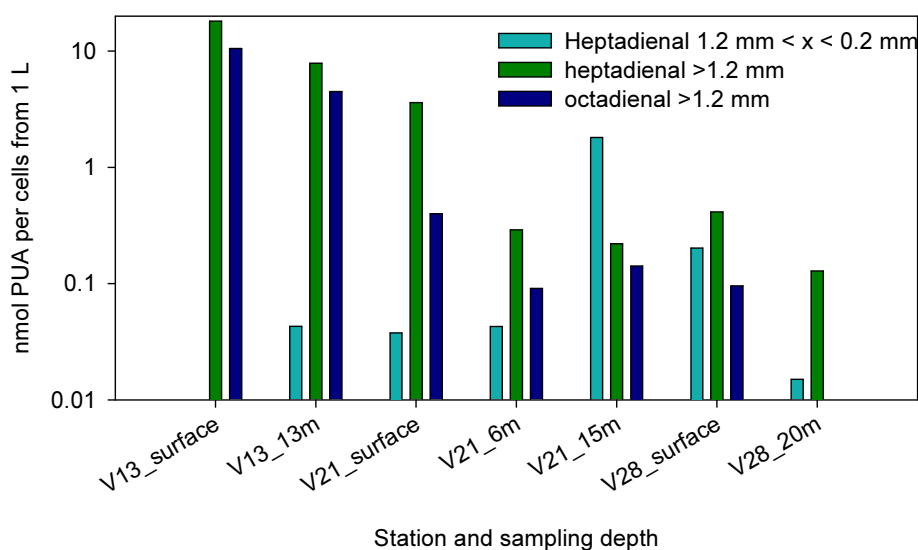


Figure 6: Production of PUA by cells from 1 litre of seawater at different depths. Note the logarithmic scale.

decreased by one order of magnitude (surface $0.8 \cdot 10^6 \text{ cells L}^{-1}$, 1 m $0.07 \cdot 10^6 \text{ cells L}^{-1}$). While I found no heptadienal produced by the picoplankton at the surface, 0.04 nmol per picoplankton cells from 1 L were produced at 13 m. At station V21, the PUA production potential of the $>1.2 \mu\text{m}$ decreased by more than 10 fold between surface and 6 m depth, but remained constant between 6 m and 15 m (Heptadienal: surface 3.6 nmol per cells from 1 L, 6 m 0.3 nmol per cells from 1 L, 15 m 0.2 nmol per cells from 1 L; Octadienal: surface 1.6 nmol per cells from 1 L, 6 m 0.08 nmol per cells from 1 L, 15 m 0.09 nmol per cells from 1 L). The production potential of the picoplankton

increased with depth until exceeding the potential of the 1.2 μm fraction (Heptadienal: surface 0.03 nmol per picoplankton cells from 1 L, 6 m 0.04 nmol per picoplankton cells from 1 L, 15 m 1.8 nmol per picoplankton cells from 1 L). At station 28, the heptadienal production potential of the $>1.2 \mu\text{m}$ fraction was similar to the picoplankton (0.4 and 0.2 nmol per cells from 1 L respectively) at the surface, but at 20 m depth the $>1.2 \mu\text{m}$ fraction had a production potential an order of magnitude higher than the production potential of the picoplankton (0.1 and 0.01 nmol per cells from 1 L respectively), while both being lower than at the surface. No octadienal was detected at 20 m depth.

We sampled all these stations during the day for both cruises, but in 2006, at the station with the *S. marinoi* bloom, I also performed a time series sampling of the production potential and dissolved PUA. The bloom was sampled at eight different time points, between 17:30 on the 19th and 20:30 on the 20st of March (**Figure 7**). The dissolved heptadienal stayed initially at constant levels (0.15

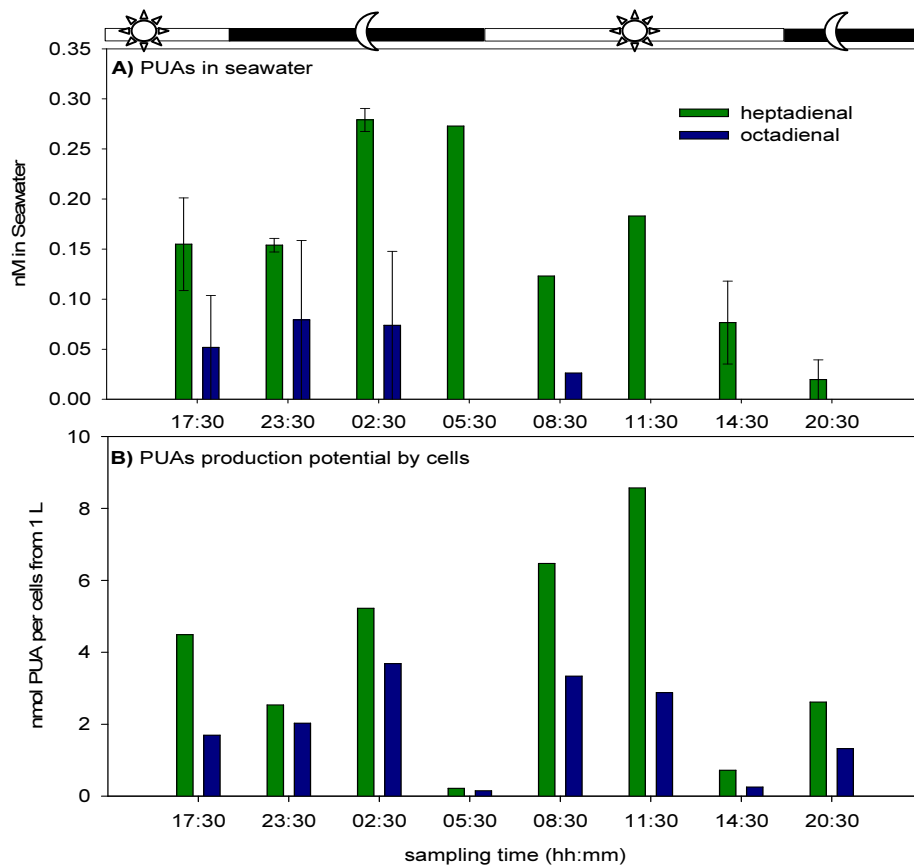


Figure 7: PUA at the site of a natural bloom of *S. marinoi* (Station 2E01, 19th and 20th march 2006). **A**, PUA dissolved in seawater. **B**, PUA produced after wounding by the cells present in 1 L of seawater. In both cases, $n = 1$ except when error bars are present (in these cases the value is average \pm range, $n = 2$). The bars on the top represent day and night time.

nM) one hour before or five hours after sunset (at 18:23). At 02:30 and 05:30, the heptadienal nearly doubled in concentration (0.27 nM) and decreased back to 0.12 nM after sunrise (sunrise at 06:15, sampling time: 08:30). The concentration remained constant until midday then decreased to

reach the very low level of 0.02 nM at 20:30. The octadienal present in the seawater remained at nearly constant levels during the first three sampling time points before decreasing to non-detectable levels.

In contrast to the dissolved PUA concentration, the production potential followed a different pattern. Both heptadienal and octadienal potential exhibited a drop at 05:30 and 14:30. At the other sampling times, the production remained relatively constant. It is impossible to determine if the observed changes and drop were significant or not, due to the lack of replicates.

2.1.2 Laboratory studies

Because the natural samples suggested that PUA are released into the seawater by diatoms, I decided to get more information on the PUA release dynamics of *S. marinoi*. Therefore I sampled three 25 L cultures every day for determination of PUA production potential and released PUA, over the entire growth curve.

PUA content of the medium and potential production by the cells

During the exponential growth phase and the early stationary phase *S. marinoi* released no or only very minor amounts of PUA into the medium (**Figure 8 A**). From day 1-9, PUA concentration was below the detection limit (around 1 pmol L⁻¹); later only trace levels were detected. On day 21 a dramatic net increase in heptadienal and octadienal concentration in the medium was observed in all three synchronised cultures (**Figure 8 A**). The concentration of PUA in the medium peaked at day 24 with values of 290 (\pm 160) nM heptadienal and 86 (\pm 39) nM octadienal. The concentration then decreased to low nM values at day 30. The peak concentration of PUA was observed directly before the cultures entered the declining phase. During the entire 5-day period of PUA release, heptadienal concentrations exceeded those of octadienal. No octatrienal or longer chain length PUA were detected. The relatively high values for the standard deviation can be attributed mostly to a slight difference (one day) in synchronisation of the three cultures, which were started at the same time. The pH of the medium remained constant (8.43 ± 0.15) during the initial phase of the experiments until day 25, but decreased to 8.00 ± 0.06 on day 30.

During the stationery phase, the PUA production potential (**Figure 8 B**) of the cells remained relatively constant until day 16, then more than doubled to reach a plateau between day 20 and 23, in the late stationery phase and finally decreased to reach very low level at day 25, for the declining phase. Repeated measures ANOVA confirmed that the observed increase in potential was significant for heptadienal ($p < 0.001$), for octadienal and octatrienal (ANOVA on ranks, $p < 0.001$

for both compounds). Post-hoc tests showed that the potential on days 20-23 was significantly different from that on days 10-16 and on days 25-30 (pairwise multiple comparison with Bonferonni t-test, $p < 0.05$) for heptadienal. For octadienal, the potential on days 19-23 was significantly higher than the one on day 10, 25 and 30. The octadienal potential was also higher on

day 15 compared to days 10, 25 or 30 (pairwise multiple comparison on ranks with Student-Newman-Keuls (SNK), $p < 0.05$). No other significant differences were identified with the post-hoc test. The significant groups could not be identified with the SNK post hoc test for octatrienal

potential (all post-hoc test $p > 0.05$ or not tested due to their rank position).

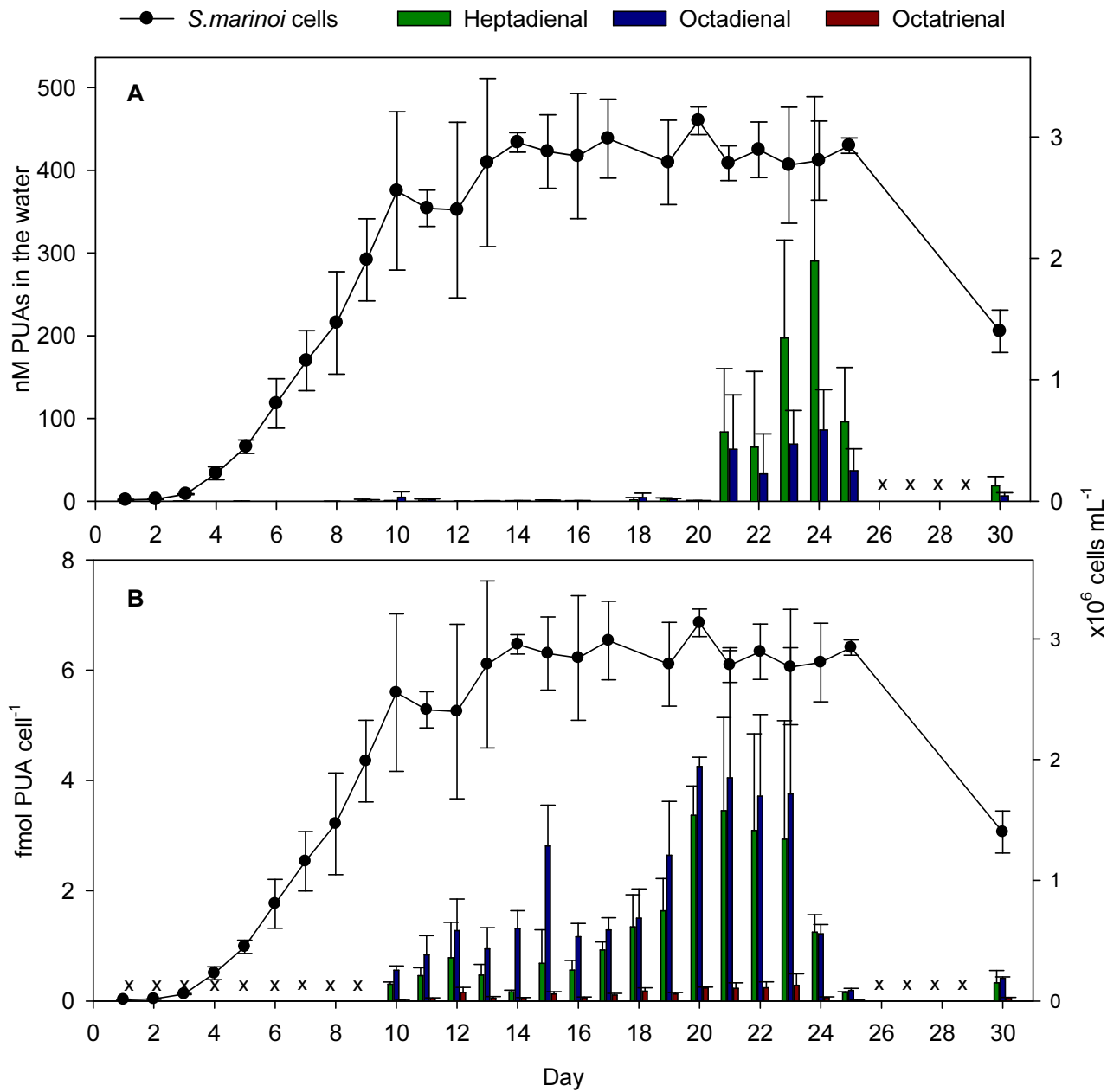


Figure 8: PUA (bars) and cell counts (dots) in a *S. marinoi* culture. **A**, PUA in the medium. **B**, PUA production potential. Values are average of three replicates \pm standard deviation. For all cases, x represents a day on which PUA were not measured.

PUA addition to a culture

In order to test the effects of exposure to biologically relevant concentrations of octadienal and heptadienal, three experiments were designed to observe the reaction of a *S. marinoi* culture to PUA addition at different time points (*cf.* material and methods chapter 4.6.3 for details). Heptadienal and octadienal were added to a *S. marinoi* RCC 75 cultures separately or at a ratio similar to that found to be released. Three different concentrations of PUA were used, one at the same concentration that

the one found in culture (250 nM heptadienal, 62 nM octadienal, referred thereafter as culture concentration), one 1000x higher and one 1000x lower. These PUA additions were performed on an exponential phase (experiment 1) or a stationary phase culture (experiment 2). Experiment 3 was conducted by adding only relevant concentrations to the culture in late stationary phase.

PUA addition during the exponential phase (experiment 1)

The growth rates before PUA-addition were not significantly different between any cultures in exponential phase as confirmed by statistical analysis (ANOVA on all growth rates before addition, $p = 0.48$). After PUA addition on day 5 at the culture concentration of heptadienal and/or octadienal, as well as at 1000x lower than culture concentrations no significant change in growth rates was observed in comparison with the controls (**Figure 9** left). Growth rates were calculated between day 5 and 8 and no statistical differences were found (ANOVA on growth rates between the treatments and the controls, $p = 0.41$). In contrast, the PUA addition at 1000x culture concentration of heptadienal and/or octadienal resulted in the drastic decrease of living cell density in the cultures. While almost no living cells were found after one day in the case of the heptadienal and the mixed heptadienal/octadienal additions, a one-day lag period with arrested growth was observed before cell density dropped in the case of the octadienal addition (**Figure 9** left).

PUA addition during the stationary phase (experiment 2)

Before PUA addition at day 16, the culture growth rates were not significantly different (ANOVA between all groups' growth rates, $p = 0.29$). As in the previous experiment, PUA additions resulting in culture concentrations, or 1000x lower, of heptadienal and/or octadienal did not result in a significant change of cell density relative to the controls (ANOVA between treatments and controls on growth rates calculated between day 16 and 17, $p = 0.36$, between day 17 and 24, $p = 0.09$) (**Figure 9** right). The addition to reach 1000x higher than culture concentration of heptadienal and/or octadienal resulted in the rapid decline of cell counts. After four days, no living cells were found in these treatments, while cell counts in the controls remained unchanged. When heptadienal was added alone at the 1000x higher (250 μM) than culture concentration, a slow but significant (t-test on growth rates before and after addition, $p < 0.03$) decrease in cell density was observed for the first day, followed by a rapid decrease of living cell density of the culture the day after. No significant changes were observed during the first two days after octadienal was added at the high concentration (t-test on growth rates before and after addition, $p = 0.07$). However the cell density decreased within the next three days.

PUA addition in late stationary phase (experiment 3)

None of the cultures that had been pre-treated with PUA in early stationary phase showed a response to the addition in late stationary growth phase (42-45 days old cultures) of a mix of

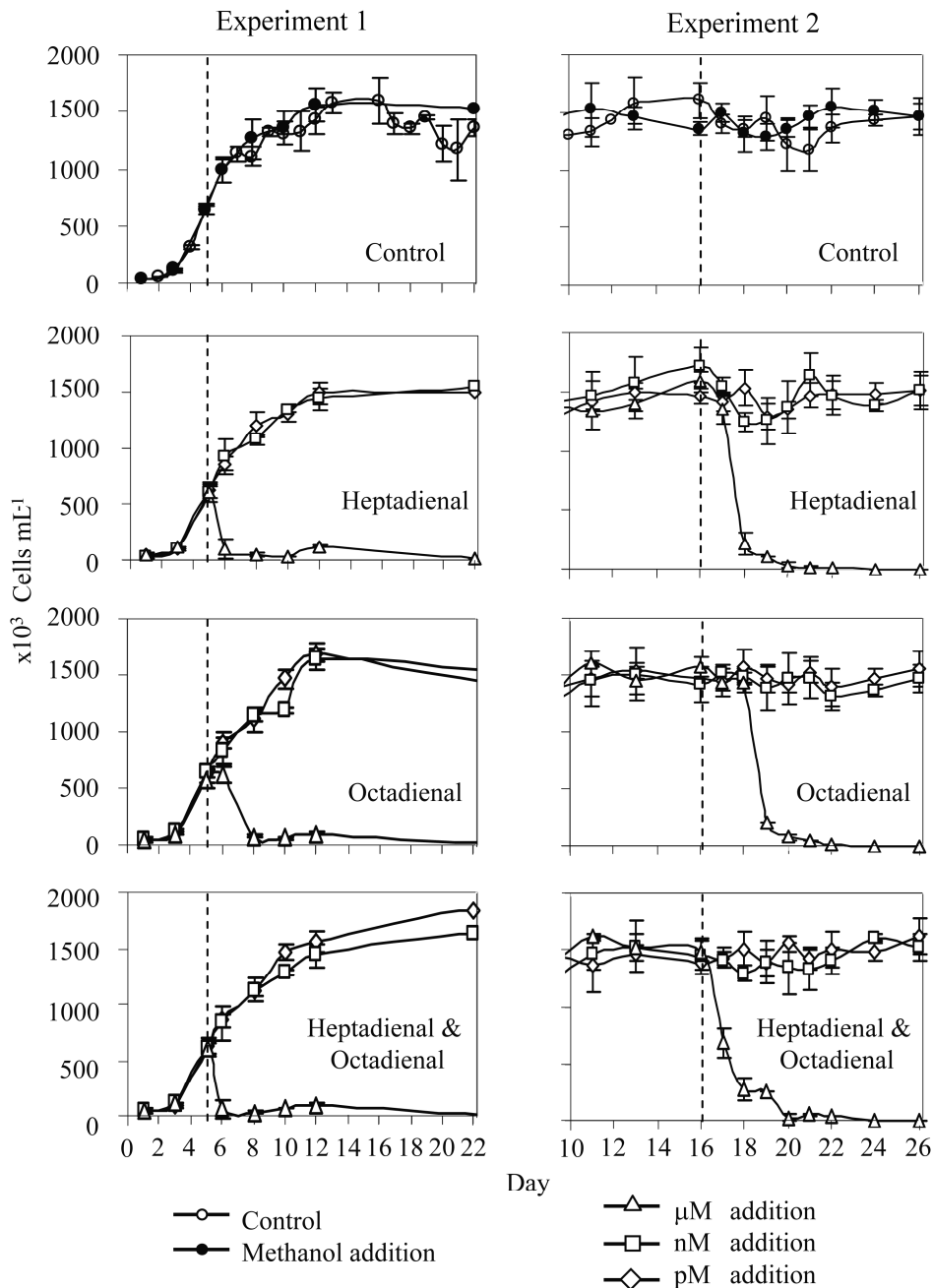


Figure 9: Cell densities of cultures after addition of heptadienal and octadienal to exponentially growing cultures (left) or stationary cultures (right). The dashed vertical lines indicate the day of addition. Heptadienal and octadienal were added to a final concentration of respectively 250 μM and 62 μM (open triangle), 250 nM and 62 nM, the concentration found in culture (open squares) or 250 pM and 62 pM (open diamonds), either alone or as mixture. Results represent the average of three replicates \pm standard deviation.

heptadienal and octadienal at the culture concentration (250 nM and 62 nM, respectively). The treated cultures and the respective controls stayed in the stationary phase for 2 to 31 days after PUA addition and then entered the declining phase simultaneously (data not shown). In contrast, the cultures that had no pre-treatment with PUA exhibited a significant response to the addition of PUA in late stationary phase (42-45 days old cultures; heptadienal/octadienal at the culture concentrations). In all replicates, PUA addition to naive cultures triggered a transient growth phase two days after the addition (**Figure 10**). Cell counts reached a maximum nine days after the PUA

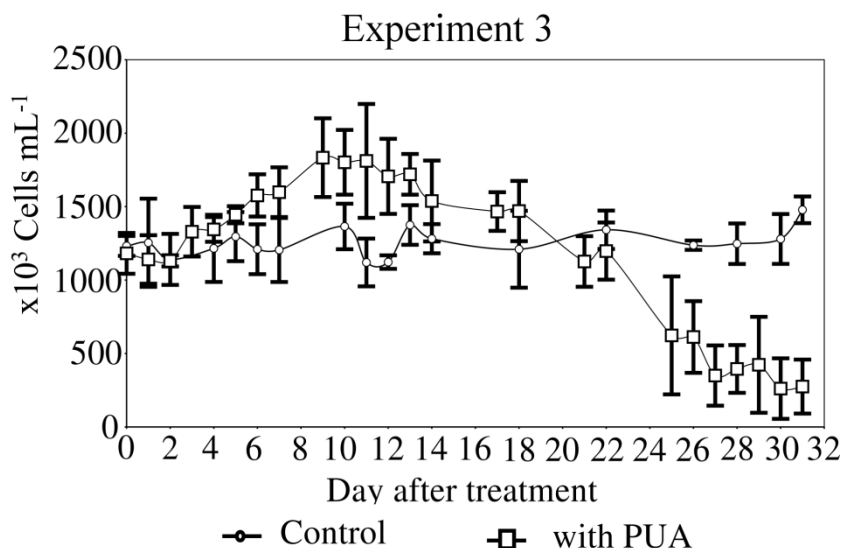


Figure 10: Cell density of naive cultures after addition of heptadienal and octadienal to a final concentration of 250 nM and 62 nM, respectively. Results are the mean of three replicates \pm standard deviation for the control (open circle) and of five replicates \pm standard deviation for the treated cultures (open square).

addition. In contrast to controls, cell-density in treated cultures then declined dramatically. A repeated measures ANOVA showed a significant interaction between treatment and time ($p < 0.0001$) with a significant difference in cell density between treatment and control on day 10 ($p < 0.05$) and day 31 after PUA addition ($p < 0.001$).

Influence of nutrient limitation on PUA production potential

The results of PUA production potential in the *S. marinoi* culture suggest that the production potential increases when environmental conditions deteriorate, potentially when nutrients become limiting. Therefore, in collaboration with François Ribalet at the Stazione Zoologica Anton Dorhn (Naples, Italy), we examined the effects of nitrogen, phosphate or silicate limitation on diatom production of PUA. Cultures of *S. marinoi*, strain CCMP 2092, were maintained in chemostats with different nutrient limited medium flowing through the culture. When the flow was kept at high rate, even the low level of nutrients in the medium was sufficient for the cells, but at low flow rate, the low nutrient concentration in the medium becomes limiting (data not shown here, see (Ribalet *et al.*, 2009)). In each treatment the production potential of heptadienal, octadienal and octatrienal was determined, as well as the PUFA cell content.

PUA produced per cell (average \pm standard deviation) in control cultures reached 1.70 ± 0.51 fmol cell⁻¹, 1.41 ± 0.35 fmol cell⁻¹ and 0.05 ± 0.02 fmol cell⁻¹ for heptadienal, octadienal and octatrienal, respectively. Total production of PUA increased 3 fold in P-limited and 7.5 fold in Si-limited cells, relative to controls, with production of PUA as high 7.5 fmol cell⁻¹ in P-limited and 27.5 fmol cell⁻¹

in Si-limited cultures (**Figure 11 A**). The increase in PUA was mainly due to an increase in octadienal (4.3 fmol cell⁻¹ and 13.4 fmol cell⁻¹ in P- and Si-limited cells, respectively) and heptadienal (3.2 fmol cell⁻¹ and 13.9 fmol cell⁻¹ in P- and Si-limited cells, respectively) (**Figure 11 C & E**). In contrast, heptadienal and octadienal production decreased dramatically in N-limited cells to 0.07 and 0.06 fmol cell⁻¹ (**Figure 11 E**). Octatrienal was present only in traces in all cultures.

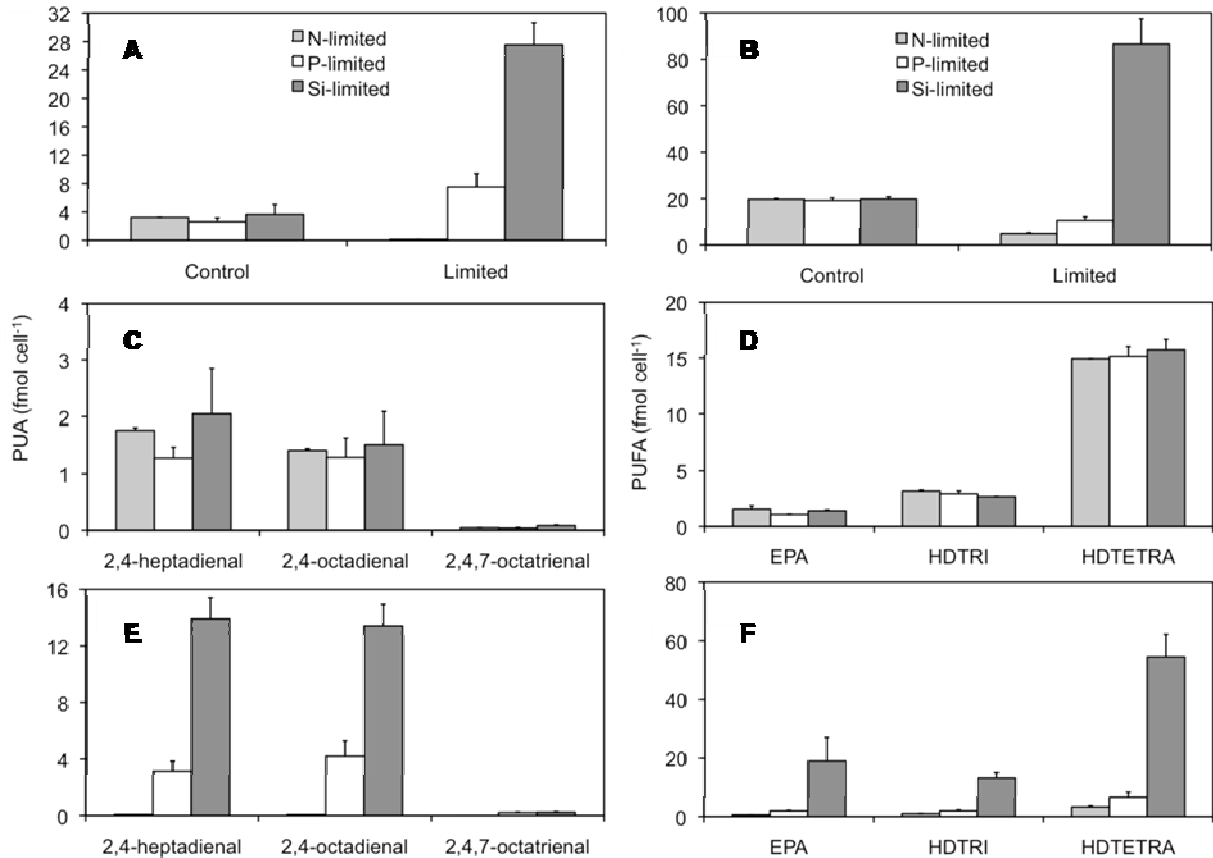


Figure 11: PUA production potential (**A, C, E**) and PUA precursor PUFA (**B, D, F**) in *S. marinoi* cells grown under nutrient limited conditions. **A**, total PUA production potential and **B**, PUFA cell content, at high (control) and low (limited) flow in N-limited, P-limited, and Si-limited growth media. **C & D**, composition of the PUA and PUFA respectively, in control, and **E & F**, in nutrient limited conditions. Error bars represent the range associated with the mean (n = 2). Adapted from (Ribalet *et al.*, 2009).

The cell content of the three PUA precursor fatty acids averaged 19.5 ± 1.0 fmol cell⁻¹ in control cultures (**Figure 11 B**). The proportion of the three PUFA that are precursors of PUA was similar in these cultures, with HDTETRA being the dominant fatty acid (**Figure 11 D**). Under nutrient limitation, total PUFA content was 4.9 fmol cell⁻¹ and 10.5 fmol cell⁻¹ in N- and P-limited cultures, respectively, which corresponded to 24.9% and 55.0% of the controls. In contrast, total PUFA content was as high as 86.6 fmol cell⁻¹ in Si-limited cells and represented 437.1% of the control (**Figure 11 F**). In N-limited cultures, all three precursor PUFA were equally reduced, while in P-limited cultures, HDTRI and HDTETRA decreased to 67.2% and 43.6% of the controls respectively,

EPA increased to 182.1% (**Figure 11 F**). Under Si-limitation, higher amounts of all three precursor PUFA were produced, with EPA increasing 1345.9% with respect to the control culture (from 1.41 fmol cell⁻¹ to 18.97 fmol cell⁻¹), and HDTRI and HDTETRA increasing 493.8% and 346.1%, from 2.66 to 13.16 HDTRI fmol cell⁻¹ and from 15.73 to 54.44 HDTETRA fmol cell⁻¹, respectively (**Figure 11 F**).

The molar EPA:heptadienal ratio was close to 1 in all controls as well as in P- and Si-limited cells. However it reached 8.5 in N-limited cells. The HDTETRA:octatrienal ratio ranged from 32.7 in P-limited cells to 701.3 in N-limited cells. The HDTRI:octadienal ratio was around 2 in all control cultures while it decreased to 1 in P- and Si-limited cells and increased to 18.0 in N-limited cells.

2.1.3 Discussion

PUA are released into the surrounding water

S. marinoi releases heptadienal and octadienal in the surrounding seawater. PUA were detected in the samples of both north Adriatic Sea cruises. The highest dissolved concentrations of PUA were observed where *S. marinoi* bloomed (**Figure 4, Figure 5**). Lower concentrations were also found at other sampling stations, with a decreasing trend when getting farther from the bloom stations.

Proportions of released PUA compared to PUA production potential at the time of sampling were clearly different between the blooms of both years. The dissolved heptadienal and octadienal corresponded to ~3% and ~1.25% of the production potential on the bloom station in 2006, while it was less than 0.5% and 1% of the respective PUA production potential in 2008. The PUA production potentials were four times higher in 2008 than in 2006, but at the same time the cell density was an order of magnitude lower in 2008 than in 2006. Although the ratio between heptadienal and octadienal production potential were similar for both years, the ratio of the dissolved PUA was inverted in 2008, with a higher concentration of octadienal than heptadienal in 2008.

Some other stations exhibited a surprisingly high amount of dissolved PUA. On station N6 (2006), dissolved heptadienal equalled ~36% of the cell production potential, and octadienal exceeded the cell potential (**Figure 4**). Both PUA exceeded their production potential on station N5 (which was not detectable for heptadienal and very low for octadienal). The lysis rates were very high on the N transect (F. Ribalet personal communication), which could provide an explanation for this phenomenon. *S. marinoi* cells may have been carried away from the bloom by the current. If the nutrient afflux from the Po River did not sustain their growth anymore, the cells would die and

release their PUA. Such a rapid dying event could result in the depletion of the cell PUA production potential and in increased concentration of dissolved PUA. However, long-lasting elevated PUA concentrations are not expected to occur, due to their high reactivity. Indeed, PUA cannot accumulate in the medium due to their reactivity and volatility (*cf.* **Figure 32** in chapter 2.5 and (Carvalho *et al.*, 2000)) and are also probably degraded by bacteria. High concentrations of dissolved PUA would then be expected only if a continuous release process is taking place.

An alternative explanation for this unexpected PUA concentration away from *S. marinoi* blooms could be the picoplankton as an additional source of PUA. In 2006, only the fraction of the plankton bigger than 1.2 μm was collected for determination of the PUA production potential. In 2008, I collected samples of the fraction of the plankton $>1.2 \mu\text{m}$ and of the plankton ranging between 0.2 and 1.2 μm (picoplankton). At station V17, the dissolved heptadienal corresponded to $\sim 50\%$ of the production potential, when this latter is measured from the $>1.2 \mu\text{m}$ fraction, but only 3% when the picoplankton potential is taken in account. It is then clear that the picoplankton fraction could contribute also to the dissolved PUA pool.

It is difficult to evaluate what part of the dissolved PUA originates from the cell lysis and if a significant part was released from healthy cells. On average, the lysis rate correlated with the amount of dissolved PUA during the 2006 cruise (F. Ribalet, personal communication), but no lysis rate data were recorded during the 2008 cruise. Therefore we cannot conclude if the different ratio between the production potential and the dissolved PUA observed between the two years is only due to differences in lysis rates.

The survey of a *S. marinoi* culture gives us the opportunity to get a better picture of the dissolved PUA's dynamic. The diatoms released heptadienal and octadienal into the surrounding seawater during a five day period in the late stationary phase (**Figure 8 A**). Our quantification method is capable of quantifying picomolar PUA-concentrations released into the medium, yet no PUA were detected throughout most of the culture's development. PUA do not accumulate in the medium (Carvalho *et al.*, 2000) and therefore a temporally limited release results in the observed transient maximum of these metabolites. As observed in the Adriatic Sea, the released concentration is not directly correlated to the production potential. The later indeed increased between day 16 and 20, while release of PUA started one day latter. Additionally, the ratio between potential and dissolved PUA changed greatly between the different days of the stationary phase. Values were $< 0.1\%$ until day 20, but this percentage reach 8% at day 23, and 20% at day 24 (**Figure 8 B**). This indicates that the release cannot be seen as a result of the availability of resources but rather as a result of a biosynthetic process which is under the control of other regulative principles.

Even though the lysis rates were not measured, release of PUA in culture cannot be attributed to cell lysis only. Indeed, autolysis and loss of the membrane integrity has been shown to be a late process in the cell death of diatoms, followed within one day by the destruction of the cell (Veldhuis *et al.*, 2001). A massive release of PUA due to autolysis would therefore likely be correlated with a decrease of the living cell density of the culture the same day. However, we have shown that the release of PUA occurs well before the culture enters the declining phase and that therefore autolysis is unlikely to contribute significantly to the release. Autolysis in the declining phase obviously does not lead to a significant accumulation of PUA in the medium even if these metabolites are still detectable (**Figure 8**). The detected dissolved PUA are only 2% of the PUA potential of the cells in the declining phase. The dynamic of PUA in the late declining phase remains unknown because the sampling was not continued after day 30, due to exhaustion of the culture volume.

The short period of PUA release from stationary cultures and the subsequent delayed decline in cell density points toward the possibility that initiation of synchronised death may be the result of PUA signalling. In this context it is interesting to note that the PUA decadienal triggers synchronisation of the diatom *T. weissflogii* in a G1 phase prior to irreversible cell death (Casotti *et al.*, 2005). However, the evolutionary advantages that would allow a selection of synchronised death in phytoplankton remain unclear (Bidle and Falkowski, 2004).

PUA can induce a declining phase

To elucidate the role of the released PUA on the regulation of the growth of diatom cultures, we tested the effect of these potential infochemicals on the *S. marinoi* RCC75 strain we also used for the survey of released PUA. In contrast to many previous studies we tested the effect of PUA at biologically relevant concentrations (i.e., the concentrations and ratios detected in the medium; **Figure 8A**). At this concentration (250 nM heptadienal and/or 62 nM octadienal), the addition of PUA to exponentially or stationary phase cultures had no effect (**Figure 9**). We also observed no synergism of the mixture of PUA compared to the treatments with the single compounds. Cultures did decline, however, in the presence of higher PUA concentrations (250 μ M heptadienal and/or 62 μ M octadienal), which is in agreement with previous studies (Ribalet *et al.*, 2007a). The somewhat delayed effect of octadienal we observed in both exponential and early stationary phase additions (**Figure 9**) could be caused by a lower active concentration due to the lower doses used in the treatments. PUA have been shown to interfere with tubulin polymerisation in sea urchin embryos (Buttino *et al.*, 1999), and therefore actively growing cells would be more susceptible to their effect. This is in agreement with our findings of a faster response in the exponential phase compared to the

stationary (**Figure 9**).

However, since the cultures did not show a response to the naturally occurring PUA concentrations, and since PUA release was restricted to the late stationary phase, I hypothesised that a temporal susceptibility to PUA might play an additional role. To verify the concept of a time-dependent susceptibility, I added PUA mixtures in the late stationary and early declining phase. Upon treatment of late stationary cultures with PUA at biologically relevant concentrations, we observed a period of increased growth resulting in a significantly higher cell density within approximately 10 days, followed by a rapid reduction of cell density (**Figure 10**). In contrast, PUA pre-treated cultures did not respond to a second PUA addition. This could be due to a desensitisation induced by the first treatment, as shown by Vardi *et al.* in experiments where NO production as response to PUA was monitored (Vardi *et al.*, 2006). Declining cultures showed no response to PUA addition (data not shown). At this stage it is not clear if the stimulating effect of PUA addition (**Figure 10**) can be interpreted as a preparation of the cells for the death of the population, neither can it be determined if the release of PUA we found in the culture is a natural signalling event leading to this reaction. However, PUA fulfil three requirements for being infochemicals: i) they are released into the medium and in the natural environment of the plankton cells, ii) they are present for a short period, and iii) they have an effect on cultures in specific stages.

The use of autoinducers to regulate cellular functions is well established for other unicellular organisms. For this type of cell to cell communication in bacteria, the term quorum sensing has been established (Fuqua *et al.*, 1994; Williams *et al.*, 2007). This type of communication has not yet been fully established for phytoplankton; however the first indications for the existence of an infochemical based stress-surveillance system are reported from the diatom *P. tricornutum* (Vardi *et al.*, 2006). The idea of a functional communication is also supported by comparative genomic analysis of the diatom *T. pseudonana* that revealed putative signalling and regulative components (Montsant *et al.*, 2007).

S. marinoi is known to form resting cells depositing in the sediments, providing inocula for next year's blooms (McQuoid and Hobson, 1996; Lewis *et al.*, 1999; McQuoid, 2002). It is tempting to postulate that an increasing pool of cells, sensing that the conditions for the bloom sustenance are degrading, releases PUA and that this signal, associated with other external conditions, may induce the population to prepare for bloom termination.

PUA have a complex dynamic

The PUA production potential of *S. marinoi* varies over the growth phases and in plankton blooms. It was stable during the early stationary phase, but then more than doubled in a span of 2 days (day

19-20, **Figure 8 B**). Previous studies have already revealed that in nitrogen or phosphate depletion, the PUA production potential increases (**Table 1**). We confirmed a response to environmental conditions in our nutrient depletion experiment (**Figure 11**). Modification of the production potential can result from a change of available substrates or from changes in the relevant enzymatic activities. Under Si- and P-limitation, an increase in heptadienal levels was observed concomitantly with a higher amount of its precursor EPA. A substrate-to-product ratio close to 1 indicates that the EPA pool was fully accessible to lipase and lipoxygenase activities, which, in turn, indicates that the amount of substrate was the limiting factor for the production of heptadienal. In contrast, only a small fraction of the HDTETRA pool was transformed into octatrienal in all three nutrient-limited growth conditions, suggesting that lipase and lipoxygenase activities were insufficient and/or this fatty acid might be only partially available for PUA biosynthesis.

Under N-limitation, the comparably low levels of all three PUA produced (0.14 fmol total PUA cell⁻¹) and an excess in their precursor PUFA (**Figure 11**) suggests a limitation in enzymatic activities involved in the biosynthesis of PUA. Since N represents a limiting factor for the synthesis of polypeptides and, therefore, for enzymatic activity in general, an N-limited adapted culture probably down regulates all non-essential enzyme expression. In a previous experiment, the cells were shown to have a slightly lower production of PUA in N-limited condition during exponential phase (Ribalet *et al.*, 2007b), and significantly higher in stationary phase (**Table 1**).

Total PUA level increased 3 fold in P-limited cells with respect to nutrient replete control cultures and reached 7.53 fmol cell⁻¹ (**Figure 11**) which is in strong agreement with production of PUA of *S. marinoi* following P-starvation in batch cultures (7.49 fmol cell⁻¹) (Ribalet *et al.*, 2007b). The similar production of PUA in P-limited and P-starved cells suggests that the physiology of cells in batch cultures reaching the stationary phase due to P-depletion approaches that of cells growing in P-limited continuous cultures. In Si-limited cells, the production of PUA increased by 10 times with respect to Si-replete controls (**Figure 11**), while their silica content decreased (data not shown, see (Ribalet *et al.*, 2009)). Therefore Si-limitation would induce a reduction in the mechanical defence against grazers (Hamm *et al.*, 2003), due to a reduction in siliceous cell wall, but would be compensated by an enhancement of its potential chemical defence capacity. This suggests that *S. marinoi* may be able to shift from mechanical to chemical defence depending on nutrient availability, resulting in an optimised defense strategy. Only when Si is limiting, and if N is present in high enough levels, the cells invest energy to produce the required enzymes for the production of PUA. The high level of PUA produced under Si-limitation (27.5 fmol cell⁻¹, **Figure 11**) may directly affect the viability of the grazer, as observed when *Temora stylifera* Dana 1849 was fed liposomes enriched with high PUA levels (Buttino *et al.*, 2008).

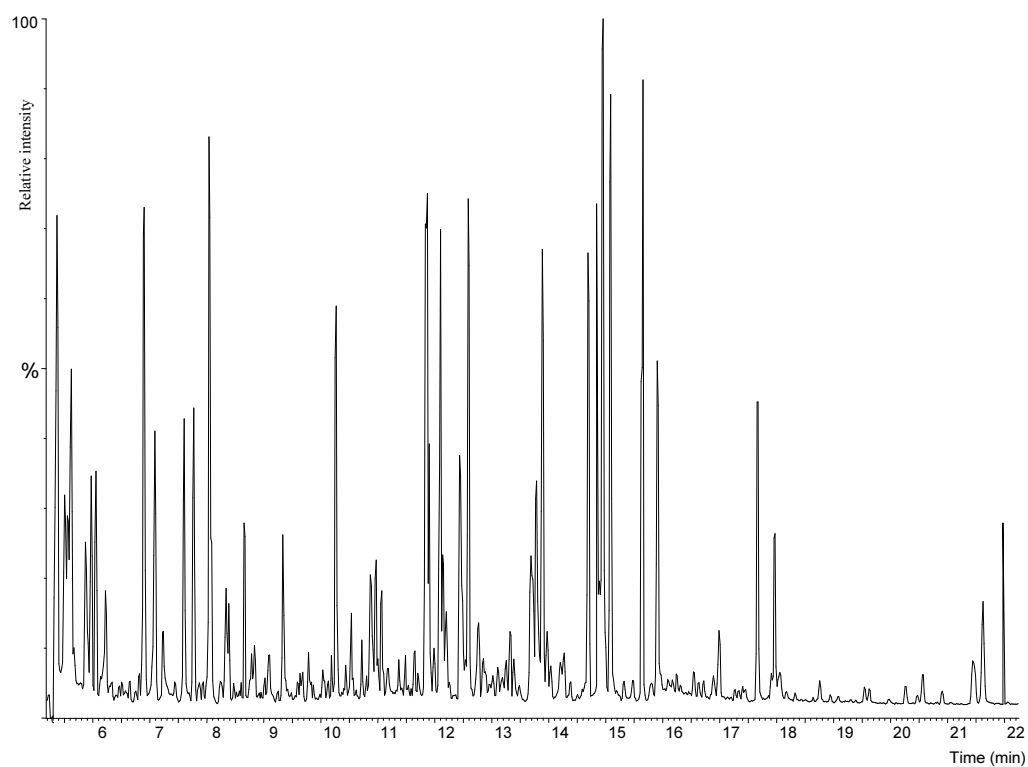
Altogether, these laboratory experiments support the view that the production of PUA is a highly dynamic process. It depends not only on growth phase, like previously shown (**Table 1**, (Ribalet *et al.*, 2007b)), but also on the nutrient levels (**Figure 11**). The response to nutrient stresses is also variable among nutrients, denoting complex interactions rather than general stress reaction. In addition, the production of PUA is highly variable among strains of the same *S. marinoi* species (**Table 1**, comparison between strain RCC 75 in **Figure 8** and strain CCMP 2092 in **Figure 11**).

Although the release of PUA in the surrounding water is not directly correlated to the production potential, and instead depends on the phases and other conditions in which the cells are. All these parameters could explain the differences observed between the field samples in 2006 and 2008. The percentage of dissolved PUA compared to production potential could suggest that the bloom in 2006 was older, close to decline, while in 2008 the bloom was younger. In addition to observation at different stations, the day-night survey in 2006 confirmed that there is no direct dependency of the released PUA and the production potential (**Figure 7**). Whether or not the increase in dissolved PUA in the night is a light regulated process is not yet clear, and further experiments should be done to examine the day-night dynamic of PUA. The huge difference in production potential between 2006 and 2008 could be explained by nutrient effects. The 2008 potentials (22 and 13 fmol heptadienal and octadienal cell⁻¹, normalised to *S. marinoi* cells only) is similar to the high potential found in Si-limited condition (**Figure 11**) while the 2006 values are closer to nutrient replete conditions. This would however be a contradiction with the idea that the bloom in 2008 is younger than the bloom in 2006, unless the nutrients inlet dynamics were very different between the years. Unfortunately, nutrient data are not available for the cruise samples. The blooms could also be dominated by different strains having very different PUA production potentials.

The 2008 cruise also revealed that the dynamic of PUA in the plankton is made more complex by actors in the plankton community other than diatoms. A substantial amount of the potential in 2008 could be contributed by another non-diatom class, potentially Cryptophytes. However, to our knowledge, no production of PUA has been reported for this class. Fractionation also revealed that heptadienal is produced by the picoplankton. This production potential becomes dominant in some location and at higher depth (**Figure 6**). The larger size fraction also seems to have an increase potential at moderate depth when compared to the surface, perhaps as a result of stress.

The production of PUA and release dynamic in nature appears extremely complex. Several actors and numerous parameters modulate the presence and the production potential of PUA. Further experiments are therefore indispensable to better understand their dynamic and to determine their exact role, particularly due to their potency as infochemicals.

2.2 Development of a metabolomic method for diatoms



GC-MS chromatogram of a metabolomic sample

In order to apply the previously developed metabolomics and metabolic profiling concepts to diatoms, a general work plan to acquire and produce data was designed. Starting from techniques common to most metabolic studies, I optimised the crucial points. This strategy is presented in a flowchart in **Figure 12**. The extraction of the cells can be designed to lead to either a wide set of metabolites, the polarity range of which depends on the extraction solvent used, or to a more restricted set of special metabolites. I chose to develop a method for metabolic profiling optimised for diatom cells (*cf.* below). The PUA potential production and analysis of the total fatty acids were also included in the work plan, to obtain a more complete picture of the cell metabolism. The total fatty acid content (lipids and free fatty acids) is indeed also an important parameter for the physiological status of the cell.

The general method was optimised to extract as many different compounds as possible in a reasonable amount of steps.

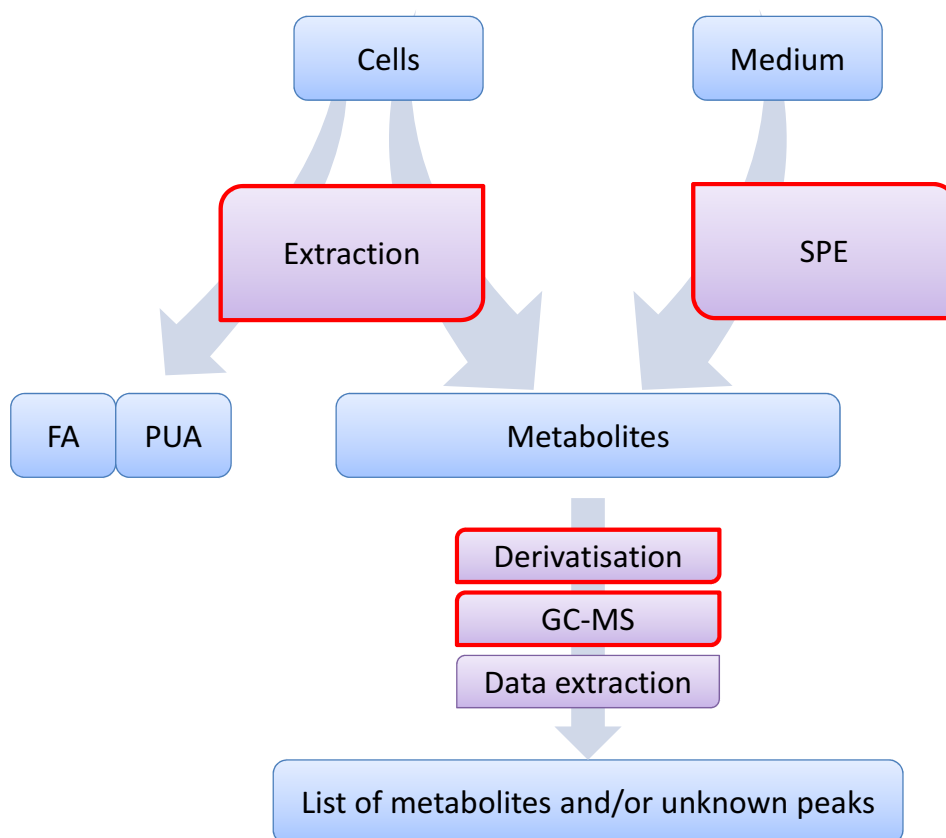


Figure 12: Diatom metabolomics work plan. The steps highlighted in red are the one that have been subject to development and optimisation. FA, total fatty acids. SPE, solid phase extraction.

Cell metabolite extraction optimisation

As mentioned in the introduction, the extraction solution has to be adapted to any new organism

type introduced in metabolomic studies. Testing different mixes of solvents allowed the determination of a better extraction than with only pure methanol (Jiye *et al.*, 2005). I followed this approach to test different extraction solvents. The 11 mixes tested contained different relative amounts of methanol, ethanol, acetone, acetonitrile and chloroform (**Table 2**). Mix 1 consists only of methanol, mixes 2 to 5 consist of methanol and another solvent, mixes 6 to 8 consist of methanol and two other solvents, mix 9 of methanol and three solvents, and mixes 10 and 11 consist of different ratios of all five solvents.

Table 2: Relative solvent composition of the 11 different extraction mixes.

Mix n°	Methanol	Ethanol	Acetone	Acetonitrile	Chloroform
1	1.0	0	0	0	0
2	0.8	0	0	0	0.2
3	0.2	0	0.8	0	0
4	0.2	0	0	0.8	0
5	0.2	0.8	0	0	0
6	0.2	0	0.6	0	0.2
7	0.2	0	0	0.6	0.2
8	0.2	0.6	0	0	0.2
9	0.43	0.23	0	0.23	0.1
10	0.2	0.23	0.23	0.23	0.1
11	0.375	0.175	0.175	0.175	0.1

Three parameters are useful to evaluate the efficiency and reproducibility of a solvent mix: the number of peaks that can be extracted from the GC-MS chromatogram, the relative standard deviation of the intensity of these peaks in replicate extraction and the relative recovery of different compounds of different polarity (Gullberg *et al.*, 2004; Jiye *et al.*, 2005).

The number of peaks detected after the extractions with the eleven mixes of subsamples of a *S. marinoi* cell sample was assessed. The reproducibility of these extractions was also determined as the median of the relative standard deviation of the quantification of the selected peaks. Results are shown in **Figure 13**. All the mixes resulted in a comparable number of peaks (from 370 for mix 4 to 380 for mix 1). In contrast, the reproducibility offered by the different mixes was extremely variable. Eight of the mixes resulted in a median of the relative standard deviation higher than 30% (mix 2, 3, 5, 6, 7, 9, 10 and 11). Mix 4 had a reasonable reproducibility with a 14% median relative standard deviation, but this was also the mix with the lowest number of peaks. Finally, mix 1 and 8 had good reproducibility with 9.2 and 9.3% median relative standard deviations respectively.

From the chromatograms, I choose 9 sugars, 9 amino acids, 6 fatty acids and 3 sterols that were present in all extractions and easily identifiable. After the quantification of their peak area, normalisation by the internal standard (ribitol), the relative recovery is reported in **Figure 14**. Several mixes showed a poor recovery (< 50%) of the amino acids (mix 3, 4, 6, 7, 9 and 10). These

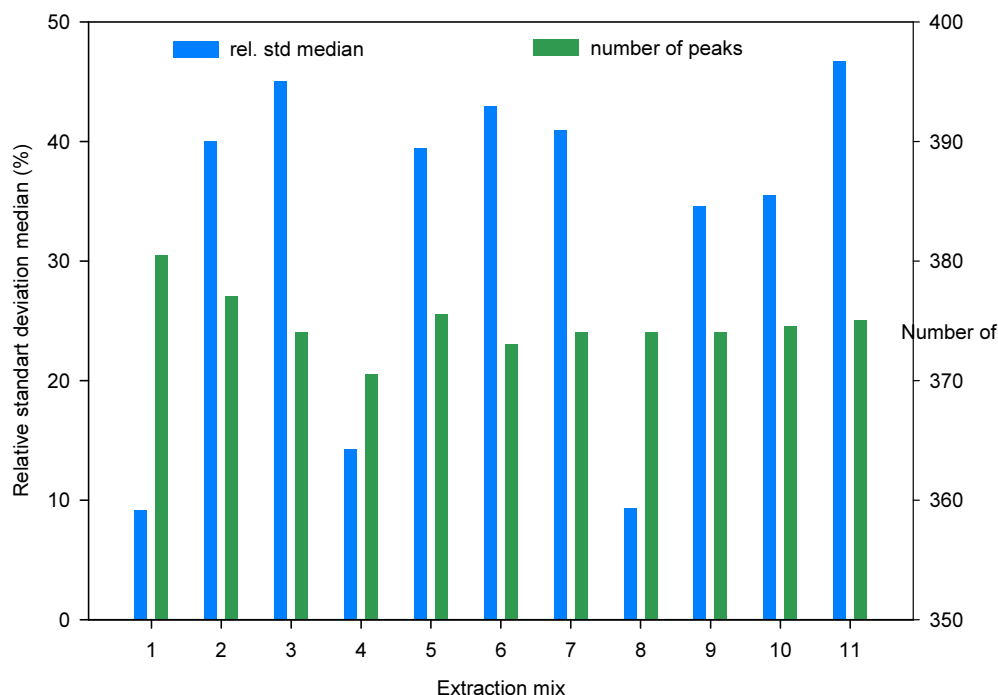


Figure 13: Reproducibility of the extraction capacity of different solvent mixes evaluated by the median of the relative standard deviation of peak intensities, and number of peaks extracted from the chromatograms with the AMDIS software for each solvent mixes.

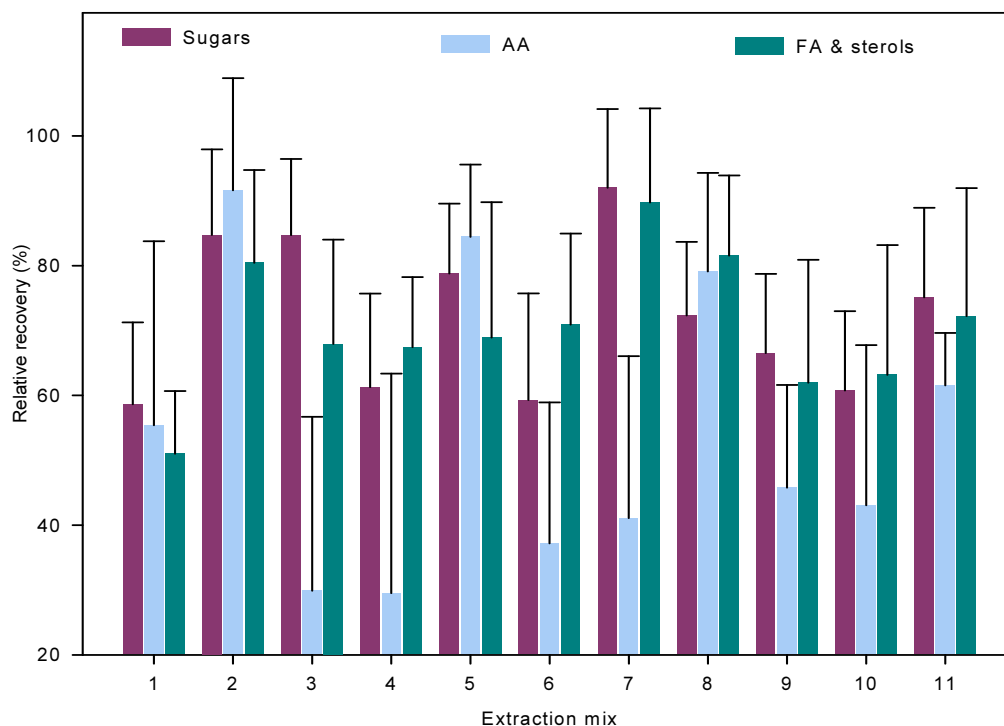


Figure 14: Relative recovery of 9 sugars, 9 amino acids (AA), 6 fatty acids (FA) and 3 sterols when cells were extracted with the different solvent mixes. Relative recoveries were determined by expressing the recovery of each compound as a percentage of the highest intensity observed for each compound. These relative recoveries were then averaged for every class of compounds and displayed with standard deviation.

are the mixes containing the lowest proportion of alcohol (methanol and/or ethanol). The two mixes that had the best reproducibility (**Figure 13**), mix 1 and 8, are also the two only ones that showed less than 10% differences between the average relative recovery of the three groups of compounds, but mix 8 had higher recovery than the mix 1 (78% and 55% in average, respectively) (**Figure 14**). Finally mix 2 had also a relatively balanced recovery (11% difference between the groups) and showed the highest overall recovery (85% in average).

In summary, mix 8 had the maximum number of peaks, mixes 8 and 9 showed the best reproducibility, and mixes 2 and 8 had high, balanced recovery rates. I therefore choose mix 8 (methanol:ethanol:chloroform in a ratio of 2:6:2), as a good compromise.

Extraction volume optimisation

The last parameter tested for the extraction was the ratio between extraction volume and number of cells. The hypothesis is that if the cell density is too high, the solvent proportion would be disturbed and/or some compounds would not be optimally recovered. Therefore, $57 \cdot 10^6$ *S. marinoi* cells were extracted with 60, 120, 180 and 300 μL of extraction mix, resulting in 0.94, 0.47, 0.32 and $0.19 \cdot 10^6$ cells per μL of extraction solution respectively. As seen in **Figure 15**, the highest extraction efficiency was achieved with the second lowest cell density tested. Also, the highest density had much lower recovery rate, thereby confirming the danger of extracting cell samples that are too dense. If possible, the preparation of metabolomic samples should be prepared with not more than $0.5 \cdot 10^6$ cells per μL of extraction solvent, and ideally between 0.2 and $0.5 \cdot 10^6$ cells. These results are for *S. marinoi* cells, and of course should be tested on other species, especially if the cell volume differs significantly from that of *S. marinoi* ($\sim 100 \mu\text{m}^3$).

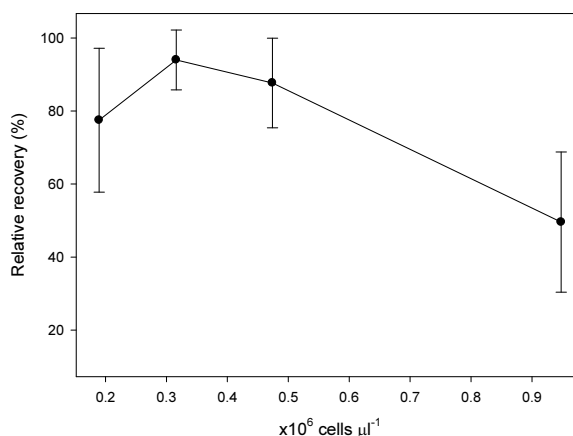


Figure 15: Effects of extraction volume on recovery. The same number of cells was extracted with different volumes of solvent mix. In abscissa, the cell density reached in the extraction volume. Values are average of relative recovery of 14 compounds over the polarity range \pm standard deviation.

Solid phase extraction optimisation

Extracting metabolites of different polarity from seawater is a tricky task. The aqueous matrix, in addition to a high salt content, makes the extraction of polar compounds difficult. We tested different Solid Phase Extraction (SPE) cartridges to compare their recovery capacity. Two of the tested sorbents are based on a polystyrene-divinylbenzene (SDB) polymer: the Bond ElutTM PPL from Varian (a functionalised SDB for polar compounds recovery), and the Chromabond[®] Easy from Macherey-Nagel (a polar modified SDB with a weak anion exchanger). Two other sorbents are based on an octadecyl phase on silica beads (C18): the Sep-Pak C18 from Waters (classic C18 phase), and a Chromabond[®] C18Hydra from Macherey-Nagel (special modification of the C18 phase for polar analytes). Finally, a graphite based sorbent, the Bond ElutTM Carbon from Varian (graphitised carbon for small organic polar compounds), was also tested. The relative recovery of glucose from seawater (acidified and un-acidified) was tested for each cartridge. The Easy sorbent showed the highest relative recovery of all SPE cartridges (**Appendix I**). The C18Hydra and the Bond Elut Carbon also recovered the glucose, but with a lower efficiency. The PPL sorbent only recovered partially glucose when the seawater was previously acidified (**Appendix I**). Based on these considerations and the easy handling, the Easy sorbent was then chosen for our metabolomic studies of the culture media and seawater.

Derivatisation optimisation

Methoxymation is usually the first derivatisation step in metabolomic sample preparation to stabilise labile aldehydes and ketones. The common technique (Lisec *et al.*, 2006) use a one hour methoxymation step at 42°C. However, Gullberg *et al.* (Gullberg *et al.*, 2004) shown that to achieve a better methoxymation, without significant degradation of metabolites, this step should be carried out at 60°C for one hour, followed by 16 hours at room temperature. This latter time could also been shorted at some extend, without big influence on the derivatisation. I therefore chose to apply this method with a final derivatisation time of 10 hours, allowing two series of samples to be prepared per day (with a set derivatising during the day, and one during the night).

The silylation has also an important impact on the recovery and the reproducibility of the analysis (Kanani and Klapa, 2007). In particular amine groups can be incompletely derivatised, leading to higher variation in the data set. I therefore tested the effect of the silylation time on the reproducibility and on the recovery of some sugars, amino acids, fatty acids and sterols from a natural sample (**Figure 16**), representing the high range of concentration that we would be encountered during lab experiments.

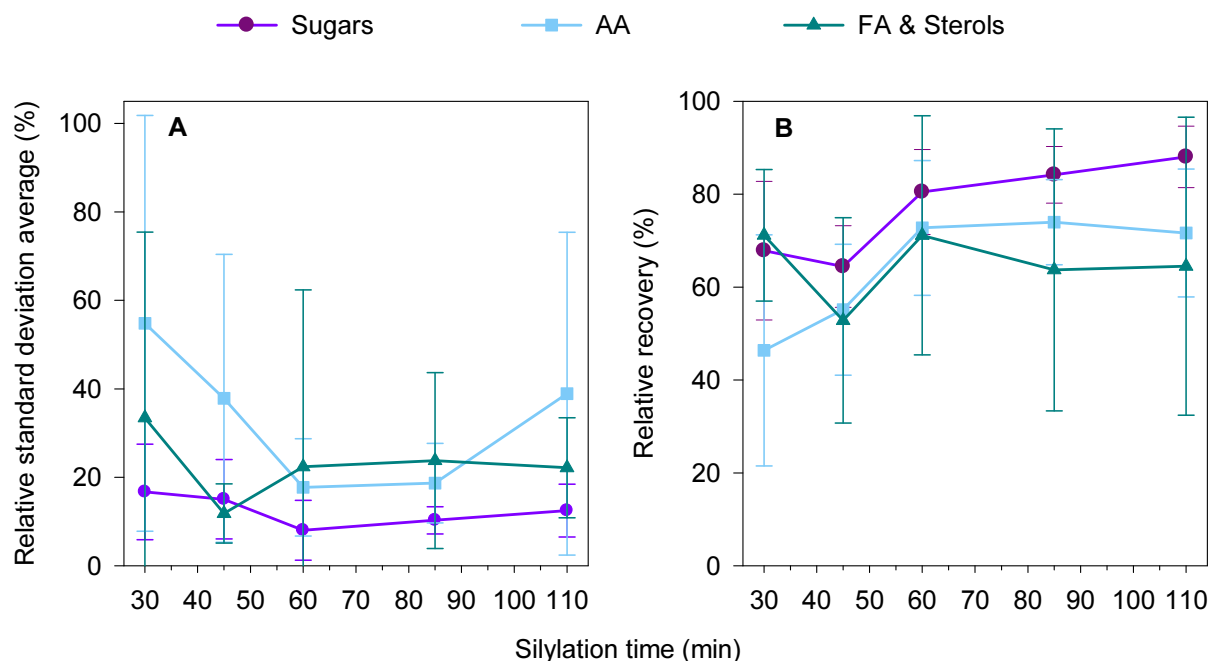


Figure 16: The influence of silylation time (at 40°C) on the recovery and variability of recovery of sugars, amino acids (AA), fatty acids (FA) and sterols. **A**, standard deviation of different classes of compounds and **B**, relative recovery of the different classes of compounds in function of the silylation time. Values are average \pm standard deviation.

Clearly the often employed 30 min for the silylation was not optimal in terms of reproducibility (**Figure 16 A**). The variability, estimated by the relative standard deviation between peak intensities of treatment with replicated silylation times, decreased from 30 min to 60 min. The amino acids showed the highest improvement, with a drop from close to 60% at 30 min to 20% at 60 min. However variability increased again after 85 min, likely due to the variability of reactivity inherent in amine groups. Fatty acids, sterols and sugars showed an improvement between 30 min and 45 min, and were relatively stable from 60 min onwards. The relative recovery follows a similar trend (**Figure 16 B**). The recovery of sugars was similar between the first two time points, improved at 60 min, and reached a plateau. The amino acids have again a pronounced improvement over the first time points to reach a plateau from 60 min onwards. Fatty acids and sterols are less influenced by derivatisation time, and except an unexplained drop at 45 min, are relatively stable from 30 min onwards.

From these results, it is clear that the silylation should be carried out for 60 min. Using this derivatisation period (at 40°C), a good recovery with minimal variability is achieved. Of course, when a batch of samples is prepared and derivatised, they cannot be run all after 60 min. However, because derivatisation is nearly complete after 60 minutes, it is unlikely that large changes occur while the samples are stored on the GC autosampler. To avoid eventual effects of storage, I constrained each derivatisation sets to a maximum of 20 samples, and therefore, every sample is analysed in less than 10 hours.

Another option would be to quench the derivatisation reagent. This happens for the methoxymation agent when the silylation solution is added. The amine moiety of methoxyamine is silylated. However such a quenching is not possible for the MSTFA, because it constitutes half of the solvent.

In conclusion, using a derivatisation time of 60 min, the error could be minimised. The variability caused by the time the samples spend on the autosampler at room temperature before injection cannot be reduced, but the effect of this variability on results is minimised by injecting replicates in a random order after the end of the silylation at 40°C.

Gas Chromatography optimisation

A final crucial parameter for the analysis of a sample via GC is the injection. Several parameters can influence the transfer of a liquid sample from the syringe into a gas phase sample in the column; A. Fiehn (Fiehn, 2007) showed that the liner surface status was the most critical parameter for reproducible results. When injecting natural samples with highly complex matrices, each sample will deposit some compounds on the surface of the liner. This results in a surface that becomes active, eventually trapping compounds that would otherwise be volatilised when contacting the hot liner surface. A. Fiehn (Fiehn, 2007) recommends changing the liner between every sample. Because this option is not feasible without a liner-exchanging robot, I tested the effect of multiple injections with the same liner on the recovery of selected compounds (**Figure 17**).

The relative intensity internal of the standard, ribitol, showed a constant decrease with injection number, and was under 50% after 20 injections. The relative intensity of sugars remained relatively constant until injection 15, then started to decrease, going under 50% after injection 20, and finally reaching a plateau after injection 30. The fatty acids and sterols showed the same trend. The amino acids were very variable, but showed a net decrease after 25 injections, and finally reached a plateau at injection 33. From this data it is clear that the activation of the liner surface is a parameter to take into account. Clearly a low number of injections with the same liner should be chosen. Additionally, the normalisation of the data should be carefully considered, to, among other reasons, counteract this decrease in intensity. Although the internal standard, ribitol, decreased at a relatively constant rate over the injection number, the other compounds seemed to follow different trends. It is possible that ribitol, widely used as derivatisation internal standard (e.g. (Lisec *et al.*, 2006)), is not the most suited to take the liner problem into account. When normalised by ribitol (**Figure 18**), the average intensities of the metabolites increased during the first 10 injections, were stable until the 25th injection and then became extremely variable. In contrast, if the intensity of the peaks are normalised by the sum of all areas considered (“sum normalisation”), the intensity of the peaks

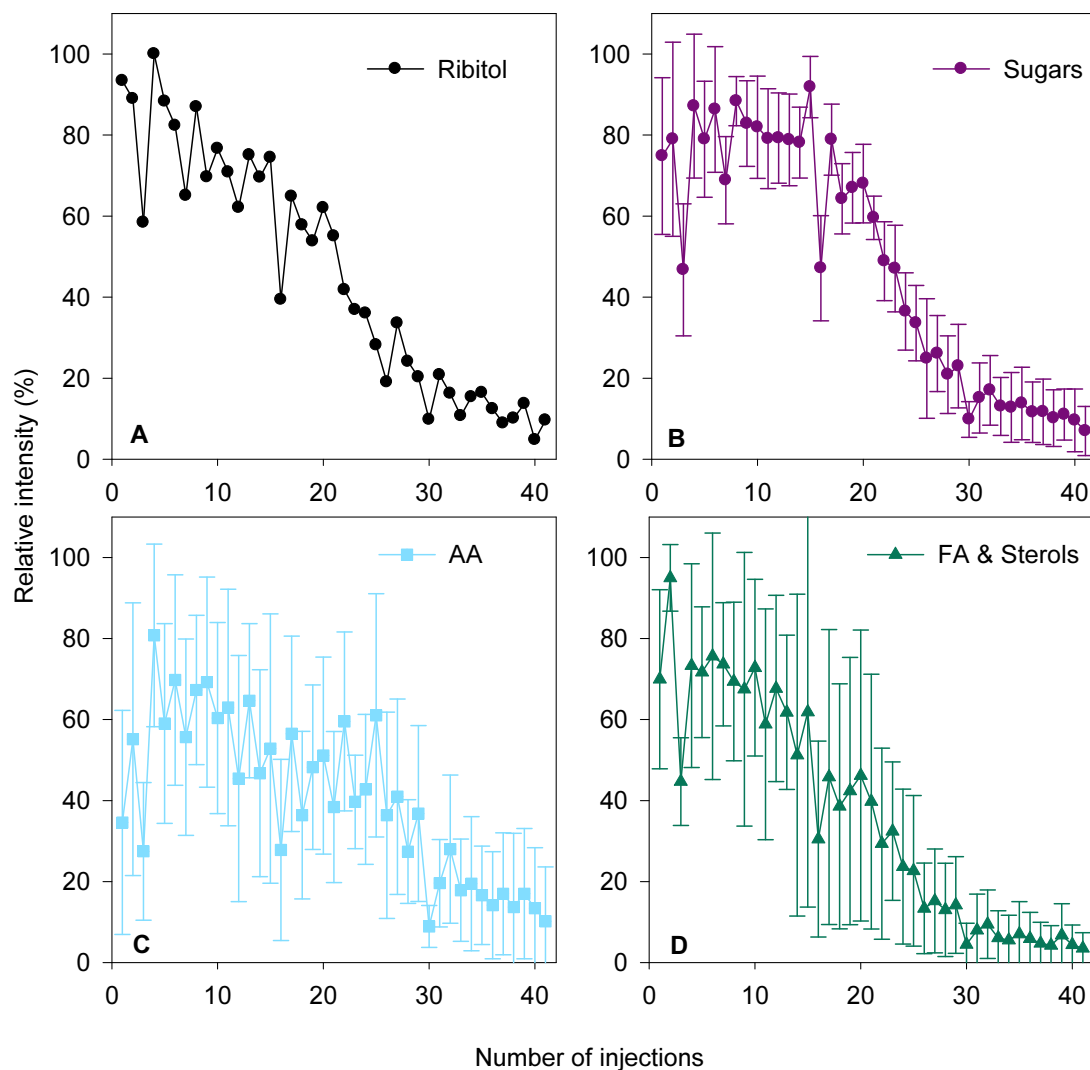


Figure 17 Signal intensity in repeated injections with the same liner. **A**, Internal standard ribitol relative intensity (peak area divided by the maximum area). **B**, **C** & **D**, relative intensity of nine: sugars, nine amino acids (AA), six fatty acids (FA) and 3 sterols, not normalised by the internal standard (ribitol). Values are averages of the relative peak areas (relative to the highest peak area of each compound) of the different compound classes \pm standard deviation.

remained stable for the 23 first injections, before decreasing (**Figure 18**). The sum normalisation, however, implies that we can assume that the total intensity of the metabolites from one cell is constant among the samples. When the samples originate from a monospecific culture, this assumption makes sense, since, even if the content of cell metabolites changes significantly, the normalised values represent a relative composition. When the samples originate from complex mixtures of species, then a more suitable normalisation should be considered. Even if the ribitol normalisation results in an error due to the liner effect, such a normalisation still makes more sense in particular in cases when the constant total intensity assumption cannot be accepted.

Irrespective of the chosen normalisation, I set a limit of 20 injections for my analysis before liner exchange. This compromise allowed running batches of 20 samples, which corresponded to

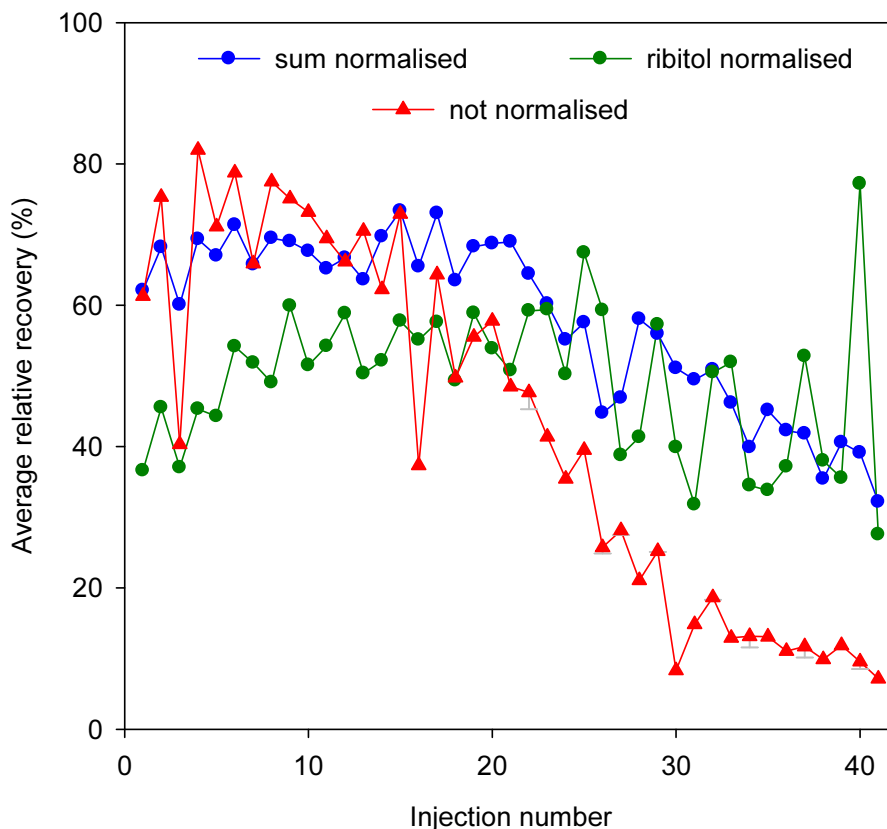


Figure 18: Normalization efficiency in repeated injections. In red, the average relative recovery of all compounds from Figure 17. In blue, average of the recovery from the same data, but normalized by the peak sum. In green, average of the recovery from the same data, but normalized by the internal standard ribitol. Values are the average of 27 compounds. Standard deviations are not shown in order to simplify the graph.

approximately 10 hours GC time between every liner change. In accord with the derivatisation times mentioned above, the final setting of the derivatisation/GC-MS-analysis work plan allows the preparation and analysis of 40 samples per day, in two batches of 20.

A SOP for diatom metabolomics

As a result of this optimisation process, I issued a Standard Operating Procedure (SOP) for preparation and analysis of diatom metabolomic samples (**Appendix XIII**).

2.3 Metabolic survey of a *S. marinoi* culture



S. marinoi 25 L culture

2.3.1 Experiment design

Deciphering the complex interactions of diatoms and their metabolic responses in their natural environment first requires a better understanding of diatoms in simpler and a more controlled environment. Dense monocultures provide two advantages. First, high cell densities mean that metabolites are more concentrated. Second, only one diatom species is present and so the changes in metabolites must be caused by physiological changes in the cells, rather than interactions with other phytoplankters.

In this context, I designed an experiment allowing a metabolic survey of *S. marinoi* in culture. The aim of the study was to evaluate the metabolomic method previously developed (described in chapter 2.2) and the variation in intracellular and extracellular metabolites over different growth phases as well as at different times of the day-night cycle. Metadata-gathering in metabolomic experiments is very important, therefore as many general culture parameters as possible were also monitored. Samples were taken from 5 replicated *S. marinoi* strain G4 cultures, as well as one blank (**Figure 19**). The strain G4, isolated from the Raunefjord in Norway, was chosen because it had also been used for the mesocosms experiments (*cf.* 2.4). This strain, though it has been isolated and purified, is not axenic. The metadata gathered daily were chlorophyll a fluorescence, as an estimate of cell density, photosystem II (PSII) efficiency, as an estimate of cell physiological state, concentration of nutrients (nitrate, phosphate, nitrite and silicate), as well as pH. Cell density of one culture was also monitored daily by counting with a microscope. Every second day, I estimated the bacterial density by plating. The lag time necessary for the diatom cells to re enter a growth phase was also assessed at some days by transferring always the same amount of cells into fresh culture medium. This parameter is assumed to be dependent on the cells physiological state. Temperature and light intensity were also monitored. For the coverage of compound classes in metabolomic profiling, the full experimental design presented in **Figure 12** was followed. Potential PUA and total fatty acid determination was thus performed in addition to the metabolomic profiling. Previous experiments monitored the metabolism on every day over the whole cultures (Barofsky *et al.*, 2009), but only at one sampling time per day. To combine the analysis of the interphasic and diurnal-nocturnal variation, I chose to sample at 8 different times of the day and night, but then only over 24 hours in each phase (**Figure 19** bottom right). At each of these sampling times the potential PUA, the total fatty acids and the metabolic profile were determined for the cells. Metabolic profiling was also conducted on the extracellular compounds present in the culturing media.

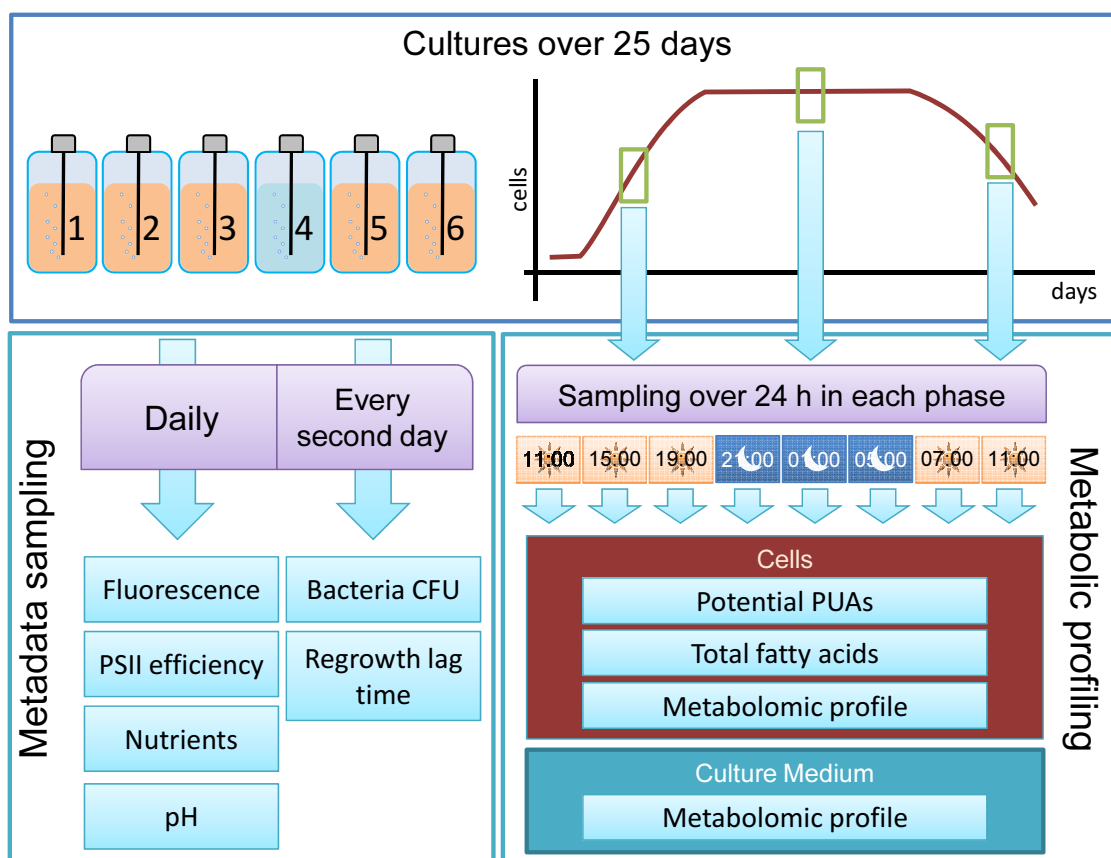


Figure 19: Experiment design for monitoring a *S. marinoi* G4 culture with extended metadata collection and metabolic profiling for day and night in exponential, stationary and declining phase. **Upper left**, 5 large cultures are used as well as 1 blank in 25 L aerated polycarbonate bottles. **Bottom left**, metadata collected every day or every second day. PSII, photosystem II. CFU, colony forming unit. **Bottom right**, Metabolic profiling of cells and medium is made at 8 different time points over 24 hours, once in every growth phase.

2.3.2 Overview of the cultures

Cell density and physiological state

Guided by fluorescence data (**Appendix III**) the exponential phase sampling was conducted at day 6-7, the stationary phase sampling at day 14-15 and the declining phase sampling at day 23-24. For this later phase, the remaining culture volume only allowed 7 sampling points; therefore the last 11:00 sample was not taken. The cell count of culture 1 (**Appendix II**) shows that the exponential phase occurred during day 2-8, followed by the stationary phase until day 19, when the cell density started to decline. The fluorescence increased until day 14-15, followed by a slow decrease (**Appendix III**). Cell density increased significantly between the first (11:00, day 6) and the last sampling (11:00, day 7) point in the exponential phase (paired t-test, $p = 0.013$). I detected no significant changes in the stationary phase sampling (paired t-test between 11:00 day 14 and 10:00 day 15, $p = 0.744$) and a significant decrease in the declining phase (paired t-test between 11:00 day

23 and 07:00 day 24, $p = 0.04$). The same trends were observed in the fluorescence measurements. The cell density did not show clear trends between day and night shifts, in contrast to fluorescence measures which decreased during the day to night transition (6%, 18% and 25% in exponential, stationary and declining phase respectively) compensated by an increase during the night-day transition (7%, 16% and 40% in exponential, stationary and declining phase respectively). The cell volume decreased significantly during the exponential phase (paired t-test between first and last sampling, $p = 0.027$) to reach $83 \mu\text{m}^3$ in average, but stayed stable in stationary and declining phase (paired t-test, $p = 0.53$ and $p = 0.93$ respectively). Finally, based on these parameters, culture 1 and 2 tended to have higher cell density than culture 3, 5 and 6; however, they exhibited the same overall behaviour and growth phases were well synchronised.

The photosystem II efficiency (**Appendix IV**) remained constant during the exponential phase, transiently decreased at day 9, recovered to previous level and stayed constant until day 17 when it started to decrease (repeated measures ANOVA, $p < 0.001$, followed by Bonferonni pairwise multiple comparison revealing significant difference between days 1-7 and days 19-23, between days 1-7 and day 9 as well as between days 10-15 and day 23). When considering the metabolomic sampling times, no significant changes appeared between the beginning and the end of the exponential sampling, but the time point at 05:00 was significantly lower than at 19:00, 01:00 and 11:00 (repeated measures ANOVA, $p = 0.001$, followed by Bonferonni pairwise multiple comparison). During the stationary metabolic sampling, no significant difference in PSII efficiency were detected (repeated measures ANOVA, $p = 0.205$), while during the declining sampling, a significant increase occurred (repeated measures ANOVA, $p < 0.001$, followed by Bonferonni pairwise multiple comparison) revealing significant differences between the last three time points (second day at 01:00, 05:00, 07:00) and the first two (first day at 11:00, 15:00).

The last physiological parameter monitored for *S. marinoi* was the lag time necessary for the cells to re-enter exponential phase (**Appendix V**). When *S. marinoi* cells were transferred into fresh culture medium from exponential phase, the cells started doubling almost the day after transfer. This lag time increased in stationary phase to ~ 4 days. Finally, from day 17 on, the cells required 5 days to restart growing. Also *S. marinoi* cells transferred from declining phase continued to decline for the first 1-2 day, before stabilising and finally restarting growth (data not shown).

Bacterial community

The bacterial abundance reached a plateau after day 5. Bacteria were also present in the blank, indicating either a cross contamination from the other bottles, a possible contamination during the filling of the bottles or an ineffective sterilisation of the equipment. However, the bacteria in the

blank stayed at densities two orders of magnitude lower than in the cultures (**Appendix VI A**). In the *S. marinoi* G4 cultures, the lowest bacterial density was measured in culture 2, which also had the highest diatom density. A basic sorting of the bacteria, based on colony colour and shape, revealed 4 obvious phenotypes. During the first half of the experiment, all four phenotypes proliferated similarly, but after day 13, phenotype II, III and IV were not detected anymore, leaving the cultivable bacterial community dominated by phenotype I (**Appendix VI B**).

Abiotic conditions

The pH in the cultures increased from 7.9 on day 1 to a peak of more than 8.4 on day 11. It then decreased to reach a plateau of 8.1-8.2 at day 18. The pH in the control culture increased slowly to reach a similar value to the diatom cultures at the end of the experiment (**Appendix VII**).

Nitrate concentration decreased rapidly until day 6-7, then more slowly until it was undetectable on day 15 (**Appendix VIII**). Phosphate seems to be depleted very quickly, with concentration near zero on day 6. However, the control culture had an extremely variable phosphate concentration, raising doubts about the reliability of the method used to detect phosphate. Nitrite was released by *S. marinoi* during the first 9-10 days of culture, before being taken up again. It was depleted by day 15. Finally, silicate was totally consumed during the first 8 days of this experiment. The concentration of this nutrient remained near to zero until day 15, and then increased again to reach ~ 2/3 of the initial concentration by day 20.

2.3.3 Polyunsaturated aldehydes and fatty acids

The G4 strain of *S. marinoi* used for this experiment produced heptadienal, octadienal and octatrienal. Heptadienal production potential was on average 0.11, 0.12 and 0.06 fmol per cell in exponential, stationary and declining phase respectively (**Figure 20**). Exponential and stationary phase PUA contents were similar and significantly higher than during the declining phase (one way ANOVA on ranks, $p = 0.002$, followed by Dunn comparison). When considering the individual sampling points, the concentration of heptadienal in the last sampling point of the declining phase proved to be the only significantly lower heptadienal concentration in comparison to any other point throughout all sampling (repeated measures ANOVA on ranks, $p = 0.033$, followed by SDK comparison). The octadienal production was always higher than heptadienal, with average potential of 0.29, 0.96 and 0.76 fmol per cell in exponential, stationary and declining phase respectively. The average octadienal production potential in exponential phase was significantly lower than in stationary or declining phase (one way ANOVA on ranks, $p < 0.001$,

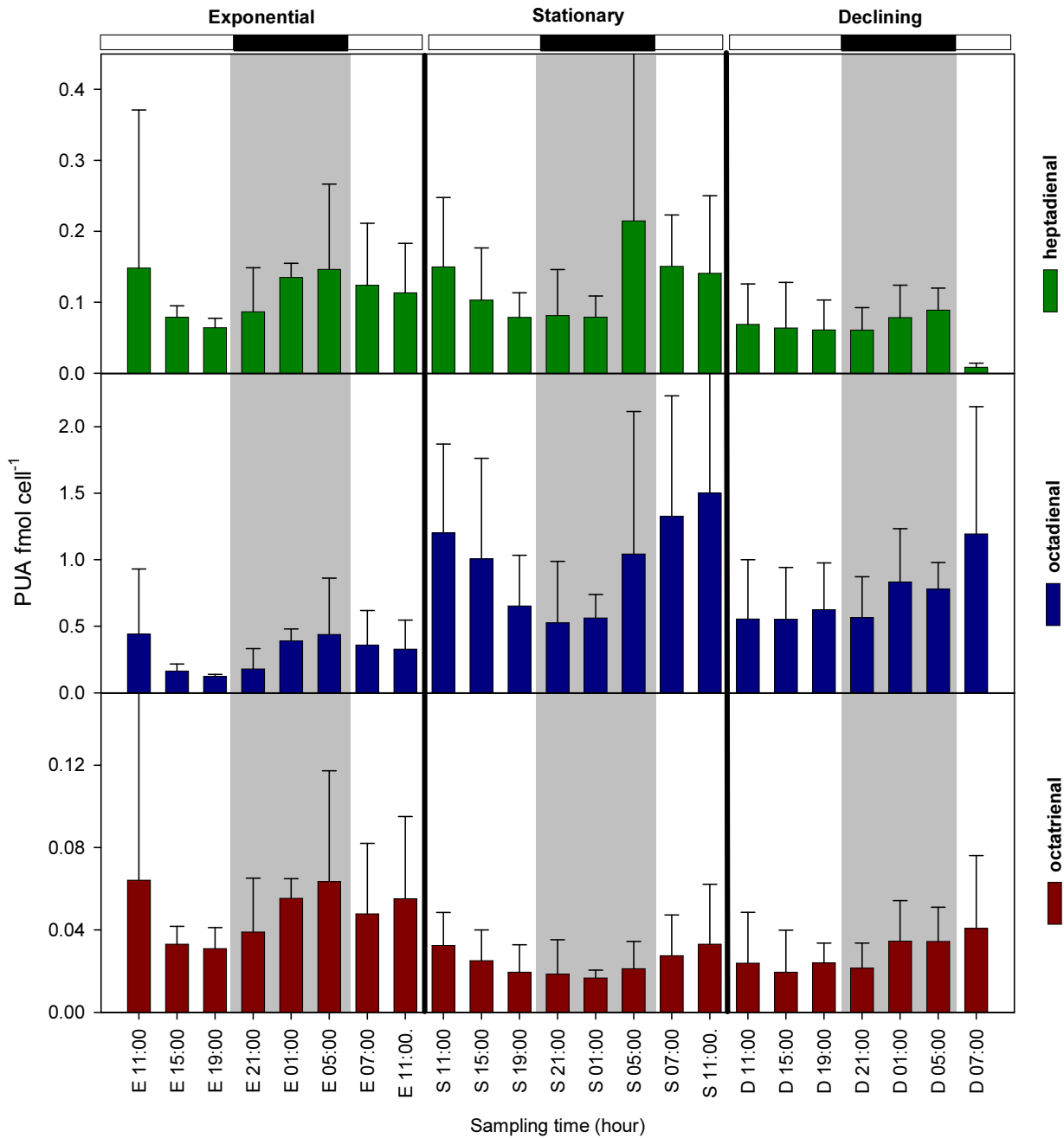


Figure 20: Polyunsaturated aldehydes production potential in *S. marinoi* G4, in exponential, stationary and declining phase, at different time of the day. The white and black boxes on the top represent day and night respectively. Values are average of the five cultures \pm standard deviation.

followed by Dunn comparison). However, if all sampling points were considered, only the potential of octadienal production on sampling times 15:00, 19:00 and 21:00 of the exponential phase was significantly lower than at any other sampling points (repeated measures ANOVA on ranks, $p < 0.001$, followed by SNK comparison). Octatrienal potential production reached on average 0.044, 0.024 and 0.029 fmol per cell in exponential, stationary and declining phase respectively. The exponential potential average was significantly higher than the averages of the

other phases (one way ANOVA on ranks, $p < 0.001$, followed by Dunn comparison). When testing all sampling points separately, no octadienal production potential was identified as significantly different from the others (repeated measures ANOVA on ranks, $p = 0.06$). The ratio between these three PUA changed between growth phases, with 1:2.7:0.4, 1:7.9:0.2 and 1:27.5:0.8 for heptadienal:octadienal:octatrienal in exponential, stationary and declining phase, respectively.

The total saturated fatty acid content (**Figure 21**, upper) was different among the time points (repeated measures ANOVA on ranks, $p = 0.001$), however the SNK post-hoc tests failed to reveal any significant differences between individual times points. A one way ANOVA on ranks on the phases supports nevertheless a significant difference between time points in different phases ($p < 0.001$). The post-hoc Dunn comparison identified that the average saturated fatty acid content in exponential phase was different (lower) from stationary and declining phases. The unsaturated fatty acid contents were more variable. Both monounsaturated fatty acids (MUFA) and polyunsaturated fatty acids (PUFA) decreased from 11:00 to 21:00 in the exponential phase and increased in stationary and declining phases (from 11:00 to 07:00 the next day). All MUFA contents of samples taken after 07:00 (second day) in stationary and in all samples taken in the declining phase were significantly higher than in the exponential phase (repeated measures ANOVA on ranks, $p < 0.001$, followed by SDK comparisons). The PUFA content of the samples taken in declining phase, as well as of the last two samples of the stationary phase, were higher than content in exponential and the remaining stationary points. Also the PUFA content in the first samples (11:00, first day) of the exponential phase was significantly higher than in the last samples of this same phase (repeated measures ANOVA on ranks, $p < 0.001$, followed by SNK comparisons).

Finally, the cell concentration of PUA precursors, eicosapentaenoic acid (EPA) for heptadienal, hexadecatrienoic acid (HDTRI) for octadienal and hexadecatetraenoic acid (HDTETRA) for octatrienal, had different patterns (**Figure 21** lower). As observed for the saturated fatty acids, the repeated measures ANOVA on ranks suggests that a significant difference exists among the HDTETRA contents ($p = 0.023$), but the post-hoc SNK comparison failed to identify differences between individual treatments. The one-way ANOVA on ranks of average content per phases then revealed that the content of HDTETRA was lower in exponential than in stationary and declining phase ($p = 0.009$, followed by Dunn comparison). HDTRI, the most abundant PUFA, followed the same pattern than the total PUFA. The HDTRI content in the samples of the first two sampling points of the exponential phase, of all sampling points after 19:00 in the stationary phase, and of all the declining phase points were significantly higher than in the samples of the 19:00-11:00 time points in exponential phase (repeated measures ANOVA on ranks, $p < 0.001$, followed by SNK comparisons). EPA, the second most abundant PUFA, also follows this pattern, with the exception

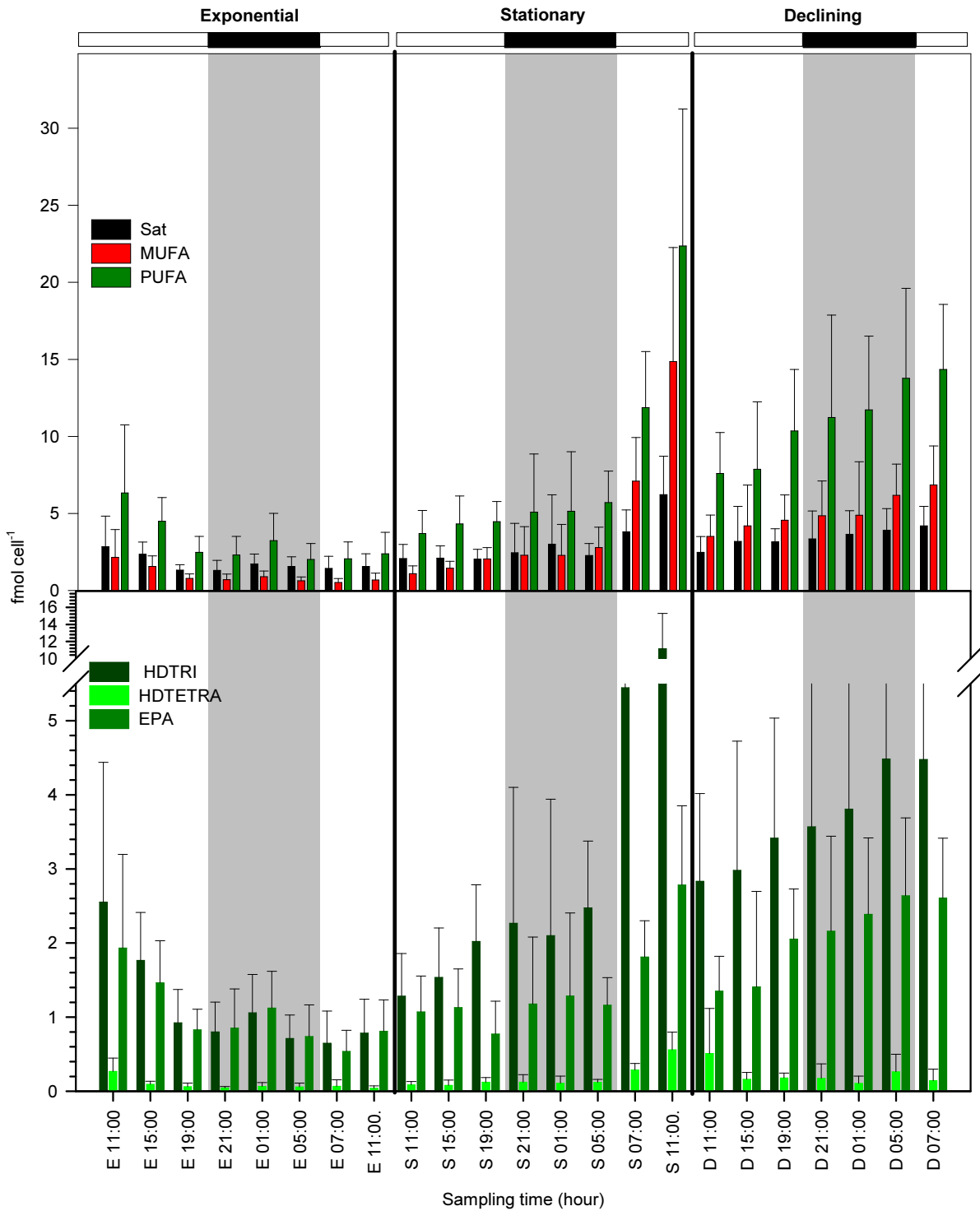


Figure 21: Fatty acid composition of *S. marinoi* G4 cells in exponential, stationary and declining phase at different time of the day. **Upper**, sum of the saturated (Sat), monounsaturated (MUFA) and polyunsaturated (PUFA) fatty acids. **Lower**, details of hexadecatrienoic acid (HDTRI), hexadecatetraenoic acid (HDETETRA) and eicosapentaenoic acid (EPA), the precursors of PUA. Values are averages of the 5 cultures \pm standard deviation. The white and black boxes on the top represent day and night respectively.

that the EPA content in the first two samples of the declining phase were not significantly higher than the samples of the last exponential phase sample (repeated measures ANOVA on ranks, $p <$

0.001, followed by SNK comparisons identifying the same differences than for HDTRI except for the samples of the first time points in declining phase).

The amount of PUA precursors was always higher than the amount of potential PUA produced and the amount of heptadienal and octatrienal was not correlated with the amount of their precursor fatty acids (Pearson correlation test, correlation coefficient = 0.09 and 0.06 respectively, with associated p-values of 0.332 and 0.519), whereas the octadienal was significantly correlated with HDTRI (Pearson correlation test, correlation coefficient = 0.419, $p < 0.001$).

2.3.4 Cell metabolites

The analysis of the chromatograms of the cell metabolites with the AMDIS-MET-IDEA softwares revealed a total of 191 quantifiable peaks. By using less restrictive parameters for AMDIS, it was possible to increase this number; however in this case MET-IDEA failed to adequately quantify a significant proportion of peaks and confused different peaks. Therefore, the analysis parameters were adjusted to produce a reasonable compromise allowing taking into account as many peaks as possible without introducing too much noise and missquantification in MET-IDEA. For each phase, most of the chromatograms resulted in a similar number of peaks (190.5 ± 0.8 , 189.3 ± 2.1 and 183.9 ± 4 in exponential, stationary and declining phase respectively). To exclude the low quality chromatograms, I set the minimum threshold for peaks number to 95% of the average. Chromatograms with fewer peaks were excluded from analysis. Among the 115 data sets produced, 11 were discarded (one in exponential, seven in stationary, and three in declining phase). All sampling points had still a minimum of three replicates. The normalisation chosen for this experiment is the peak sum normalisation (*cf.* 2.2). The use of monospecific cultures in this experiment allowed this normalisation without restriction. All the metabolite intensities used in the multivariate analyses therefore represent a relative concentration of the compound in the cells rather than an absolute value of the metabolite. This normalisation also has the advantage of taking into account all variations due to the sample preparation (volume of culture filtered, cell density, cell volume, extraction volume, derivatisation variations) in a one-step normalisation, independent of measure errors of all these parameters (such as manual cell counts or volume determination).

First, a canonical analysis of principal coordinates (CAP) was performed with the growth phases defined as groups (**Table 3**, **Figure 22 A**). The separation of the groups is clear and no samples overlapped between groups. The diagnostic values for this CAP (**Table 3**) confirmed that the two axes are very efficient in separating the groups (high eigenvalues) and that these axes are highly related to differences between the groups (high correlations Δ^2). The crossvalidation results in 0% misclassification, meaning that the groups were extremely distinct in the multivariate space.

Furthermore the permutation test confirmed that the groups had significantly different locations in the multivariate space. Finally, the correlation coefficient of the first axis is significant, meaning that the difference explained by this axis is statistically significant. It is therefore clear that there were significant changes in the cell metabolites through the phases of growth.

In order to decipher which metabolites are important for the separation, one can consider the **Table 3**: Eigenvalues (λ), correlation (Δ^2) and diagnostics statistics of the Interphasic CAP on cell metabolites diagnostics

Constrained canonical axes				Statistics		
1 st axis		2 nd axis		Crossvalidation Misclassification	Permutatest	
λ	Δ^2	λ	Δ^2		Trace stat.	1 st Δ^2
0.97698	0.95449	0.94987	0.90225	0%	p = 0.001	p = 0.001

absolute correlation of each metabolite with the canonical axes, and if significant, display a vector representing the contribution of this particular metabolite to the ordination. This graphical representation allows the determination of metabolites important for the separation of each group formed by the CAP. A vector pointing toward such a group is contributing to the separation of this group, and the length of the vector is directly related to the importance of this contribution. Also, a vector pointing in the opposite direction is also contributing to the separation, meaning that this metabolite's absence or low abundance is important to define the group.

Such vectors for the interphasic CAP are shown on **Figure 22** B-E. All the compounds having a significant correlation with one of the two constrained canonical axes were investigated to identify the metabolite structure. A list of these significant metabolites, with or without identification, is found in the **Appendix IX**, as well as in **Table 4**. Twenty-six metabolites were not identified, and their spectra were added to a mass spectra library that can be used to find these unknown metabolites in other experiments (library available on the appendix CD). The vectors of these unknown metabolites (**Figure 22** B) were separated in 5 groups: the first group (metabolites 21, 30, 31, 33, 62, 65, 99, 131, and 183) had vectors pointing toward the exponential phase group. The average relative intensity of these metabolites (**Table 4**) confirmed that they had a higher concentration in exponential phase, and a similar concentration in declining and stationary phases. A small second group consisted of metabolites 61 and 6, which pointed directly away from the exponential phase group, in between stationary phase and declining phase groups. These metabolites were then low in exponential phase and high in both stationary and declining phases. The third group consisted of 10 metabolites whose vectors pointed to the declining phase group (69, 129, 5, 57, 96, 169, 3, 2, 85, and 145). The stationary phase was defined by the two last groups, one pointing toward this group, (metabolite 91) and one outwards (metabolites 166, 29, and 50).

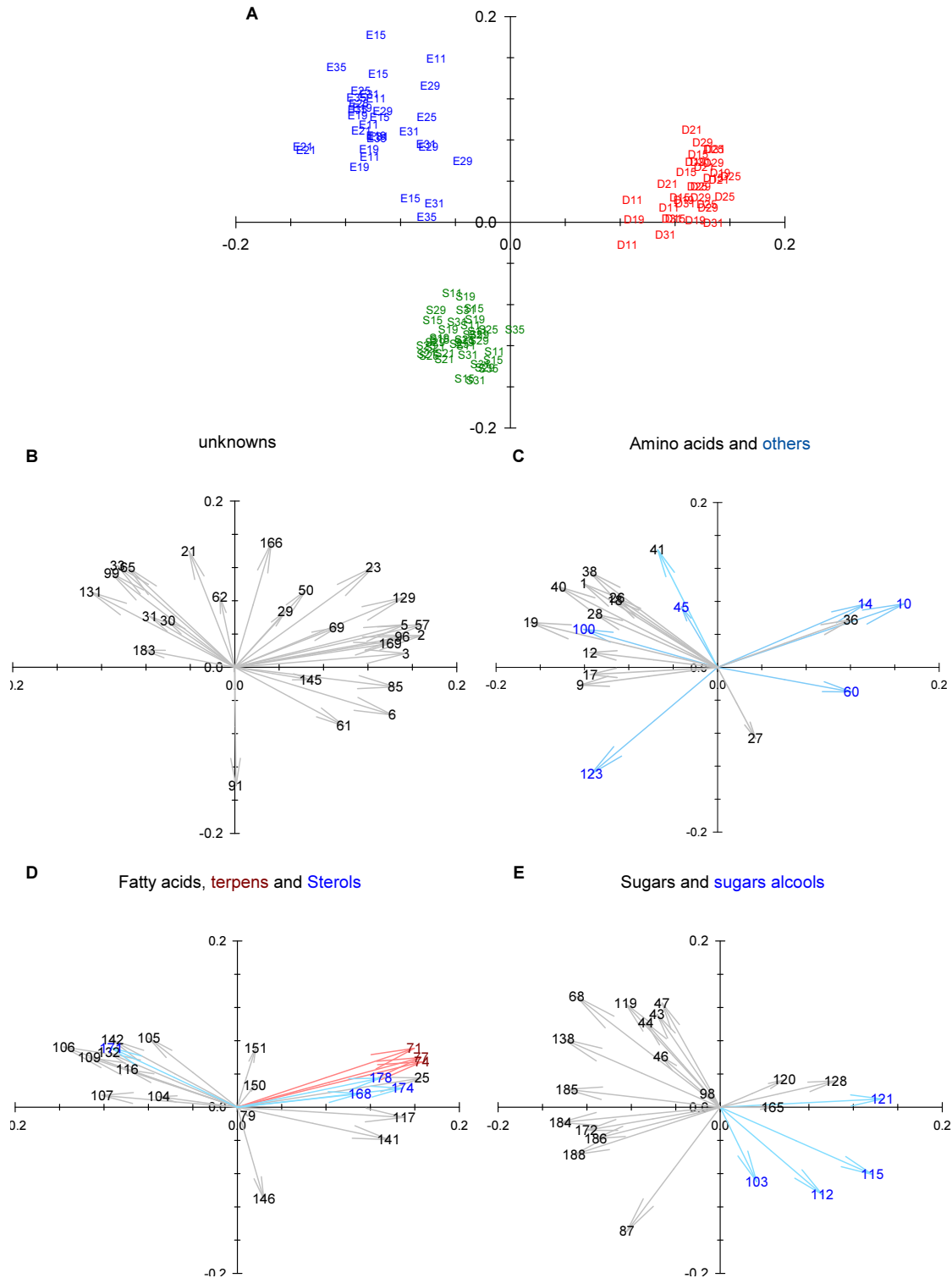


Figure 22: Interphasial separation of *S. marinoi* G4 cell metabolites. **A**, CAP separation of the cell metabolite samples. In blue, exponential samples, in green, stationary samples and in red declining samples. Numbers represent the sampling hour. **B-E**, scaled vectors of the metabolites significant for the separation. The numbers are the metabolites numbered referred in **Table 4**. X-axis is always the first constrained canonical axis and y-axis the second constrained canonical axis. Metabolites 79 and 98 are also shown, as examples of non significant compounds.

A high relative concentration of amino acids was characteristic of the exponential phase (**Figure 22 C & Table 4**). Indeed almost all amino acids identified as important for the CAP separation had a high intensity in exponential phase, while their concentration in the stationary phase was intermediate and very low in the declining phase. The only major exceptions to this pattern were hydroxy-proline (metabolite 36, characteristic for declining phase) and pyroglutamic acid (metabolite 27, higher in declining and stationary phases). Pyroglutamic acid is the product of a transformation of derivatised glutamate and glutamine, occurring when the sample is injected into the hot liner of the GC (Kanani and Klapa, 2007). Phenylalanine, glycine, alanine, n-acetylglutamic acid, threonin, proline and serine (metabolites 40, 19, 1, 38, 28, 18, and 26) had vectors directly pointing to the exponential phase group (**Figure 22 C**) and their intensities in stationary phase were similar to the intensities declining phase (**Table 4**). Two metabolites were identified as isoleucine (metabolites 17 & 12). This is possible because amino acids can have different derivatisation levels. However these metabolites behaved very similarly, having, like valine (metabolite 9), their vectors which pointed in between exponential and stationary CAP groups, opposite of the declining phase group (**Figure 22 C**). Their relative intensities reflected this positioning, being high in both exponential and stationary phase (**Table 4**).

A major group of lipids had vectors pointing to the exponential phase (**Figure 22 D**). This group was only composed of free fatty acids, namely hexadecanoic acid (metabolite 116), hexadecenoic acid (metabolite 105), hexadecadienoic acid (metabolite 109), HDTRI (metabolite 106), EPA (metabolite 142), and linoleic acid (met 132). Although these fatty acids had a higher intensity in the exponential phase, they were also relatively intense in the other phases (**Table 4**). The vector of two fatty acids (metabolites 104 & 107, hexadecenoic acid and an undetermined fatty acid, respectively) pointed between exponential and stationary phases groups. Two monoacylglycerols (metabolites 150 & 151, with a hexadecadienoic acid and a hexadecenoic acid moiety respectively) were identified as contributing to the separation of the stationary phase from the other phases, even if this contribution is not very significant (short vectors). Structure identification of these compounds was made by comparison of their spectra with the spectrum of metabolite 146, a monoacylglycerols with a hexadecanoic acid moiety identified by library. However metabolite 146 had an opposite pattern, as it was significantly higher in the stationary phase. Finally myristate-glycerol (metabolite 141), hexadecatetraenoic acid (metabolite 117) and 3-octenoic acid (uncertain identification, metabolite 25) were significantly correlated declining phase.

Three terpenes and four sterols were important for the separation of the groups and, with the exception of metabolite 171, all significantly contributed to the declining phase separation (**Figure 22 D**). The metabolite 171 has been identified by comparison with library entries as

Table 4: Interphasic intensities of metabolites significant for phase separation of *S. marinoi* G4 cells in culture, identified by CAP.

N ^{o1}	Metabolite	Class ²	Exp. ³	Stat. ³	Decl. ³
23	?	?	39±12	13±10	67±20
29	?	?	24±22	13±10	29±20
50	?	?	22±20.7	11±5.2	30±11.7
129	?	?	16.2±7.1	6.6±5.4	49.7±20.6
69	?	?	13±17.3	12±7.6	29±15
2	?	?	13±11.3	17±7.7	63±22.4
6	?	?	13±6.9	38±16.4	57±18.6
61	?	?	12±15	36±18	43±21
57	?	?	7.9±4.3	6.8±3.7	50.4±20.8
3	?	?	6.9±4.1	14.3±11	47.4±22.9
169	?	?	5.7±2	8±2.2	31±20
5	?	?	5.1±5.4	3.2±3.1	43.4±25.7
145	?	?	3.4±1.3	7±2.1	12.3±16.3
85	?	?	3.1±2.9	19.8±16.5	44.4±19.2
96	?	?	1.2±3	2.4±1.2	31.2±20.1
91	?	?	17±6.7	57±15.9	30±21.3
21	?	?	45±25.4	11±6.4	25±5.6
33	?	?	42±27.9	3.2±2.9	2.7±3.3
99	?	?	40.3±25	5.4±3.2	3±3.8
131	?	?	39.5±22.7	10.3±5.5	2.3±3.1
183	?	?	35±24.5	25±20.5	13±7
166	?	?	34.5±20.6	6.9±2.3	32.2±12
65	?	?	29.7±18.5	4.2±3	5.2±4.3
62	?	?	21.2±25.7	6.8±2.3	15.3±4.7
31	?	?	14.4±18.6	4.3±2.7	1.3±1
30	?	?	12.4±19.3	3±2.5	0.7±0.6
36	Hydroxy-proline	aa	9.1±8.7	3.4±2.2	31.4±24.8
9	Valine*	aa	34±17.6	36±25.7	4.8±2
27	Pyroglutamic acid?	aa	12±12	35±20	26±13
40	Phenylalanine?	aa	52.3±20.5	13.8±14.2	1.9±1.4
19	Glycine*	aa	47.8±15.7	26.6±10.4	3.6±2
1	Alanine*	aa	37.9±24.8	10±4.9	4.6±2
38	N-acetyl-glutamic acid?	aa	36.2±25.2	3.3±2.7	1.7±1
12	Isoleucine?	aa	31.6±21.5	23.2±23.6	2.7±1.6
28	Threonin?	aa	29.8±29.3	10.6±10.7	0.4±0.7
17	Isoleucine	aa	29.1±17.7	27.2±24.7	2.8±1.7
18	Proline*	aa	25.3±26.3	3.7±3.4	0.8±0.8
26	Serine*	aa	22.6±27.2	2.6±3.2	0.3±0.5
141	Myristic-glycerol?	FA	28±8.8	45±7.3	62±19.7
117	Hexadecatetraenoic acid?	FA	23±14.3	34±8.7	59±16.5
150	C16:2-glycerol?	FA	19±6.5	16±2.5	20±18.3
25	3-octenoic acid??	FA	6.2±3.1	7±4.5	52.6±19.9
79	Unidentified fatty acid	FA	3.1±0.7	4.8±16.1	5±1.2
146	C16:1-glycerol??	FA	29±14	58±19	44±24
107	Hexadecenoic acid?	FA	72±14	61±16	43±15
106	Hexadecatrienoic acid (HDTRI)	FA	68±17	36±11	16±12
116	Hexadecanoic acid	FA	68±14	56±12	47±11
109	Hexadecadienoic acid?	FA	58±17	36±12	22±15

N ^{o1}	Metabolite	Class ²	Exp. ³	Stat. ³	Decl. ³
151	C16:1-glycerol?	FA	56±18.4	42±9.9	55±16
104	Unidentified fatty acid	FA	47±33	38±17	26±19
105	Hexadecenoic acid*	FA	39±15.6	15±7.8	16±24.2
142	EPA	FA	34.6±17.8	10.6±12.5	7.2±7.3
132	Linoleic acid*	FA	32.7±20.8	13.1±10.3	5.5±7
14	Glycerol	Other	46±17.5	36±17.3	76±9.5
60	Putrescine*	Other	18±8.8	35±17.8	51±20.8
10	Diethylenglycol	Other	15.8±6.4	6±5.3	65.1±20.4
123	Terpenoid	Other	43±15.3	71±14.3	21±9.9
100	Hexonic acid	Other	27.4±19.3	15.1±7.6	4.4±3.3
41	Threonic acid	Other	38.7±20.9	6.6±3.3	18.6±6.9
45	Trishydroxybenzen	Other	12.4±7.5	3.4±1.7	5.5±17
168	Sterol?	Sterol	35±16	38±13	60±27
178	Sterol	Sterol	25±12	25±11	55±27
174	Cholesterol*	Sterol	14±7.2	18±4.5	55±27.7
171	Cholesterylpelargonate?	Sterol	31.4±21	8.9±4.4	2.1±2.2
128	Unidentified sugar	Sugar	43±20	43±16	64±13
120	Hexose?	Sugar	7.3±7.3	2.8±1.5	17±28
165	Disaccharide	Sugar	3.2±1.3	3.8±1.4	8.1±16.7
188	Trisaccharide	Sugar	37.6±20.5	41.4±18.7	5.6±7
87	Glucose*	Sugar	26±14.4	62±19.9	15±5.1
186	Trisaccharide	Sugar	17.1±8	18.6±14.2	1.5±0.7
68	Hexofuranose?	Sugar	50.8±17.4	6.3±4.2	3.9±3.4
185	Trisaccharide	Sugar	45±19.7	33±8.9	15±5.8
119	Hexose	Sugar	41.6±24.5	5.1±6.8	9.3±6.9
184	Trisaccharide	Sugar	39.6±19.6	35.4±13.1	7±5.3
47	Pentafuranose	Sugar	29.7±19.7	3.8±4.2	12.6±11.8
43	Pentafuranose	Sugar	25.4±19.2	4.4±4.1	10±9
46	Pentafuranose	Sugar	24.5±22	6.7±16	8±11
44	Pentafuranose	Sugar	23±18.9	3.6±2.7	7±6
98	Hexose?	Sugar	8.6±2.9	5.3±3.7	6.5±19.1
172	Digalactosylglycerol?	Cplx-Sugar	52±13	56±17	25±19
138	2-GalactosylGlycerol	Cplx-Sugar	36.4±17.4	15.4±8.1	5.2±4.3
121	Inositol isomer	Sugar alcohol	30±10	35±13	62±15
115	Inositol isomer	Sugar alcohol	20±8.9	50±15.4	62±15.4
112	Inositol isomer	Sugar alcohol	25±13	58±21	56±15
103	Inositol isomer	Sugar alcohol	14±5.6	34±17.6	27±13.5
71	3,7,11,15-tetramethyl-2-hexadecen-1-ol?	Terpene	17±9.7	10±5.9	52±17.3
77	3,7,11,15-tetramethyl-2-hexadecen-1-ol?	Terpene	13.6±6.8	9.6±5.6	51.8±18.5
74	3,7,11,15-tetramethyl-2-hexadecen-1-ol?	Terpene	12.3±6.4	9.6±6	49.9±18.1

¹ metabolite number and ² classification of metabolites, as in **Appendix IX**. ³ average ± standard deviation in each phase of the intensity of the metabolites relative to the maximum intensity observed during the whole experiment. The colour shades are based on values, red: maximum average, cyan: 0. * metabolite identification confirmed by comparison with a standard. Metabolites are tagged with "?" if the reverse match of the comparison with the library was lower than 800 and with"??" if the score was lower than 700 (cf. **Appendix IX**).

cholesteryl-pelargonate and significantly contributed to the exponential phase; however, because the retention time of metabolite 171 did not match the expected retention time of cholesteryl-pelargonate, it is not correctly identified, and was most likely a steroid.

The sugars showed four different behaviours (**Figure 22 E**). A first group characterised the exponential phase (metabolites 47, 43, 46, 44, 119, 68, and 138), all monosugars (hexose or pentose), with the exception of metabolite 138, identified as galactosyl-glycerol (floridoside). All the trisaccharides identified by the CAP (metabolites 184, 185, 186, and 188) had vectors pointing between exponential and stationary phases groups, and had accordingly high and similar relative intensities in these two phases (**Table 4**). Metabolite 172, a digalactosyl glycerol, had the same behaviour. Three sugars were characteristic for the declining phase (metabolites 120, 128 and 165, a hexose, an unidentified sugar and a disaccharide respectively). Glucose showed a unique behaviour for the sugars. It was significantly higher in stationary phase than in either of the other phases (very distinct and long vector toward the stationary group). The inositol isomers (**Figure 22 D**, sugar alcohol), were characterised by low intensities in exponential phase and high intensities in stationary and declining phase (except metabolite 121, with a comparable level in exponential and stationary phases and a high level in declining phase).

Seven metabolites important for the CAP separation were structurally identified, but could not be classified in the previous classes. Threonic acid (metabolite 41), trishydroxybenzene (metabolite 45) and hexonic acid (metabolite 100) were characteristic for the exponential phase. An undetermined oxo-terpene (metabolite 123) had a higher concentration in the stationary phase compared to the other phases. Finally, the vectors of glycerol (metabolite 14), diethylenglycol (metabolite 10) and putrescine (metabolite 60) pointed towards declining phase (**Figure 22 C**). The first two metabolites had similar intensities in exponential and stationary phase, followed by a high intensity in declining phase, while putrescine increased throughout the phases (**Table 4**).

Two metabolites (metabolite 98 & 79, a hexose and a fatty acid) were also included in **Figure 22**, as example of compounds not significant for the separation. Their vectors are very small, and their relative intensities do not vary significantly between phases.

In a second approach, the phases were considered independently. The eight sampling times over 24 hours, were considered first as independent groups, and then separated in day and night groups. The first separation allowed identification of compounds with a short response time and which are characteristic for one time point, while the second grouping spotted the compounds related to photosynthesis and other photic/aphotic related processes.

In exponential phase, both groupings achieved separation by CAP (**Figure 23 A & C**). When considered as distinct groups, the different time points separated mainly on two axes (**Table 5**). Because the third axis had a low eigenvalue, only the first two axes were considered. The first constrained CAP axis separated the last two sampling times (07:00 and 11:00, the second day of the

exponential sampling) from the first 6 sampling times. The second constrained axis separated mainly the first three sampling points (11:00, 15:00 & 19:00, day) from the next three (21:00, 01:00 & 05:00, night). The time point 21:00 is not well separated in between these groups, and is probably a transition time point. This overlap is reflected in the crossvalidation test, which resulted in a high misclassification. This means that the groups are not very distinct, even if the trace statistics of the permutation test confirmed that they occupy significantly different location of the multivariate space. The first axis is also significantly correlated with the separation (**Table 5**).

Table 5: Eigenvalues (λ), correlation (Δ^2) and diagnostics statistics of the CAP analysis of the exponential phase.

	Constrained canonical axes						Statistics		
	1 st axis		2 nd axis		3 rd axis		Crossvalidation	Permutatest	
	λ	Δ^2	λ	Δ^2	λ	Δ^2	Misclassification	Trace stat.	1 st Δ^2
G [†]	0.95373	0.9096	0.90495	0.81894	0.76634	0.58727	65%	p = 0.001	p = 0.001
D/N [‡]	0.93717	0.87828	-	-	-	-	12.50%	p = 0.001	p = 0.001

[†], sampling time as individual groups. [‡], sampling time grouped as day and night

Six sugars and sugar alcohols were identified as significant for the separation. All of them, except the metabolite 119 (a hexose), were characteristic for the group made up of samples taken on second day of light sampling (Day2 group) (**Figure 23 B**). They had similar relative intensities in the first 5-6 sampling times, and then increased at the night-day shift (**Table 6**). Metabolite 119 had a vector pointing in the direction of the group formed by the night sampling time (Night group), and indeed its relative intensity peaks in the night (**Table 6**). In contrast to sugars, all the vectors of the fatty acids and related compounds identified as significant pointed toward the group of the first day of light samples (Day1 group) (**Figure 23 B**). Additionally, their relative intensities peaked just before the day-night shift (**Table 6**). The only exception is HDTETRA (metabolite 117), with the highest intensity at 7:00, on the second day (**Table 6**).

Across the 10 amino acids identified, no specific pattern emerges. Six of them (alanine met. 1, isoleucine met. 12 & 17, valine met. 9, threonine met. 28 and pyroglutamic acid met. 27) were intense in the Night group. The vector of proline (metabolite 18) pointed towards the Day1 group. The last three amino acids (hydroxy-proline met. 36, glycine met. 19 and serine met. 19) tended to point towards the Day2 group. However, it has to be noted that most of the corresponding vectors are not very long, and therefore their contribution to the separation was small.

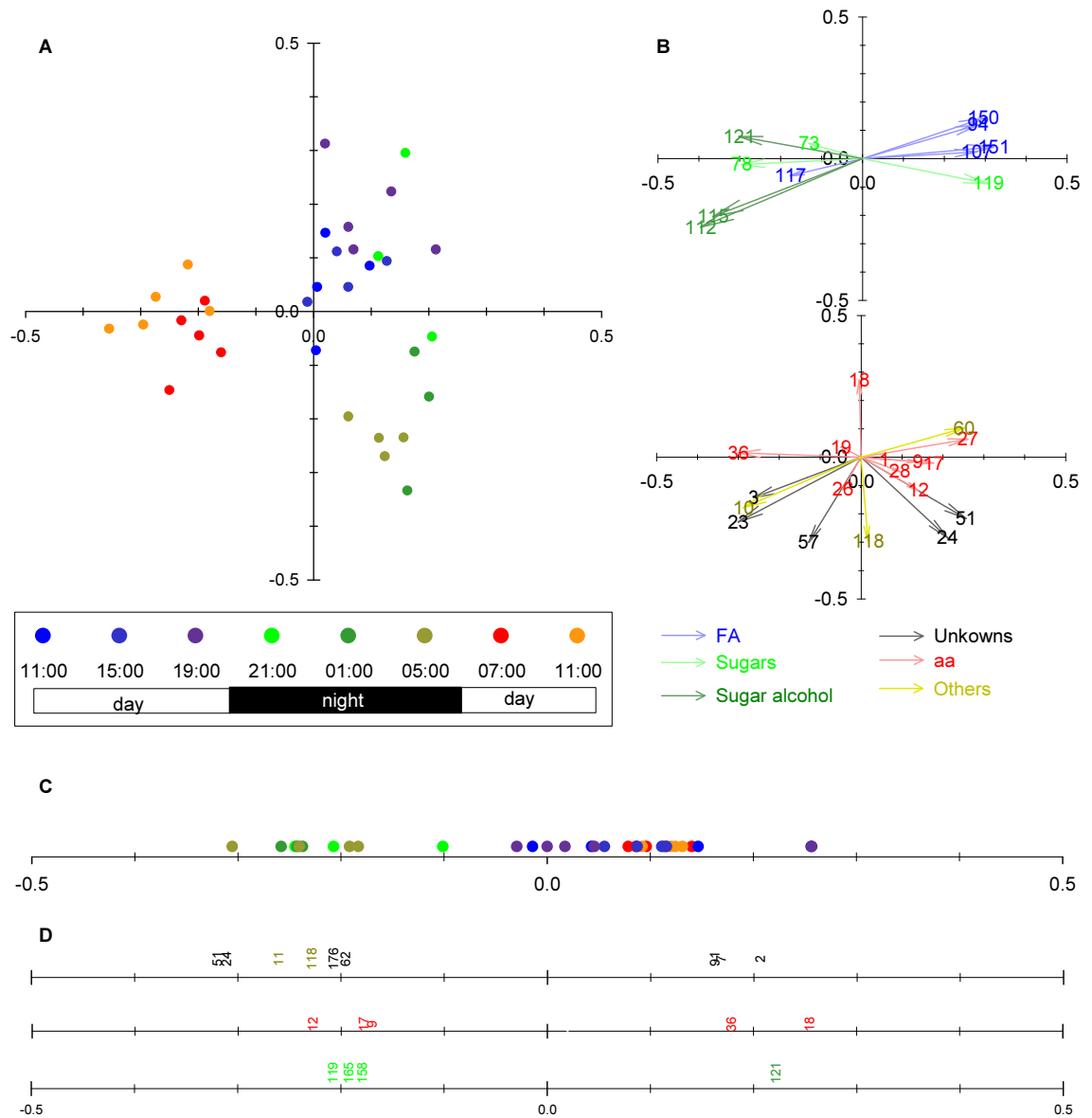


Figure 23: Intraphasic separation based on *S. marinoi* G4 cell metabolites in exponential phase. **A**, separation by CAP with every sampling time as a group (see legend in box for the colour code). **B**, scaled vectors of the metabolites with a significant contribution to the CAP axes from **A**. **C**, separation by CAP with day and night sampling as groups. **D**, scaled vectors of the metabolites with significant contribution to the CAP axis from **C**. For a clearer view, the arrows have been omitted. The numbers are the n° of the metabolites, as in **Appendix IX** and **Table 6**.

Three other metabolites were identified as significant for the separation. Diethylenglycol (metabolite 10) is characteristic for the Day2 group, while the 2,5-furandicarboylic acid (metabolite 118) peaked in the Night group and putrescine (metabolite 60) decreased over the 24 hours.

Table 6: Intensities of metabolites in *S. marinoi* G4 cells, over 24 hours in the exponential phase. Shown here are only the metabolites with a significant contribution to the CAP axes.

N ^{o1}	Metabolite	Class ²	CAP ³	Intensity at sampling time (average ± standard deviation)(n indicated in brackets)							
				11:00 (4)	15:00 (4)	19:00 (5)	21:00 (3)	01:00 (3)	05:00 (4)	07:00 (5)	11:00 (5)
2	? ⁿ	?	o	36±46.3	19±22.5	23±13.2	12±5	17±4.2	14±8.7	24±8.5	20±5.5
7	?	?	o	57±33.4	55±39.8	54±16.5	14±7.3	18±4.7	24±15	10±7.6	23±14.9
51	?	?	x o	11.6±5.4	35.6±43.6	12.9±4	6.5±2.7	8.4±2.1	9.1±3.4	5.1±1.5	5.9±3.6
62	? ⁿ	?	o	24±9.2	12±6.8	12±4.6	40±49.2	39±52.7	34±42.4	12±3.3	12±9.4
24	?	?	x o	5.9±6	10.5±14.1	4.5±2.7	16.3±19.3	56.8±38.1	24.6±12.1	0.8±0.6	4±7.1
57	? ⁿ	?	x	36±17.9	30±7.6	14±8.6	21±3.7	50±43.5	35±7	39±11.2	38±11.2
176	?	?	o	43±15.6	39±20.7	11±3.2	50±19.9	32±9.7	60±33.6	25±5.5	27±8.2
3	? ⁿ	?	x	30±6.4	27±9.4	17±4.4	21±2.3	25±3.1	37±5.2	28±27.1	55±25.9
23	? ⁿ	?	x	59±10.6	61±16.5	41±10.3	49±14.2	73±1.5	62±12.6	74±23.6	87±13.5
91	? ⁿ	?	o	46±8.9	43±16.1	34±5.4	37±12.8	27±2.7	37±17.1	41±9.3	56±28.9
18	Proline* ⁿ	aa	x o	41.7±46.2	28.6±27.8	51±22.5	6.2±3.5	6.2±4.9	4.9±2.7	16.9±16.6	31.4±18.7
1	Alanine* ⁿ	aa	x	29±16	25±19	43±27	45±12	60±37	36±28	28±12	44±37
9	Valine* ⁿ	aa	x o	34±19	36±15	62±19	59±22	83±19	52±30	28±19	60±31
12	Isoleucine? ⁿ	aa	x o	18±9.5	23±11.1	46±21.9	44±23.6	83±21.7	48±36	29±28.4	40±22.3
17	Isoleucine ⁿ	aa	x o	25±14	35±24	69±30	52±26	81±11	50±34	31±30	43±22
26	Serine* ⁿ	aa	x	8.4±13	11±8.1	6±6.1	23.4±20.8	64.8±42.6	13.3±14.7	19.2±20.8	44.5±35.9
27	Pyroglutamic acid? ⁿ	aa	x	42.6±36.9	32.2±28.3	65.5±20.2	25.7±42.3	68.3±41.8	28.7±26.4	7.2±3.6	9.3±7.5
28	Threonine? ⁿ	aa	x	8.3±13	18±27	35.6±21	42.5±32	64.4±19	27.6±24	11.6±21	42±44
19	Glycine* ⁿ	aa	x	42±2.7	45±15.8	49±15.1	57±2.4	49±10.9	42±12.6	41±20.4	58±25
36	Hydroxy-proline ⁿ	aa	x o	15.3±9	23±6.2	15.9±3	8.8±3.1	5.9±0.3	13.3±6.7	27.5±27.1	41.5±34.6
94	Pentadecanoic acid?	FA	x	67±19.9	70±21.5	75±6.6	48±7.8	59±3.7	59±5.7	43±4.3	42±4.3
107	Hexadecenoic acid? ⁿ	FA	x	76±15.6	72±15.4	85±12.7	62±12.7	81±11.1	77±8	62±5.9	60±15
150	2-C16:2 glycerol? ⁿ	FA	x	78±22.9	65±16	84±6.7	50±11.1	70±8.8	54±6.2	42±4.8	35±6.3
151	2-C16:1 glycerol? ⁿ	FA	x	80±18.8	60±16.3	89±8.5	57±22.2	90±9.1	66±11.3	53±9.5	39±15.1
117	Hexadecatetraenoic acid? ⁿ	FA	x	36±17.4	26±10.2	19±5.1	28±11.1	19±3.3	30±15.3	51±32.3	34±22.4
60	Putrescine* ⁿ	Other	x	71±30.5	79±18.8	64±9.6	50±4.1	50±10.4	60±13.2	21±19.3	32±17.6
11	Ethanolamine	Other	o	39±13	26±17	49±16	47±43	88±10	61±29	40±11	39±19
118	2,5-Furandicarboxylic acid?	Other	x o	25±23	22±17	26±22	36±26	69±34	58±21	46±17	43±23
10	Diethyleneglycol ⁿ	Other	x	56±30	50±17.5	30±11.3	41±8	42±6.4	59±24.3	71±18.5	70±12.6
119	Hexose ⁿ	Sugar	x o	44±22.2	48±40.7	47±17.1	42±20	66±11.3	62±24.6	23±4.5	17±7
158	Maltose*	Sugar	o	26±19.8	33±14.2	30±16.2	45±11.8	50±7.1	67±17	55±26.9	45±21.9
165	Disaccharide ⁿ	Sugar	o	36±21.1	44±12.7	32±7.8	53±13.7	55±6.6	74±18.3	60±19.7	52±20
73	Hexofuranose?	Sugar	x	45±16.8	41±4.8	63±19.9	67±6	65±13.7	52±12.3	66±24.7	74±20.2
78	Hexopyranose??	Sugar	x	34±24.5	32±12.4	32±7.8	36±6.6	40±20.5	27±4.5	56±19.9	66±23
112	Inositol isomer ⁿ	Sugaralcohol	x	31±8.4	28±4	23±5.1	30±5.4	41±8.9	57±7.1	77±13.2	80±18
115	Inositol isomer ⁿ	Sugaralcohol	x	42±6.1	29±18	34±5.7	38±12.3	39±8	65±11.1	77±13.2	82±18
121	Inositol isomer ⁿ	Sugaralcohol	x o	53±14.5	56±8.6	53±9.7	47±18.9	28±5.5	43±19	62±20.6	74±16.8

¹metabolite number and ²classification of metabolites, as in Appendix IX. ³x: metabolite contributing to separation of every time point; o: contributing to the separation of day/night samples, as identified by CAP. * metabolite identification confirmed by comparison with a standard. Metabolites are tagged with “?” if the reverse match of the comparison with the library was lower than 800 and with “??” if the score was lower than 700 (cf. Appendix IX). ⁿ metabolite also changing during phases of growth.

Finally, five unknown compounds were also associated with groups' separation. Compound 3 and 23 had the highest intensity in the Day2 group, while compound 57 was characteristic for the last 5 sampling times (pointing at the opposite direction from the first 3 sampling times) (Figure 23 B,

Table 6). Vectors of compounds 51 and 24 pointed towards the Night group. For compound 51, this seems in contradiction with the relative intensity averages displayed in **Table 6**, because the intensity peaked in Day1 group. However, these intensities are highly variable (large standard deviation), and therefore the trend that should be considered is a relatively similar intensity in the first six sampling points followed by a decrease in the last sampling points.

When considering only two groups of sampling time, defined by day and night sampling, a CAP achieved a good separation (**Figure 23 C**, **Table 5**). When only two groups are considered, one constrained axis is produced. The separation along this axis is good (high eigenvalue), and the two groups do not overlap (trace statistic were significant and low misclassification occurred in the crossvalidation). Additionally, this axis is significantly correlated with the separation of the two groups (**Table 5**).

Seven unknown compounds were identified as significant for the day-night separation, two of which were already found in the previous grouping (metabolites 51 and 24). Along with the metabolites 176 and 62, these compounds were highly significant for the night sampling, while the metabolites 2, 91, and 7 were higher during the day samplings. Ethanolamine, together with the previously identified 2,5-furandicarboxylic acid, was also characteristic of the night sampling. The amino acids revealed by these CAP were already identified in the previous CAP, with isoleucine (metabolites 17 & 12) and valine (metabolite 9) as night compounds and hydroxy-proline and proline as major day compounds (the latter being extremely low during the night).

Two additional sugars were identified, with maltose (metabolite 158) and an unknown disaccharide (metabolite 165) increasing during the night time. These two sugars grouped with the hexose 119 already previously identified as night compound. Finally the inositol isomer 121 was higher during the day.

It should also be noted that 27 of the 37 compounds identified as contributing to the separations within the exponential phase were also important in the separation of the different growth phases, indicating very dynamic compounds (**Table 6**).

In stationary phase, the eight sampling times were also submitted to the CAP as independent groups or as day and night groups (**Figure 24**). Neither of the two groupings allowed a separation with CAP. The eigenvalues of the constrained axes (0.37559 and 0.25749 for the first axes in both grouping strategies) confirmed that the separation was not possible. Diagnostic statistics were non-significant as well ($p > 0.6$ in all cases).

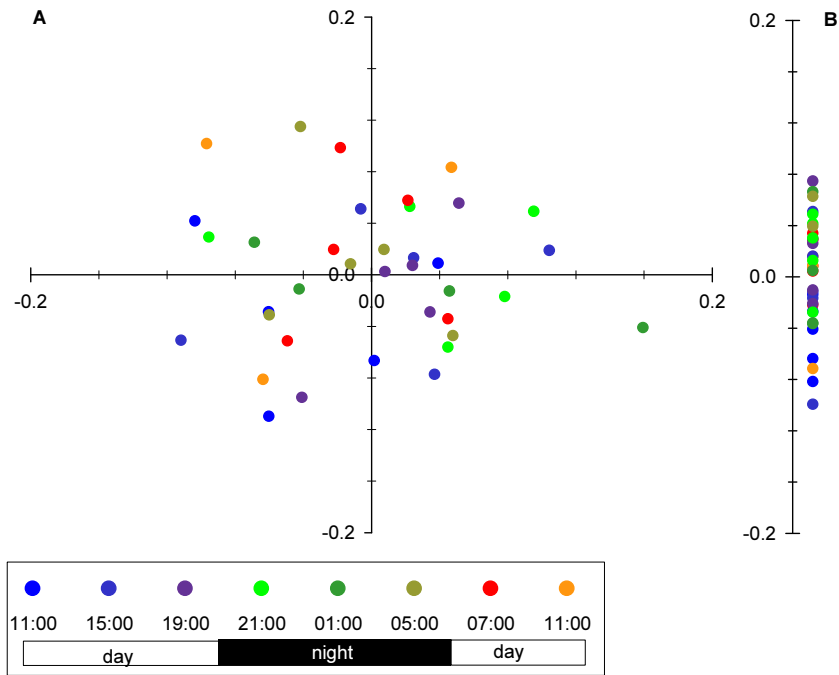


Figure 24: Intraphasic separation based on *S. marinoi* G4 cell metabolites in stationary phase, over 24 hours. **A**, Separation by CAP with every sampling time as group (*cf.* legend in box for the colour code). **B**, Separation by CAP with day and night sampling as groups.

In an attempt to detect any other grouping, I used a non-supervised method, the principal coordinate analysis (**Appendix X**). However, this method did not determine a grouping as well. Therefore no significant metabolite changes could be detected within the eight sampling times of this phase.

In the declining phase, the CAP on the two grouping strategies resulted in contrasted results. The night/day grouping CAP showed no clear separation (see low eigenvalue and high p values in **Table 7**).

Table 7: Eigenvalues (λ), correlation (Δ^2) and diagnostics statistics of the CAP analysis of the declining phase.

	Constrained canonical axes				Statistics		
	1 st axis		2 nd axis		Crossvalidation	Permutatest	
	λ	Δ^2	λ	Δ^2	Misclassification	Trace stat.	1 st Δ^2
G [†]	0.91243	0.83262	0.54342	0.2953	72.23%	p = 0.281	p = 0.001
D/N [‡]	0.56912	0.32389	-	-	33.33%	p = 0.05	p = 0.052

[†], sampling time as individual groups. [‡], sampling time grouped as day and night

However, when every time point was considered as an independent group, the separation was better. The first axis achieved a good separation (high eigenvalue and correlation), and significantly

explained the separation (see p-value in the permutation test for the significance of the correlation of the first axis, **Table 7**). The second axis was not as good, and did not contribute much to the separation. The trace statistics showed that the different time points were not significantly separated in the multivariate space. This is confirmed by the high misclassification in the crossvalidation. This is not surprising, since 7 groups are separated on only one axis. The CAP revealed larger separation corresponding to a transition between day-night-next day (**Figure 25**).

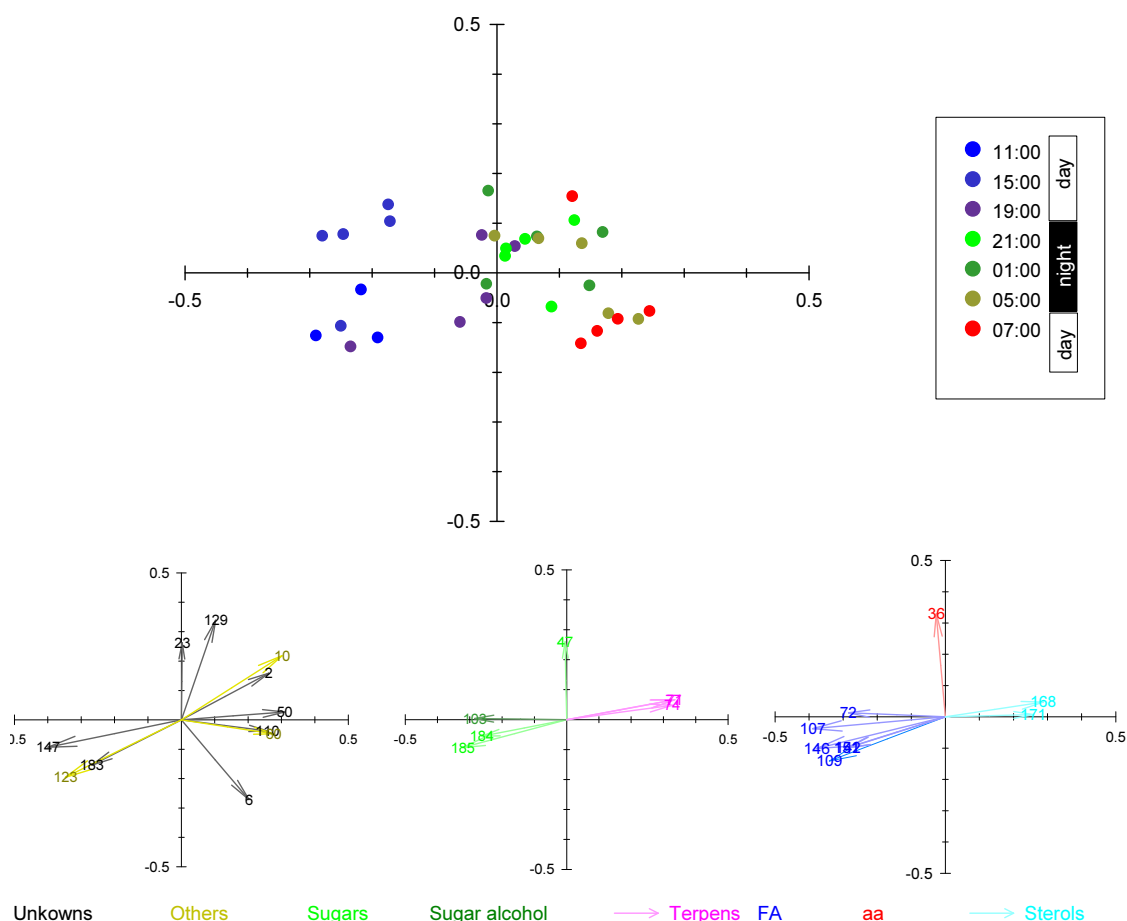


Figure 25: Intraphasic separation based on *S. marinoi* G4 cell metabolites in the declining phase. **Upper**, separation by CAP with every sampling time as group (see legend in box for the colour code). **Lower**, scaled vector of the metabolites with a significant contribution to the CAP axes.

Twenty seven compounds significantly contributed to the separations on the first two axes (23 for the first axis). Unidentified compounds 147 and 183 were significantly higher in the first two samplings compared to the others (long vectors in the direction of the group of the first sampling point, **Figure 25**). Compounds 2, 10 and 50 had the opposite behaviour, significantly increasing in the last sampling points. The behaviour of compounds 6, 23 and 129 was not clear, because they were mainly associated with the second axis. However compound 6 had a vector pointing to the last sampling point (07:00), while the vectors of compound 23 and 129 pointed towards the 21:00-05:00

sampling points. This is reflected in their intensities (**Table 8**) which are the highest at the corresponding sampling points. Diethylene glycol (metabolite 10) and putrescine (metabolite 60) clearly increased over the 7 sampling points, as shown by their relative intensities in **Table 8** and their vectors pointing in the positive direction of the first constrained axis (i.e. towards the last samples)(**Figure 25**). Two trisaccharides were identified as contributing to the separation (metabolites 184 & 185). Their vectors pointed toward the negative pole of the first constrained axis and their relative intensities accordingly decreased over the sampling period. The only contributing inositol isomer followed the same pattern (metabolite 103). One sugar, a pentafulfuranose (metabolite 47), contributed to the second axis, and had a peaking intensity at the light-dark transitions (**Table 8**). Three terpenes (met 71, 74 & 77) appeared to increase over the sampling points, and had long vectors pointing to the positive pole of the first axis.

The only amino acid showing up in this analysis was hydroxy-proline (metabolite 36). It contributed to the second axis, and had a peak intensity in the middle of the night. Fatty acids and sterols presented an opposite pattern. The six fatty acids that significantly contributed to the separation (tetradecanoic acid met. 72, hexadecenoic acid met. 107, hexadecadienoic acid met. 109, EPA met. 142, mono-hexadecenoic acyl-glycerol met 151 & 146) had vectors pointing towards the first sampling points while the two sterol vectors (metabolites 168 & 171) pointed in the opposite direction (**Figure 25**). This is reflected by the intensity of the fatty acids and related compounds, decreasing over the sampling period, while the sterols increased (**Table 8**).

Of these 27 compounds, only three (metabolites 110, 147 and tetradecanoic acid met. 72) did not also contribute to the separation of the growth phases (**Table 8**).

Table 8: Intensity of metabolites in *S. marinoi* G4 cells, over 20 hours in the declining phase. Shown here are only the metabolites with a significant contribution to the CAP axes.

N ^{o1}	Metabolite	Class ²	Intensity at sampling time (average \pm standard deviation)(n indicated in brackets)						
			11:00 (3)	15:00 (5)	19:00 (5)	21:00 (5)	01:00 (5)	05:00 (5)	07:00 (5)
183	? ⁿ	?	74 \pm 37.8	37 \pm 5.4	32 \pm 11.4	26 \pm 16.1	24 \pm 6.7	22 \pm 3.9	24 \pm 7.7
147	?	?	80 \pm 17.4	77 \pm 5.6	48 \pm 17.9	30 \pm 8.6	34 \pm 12.9	30 \pm 16.5	27 \pm 3.3
6	? ⁿ	?	57 \pm 15.1	38 \pm 7.2	65 \pm 26.7	37 \pm 10.8	48 \pm 4.6	64 \pm 16.5	60 \pm 14.1
129	? ⁿ	?	31 \pm 12.4	55 \pm 14	60 \pm 11	78 \pm 19.5	55 \pm 35.9	56 \pm 8.6	50 \pm 27.1
23	? ⁿ	?	57 \pm 14.4	58 \pm 12.8	75 \pm 17.8	83 \pm 7.7	77 \pm 19.7	65 \pm 14.7	49 \pm 47
50	? ⁿ	?	35 \pm 14.4	49 \pm 3.1	59 \pm 11.9	48 \pm 13.3	80 \pm 23.7	71 \pm 5.9	69 \pm 13.5
110	?	?	29 \pm 18	36 \pm 20	45 \pm 19	40 \pm 39	59 \pm 18	62 \pm 23	65 \pm 38
2	? ⁿ	?	35 \pm 4.3	57 \pm 16.4	54 \pm 20.2	65 \pm 27	69 \pm 24.2	71 \pm 18.7	79 \pm 21.7
36	Hydroxy-proline ⁿ	aa	21 \pm 23.5	46 \pm 13.3	37 \pm 6.2	42 \pm 47.6	55 \pm 40	25 \pm 26.4	30 \pm 34
109	Hexadecadienoic acid? ⁿ	FA	66.1 \pm 31.9	40 \pm 6.2	25.1 \pm 5.3	15 \pm 15.4	9.3 \pm 11.2	14.9 \pm 15.2	10.8 \pm 1.1
142	EPA ⁿ	FA	66.7 \pm 36.9	23.7 \pm 2.5	26.7 \pm 22	5.8 \pm 9.6	6.3 \pm 10.4	14.8 \pm 19.1	2.6 \pm 1.6
72	Tetradecanoic acid	FA	71 \pm 24.8	58 \pm 8	43 \pm 3.6	38 \pm 4.1	36 \pm 10.3	38 \pm 11.1	33 \pm 7.8
146	C16:1-glycerol?? ⁿ	FA	78 \pm 20.1	73 \pm 5	43 \pm 15.9	23 \pm 11.9	28 \pm 16.9	24 \pm 22.2	16 \pm 4.2
107	Hexadecenoic acid? ⁿ	FA	81 \pm 16.9	69 \pm 9.6	48 \pm 12.6	44 \pm 18.2	37 \pm 13.3	38 \pm 13.9	34 \pm 5.3
151	C16:1 glycerol? ⁿ	FA	73 \pm 23.2	67 \pm 7.1	53 \pm 15.3	46 \pm 11.1	35 \pm 22.1	51 \pm 15.9	43 \pm 9
123	Terpenoid ⁿ	Other	74 \pm 26.6	47 \pm 4.3	35 \pm 12.3	25 \pm 6.4	26 \pm 4.8	22 \pm 4.3	27 \pm 4.5
10	Diethylenglycol ⁿ	Other	35 \pm 7.6	61 \pm 17.3	64 \pm 13.7	93 \pm 8	80 \pm 15.7	78 \pm 8.3	89 \pm 3.3
60	Putrescine * ⁿ	Other	42 \pm 16.9	54 \pm 10.9	46 \pm 21.5	47 \pm 15.2	63 \pm 33.2	60 \pm 24.2	80 \pm 4.9
168	Sterol? ⁿ	Sterol	33 \pm 16	38 \pm 30.8	76 \pm 15.6	84 \pm 11.4	85 \pm 12.8	57 \pm 45	72 \pm 4.2
171	Cholesterylpelargonate? ⁿ	Sterol	0 \pm 0	14.1 \pm 12.2	44.7 \pm 10.8	26.6 \pm 28.3	27.8 \pm 24.4	28.6 \pm 29.6	63.4 \pm 29.8
184	Trisaccharide ⁿ	Sugar	44.8 \pm 12.2	32.6 \pm 14.1	15.2 \pm 9.8	14.6 \pm 14.2	19 \pm 9.3	12.1 \pm 7.3	6.7 \pm 1.1
185	Trisaccharide ⁿ	Sugar	85 \pm 25	71 \pm 18	51 \pm 17	53 \pm 21	41 \pm 11	41 \pm 20	41 \pm 13
47	Pentafuranose ⁿ	Sugar	18.4 \pm 13.9	18.9 \pm 9.1	19.5 \pm 9.3	43 \pm 21.6	8.8 \pm 3.6	36.5 \pm 40.7	30.8 \pm 34.4
103	Inositol isomer ⁿ	Sugar alcohol	81 \pm 19.3	74 \pm 3.9	60 \pm 18.5	26 \pm 13.1	51 \pm 20.4	48 \pm 11.7	44 \pm 29
77	Hydroxy-terpene? ⁿ	Terpene	30 \pm 1.9	30 \pm 2.7	37 \pm 11.9	54 \pm 8.6	60 \pm 6.4	49 \pm 4.7	59 \pm 10.9
74	Hydroxy-terpene? ⁿ	Terpene	30 \pm 1.4	28 \pm 4.5	37 \pm 9.3	50 \pm 10.6	58 \pm 5	50 \pm 4.3	53 \pm 8.4
71	Hydroxy-terpene? ⁿ	Terpene	33 \pm 2.6	30 \pm 4.1	40 \pm 12.5	55 \pm 7	57 \pm 6.3	55 \pm 3.8	57 \pm 8.4

¹ metabolite number and ² classification of metabolites, as in Appendix IX.* metabolite identification confirmed by comparison with a standard. Metabolites are tagged with “?” if the reverse match of the comparison with the library was lower than 800 and with“??” if the score was lower than 700 (cf. Appendix IX). ⁿ, metabolite also changing during phases of growth.

2.3.5 Metabolites released in the medium

The chromatograms generated from the Easy extracts of the culture media revealed a large number of peaks. Using the same criteria in the AMDIS-MET-IDEA as described for the cell metabolites, a third more peaks can be quantified from the media samples compared to the cellular metabolites. However, almost all the peaks found in the chromatograms of the Easy extracts are to be also found in the chromatograms from the Easy extracts of the blank culture (**Figure 26**). In order to concentrate on the compounds related to the presence of the algae, I used a subtraction strategy. First, all the peaks were quantified in all samples, including the blanks, with AMDIS-MET-IDEA. Then, for every time point in every phase, the corresponding blank peak intensities were subtracted

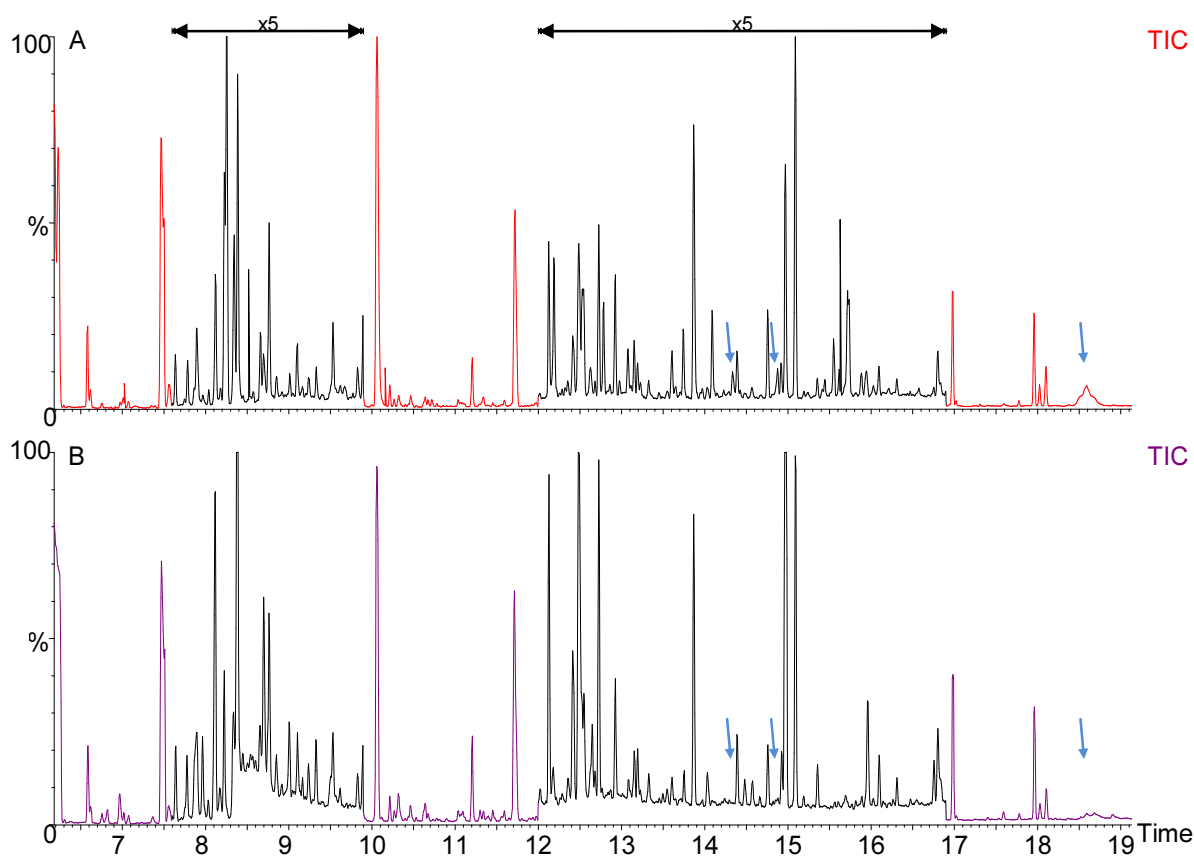


Figure 26: Total ion count chromatograms of Easy extracts in exponential phase at time 19:00. **A**, culture 3. **B**, control. The intensity of the highest peak is normalised to the same value. Traces in black are magnified 5 fold. The blue arrows point to examples of differences.

three times from the five corresponding replicates data set. Because MET-IDEA software attempts to find each peak in all samples, the software sometimes integrates background noise and a non-zero value is assigned to compounds not present in the blank sample. Therefore, I accepted peaks as present in sample chromatograms and not blank chromatograms when the relative intensity in the sample chromatogram was at least three times more intense than the intensity of the same peak in

the blank. The factor three was chosen as a compromise to overcome small variations in the intensities between the samples and the blank, without excluding too many peaks. Each peak that satisfied this condition was then manually confirmed. Forty peaks were finally confirmed and the next steps of the analysis were performed on this data set (**Table 9**).

Table 9: Summary of MET-IDEA peak detection and blank subtraction

Culture phase	Peaks detected	Peaks detected in blank	Peaks after 3 fold blank subtraction	Peaks after manual confirmation
Exponential	334.5±2.2	333.1±3.4	34.0±8.9	
Stationery	336.1±1.7	333.7±1.2	40.6±6.9	40
Declining	329.4±5.0	315.7±14.5	59.4±15.3	

Using the available libraries, only 11 peaks could be assigned to a specific metabolite. In addition, nine of them were also compounds found in the cells (**Appendix XI**). The identified compounds were sugars, fatty acids and hydroxybenzoic acid.

This data set was analysed by CAP, with every sampling point grouped by growth phase. The separation was very good (**Table 10, Figure 27 A**). The exponential phase was separated from the stationary and declining by the first axis. This axis was good at explaining the difference between these phases (high eigenvalue and correlation). Additionally the permutation test confirmed that this axis had a significant correlation with the separation. The second axis separated the stationary phase from the declining phase. This separation was not total, and a small overlap can be observed. The crossvalidation reflects this small overlapping with a small misclassification. However, the trace statistic confirmed that the groups occupied significantly different locations in the multivariate space (**Table 10**).

Table 10: Eigenvalues (λ), correlation (Δ^2) and diagnostics statistics of the CAP analysis of the culture medium metabolites in between growth phases.

Constrained canonical axes				Statistics		
1 st axis		2 nd axis		Crossvalidation Misclassification	Permutatest Trace stat.	1 st Δ^2
λ	Δ^2	λ	Δ^2			
0.98422	0.9687	0.82245	0.67643	4.46%	p = 0.001	p = 0.001

Out of the forty metabolites consisting the data set, thirty had significant contribution to the separation. The majority of them increased over the phases and peaked in declining phase. This is also reflected by their vectors pointing toward the declining phase group (**Figure 27 B & C**). Among the unidentified compounds, only two (metabolites 231 & 204) had vectors pointing to the exponential phase. Both had long vectors and were therefore significant for this phase, as confirmed by their relative intensities (**Table 11**). Only one other compound followed this trend, hexadecanoic

acid (metabolite 254), but its vector was shorter, indicating a lower importance for the separation. Two unidentified compounds were characterised by a high intensity in both declining and stationary phase, metabolite 259 & 168, but peaked in the stationary. This trend was also found for

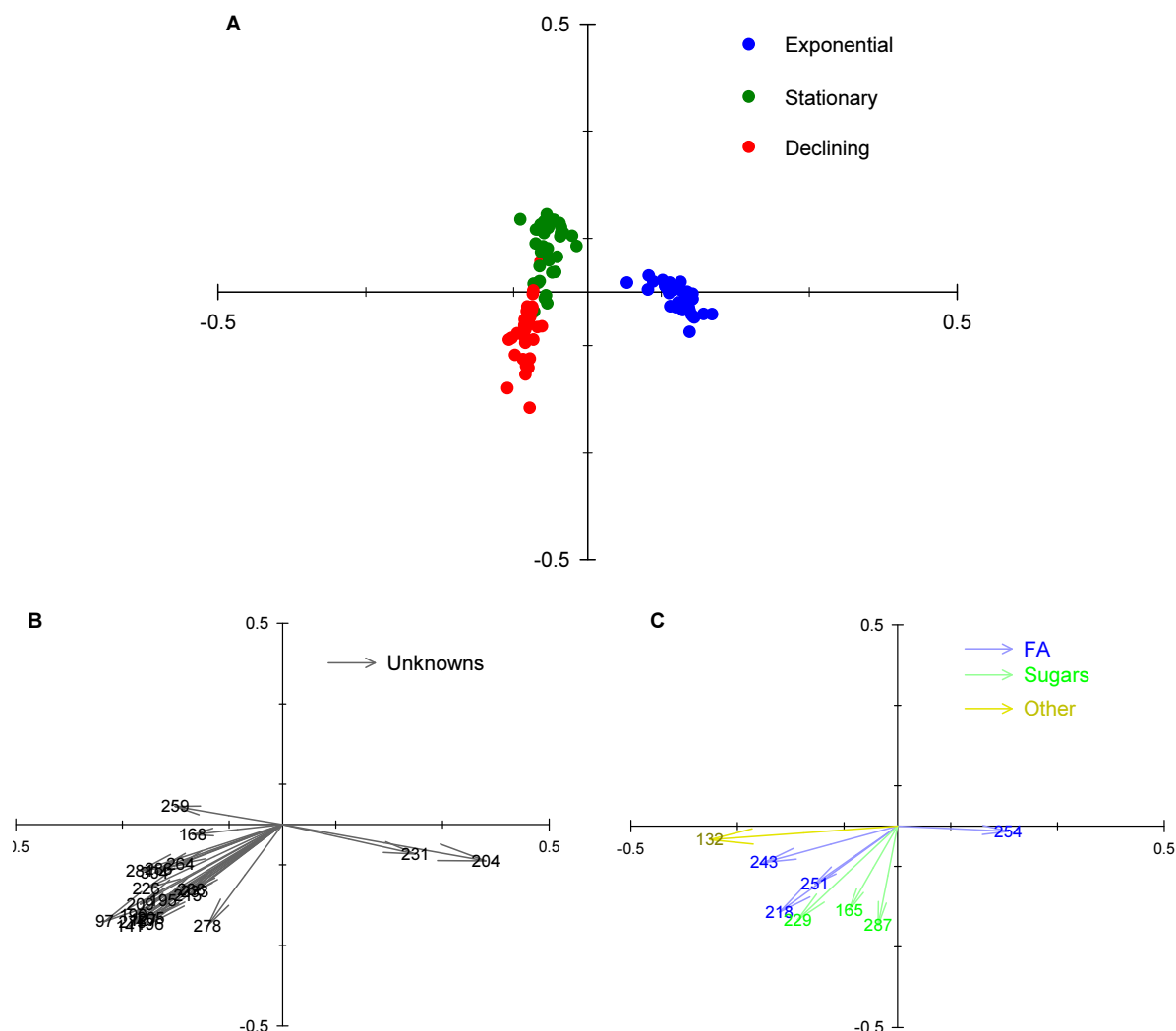


Figure 27: Interphasic separation of *S. marinoi* G4 metabolites found in the culture medium. A, CAP separation of the samples with phases as groups. B & C, scaled vectors of the metabolites significant for the separation. The numbers refer to metabolites in **Appendix XI**. In abscissa is always the first constrained canonical axis and in ordinate the second constrained canonical axis.

hydroxybenzoic acid (metabolite 132) (**Table 11**). All the other identified and unidentified peaks were most intense in declining phase, with varying intensities in stationary phase. No compounds were found to be highly present only in stationary phase. Galactosyl-glycerol (metabolite 287), seemed to characterise the stationary phase with a lower concentration than in other phases. It had the only vector clearly pointing almost only toward the negative pole of the second axis (**Figure 27 C**), and the relative intensity of this metabolite confirmed this trend (**Table 11**).

Table 11 Intensity of metabolites in *S. marinoi* G4 culture medium, in exponential, stationary and declining phase. Shown here are only the metabolites with a significant contribution to the CAP axes.

N ^{o1}	Metabolite	Exponential ²	Stationary ²	Declining ²
204	-	36.3±17 (0.4±0.6)	3.5±1.8 (0±0)	5.9±3 (0.3±0.7)
231	-	28.4±24.2 (1±1)	7.5±7.8 (0.9±1.6)	7.7±11.4 (1.1±1)
254	Hexadecanoic acid *	27.5±25.8 (1±0.7)	14.2±4.8 (0.6±0.2)	6.8±2.6 (0.3±0.3)
287	Galactosyl-Glycerol?	19±18.1 (0.3±0.1)	14±4.9 (0.3±0.2)	17±10.3 (0.3±0.1)
281	-	12±10 (6±4)	33±24 (5±4)	33±20 (4±2)
168	-	17±15 (4±4)	26±24 (1±0)	16±17 (1±1)
259	-	4±4.3 (0±0)	25.7±33.4 (0.1±0.2)	15.4±11.2 (0±0)
132	3 or 4 hydroxybenzoic acid?	29±8 (9±3.1)	53±14.2 (6±0.7)	41±15.7 (3±1)
190	-	12±6.2 (3±3.5)	19±7 (0±0.3)	40±28.6 (0±0.6)
233	-	2.9±2.5 (0.1±0)	9±8.8 (0.1±0)	20.5±29.5 (0±0)
288	-	8.1±9.3 (1±0.4)	10.6±12.5 (1±0.4)	25.8±27.8 (0±0.2)
165	Pentafuranose?	5.4±3.8 (0.4±0.2)	6.4±4.8 (1.4±0.9)	15.9±27.4 (0.8±0.6)
97	-	7.2±2.7 (0.2±0.1)	33.3±11.2 (0.8±0.1)	56.6±14.2 (1±0.2)
127	-	7.2±4.3 (0.1±0.1)	29.9±15.9 (0.1±0.1)	61.8±18.5 (0.1±0.1)
141	-	3.9±2.2 (0.2±0.1)	20.5±12.1 (0.2±0.1)	45.5±20.3 (0.2±0.1)
195	-	17±7.8 (8±4.1)	27±13.1 (6±0.6)	40±24.9 (7±8)
196	-	16±7.9 (2±1.1)	28±13.5 (2±0.9)	53±21.4 (2±0.8)
205	-	15±7.3 (0±0.1)	31±15.1 (1±0.4)	49±20.1 (0±0.2)
209	-	9.5±5.9 (4.2±3.3)	24.8±20 (0.2±0.2)	47.4±28.6 (0.1±0.1)
215	-	27±12 (6±3)	47±25 (8±4)	59±24 (6±3)
226	-	9.6±10 (0±0)	26.3±23.6 (0.1±0)	39.8±27.4 (0±0)
264	-	15±8.2 (0±1)	27±24.9 (1±1)	34±32.5 (0±0)
275	-	11±8 (1±0.4)	31±18.4 (0±0.3)	44±22.8 (0±0.2)
278	-	40±18 (0±0.3)	38±13 (2±1.8)	54±23 (0±0.1)
286	-	3±2.3 (0±0)	28.1±29.4 (0±0)	36.3±29.7 (0±0)
304	-	7.7±5.8 (0±0)	27.1±15.5 (0±0)	42.8±32.5 (0±0)
243	Unidentified fatty acid?	6.7±6.1 (0.5±0.7)	28.2±32.9 (0.5±0.7)	32.9±23.7 (0.2±0.3)
251	Hexadecenoic acid	24±19 (1±0)	29±25 (1±1)	38±26 (0±0)
229	Hexose	32±10 (23±6)	38±20 (14±3)	49±21 (8±4)
218	Tetradecanoic acid*	23±12 (7±3)	29±17 (6±1)	41±25 (3±1)

¹ metabolite number as in **Appendix XI**. ² average intensity of the metabolites ± standard deviation (blank average ± standard deviation). n = 39, 38 et 35 for the exponential, stationary and declining phase respectively (n = 8, 8 and 7 for the respective blanks). * metabolite identification confirmed by comparison with a standard. Metabolites are tagged with “?” if the reverse match of the comparison with the library was lower than 800 and with“??” if the score was lower than 700 (cf. **Appendix XI**).

As for the cell metabolites analysis, I also considered each phase separately to identify compounds that would change over 24 hours, or over the day-night transition. In all cases, the separations were not good. The eigenvalues of the first axes did not exceed 0.85, the crossvalidation resulted in high misclassifications and almost all correlations of the first axis were not significant (**Table 12**). Additionally the trace statistics revealed that in all but one case the groups did not occupy

significantly different locations. Neither did the CAP result in visually clear separation (**Figure 28**). Particularly in stationary phase, the day-night grouping resulted in no grouping at all, all samples being clumped together. A slight separation between the first day-night-second day was achieved when every sampling time was considered separately, but results were not significant.

Table 12: Eigenvalues (λ), correlation (Δ^2) and diagnostics statistics of the CAP analysis of the exponential (E), stationary (S) and declining (D) phase.

		Constrained canonical axes				Statistics		
		1 st axis		2 nd axis		Crossvalidation	Permutatest	
		λ	Δ^2	λ	Δ^2	Misclassification	Trace stat.	1 st Δ^2
E	G [†]	0.8488	0.72059	0.65078	0.42351	71.79%	p = 0.11	p = 0.04
	D/N [‡]	0.6568	0.4314	-	-	41.03%	p = 0.031	p = 0.031
S	G [†]	0.7651	0.5855	0.70713	0.50004	84.21%	p = 0.491	p = 0.2
	D/N [‡]	0.04968	0.00247	-	-	47.37%	p = 0.796	p = 0.796
D	G [†]	0.75264	0.56647	0.44463	0.02498	85.71%	p = 0.93	p = 0.122
	D/N [‡]	0.51767	0.26798	-	-	51.43%	p = 0.131	p = 0.131

[†] sampling time as individual groups. [‡] sampling time grouped as day and night

The only case of significant statistics was the day-night grouping in exponential phase. This was then the only case in which the significant contributing metabolites were examined (**Figure 28 C**). The one constrained axis managed to separate day and night, but with overlapping of the groups. The last two sampling times of the night (01:00 and 05:00) were the best separated from the others. Nine metabolites were identified as significantly contributing to this separation (**Figure 28 C**, **Table 13**). Only tetradecanoic acid (metabolite 218) characterised the day samples. All other metabolites had a higher global intensity in the night, and also tended to increase over the 24 hours. A notable exception is glucose, which peaked in the night and returned to previous levels in the day. It was also the most significant compound for the night group (**Figure 28 C**).

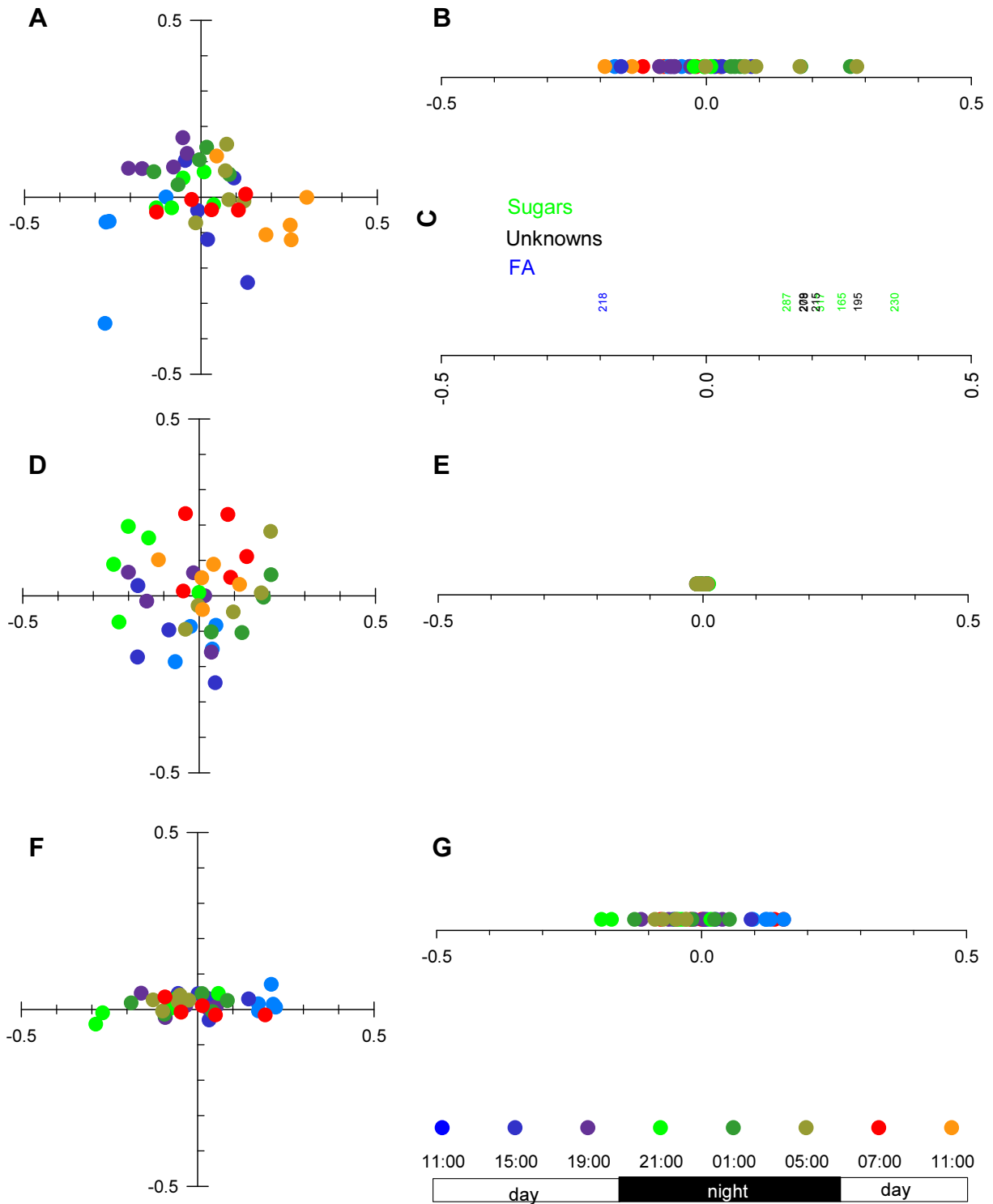


Figure 28: Intraphasic separation of *S. marinoi* G4 metabolites found in the culture medium. **A, D & F,** CAP with every sampling time considered as a group. **B, E & G,** CAP with day and night sampling times considered as groups. **A & B,** exponential phase samples. **C,** scaled vectors of the metabolites significantly contributing to the CAP axis in **B.** For clarity, the arrows are omitted, the numbers correspond the metabolite's number as in **Appendix XI.** **D & E,** stationary samples. **F & G,** Declining phase samples. In abscissa is always the first constrained canonical axis and in ordinate the second constrained canonical axis.

Table 13: Intensities of metabolite in *S. marinoi* G4 culture media, over 24 hours in the exponential phase. Shown here are only the metabolites with a significant contribution to the CAP axis when separating day and night groups.

N ^{o1}	Metabolite	Intensity at sampling time (average ± standard deviation)(Blank value indicated in brackets)							
		11:00 (n=4)	15:00 (n=5)	19:00 (n=5)	21:00 (n=5)	01:00 (n=5)	05:00 (n=5)	07:00 (n=5)	11:00 (n=5)
209	? ⁿ	17±8 (4)	32±28 (12)	47±26 (41)	39±18 (15)	48±25 (31)	54±25 (0)	46±34 (13)	51±34 (30)
278	? ⁿ	23±7 (6)	30±16 (6)	47±24 (17)	52±19 (4)	65±23 (6)	63±16 (7)	44±17 (4)	39±12 (4)
218	Tetradecanoic acid ⁿ	18±9 (15)	50±33 (16)	39±13 (22)	29±16 (9)	32±15 (15)	41±16 (9)	35±19 (10)	48±23 (9)
215	? ⁿ	27±10 (11)	54±31 (18)	45±14 (11)	44±28 (7)	43±13 (3)	47±15 (3)	47±26 (19)	63±21 (12)
287	Galactosyl-Glycerol? ⁿ	9±8 (0)	18±16 (1)	18±13 (2)	14±12 (0)	30±40 (1)	25±15 (1)	16±15 (1)	23±10 (1)
165	Pentafuranose? ⁿ	12±13 (1)	20±18 (3)	21±13 (2)	19±7 (1)	35±16 (1)	53±29 (3)	25±17 (4)	28±8 (2)
195	? ⁿ	39±25 (16)	36±19 (31)	31±12 (31)	31±12 (20)	49±30 (19)	56±17 (16)	37±11 (24)	40±17 (20)
230	Glucose	8±12 (1)	26±29 (2)	32±11 (1)	14±10 (3)	52±37 (2)	63±40 (2)	33±20 (4)	12±8 (1)
317	Trisaccharide?	8±16 (0)	6±8 (0)	2±3 (0)	4±5 (0)	4±2 (0)	23±43 (0)	3±2 (0)	1±1 (0)

¹ Metabolite number, as in Appendix XI. Metabolites are tagged with “?” if the reverse match of the comparison with the library was lower than 800 (cf. Appendix XI). ⁿ metabolite also changing during phases of growth.

2.3.6 Discussion

Cell states at different metabolomic sampling points

The chlorophyll a fluorescence was used as the first approximation of the cell growth, and the metabolomic sampling periods were determined based on this parameter. However, the chlorophyll a increased until day 14 (Appendix III), while the cell density already had reached a plateau at day 8 (Appendix II). It is then clear that the fluorescence measure should be used with care in estimating the growth phases. The exponential phase metabolomic sampling, on days 6-7, thus reflects late exponential phase conditions. The cell density continued to increase during the exponential phase metabolomic sampling, and therefore the cells were still actively dividing. The second metabolomic sampling period was made during the middle of the stationary phase according to cell counts, and just after the chlorophyll a concentration stabilised. The exact start of the declining phase was difficult to define, but there is little doubt that the metabolomic sampling period chosen for this phase (day 23-24) was within this phase. Indeed, the cell density, as well as the chlorophyll a fluorescence signal, significantly decreased during these days. The chlorophyll a fluorescence measures, in addition, were dependent on the time of day and especially on the day-night conditions. This is in good accordance with previous reports on the diurnal cycle of the chlorophyll a content in *S. costatum* (Owens *et al.*, 1980). Chlorophyll a fluorescence should thus not be used for normalisation purposes, if the samples are not taken at the same time of the day.

The cell volume is an important parameter allowing an estimation of total biomass in the culture. Biomass could be a preferred normalisation parameter to cell density when describing an absolute variation of a compound in different conditions. A significant change in cell volume would modify the absolute content of a compound per cell, if the concentration of this compound does not change. This is important to keep in mind when interpreting the PUA and fatty acids results, reported to the amount per cell, but not for the metabolomic results, because the sum normalisation approach chosen compensates for the volume effect. The cell volume of *S. marinoi* G4 decreased during exponential phase (**Appendix II**), which is expected because it is a direct consequence of the characteristic cell division of diatoms. It would be interesting to observe the metabolic changes during the division. However, at no specific time point could a defined shift in the cell density or in the cell volume be detected. It is thus probable that the cells do not divide in a synchronous manner at a specific point of the day, making it impossible to define samples from specific sampling time points as “pre-division” and “post-division” samples.

The photosystem II efficiency was relatively stable over the course of the culture, with the exception of the exponential-to-stationary phase transition (**Appendix IV**). The drop in PSII efficiency at this point was probably due to a temporal metabolic mismatch with the nutrient status (Kolber *et al.*, 1988), and the efficiency returned to previous levels after the adaptation of the cellular metabolism. The small increase observed during the declining phase metabolomic sampling could be caused by a slight amelioration of the cell’s physiological status due to the frequent mixing of the culture.

Different nutrient starvation states

Silicate limitation induced the stationary phase. The first limiting nutrient in the cultures seemed to be phosphate (**Appendix VIII**), which reached low level by day 7. Silicate reached the bottom level on day 8, just after the sampling. However, the high variability in phosphate measurements makes it difficult to assign definitively which of the two nutrients was really limiting first. The stationary phase started, according the cell counts, at the onset of the silicate limitation.

Nitrogen resources are depleted only in the middle of the stationary phase. The nitrate uptake rate was slowed down after the entry of the cultures into stationary phase. When nitrate was at a high concentration, the cells excreted nitrite. This has been shown previously, and could be used by the cells to divert part of the excessive energy collected by photosystems (Serra *et al.*, 1978). After day 10, when the nitrate concentration in the medium reached low levels (< 20% of the initial concentration), nitrite was also decreasing. Nitrogen levels reached very low (and probably limiting) levels by days 12-14, just before the stationary phase metabolomic sampling. The chlorophyll a fluorescence reached a plateau when nitrogen became limited, confirming the direct relation

between chlorophyll a and nitrogen levels found in previous studies (Harrison *et al.*, 1977).

Silicate is re-solubilised in the culture. Silicate concentration started to increase again after day 15. This is probably caused by the re-solubilisation of dead diatom frustules by bacteria. Bacteria have been shown to be more efficient than abiotic processes in the re-solubilisation of silicon from diatom frustules (Roubeix *et al.*, 2008). The start of the increase in dissolved silicate corresponded with nitrogen limitation. If we assume that the re-solubilisation was occurring during most of the stationary phase, we could hypothesise that the diatoms were taking up all the newly available silicate until nitrogen became the limiting factor and stopped or reduced greatly the formation of new cells. Alternately, the rate of dying cells may have increased due to the nitrogen limitation.

The observed lag time before re-entering exponential growth phase after transfer to fresh medium (**Appendix V**) was also related to the nutrient status and growth phases. In exponential phase, when no nutrients were depleted, the lag time was short or nonexistent. In the early stationary phase, when Si and P were limiting, the lag phase was longer, and finally reached 5 days in the late stationary phase. At that point, the cells' physiology changed to a starvation status and restarting the growth probably required replenishment of the nutrient reserves and reinitiating the growth machinery. Such variations in lag time caused by different nutrient limitation pulses have already been reported (Collos, 1986).

Bacteria community changed over the different growth phases

Despite our attempt to keep the culture bacterial level as low as possible, the bacterial community proliferated from the first day of the culture onwards (**Appendix VI**). After day 5 the concentration of bacteria reached a plateau, possibly due to combination of the depletion of phosphate and slowing of the diatom growth. Interestingly, three of the four major colony phenotypes observed were not detectable before day 3 or after day 15. The period during which these three phenotypes were present corresponded to the nitrite presence. However, a study reported an antibiotic activity of *S. costatum* increasing in the middle of the stationary phase (Terekhova *et al.*, 2009). It is therefore unclear if this modification of the bacterial community is linked to the nitrite dynamics (the three phenotypes representing then denitrifying bacteria) or if *S. marinoi* G4 directly influenced the bacterial community. *S. costatum* and *T. rotula* are known to be associated with distinct bacterial communities (Grossart *et al.*, 2005), supporting the hypothesis of a direct influence. However, a recent study showed that the interactions are very complex with nutrient influences the relations between diatom and bacteria (Grossart and Simon, 2007). Because the densest cultures also had the lowest bacterial density, it is possible either that a higher density of *S. marinoi* slowed the growth of the bacteria or that a stochastically lower bacteria density of these cultures permitted a higher *S. marinoi* density. However, the bacterial community evaluation methods used here are not

precise and reproducible enough to postulate more than general hypothesis. These interactions between *S. marinoi* and the bacterial community require more experiments in order to be clarified, and were not the subject of this study.

Large pH variations are observed

The pH in the cultures changed during the experiment (**Appendix VII**), reaching more than 8.6 after day 10. Reasons for this change are unknown. The cultures were continuously bubbled, excluding any effect caused by a modification of carbonate ratio dissolved in the medium. The algae were cultured in artificial HEPES-buffered seawater. A possible explanation for the pH change is the use of the HEPES as carbon source by the bacteria. This hypothesis is supported by the increased pH which was also observed in the control culture, where only bacteria were present. The slower change in the control is consistent with the lower bacterial density in the control. However, the change of pH in the *S. marinoi* culture was certainly caused by multiple factors including not only the bacterial effect, but also the uptake and excretion of compound affecting the pH. The increase in pH could also participate in the transition of *S. marinoi* between growth phases, because phytoplankton growth rates can be greatly affected by pH variation (for a review, see (Hinga, 2002)). However, even different strains of the same species show huge differences in pH tolerance (Hinga, 2002), and therefore the pH effect on our culture growth rate cannot be estimated.

In summary, we could depict the conditions of the *S. marinoi* cells in the different phase sampling as follow:

- During the exponential phase sampling, cells were already phosphate limited, near silicate limitation but not nitrogen limited. Cell counts were still increasing, but the cultures were near the transition to stationary phase. Their metabolism was still adapted to a high growth rate and they were excreting nitrite. They were experiencing optimal pH, but already possessed a relatively stable and high bacterial community.
- During the stationary phase sampling, cells were at the onset of nitrogen limitation. They were experiencing a high pH and were at a transition point of the bacterial community.
- During the declining phase sampling, cells were limited in all nutrients except silicate. Their density was decreasing, and their photosynthetic machinery had started to degrade. The pH has returned to near initial values, and the bacterial community was dominated by one phenotype.

PUA production potential in S. marinoi G4 follows a different dynamic

S. marinoi G4 in culture has the potential to produce more octadienal than heptadienal (**Figure 2**), which is in contrast to previously studied strains (**Table 1**). This inverted relation has been verified several times with independent cultures of the same strain (data not shown).

The heptadienal production potential ($< 0.2 \text{ fmol cell}^{-1}$) was on the low side of the production range, when compared to other strains in culture or the measures in the Adriatic Sea (**Table 1**, **Figure 8**). In contrast to previous reports for other strains, the heptadienal production potential did not significantly increase when nutrients were limiting (in the stationary sampling). The production potential of heptadienal was also always much lower than its precursor's concentrations, EPA (**Figure 20**, **Figure 21**). In addition, the potential was not correlated with the level of EPA, suggesting that the production potential was not substrate limited. It is thus most likely the enzyme levels that were limiting. An alternate hypothesis would be that a part of the EPA was bound to another lipid pool that cannot be immobilised by phospho- and galacto-lipases.

In contrast, octadienal production potential was higher in stationary and declining phase, in accordance with the up regulation of the octadienal production pathway during nutrient limitation (*cf.* 2.1). In this case, the limiting factor was the substrate. Indeed, octadienal production potential was significantly correlated with its precursor HDTRI. The increase of this potential in stationary and declining phase was apparently due to the significant increase of PUFA during these phases (**Figure 21**). The content in EPA and HDTRI followed the same trends but the corresponding PUA did not. It is therefore clear that octadienal and heptadienal pathways are differently expressed.

Octatrienal production potential was in accordance to the potential of other strains (**Figure 20**, **Table 1**), and was not substrate limited. Octatrienal dynamics are less studied than the dynamics of other PUA, because the production potential levels of this compound are much lower and it is therefore more difficult to detect. In this experiment, it showed a dynamic that was the inverse to octadienal, with a significantly higher production potential in exponential phase than in either of the other phases (**Figure 20**). However, the lack of data from previous experiments makes the comparison difficult, and it is unclear if this dynamic is spread among the *S. marinoi* strains.

In addition to the phase-related dynamics, all PUA production potentials tended to decrease before the day to night transition in exponential and stationary phase. This trend, however, was not significant.

The total amount of fatty acids (1.5 ± 1 , 3.8 ± 3 , $5.1 \pm 2 \text{ pg cell}^{-1}$ in exponential, stationary and declining phase respectively) was in good accordance with previously reported data for a *S. costatum* strain of similar volume (Volkman *et al.*, 1989). In contrast, the PUFA relative composition was different when compared to previous data (**Figure 3**, **Figure 21**): EPA was only the second most abundant PUFA in *S. marinoi* G4, while HDTRI was the most abundant. This finding supports the altered PUA production potential of this strain.

A general increase of fatty acid content was observed between exponential phase and the two other

phases, with PUFA increasing the most. Particularly, a net increase in fatty acid content was observed the second day of the stationary sampling. This may reflect a response of the cell metabolism to nitrogen limitation. This increase in PUFA could contribute to the preference of copepods for late stationary phase *S. marinoi* G4 cells (Barofsky *et al.*, 2010). It should also be noted that this net increase in fatty acids at the end of the stationary phase could originate from normalisation errors. However, such an error would have also propagated on the PUA normalisations, which was not observed.

Intracellular metabolites significantly vary among growth phases

A distinction of the intracellular metabolites profiles between the growth phases was possible. The CAP method I used succeeded in identifying metabolites that were differently present in each phase. The majority of the differences were observed between exponential and declining phase, with metabolites often present in only one or the other of these two phases. Only a few metabolites characterised the stationary phase. A small part of the metabolites also characterised two phases. The optimised metabolomic method proved to be efficient in detecting changes in the intracellular metabolites of diatom cells.

Amino acids metabolism adapts to the growth phase

During the exponential phase, the cells require high amount of building blocks, including amino acids, to produce new cells, and nitrogen is not limiting. This very active metabolism explains why we observe high amounts of free amino acids in the cells in this phase (**Table 4**). In contrast, pyroglutamic acid, the derivative of glutamate and glutamine (Kanani and Klapa, 2007), was higher in the cells during stationary and declining phase. Glutamate is the major mediator of nitrogen introduction into the metabolism (Stryer, 1995), and it is a highly controlled metabolite. Recently, Brown *et al.* showed that the enzymes controlling the amination and use of glutamate in diatoms respond to nitrogen levels (nitrate, nitrite) and to diurnal cycles (Brown *et al.*, 2009). Because the amino acid metabolism is so active in exponential phase, glutamate is in high demand to provide the necessary amine groups and therefore its concentration remains low. We could expect a correspondingly higher concentration in α -ketoglutarate, the deaminated glutamate. However, the derivatisation methods I used are likely to degrade this compound (*cf.* Chapter 1). When nitrogen becomes limiting, in the stationary and declining phase, the *de novo* amino acid biosynthesis is reduced, leading to our observation of lower levels of amino acids. The activity of glutamate dehydrogenase (EC 1.4.1.4) is reduced in diatoms when nitrogen is limiting (Eppley and Renger, 1974). Higher level of glutamate can therefore build up in the cells, as observed (**Table 4**). The mechanisms leading to the accumulation of hydroxy-proline in the cell in declining phase are

unclear.

High metabolism in exponential phase

In addition to the amino acid metabolism, high relative levels of several sugars and fatty acids were observed in the exponential phase (**Table 4**). C16 fatty acids were the dominant metabolites of this latter class. EPA and linoleic acid were also at high levels. It is conceivable that the high metabolism in the exponential phase lead to the production of high relative levels of free fatty acids, however the total fatty acid content (**Figure 21**) was significantly lower in the same phase. This would indicate that the biosynthesis of high levels of lipids would be a later process occurring after the exponential phase.

The majority of the monosaccharides varying in between phases characterised the exponential phase, and the di- and tri- saccharides were at high level in both exponential and stationary phase samples (**Figure 22**). When resources (like iron or other nutrients) are not limiting, the whole metabolism is active and high photosynthesis rates lead to the accumulation of monosaccharides that are then incorporated into polysaccharide reserves or building blocks. In the stationary phase, the resources have become limiting, but photosynthesis still fuels the energy needs of the cells. The monosaccharides are not produced in high amount, and their levels are thus lower, but the reserve polysaccharides level remains high. The high level, in the exponential phase cells, of a hexonic acid and threonate, intermediates in sugar metabolism, is also probably linked to the high sugar metabolism during this phase (Stryer, 1995).

Glucose accumulates in the stationary phase

One of the only monosaccharides that were not observed at high levels in the exponential phase cells was glucose (**Table 4**). During this phase, most of the sugar metabolism is diverted to polysaccharide production, and glucose does not accumulate. In stationary phase, the lower metabolism probably allowed the accumulation of glucose.

Glycolysis is activated in the declining phase

In the declining phase, photosynthesis is impaired (**Appendix IV**). Activation of the glycolysis has been shown to be a response to iron limitation in *P. tricorutum* (Allen *et al.*, 2008). Such an iron limitation is possible in the declining phase. Because photosynthesis, dependent on iron, no longer fuels the cells with energy, the Calvin cycle is interrupted. The glucose pool is depleted, and the polysaccharides are degraded. This is supported by the low level of glucose and other saccharides in the cells sampled during declining phase. The observed increase in inositol in the cells in declining

phase could result from the degradation of lipids, but could also originate from glycolysis, via glucuronate. The use of an inositol shunt in diatoms to increase the exchange of reducing equivalents to the mitochondria under iron limitation has been suggested (Allen *et al.*, 2008). This could be used to mitigate the production of reactive oxygen species (ROS) in the mitochondria. The observed increase in glycerol could be a result of lipid catabolism.

The metabolic activity is lower in stationary phase compared to the other phases

Numerous unidentified metabolites are reported here to have high relative level in exponential phase, which is in good accordance with the overall high metabolic level already discussed. In declining phase, even more unidentified metabolites are detected at a high relative level. As discussed above, the catabolism (e.g. glycolysis) is high in this phase; therefore it is not surprising to find so many metabolites.

In the stationary phase, only a few metabolites have their peak relative concentration. The metabolism is then probably at lower level in this phase than in the other phases, and the majority of observed activity is in production of glucose by the photosynthesis, and the increase of lipid content (**Figure 21**).

Diurnal cycles are more difficult to characterise

Of the six CAP analyses performed separately on the different sampling points in each growth phase, only three led to significant groupings (**Figure 23**, **Figure 24** & **Figure 25**). The exponential phase cell metabolites profile harboured the most variation between the sampling points. Two patterns could be identified by the two CAP performed on these samples: first, when each sampling point was considered as distinct group, the CAP mainly separate the first day from the second (day-to-next-day); second was that CAP analyses detected the day-night differences. This latter pattern was not identified in the cell metabolite profile of any other phase. Only the day-to-next-day pattern was found in declining phase. The main patterns that can be seen were therefore more related to changes of the general metabolism and catabolism of the cells rather than to diurnal cycle.

The intracellular metabolite profiles of the stationary phase did not vary significantly enough over the course of the eight sampling points in this phase to allow separation with CAP. This is in good accordance with the hypothesised low level of metabolism in stationary phase.

Sugars and free fatty acids have an inverse day-to-next-day pattern in exponential phase

Sugars increased while fatty acids decreased over the exponential sampling. Only a few sugars

showed significant differences in the metabolite profile of the exponential phase samples. Their corresponding vectors in the CAP clearly indicated that they were accumulating over the course of the sampling (**Figure 23**). They were mainly produced at the end of the night and accumulate in the day-to-next-day pattern. In contrast, it appears that the free fatty acids were decreasing in a day-to-next-day pattern. This decrease in fatty acids was also observed in the total fatty acid content (**Figure 21**). It is clear that the total fatty acid content of cells decreased in the exponential phase. This may be attributed to the decrease of cell volume in the case of the total fatty acid content, but not in the case of the sum normalised free fatty acids relative level. This supports a lowering of fatty acid metabolism during the exponential phase. The majority of the carbon resources are then used for the sugar metabolism. It should be noted that the intensities of both classes decreased over the course of sampling in the declining phase, in accordance with catabolic pathway activated during this phase.

Amino acids are mainly biosynthesised during the night

During the exponential phase, where metabolism is the highest, most amino acids are biosynthesised in the night. From the vectors plot and the relative intensities (**Figure 23, Table 6**), it appears that most of the amino acids with intensities significantly varying were produced in the middle of the night. Glutamate concentration, on the other hand fluctuated. The nitrogen assimilation has been reported to potentially follow two similar enzymatic pathways, one activated during the day, and one activated during the night (Brown *et al.*, 2009). Both pathways, however, produce glutamate or glutamine. This accords well with the glutamate levels we observed. We can therefore suppose that the nitrogen assimilation occurs both at day and night time, and the energy accumulated during the day is also used during the night to produce amino acids. The variation of glutamate levels are the results of activation of two nitrogen assimilation pathways combined with amino acid metabolism demands. The only amino acid I observed which was not produced at night is proline. The production of proline in diatoms has already been reported to be very low at night in comparison to much higher rate for the other amino acids (Liu and Hellebust, 1976). One reason could be that the proline biosynthesis is very energy demanding (Krell *et al.*, 2007) and would therefore be reduced in the night. But proline could also play the role of an osmolite, and its level is reported to vary in response to osmotic stress (Krell *et al.*, 2007). The low level of proline observed when other amino acids levels peak could therefore also be a response to equilibrate the osmotic pressure.

Putrescine has a complex dynamic

Putrescine, a double aminated compound, globally increased in the intracellular profiles over

sampling of the three phases (**Table 4**) although it temporally decreased across the exponential phase sampling points (**Table 6**). This decrease during the actively growing phase could be attributed to the high needs in putrescine and higher polyamines for the formation of the siliceous frustules (Kröger *et al.*, 2000). On the other hand, the general increase in putrescine levels over the growth phases could be somewhat unexpected with regard to the nitrogen limitation that occurs in the stationary and declining phase. In plants, an increase in free putrescine levels has been associated with senescence (Paschalidis and Roubelakis-Angelakis, 2005). In addition, putrescine could be employed in photosynthesis quenching, when there is a mismatch between the energy collected by the chlorophyll antenna and the photosynthesis related metabolism (Sfichi-Duke *et al.*, 2008). Putrescine is also included in nucleosomes, and could therefore be released during senescence when DNA degrades (Ballestar *et al.*, 1996). Putrescine has therefore several important roles in the diatom metabolism and harbours a complex dynamics.

Other intracellular metabolites

The production of terpenes and terpenoids has been reported in diatoms in general (Rowland *et al.*, 2001) and in *S. costatum* in particular (Noureddine Yassaa *et al.*, 2008), but their specific roles in diatoms remain unknown. High relative levels of terpenes and related compounds were significantly associated with the declining phase. The roles of terpenes and terpenoids could therefore be related to the general stress state that the cells encounter in declining phase or in processes associated with resting stage cell formation.

Trihydroxybenzene observed at higher levels in exponential phase cells could be a UV protection (Amsler and Fairhead, 2005) induced by a higher light level received by the cells while the culture density is not maximal. However, this compound has not been previously reported from diatoms.

Diethylene glycol was detected in several intracellular metabolite profiles and shows significant variation between phases as well as among the sampling points of the exponential and declining phase. Diethylene glycol is not reported to be naturally produced and shows moderate toxicity to algae (Staples *et al.*, 2001). Its origin in our sample may be due to a contamination. Contamination after the sampling is unlikely, because its concentration increased over the growth phases. A release from the culturing vessel or aeration tube is more likely, followed by the absorption by the cells of this compound that easily translocates through the plasmalemma. In addition, diethylene glycol was not detected in the controls of the intracellular metabolite profiles, but was detected in the Easy extracts of the media.

Extracellular metabolite profiles significantly vary among growth phases

The method used to extract the metabolites from the seawater resulted in a high number of compounds not specific to diatom culture, as revealed by the blanks. An efficient correction strategy was therefore necessary. Great care had to be taken, when conducting experiments on the extracellular metabolites, to prepare and analyse the appropriate blanks along with the cultures. Despite this problem, the analysis of the metabolites present in the culture media revealed differences between the growth phases. CAP analysis of these extracellular metabolites succeeded in identifying differences associated with the different growth phases (**Figure 27**). The exponential phase extracellular metabolite profiles distinctly separated from the stationary and declining phase profiles. The primary observed pattern was an accumulation over the growth phases of extracellular metabolites. The exponential phase was therefore characterised by low levels of these metabolites, the stationary by either low or high levels, and the declining phase by high levels. In the context of the extracellular metabolite profiles, the stationary phase is only a transition phase between the exponential and the declining phase. The accumulation of different metabolites in the media is not surprising, and probably results from a constant excretion of compounds by the cells.

Only three compounds were detected at higher relative levels in the exponential phase samples, two of which remained unidentified. The third metabolite is hexadecanoic acid. This is probably a reflection from the high relative concentration of this fatty acid in the exponential phase cell metabolite profile. However, the other fatty acids present at high levels in these cells were not detected at high level in the media of the exponential phase. The release of fatty acids from diatoms has been reported; e.g., EPA has been suggested as autoinhibitor in a *S. costatum* culture (Imada *et al.*, 1992) and may play other roles including antibacterial activities (Desbois *et al.*, 2009). Several other fatty acids were present in the culture medium, with relatively high levels in all phases and with increasing levels in the declining phase. In contrast, metabolite 243, an unidentified fatty acid, was found at low levels in the exponential phase samples and showed a net increase in stationary. Given that free fatty acids could affect bacteria (Desbois *et al.*, 2009), the differential release of fatty acids could be associated with the bacterial community changes (**Appendix VI**). However several other unidentified metabolites showed similar patterns and could also be implicated in the interaction with the bacterial community. Further experiments will be required to test if these extracellular compounds released by *S. marinoi* affect the bacterial community.

Hydroxybenzoic acid was also detected in the media. Its relative levels increased in stationary phase samples and remained high in declining phase samples. Potentially this compound could serve as an iron chelator, excreted by the diatom to scavenge this important metal. The iron level was not measured, but it is probable that it is also depleted during the culture. This result is of

special importance since the reports of siderophore excretion by eukaryotic phytoplankton are not very extensive or reproducible (e.g. (Wells *et al.*, 2005)).

Galactosyl-glycerol is the only detected compound that was characterised by high levels in exponential and declining phase samples and a lower level in the stationary phase. Galactosyl-glycerol can originate from the degradation of galactolipids. This compound also serves as a regulator for the osmotic pressure in red algae (Ben-Amotz and Avron, 1983; Dickson and Kirst, 1987). High amounts of this compound could therefore be released when cells are dying and that lipase activities degrade the lipids or if the osmotic equilibrium changes rapidly. This latter case could occur when the metabolism is highly active in the cells in exponential phase or in declining phase. This compound could be excreted to compensate for the increase in other intracellular osmolites.

Finally, no amino acids and only a few sugars were identified in the medium. This is surprising, because diatoms are known to excrete high levels of these compounds (Myklestad and Haug, 1972; Myklestad *et al.*, 1972; Sharp, 1977). It is possible that due to the blank subtraction strategy required to eliminate unspecific peaks, a part of the extracellular compounds was not represented in the data analysed. Additionally, the SPE cartridges are not very efficient at extracting these polar compounds out of a seawater matrix. Serious development of the extraction of the metabolites from seawater is therefore required to achieve a good metabolomic profiling of the extracellular compounds released by diatoms.

Extracellular metabolite profile only reveal diurnal cycle in the exponential phase

As observed with intracellular metabolite profiles, diurnal cycle variations are difficult to detect with our technique. Only the exponential phase samples, when considering the groups of day and night sampling, revealed identifiable variation in the extracellular profiles (**Table 13, Figure 28**). All the highlighted metabolites increased in the night, except tetradecanoic acid. Once again, this shows potentially different dynamics for some fatty acids compared to other primary metabolites. Every metabolite, which increased in the night, remained at higher level the second day compared to the first day, except glucose and a trisaccharide. This supports the general dynamics of slow compound accumulation in the medium over the growth phases. Glucose and the trisaccharides are also released during the night, but they are probably rapidly consumed by the bacterial community. This cycle also supports the previously discussed hypothesis of a higher metabolism in the night discussed above.

2.4 Mesocosms



Mesocosms in Raunefjord, Norway

Experiment design

After having tested the metabolomic methods on *S. marinoi* G4 in culture, the method was adapted to field sampling. During 14 days in April 2008 (15-28.04.2008), in collaboration with Dr. Jens Nejstgaard and other groups, we conducted a mesocosm experiment in order to determine if we can induce a *S. marinoi* G4 bloom, and in that event follow the community on a metabolic level. Six 10 m³ enclosures were filled with seawater from the Raunefjord, near Bergen, Norway. These mesocosms, floating in the fjord, represent a good compromise between totally uncontrolled natural samples and lab cultures. They experience to the same weather conditions than the fjord, but the composition of nutrients and of the plankton community could be altered artificially. From the six enclosures, mesocosms A-C were designed as controls. Mesocosm A consisted of only fjord water. At day 1, B was supplemented with N and P, while mesocosm C was supplemented with N, P and Si. Mesocosms D-F were supplemented with the same nutrients as C, but, in addition, *S. marinoi* G4 in exponential phase was added as such that the cell density of this diatom reached ~100 cells mL⁻¹ (mesocosm D), ~400 cells mL⁻¹ (mesocosm E) or ~1000 cells mL⁻¹ (mesocosm F) (**Figure 29**). The mesocosm setup is described in (Barofsky *et al.*, 2010).

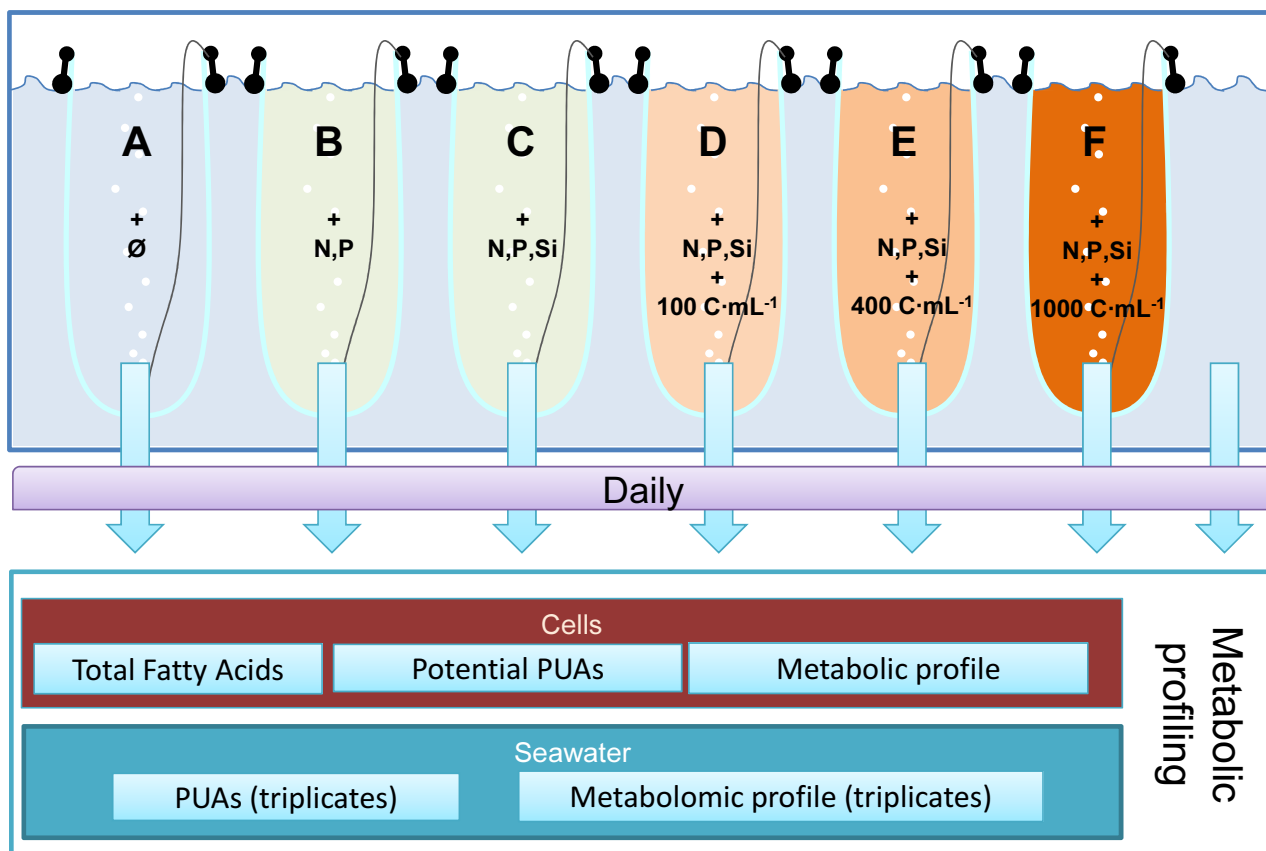


Figure 29 Mesocosm design. **Upper**, the 6 mesocosms of 10 m³ in the Raunefjord. A-F, mesocosms code, with the different nutrients and *S. marinoi* cells addition at day 1. **Lower**, the daily sampling design.

The full metabolomic design (**Figure 12**) was again used for this experiment. For the cells, samples for the total fatty acids, the potential production of PUA and metabolic profiling were taken daily from each mesocosm as well as from the fjord. For the profiles of extracellular metabolites, samples for dissolved PUA and metabolic profiling were also taken daily from the mesocosms and the fjord in triplicates (**Figure 29**). Samples were taken for 14 days (day 0-13). Fluorescence and plankton composition samples were gathered at the same time. However, the species composition and densities, analysed by another group, were not fully available at the time this thesis was written. Only cell counts for *S. marinoi* and *Phaeocystis* sp. are available. Therefore I will not present the cell metabolites and total fatty acid data, although I analysed them, as their major significance is in conjunction with the plankton community composition and density. However, a preliminary analysis revealed 329 quantifiable metabolites, 69 of which were identified (data not shown). Within the identified metabolites, 47 were also found in the *S. marinoi* cultures described in chapter 2.3.

The other data are presented, even though a more complete picture is likely to emerge when information about the plankton community is available.

2.4.1 Bloom development

In mesocosm A, a background level of *S. marinoi* was observed, but did not exceed 100 cells mL⁻¹ (**Figure 30 A**). When nitrate and phosphate, but no silicate, were added, the *S. marinoi* density increased slowly to a maximum of 600 cells mL⁻¹ at day 10 (**Figure 30 B**). With all nutrients (mesocosm C), *S. marinoi* increased until reaching 1000 cells mL⁻¹ at day 10 (**Figure 30 C**). In mesocosm D, with an addition of 100 cells mL⁻¹, *S. marinoi* did not bloom more than in mesocosm C and reached a maximum (780 cells mL⁻¹) at day 7 (**Figure 30 D**). With the two high inoculation treatment (400 and 1000 cells mL⁻¹, mesocosm E and F), *S. marinoi* entered a rapid growth phase and bloomed. The densities reached their maxima at day 8 (~17·10³ cells mL⁻¹) and day 7 (~70·10³ cells mL⁻¹) for mesocosm E and F respectively (**Figure 30 E&F**). In all mesocosms B-F, we also observed a bloom of *Phaeocystis* sp. (no data available for mesocosm A). This prymnesiophyte reached a maximum at day 9-10 in mesocosms B-E and at day 7 in mesocosm F (the same day as the *S. marinoi* bloom). In mesocosms B and C, the maximum *Phaeocystis* sp. densities were > 80·10³ cells mL⁻¹, while for mesocosm D-F they did not exceed 47·10³ cells mL⁻¹ (**Figure 30**). It is to be noted is that the lowest peak density of *Phaeocystis* sp. was attained in mesocosm F, in which *S. marinoi* formed the most intense bloom. Finally in mesocosms B-D, *Phaeocystis* sp. stayed relatively stable after peaking, while in the mesocosm E and F, concentrations started to decrease.

Preliminary analysis also revealed that *S. marinoi* and *Phaeocystis* sp. together contributed less than 10% of the total biomass present in the mesocosms (H. H. Jakobsen personal communication).

2.4.2 PUA

PUA production potential

In mesocosm A, no PUA other than trace amounts of decadienal were produced by the plankton (**Figure 30 A**). Decadienal was expected to be found in some samples because *Phaeocystis* sp. has been shown to produce this PUA (Hansen *et al.*, 2004). The plankton in the fjord water did not produce any PUA (data not shown). In mesocosms B, C and D, low heptadienal and decadienal production potential was detected. In these mesocosms, the decadienal potential slowly increased until reaching 0.8-0.9 nmol L⁻¹ at day 6. Then at day seven, the day when *Phaeocystis* sp. entered stationary phase, the production jumped to over 1.5 nmol L⁻¹, and stayed relatively stable until day 12 (**Figure 30 B-D**). If *Phaeocystis* was the only decadienal producer, the potential production of PUA was of 18-38, 8-48 and 56-97 amol decadienal cell⁻¹ in mesocosms B, C and D respectively. In mesocosms E and F, the decadienal increased to peak at day 8, with 8.7 and 5.7 nmol L⁻¹ respectively, before decreasing the next day (**Figure 30 E & F**). With these values, if *Phaeocystis* sp. was still the only producer, the potential production reached 300 and 290 amol decadienal cell⁻¹. Additionally, the per cell decadienal potential in mesocosms E-F was always higher than in the other mesocosms.

In mesocosm B, heptadienal production potential slowly increased until day 10, also the day of the highest *S. marinoi* density in this mesocosm, reaching 0.56 nmol cell⁻¹ (**Figure 30 B**). In mesocosms C and D, the heptadienal potential reached its maximum at day 8, following the *S. marinoi* density, eventually measuring 0.88 and 0.69 nmol L⁻¹ (**Figure 30 C & D**). In mesocosm E, the potential reached its maximum, 5.96 nmol L⁻¹, at day 7, one day before the maximum of *S. marinoi* density, while in mesocosm F, it reached a maximum of 6.8 nmol L⁻¹, at day 8, one day after the maximum of *S. marinoi* (**Figure 30 E & F**). If normalised by the *S. marinoi* cell density, the potential production values was similar in all mesocosms (0.3-1.3 fmol cell⁻¹).

Octadienal was detected only when the *S. marinoi* density was highest, in mesocosm E and F (**Figure 30 E&F**). The potential reached its maximum at day 8, measuring 0.17 and 0.21 nmol L⁻¹ respectively (10 and 6 amol *S. marinoi* cell⁻¹).

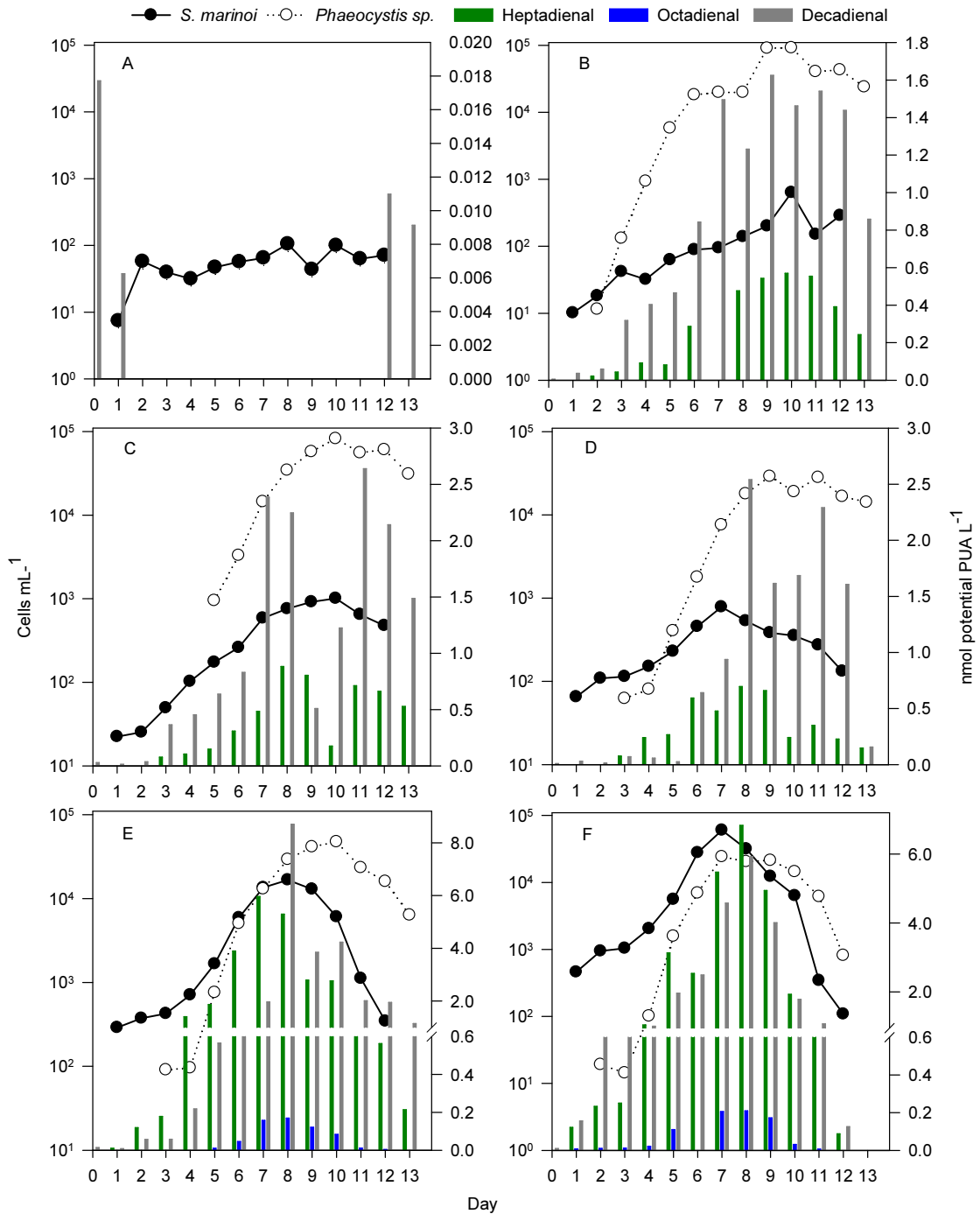


Figure 30: PUA production potential by the cells of one litre of mesocosms water, *S. marinoi* and *Phaeocystis sp.* densities. **A-F**, mesocosms A-F. Note the logarithmic scale on the right for the cell counts and the different scales on the left for the PUA production potential.

PUA in the seawater

Low background levels of heptadienal, octadienal and decadienal were detected in mesocosm A ($<0.025 \text{ nM}$), but with extreme variations (**Figure 31 A**). No PUA were detected in the open fjord water (data not shown).

In mesocosms B-D, the decadienal concentration in the water remained very low until day 7-8.

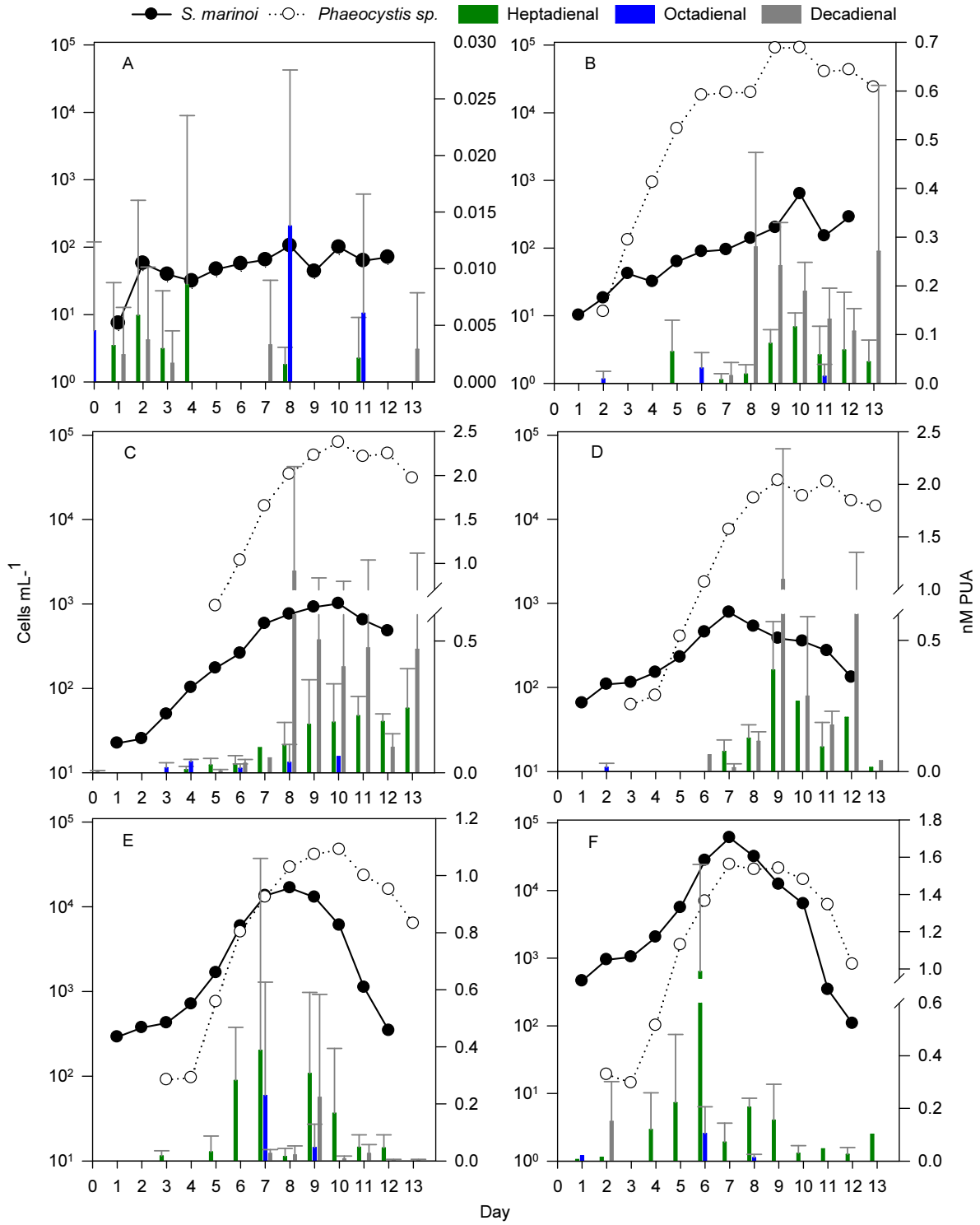


Figure 31: Dissolved PUA, *S. marinoi* and *Phaeocystis sp.* in mesocosms A-F. PUA values are average \pm standard deviation (n = 3). Note the logarithmic scale on the left for the cell counts and the different scale on the right for the PUA nM.

The next day, corresponding to a jump in the production potential, the concentration drastically increases to reach 0.28 ± 0.19 , 1.0 ± 1.0 and 1.09 ± 1.0 nM (**Figure 31 B-D**). It then decreased gradually on the next days before re-attaining the initial value in the last or penultimate day (**Figure 31 B-D**). In mesocosms E and F, decadienal was found only in very low concentrations (**Figure 31 E&F**).

The heptadienal remained low in mesocosm B and C, increasing to ~0.1 nM towards the end of the experiment. In mesocosms E and F, it increased to reach ~1 nM on the day before *S. marinoi* reached its maximum density, dropped on the day of *S. marinoi* maximum, re-increased to 0.2-0.3 nM the first day of the *S. marinoi* decline and then declined until the end of the experiment (**Figure 31 E & F**). These are only trends, the differences between the days are not significant, except between day 6 and 7 in mesocosm F (t-test, $p = 0.049$).

Finally only very low levels of octadienal were detected, in mesocosms B, C, E and F, without clear trends.

2.4.3 Dissolved metabolites

Like in the case of the dissolved metabolites from the culture, very high numbers of peaks were detected (a maximum of 469). However, a large proportion of these peaks were also present in high intensity in the blank mesocosms (A). I therefore applied the same subtraction strategy as in the culture survey. This resulted in 79 peaks that were more than 3-fold more intense in at least one of the triplicate sets of mesocosms B-F compared to the corresponding day of mesocosm A. The resulting list of metabolites was examined manually for structure identification (**Appendix XII**). As a first analysis, I calculated the correlation of each compound found with the cell density of *S. marinoi*, *Phaeocystis* sp. and the total chlorophyll a. Secondly a K-mean clustering allowed a further classification of the uncorrelated compounds (**Table 14**). Thus the compounds were separated in 9 groups.

First, 22 compounds correlated significantly with *Phaeocystis* sp. density. This included saccharides, disaccharides, myristic acid, an unknown C20 fatty acid, a terpene, a hydroxy fatty acid and galactinol. All these compounds generally increased with the *Phaeocystis* sp. density.

A second group was formed by 15 compounds which correlated with *S. marinoi* density. They were mainly present in mesocosm F. This group included glucose, several other saccharides, hexadecenoic acid, hexadecenoic acid, a sterol, an inositol isomer and two unidentified compounds that were also found in the *S. marinoi* cell during the culture experiment (*cf.* 2.3).

A third group of 8 compounds significantly correlated with the chlorophyll a content. Aspartic acid, hexadecadienoic acid and two sugars were the only identified metabolites in this group.

The last six groups were formed by the K-mean clustering. A first group (cluster 1) was only formed of pentafuranoses, characterising the declining phase of *S. marinoi* in mesocosm F, but which was also present in the last days of mesocosm B. The next group was composed of three

Table 14: Dissolved metabolite intensities in the 6 mesocosms and in the sea. The intensity of each metabolite is reported relative to the highest value for the compound in all samples. The highest intensity is in red, not detected in blue. For each mesocosm column, each day is represented from left to right. Each coloured rectangle represents the average of three measures.

N°1	Mesocosm						SEA	Correlation			
	A	B	C	D	E	F		Sk ²	Ph ³	Chl ⁴	Class ⁵
<i>S. marinoi</i>											
<i>Phaeocystis</i> sp.											
Chlorophyll A								0.6	0.48		
136 -									0.32		6
222 -									0.32		6
200 Terpen??									0.33	0.6	6
261 Hydroxy-octadecanoic a									0.34		6
151 Pentafuranose									0.35		6
195 -									0.36		6
185 Sugar alcohol									0.39	0.3	9
232 -									0.4	0.3	6
269 C20:x??									0.42	0.4	9
246 -									0.44	0.4	6
75 Phosphate??									0.45	0.4	10
237 -									0.46	0.5	2
336 -									0.49		6
419 Saccharide									0.51	0.4	8
291 Galactinol??								0.34	0.55	0.7	4
202 Tetradeconoic acid									0.59	0.5	5
413 Saccharide									0.59	0.3	2
289 Galactosyl glycerol								0.31	0.64	0.7	5
421 Saccharide									0.7	0.4	7
296 Disaccharide?									0.74	0.6	6
226 -									0.75	0.5	6
395 Disaccharide									0.77	0.6	8
213 Glucose								0.31			6
248 -								0.31			6
446 Trisaccharide								0.31		0.4	6
115 Tetrose?								0.33		0.3	6
168 Pentose								0.34		0.3	6
343 -								0.37		0.4	9
162 Pentafuranose								0.39		0.3	6
238 Hexadecenoic acid								0.41		0.3	6
267 Skel-cell 128								0.43		0.5	6
429 Trisaccharide								0.44		0.4	6
401 Sterol								0.45		0.5	2
273 Skel-cell 131								0.49		0.4	6
266 -								0.5		0.6	2
240 Inositol isomer								0.52		0.6	6
242 Hexadecenoic acid								0.6		0.4	6

N°1	Mesocosm						SEA	Correlation			
	A	B	C	D	E	F		Sk ²	Ph ³	Chl ⁴	Class ⁵
<i>S. marinoi</i>											
<i>Phaeocystis</i> sp.											
Chlorophyll A							0.6	0.48			
129 Aspartic acid									0.3	6	
432 Trisaccharide									0.3	4	
235 Hexadecadienoic acid?									0.3	9	
141 -									0.3	9	
60 -									0.4	9	
180 -									0.4	6	
279 -									0.4	4	
187 Desoxyhexose ?									0.5	9	
149 Pentafuranose										1	
148 Pentafuranose										1	
145 Pentafuranose										1	
155 Pentafuranose										1	
124 Hydroxybenzoic acid										2	
329 -										3	
327 -										4	
134 -										6	
123 -										6	
52 -										6	
218 -										6	
225 -										6	
320 C20:0??										6	
444 Trisaccharide										6	
229 -										6	
311 -										6	
449 -										6	
214 -										6	
56 -										6	
209 -										6	
326 Hexosephosphate?										6	
53 -										6	
349 Sugar alcohol??										6	
167 Pentose										6	
101 -										6	
353 Disaccharide?										6	
346 Disaccharide										8	
447 -										8	
147 -										9	
143 -										9	
230 -										9	
319 -										10	
301 Inositolphosphate										10	
345 -										10	

¹ metabolite number, as in **Appendix XII**. ^{2,3,4} significant Pearson product moment correlation (p<0.001), between metabolite intensity and *S. marinoi* (²), *Phaeocystis* sp. (³) or total Chlorophyll A (⁴). ⁵ classification by K-mean clustering based on Euclidian distance, with 10 clusters. Metabolites are tagged with "?" if the reverse match of the comparison with the library was lower than 800 and with "??" if the score was lower than 700.

compounds each clustering separately (cluster 2, 3 &4), without identifiable pattern. The only identified compound in this group is hydroxybenzoic acid, which was present along almost every sampling point, with a higher intensity in mesocosm F.

The cluster 6 formed the next group. This was the largest group identified with 19 compounds; however most of the metabolites remained unidentified. The general trend observed in this group was an increase in the last days of mesocosm B-F, with the highest intensity in mesocosm F, during the *S. marinoi* decline. The only identified metabolites in this case were sugars and eicosanoic acid.

The last three groups were each formed by 2-3 compounds, without clear patterns. The only two metabolites identified in these groups were a disaccharide and inositol-phosphate. Almost all compounds remained very low in mesocosm A and in the fjord water.

2.4.4 Discussion

A bloom of *S. marinoi* can be caused by initial cell density

The modification of the phytoplankton ratio at the beginning of the experiment proved to be sufficient to trigger a bloom of *S. marinoi*. The two highest *S. marinoi* inoculations triggered distinct blooms of this species, even in the presence of *Phaeocystis* sp. as a competitor, while the lowest inoculation failed to do so. We can therefore conclude that the starting cell density at the moment of nutrient increase can determine which species will bloom. The threshold for allowing a bloom of *S. marinoi* is somewhere between 200 and 400 cells L⁻¹.

High decadienal production potential is associated with *Phaeocystis* sp. peak density

Phaeocystis sp. also bloomed in the mesocosm, and a decadienal production potential was detected (**Figure 30**). *Phaeocystis pouchetii* has previously been shown to produce decadienal (Hansen *et al.*, 2004), although our laboratory tests did not confirm this potential (data not shown). The decadienal production potential was associated with *Phaeocystis* sp. density, and a net increase was detected when this alga was in stationary phase in the mesocosms. It is possible that the PUA production potential in *Phaeocystis* sp. is, as found for *S. marinoi*, dependant on several factors including strains, nutrient status and growth phase. The potential is higher in the mesocosm with high *S. marinoi* density. This could be a stress response or defence mechanism produced by *Phaeocystis* sp. in response to cues released by *S. marinoi*, as suggested by (Hansen and Eilertsen, 2007). It could alternatively be a response to lower concentrations of some nutrients due to the higher biomass of *S. marinoi*.

Heptadienal and octadienal ratio indicates a strong regulation of the PUA production potential

The heptadienal production potential per *S. marinoi* cell was higher than the octadienal production potential, in opposite to the culture observations with *S. marinoi* G4. However the majority of the *S. marinoi* in the mesocosms E and F is assumed to be the G4 strain, because this is the one used for the inoculation. This inverted ratio was also observed in a preliminary mesocosm experiment with the G4 strain (data not shown). The normalised value per cell (0.3-1.3 fmol heptadienal cell⁻¹, 10 amol octadienal cell⁻¹) showed a higher potential for heptadienal than in culture and a much lower potential for octadienal than in culture. This indicates that extreme modifications of the PUA production potentials can be observed in the same strain in response to different environments. The mesocosm conditions are closer to the natural competition conditions, and such a modification of the PUA production potential indicates a strong regulation of this pathway. In addition, alternative sources for the PUA might have to be taken in account.

Decadienal concentration in the water is reduced in the presence of high densities of *S. marinoi*

The concentration of decadienal in the seawater followed the production potential in mesocosms B to D, with a net increase when *Phaeocystis* sp. was in a stationary phase. However, almost no decadienal was detected in the water of mesocosms E and F. Either the decadienal was absorbed more quickly because the biomass was denser in these mesocosms, or its release was reduced. In both cases, a potential defensive role against *S. marinoi* from *Phaeocystis* sp. (Hansen and Eilertsen, 2007) seems to not be supported because the competition with *S. marinoi* was the highest in these mesocosms.

Heptadienal is released just before *S. marinoi* peaks

Two different patterns of dissolved heptadienal concentration could be identified. First, in all mesocosms heptadienal was released at the end of the experiment. This could be attributed to the cell lysis during the decline of *S. marinoi*. The second pattern was seen in the mesocosms where *S. marinoi* bloomed. In both mesocosms E and F, a peak of heptadienal was observed the day before the cell density peaked and then started to decline. This supports the potential role of heptadienal in preparing the cell to enter a declining phase, as observed in culture (**Figure 8**).

Extracellular metabolite profiles are correlated with *Phaeocystis* sp. and *S. marinoi* densities

The extracellular metabolite profile analysis was affected by the same problem as in the culture,

namely a high number of unspecific peaks. However, the use of mesocosm A as a blank allowed us to bring out 79 compounds, a majority of which could be identified (**Table 14**). The intensities of 22 compounds were correlated to *Phaeocystis* sp. density. These compounds were mainly sugars, which is not surprising. *Phaeocystis* is indeed known to excrete high amounts of saccharides, partly to form its colonial matrix (for a review, (Alderkamp *et al.*, 2007)). It is probable that the matrices of *Phaeocystis* colonies are also at least partly retrieved on the SPE cartridge during sampling.

Fifteen metabolites were correlated with *S. marinoi* cell density. These were mainly sugars, but also hexadecenoic acid. This latter was also identified in the extracellular metabolites from *S. marinoi* cultures (*cf.* 2.3.5). Two unknown metabolites found in the metabolite profile of *S. marinoi* cells in culture were also identified in this group. This supports the association of this group of metabolites with *S. marinoi*.

Other fatty acids were also detected (hexadecadienoic and tetradecanoic acid), further supporting a potential role of fatty acids in the plankton interactions.

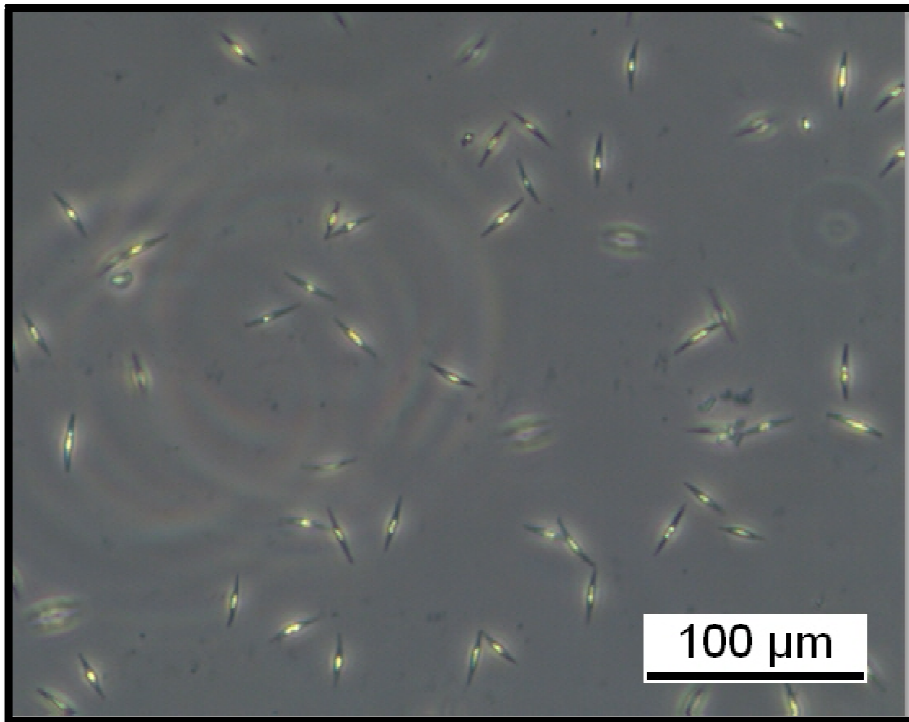
Some other metabolites were correlated with chlorophyll a concentration, therefore indicating general release of these compounds by photosynthetic organisms.

A big group of metabolites had their peak concentrations at the end of the experiment, especially in mesocosm F, when the blooming species were declining. These compounds are therefore probably released by cell lysis and degradation.

Hydroxybenzoic acid was again detected in the water, with high relative concentration in mesocosm F while *S. marinoi* was actively growing. This supports the hypothesis that *S. marinoi* actively release this compound, possibly to gather iron.

Deciphering the origin, fate, and function of released metabolites in a mesocosm experiment is a complex task. The knowledge of the species or class composition is required for more detailed analysis, but here we show that some metabolites can already be attributed to specific species.

2.5 Decadienal treatment on
Phaeodactylum tricornutum



Phaeodactylum tricornutum

In 2005, an Expressed Sequence Tag (EST) library resulting from different treatments on *P. tricornutum* was made available (Maheswari *et al.*, 2005). Two of the treatments included in this library are addition of decadienal. A “high treatment” (final concentration in the culture $5 \mu\text{g mL}^{-1}$, $\sim 33 \mu\text{M}$) and a “low treatment” ($0.5 \mu\text{g mL}^{-1}$, $\sim 3.3 \mu\text{M}$) were applied for 6 hours before extracting the RNA for the EST generation (<http://www.diatomics.biologie.ens.fr/EST3/>, 2005). These treatments were motivated by the earlier observation of the complex Ca^{2+} / NO response triggered by decadienal in *P. tricornutum* (Vardi *et al.*, 2006).

I decided to repeat the “low treatment” experiment and to perform a metabolomic analysis on the intracellular metabolites and those released in the medium. Only a limited sampling design was used. The cells and medium were sampled in exponential phase before decadienal addition and 6 hours (as for the ESTs), 24 hours and 48 hours after the decadienal treatment.

2.5.1 ESTs preliminary analysis

A preliminary analysis of the EST library for the “low treatment” revealed 409 genes that were specifically up-regulated (**Table 15**). The major identified genes are related to signalling and DNA/RNA associated proteins (e.g. histone deacetylases). Next come genes associated with transport, detoxification, lipid and membrane related proteins. A few genes of other pathways of the central metabolism (amino acids and sugars mainly) are up-regulated (**Table 15**). Based on this preliminary analysis, the “low treatment” seemed appropriate for metabolic profiling.

Table 15: Gene classes up-regulated in the low decadienal treatment.

Gene class ¹	Number up regulated	Gene class ¹	Number up regulated
Other/unidentified	233	Stress response	5
Signalling	34	Cell cycle	5
DNA/RNA associated	32	Defence related	3
Transport	18	Protein synthesis	2
Detoxification	15	Light associated	2
Lipid metabolism	12	Heat shock protein	2
Membrane related	10	Other in central metabolism	2
Sugars metabolism	7	DNA repair	2
Proteasome related	7	Nucleotide metabolism	2
Proteases	7	Oxidoreduction related	1
Amino acids metabolism	7	Inositol metabolism	1

¹, Class assigned based on the predicted proteins

2.5.2 Metabolomic profiling

The cultures were in exponential phase at the time of decadienal addition and the treatment had no effect on the cell growth (**Figure 32 A**). At the time points $T = 0\text{h}$, 6h , 24h and 48h , the concentration of decadienal was assessed in the treated cultures as well as in one control culture. No decadienal could be detected in the medium before the addition (data not shown). Six hours after decadienal addition to a final concentration of $3.3\ \mu\text{M}$ in the culture, the concentration of decadienal had decreased to $76.2 \pm 30.9\ \text{nM}$. At $T = 24\text{h}$ and 48h , the concentration were $2.4 \pm 0.5\ \text{nM}$ and $1.6 \pm 0.6\ \text{nM}$ respectively (**Figure 32 B**). In the control culture, low concentrations of decadienal, 0.87 and $0.91\ \text{nM}$ at $T = 6\text{h}$ and $T = 48\text{h}$ respectively, could be detected as well. Decadienal was not detected anymore at $T = 48\text{h}$ for the control (**Figure 32 B**).

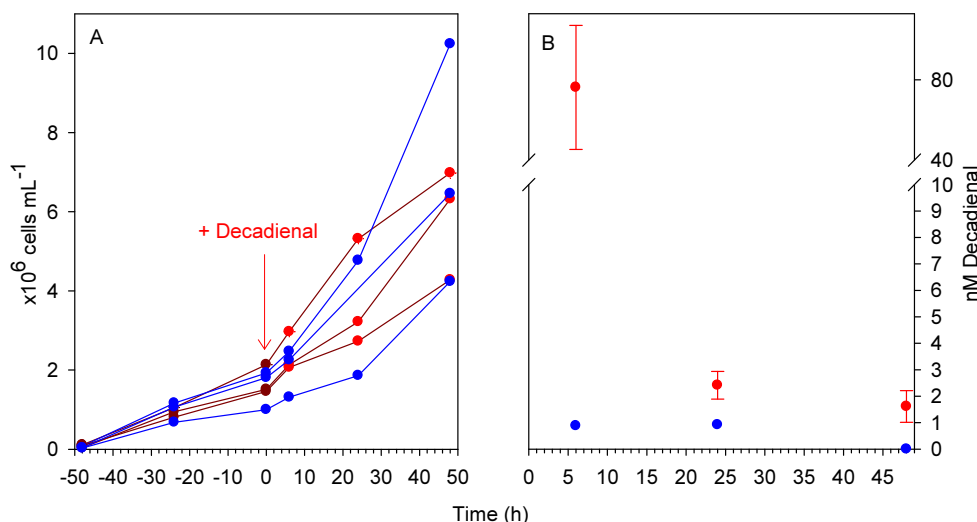


Figure 32: **A**, *P. tricornutum* cell density. In red, cultures treated (at $t = 0$, indicated by an arrow). In blue, control culture (methanol treated). **B**, decadienal concentration in the culture medium after treatment. In red, in the treated culture, (average \pm standard deviation, $n = 3$). In blue, in a control culture ($n = 1$).

A total of 283 peaks could be extracted and quantified from the chromatogram of the cellular metabolites. In the chromatogram of the metabolites released into the medium, after correction for blank peaks (*cf.* 2.3), 74 peaks were retained for analysis.

The CAP analysis of the cellular metabolites proved unable to find a difference between the control and the treated cultures, at any sampling point. The eigenvalues and Δ^2 are low, the misclassification high, and the statistics were not significant in any case. This means that the control and treatment cannot be separated and are not significantly different (**Table 16**). Visual evaluation of the separation confirmed these results (**Figure 33 left**).

Table 16: Eigenvalues (λ), correlation (Δ^2) and diagnostic statistics of the CAP analyses on the cells and medium metabolites, before ($T = 0$) and after 6, 24 and 48 hours ($T = 6$, $T = 24$ and $T = 48$) after the decadienal treatment.

	Constrained canonical axes			Statistics		
	T	λ	Δ^2	Crossvalidation Misclassification	Permutatest Trace stat.	1 st Δ^2
Cellular metabolites	0	0.37830	0.14311	83.3%	$p = 0.989$	$p = 0.989$
	6	0.20337	0.04136	80.0%	$p = 0.793$	$p = 0.793$
	24	0.00701	0.00005	10.0%	$p = 1.000$	$p = 1.000$
	48	0.67217	0.45181	50.0%	$p = 0.683$	$p = 0.683$
Medium metabolites	0	0.82909	0.68740	33.3%	$p = 0.187$	$p = 0.187$
	6	0.44496	0.19799	83.3%	$p = 0.777$	$p = 0.777$
	24	0.64392	0.41463	66.6%	$p = 0.513$	$p = 0.513$
	48	0.61991	0.38428	66.6%	$p = 0.621$	$p = 0.621$

In the case of the dissolved metabolites, a preliminary analysis detected a grouping at $T = 6$ (data not shown). This grouping relied on a single metabolite that was significantly higher in $T = 6$ and decreased rapidly in $T = 24$ and 48. The analysis of the spectrum resulted in the identification of methoxymated decadienal. When the CAPs were conducted excluding the metabolite corresponding to decadienal, no grouping was achieved, similar to the cellular metabolites (**Figure 33** right, **Table 16**).

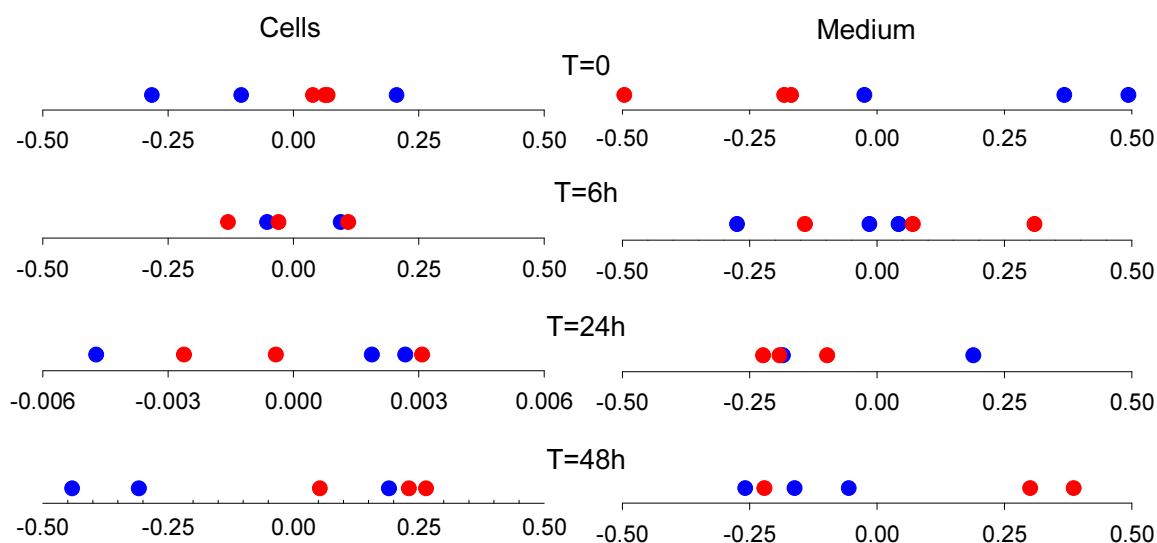


Figure 33: CAPs grouping of *P. tricornutum* metabolites, based on cellular metabolites (left) or on metabolites from the medium (right), before, 6 hours, 24 hours, and 48 hours after decadienal addition. Blue circles, control (methanol treated); red circle, treated cultures.

2.5.3 Discussion

Decadienal did not trigger a detectable metabolic response

Despite the large number of metabolites detected in the cells, no modifications of the intracellular profiles were detected when decadienal was added, in comparison to the control culture. Similarly, no effect on the culture growth was observed. It is possible that no significant metabolism alteration was triggered by the low treatment, and that the active metabolism of the exponential growth was only minimally disturbed. The profiles were different between the different sampling points, but were similar in both the treated and control at the same sampling time (data not shown). An active metabolism in the exponential phase could then mask a small metabolic response to the treatment. It is also possible that the metabolic response to the treatment was only transient and only an early sampling would have detected it.

The analysis of the extracellular metabolite profile revealed many metabolites, but here also, no alteration was observed in comparison with the control culture. The CAP succeeded in identifying one different compound present only in the treatment, at low concentration, but this compound was decadienal. This proves that the method is able to pinpoint differences in the extracellular metabolite profile, even if it is only one compound in low concentration.

Another explanation of the absence of response of the cultures on the metabolic level, despite the evidence of a genetic response, lies in a possible different exposition of the cells to decadienal. The analysis of the decadienal concentration in the treated culture showed a rapid decrease. In six hours, the concentration dropped from the 3.3 μM reached directly after the addition to 80 nM. The concentration was only 2 nM after 24 hours. This proves that PUA are quickly eliminated from a bubbled culture, and therefore the exposition of cells to a high enough concentration of decadienal may have not lasted long enough to trigger the response. This highlights the absolute need for precise and detailed description of the culture parameters in order to allow comparison of “omics” experiments.

3. Conclusion

The purpose of my PhD research was to characterise the physiological changes in diatoms in response to environmental stimuli. To that end, I designed a metabolic profiling technique, optimised from plant metabolomics. I successfully applied this technique to the survey of *S. marinoi* metabolism in culture and field experiments. It led to the identification of fluctuations within both the intra- and extra-cellular metabolites of *S. marinoi* depending on the growth phases. I also specifically investigated the dynamics and roles of proposed signalling molecules, the polyunsaturated aldehydes (PUA).

Several factors modified the amount of PUA produced by the cells after wounding (PUA production potential). Complex influences of the nutrient status on PUA production potential were observed. Si and P limitation increased the potential, while N limitation decreased the potential. PUA were previously considered to be only released after cell wounding, but I showed that PUA are released by healthy cells in cultures. PUA were released in a short period before the initiation of the declining phase. This pulse was also observed the day before the cells peaked and started declining in mesocosms where *S. marinoi* was blooming. The presence of PUA in the seawater was also detected in the north Adriatic Sea, and could be correlated with *S. marinoi* blooms. An addition of PUA at a biologically relevant concentration to a late stationary phase culture triggered the declining phase in this culture. The presence of PUA in the medium associated with other factors, probably a nutrient limitation, can thus cause diatoms to transition to declining phase, and possibly synchronise bloom termination.

The metabolic survey of a *S. marinoi* culture allowed me to draw a hypothetical picture of the main metabolic changes observed during the different growth phases (**Figure 34**). In exponential phase, the metabolism is very active, and produces many primary metabolites. The energy collected during the day allows, among others, the assimilation of nitrogen into glutamate. During the night, this energy is used to fuel the biosynthesis of amino acids as well as mono- and poly-saccharides. The fatty acid metabolism on the other hand seems to be reduced and the fatty acid pool is low in exponential phase (**Figure 34** upper). When silicate and phosphate become limited, the cells enter stationary phase and finish assimilating the nitrogen resources. When nitrogen becomes limiting, the amino acid metabolism is shut down, and a relative increase in glutamate is observed. The sugar metabolism is reduced, leaving mainly the polysaccharide pool. The energy collected by photosynthesis in this phase fuels the formation of glucose and the replenishment of the fatty acid pool (**Figure 34** middle). The cells enter declining phase, maybe under the control of increased PUA concentration in the medium, and other factors (iron limitation). Glycolysis is activated and the saccharide pool is used up. An inositol shunt is perhaps activated to convey reducing

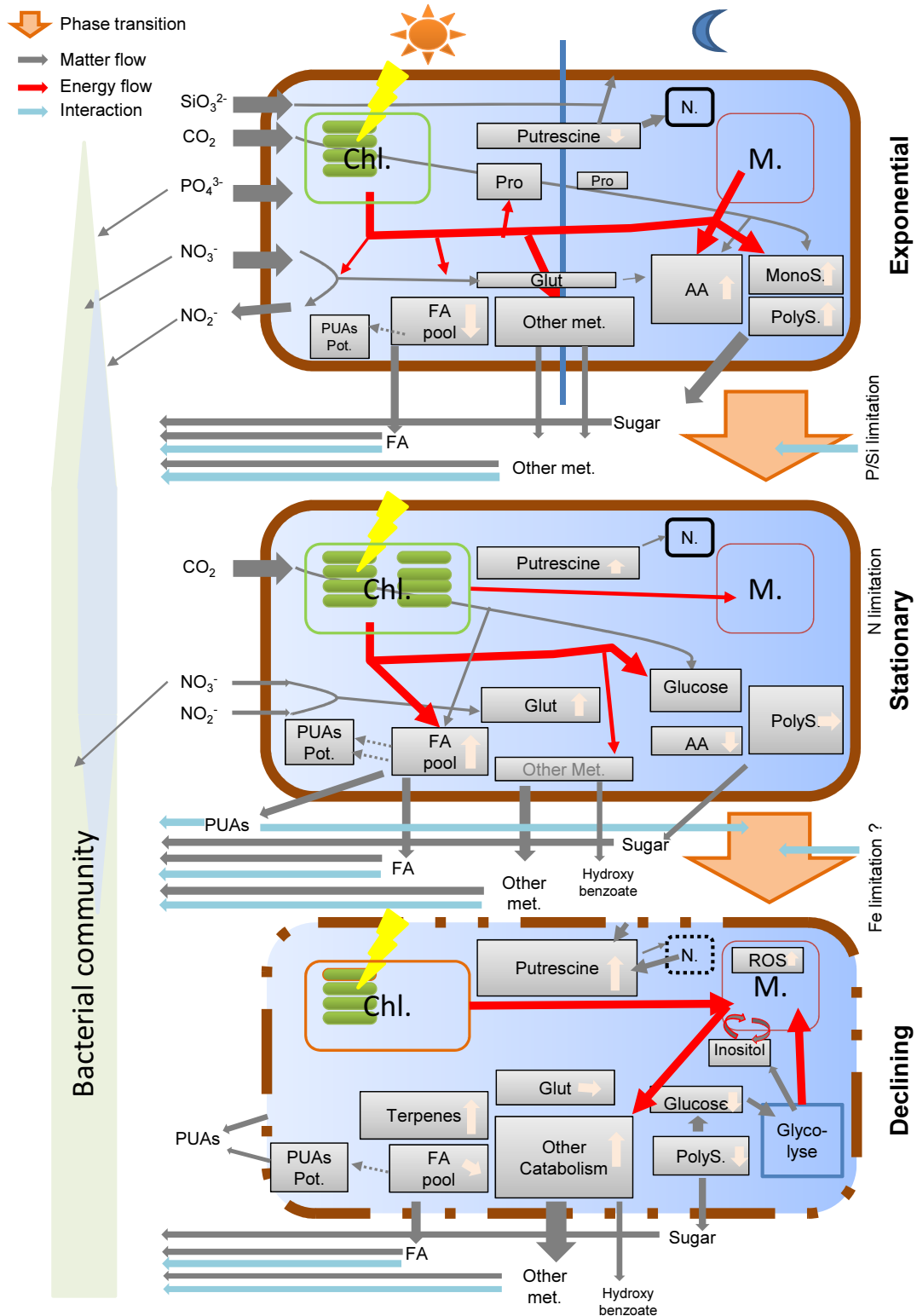


Figure 34: Scheme of the *S. marinoi* metabolism in different growth phases and factors influencing transitions between phases (orange arrows). Chl.: chloroplasts. M.: mitochondria. N.: nucleus. MonoS: monosaccharides. PolyS: polysaccharides. AA: amino acids. Pro: proline. Glut: glutamate. PUA Pot: PUA production potential. The sun and moon indicate the day and night cycle in exponential phase. The arrows in the boxes represent the changes in metabolite pools. The grey arrows represents the matter flow, the red arrows the energy flow and the light blue arrows represent the potential interactions on the bacterial community and on the transitions.

equivalents to the mitochondria, probably to mitigate the reactive oxygen species (ROS) building up. ROS could occur because of impaired photosystems. An increase of terpene and putrescine concentrations is observed in this phase, as well as of numerous other unidentified metabolites (**Figure 34** lower).

Over the phases, diverse metabolites are released in the medium, including sugars, fatty acids, steroids and other metabolites. Some of these metabolites were also found to be released in close to natural bloom conditions (mesocosms). These metabolites can on one hand provide food to the microbial community, but on the other hand, evidence accumulates that they could also influence the bacterial community composition.

My results provide valuable insight into the diatom metabolism in different growth phases. This novel comprehensive metabolic analysis of diatom physiology reveals interesting differences in major pathways of the central metabolism. The sugar and amino acid metabolisms seem to be predominant in exponential phase while fatty acid accumulation occurs in stationary phase.

This basic picture of the physiology change during the phases and the complex regulation of the PUA pathways will be very useful for studies that want to understand the interactions in the phytoplankton and with the zooplankton.

Future research will be needed to optimise the extraction of metabolites from seawater, but already with the methods I developed it will be possible to go more into detail concerning the relation between diatoms and the other members of the plankton community. The fatty acid are a promising class to study for the regulation of the bacterial community, but a comprehensive picture can only be drawn if the sugars are also analysed. The completely unknown roles of terpenes, hydroxybenzoic acid and putrescine are also of great interest.

4. Materials and Methods



SPE of mesocosms samples

Preliminary note:

Unless otherwise mentioned, chemicals and supplies were obtained from Roth (Karlsruhe, Germany), Sigma-Aldrich (Munich, Germany) or VWR (Dresden, Germany). Liquid volumes < 5 mL were handled with Eppendorf pipettes and Eppendorf Tips (Eppendorf, Hamburg, Germany). High grade methanol (Chromasolv © Plus >99.9%, Sigma-Aldrich) and hexane (Suprasolv, Merck, via VWR) were used for all experiments. The grades of other solvents are described in subsequent sections.

4.1 Culturing

4.1.1 Strains

Skeletonema marinoi strain RCC75 was obtained from Roscoff culture collection, Roscoff, France.

Skeletonema marinoi strain G4 was obtained from Jens Nejstgaard, Department of Fisheries and Marine Biology, University of Bergen, Norway. This strain was isolated from Raunefjord (60.269° N, 5.219° E).

Skeletonema marinoi strain CCMP 2092, originally isolated from the Adriatic Sea, was obtained from the Provasoli-Guillard National Center for Culture of Marine Phytoplankton, Booth Bay Harbor, USA.

Phaeodactylum tricornutum strain UTEX 646 was obtained from the Culture Collection of Algae at the University of Texas in Austin, USA.

4.1.2 Media

All lab experiments were conducted on diatoms cultivated in artificial seawater, prepared as described in Maier and Calenberg (Maier and Calenberg, 1994). This medium was HEPES-buffered (5.0 mM) to pH 7.8 prior autoclaving (121°C, 30 min, in Nalgene Polypropylene (PP) 1 L bottle). Nutrient levels were 14.5 µM phosphate, 620 µM nitrate and 320 µM silicate.

4.1.3 Culture conditions

Unless otherwise stated, all cultures were grown under 30-40 µmol photons s⁻¹ m⁻² (measured as photosynthetic active radiation (PAR) with a quantum meter, model QMSS, Apogee, Logan USA),

at $14.5^{\circ}\text{C} \pm 1.5^{\circ}\text{C}$, under a 14/10 hours light/dark cycle. The light was provided by fluorescent tubes (Osram T8 36W 840).

Stock cultures were grown in heat sterilised (350°C for 5 hours) 300 mL glass containers (Weck, Germany). Higher volumes for inoculation were grown in autoclaved (121°C , 20 min) glass Erlenmeyer flasks with aluminium foil caps.

All manipulations were performed using standard sterile handling techniques in a vertical flow sterile bench (BDK, Germany).

4.1.4 Microscopy

All cell counts and microscopy was performed with an upright microscope with phase contrast (DM2000, Leica, Heerbrugg, Switzerland). Pictures were taken with a digital firewire colour camera (DFC280, Leica, Heerbrugg, Switzerland). *S. marinoi* cell volume was calculated based on a cylindrical shape; length and width of at least 20 cells were measured from pictures taken at 400x magnification with the Leica IM50 software (Version 4.0 release 132). Cells were counted in a Neubauer or Fuchs-Rosenthal haemocytometer (Marienfeld, Lauda-Königshofen, Germany) depending on cell density. The same haemocytometer type was used for all cell counts within one experiment. At least 400 cells were counted for each sample, in order to obtain $\pm 10\%$ approximates with 0.95 confidence (Lund *et al.*, 1958).

4.1.5 Large volume cultures (10 L and 25 L)

Unless otherwise stated, all supplies were purchased from Roth (Karlsruhe, Germany)

Culture vessel design

Large volume cultures were grown in 10 L or 25 L polycarbonate (PC) bottles (Nalgene, via VWR, Dresden, Germany). The culturing vessel is described in **Figure 35**. The bottles had one inlet and two outlets. The air inlet was connected inside the bottle to a glass tube (**Figure 35 B**) with the exit at ~ 1 cm from the bottom of the bottle. Air was pumped by an aquarium air pump through a glass wool pre-filter and a HEPA-Vent (Ø 50 mm, Whatman) filter for sterilisation (**Figure 35 F, G&H**). The outlet of the filter was connected to the inlet of the bottle, allowing bubbling of the cultures via the glass tube. A hose clamp was attached to the connecting tube in order to control the airflow. Two liquid inlets were also connected via PP T-pieces to this inlet tubing. One of these inlets was fitted with a $0.22 \mu\text{m}$ filter (polyethersulfone, PES, Ø 25 mm) to fill the bottle with the culture medium (**Figure 35 L**). The second liquid inlet was used to inoculate the culture (**Figure 35 M**). For sampling, one end of a Teflon tube (inner Ø : 1 mm) was fitted through the first outlet and the

other end was lying on the bottom of the bottle (**Figure 35 C**). This outlet was connected via silicon tubing to a dripping chamber (**Figure 35 E**). This chamber, built by inserting a 1 mL PC syringe into a 2.5 mL PC syringe, prevented contact between the sterile liquid of the bottle and the liquid at the sampling outlet (**Figure 35 D**). The second outlet of the bottle served as an air outlet and was connected to silicon tubing. This tubing was inserted in a 50 mL Falcon tube, used as liquid trap (**Figure 35 Q**). Illumination was provided by a rack of 8 fluorescent tubes placed horizontally on the side of the bottle (**Figure 35 O**). The distance between the bottle and the light rack was adjusted to have a PAR of 60-80 $\mu\text{mol photons s}^{-1} \text{m}^{-2}$ at the middle part of an empty bottle. Fans were used to create airflow into the space between the bottle and the light racks in order to prevent heating of the cultures (**Figure 35 N**).

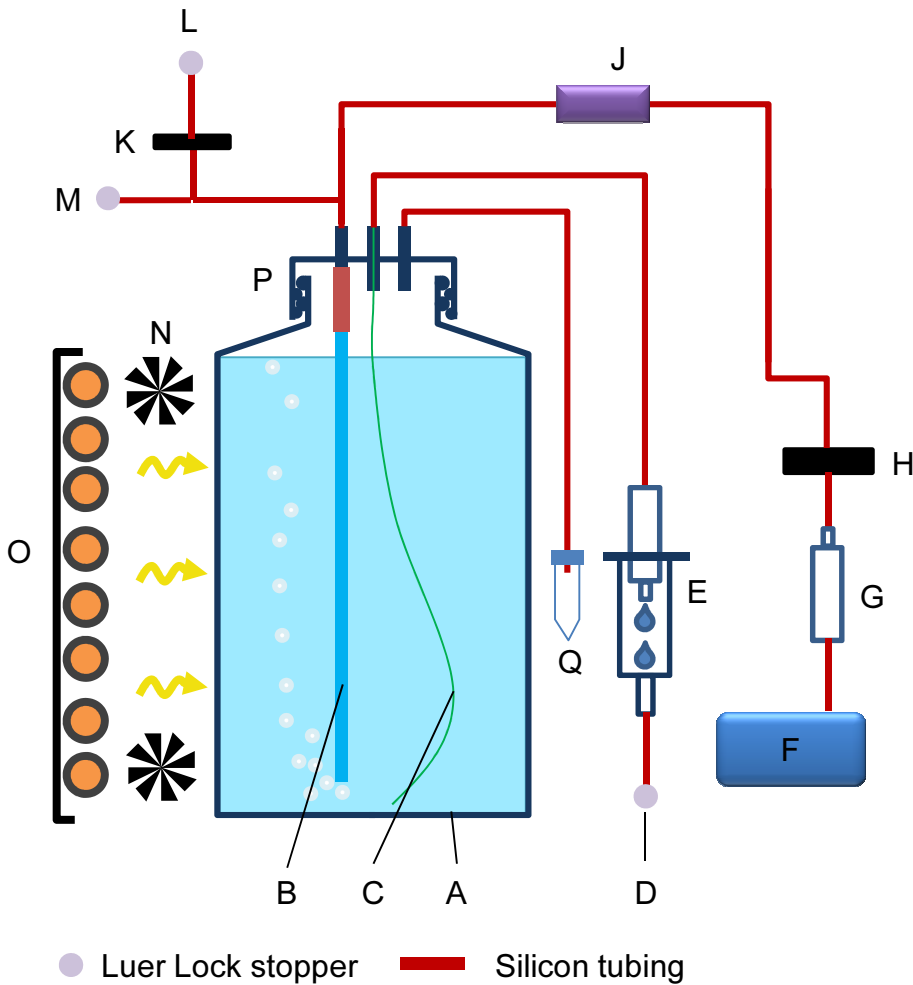


Figure 35: Scheme of the large volume culture vessel. **A**, 10L or 25L bottle (PC, Nalgene). **B**, Bubbling tube (Duran glass, $\text{\O} 4 \text{ mm}$). **C**, sampling tube (Teflon, $\text{\O} 1 \text{ mm}$). **D**, sampling outlet. **E**, dripping chamber, made of a 1 mL syringe inserted into a 2.5 mL syringe (PC). **F**, Aquarium air pump. **G**, Air pre-filter made of a 1 mL syringe (PC) filled with glass wool (Duran). **H**, Sterile filter HEPA-Vent (Whatman). **J**, Hose clamp to regulate the airflow. **K**, Sterile filter ($0.22 \mu\text{m}$, PES). **L**, Non-sterile liquid inlet. **M**, Sterile liquid inlet. **N**, Fans to remove the heat generated by the lights. **O**, Fluorescent tube rack. **P**, Transfer cap (PP, Nalgene). **Q**, Air outlet embedded in a Falcon tube.

Culture vessel preparation

Before each experiment, the bottles were acid washed several hours with ~ 3 L of 1% acetic acid in deionised water with repeated rigorous shaking. The bottles were then thoroughly rinsed with deionised water and left overnight (O/N) filled with deionised water. The next day, the bottles were again rinsed with deionised water before attaching the transfer cap and tubing. The bottles were autoclaved (121°C, 20min) with all tubing and air filters already attached. The liquid filters were added afterwards under sterile conditions. The bottles were filled by pumping autoclaved medium through the 0.22 µm filter of the liquid inlet with a peristaltic pump (MV-GES, Ismatec, Glattbrugg, Switzerland) (**Figure 35 L**). The bottles were then stored O/N at 14°C with bubbling in order to equilibrate the CO₂ concentration and the temperature. The airflows were adjusted to ensure similar bubbling in all bottles (visual estimation). Sterile glass 1 L bottles containing the inoculation cultures were sterilely connected via silicon tubing to the liquid inlet (**Figure 35 M**). The inoculation cultures were then pumped in by creating a slight vacuum in the large bottle (a membrane vacuum pump was connected to the air outlet, **Figure 35 Q**).

Sampling process

Sampling of the cultures was achieved as follows: the bottle was shaken to ensure a homogenous culture. The air outlet was closed, resulting in the building of slight overpressure in the bottle. The sampling outlet (**Figure 35 D**) was then opened and the culture was pushed out by the overpressure. The first 20 mL were discarded and then the culture was collected in 1 L glass bottles. The sampling outlet was finally closed before re-opening the air outlet.

4.2 GC-MS specification

A Waters GCT premier (Waters, Manchester, UK) orthogonal reflectron time-of-flight (oTOF) mass spectrometer (MS) coupled to an Agilent 6890N gas chromatograph (GC) equipped with a DB-5ms 30 m column (0.25 mm internal diameter, 0.25 µm film thickness, with 10 m Duraguard pre-column, Agilent, Waldbronn, Germany) was used for GC-EI-MS measurements. The parameters in **Table 17** were kept constant for all experiments. The split/splitless injector was fitted with a gold plated inlet seal with dual Vespel rings (Restek, Bad Homburg, Germany) and a deactivated glass liner (4x6.3x78.5 mm inner Ø x outer Ø x length, Agilent, Waldbronn, Germany). The samples were injected with an 7683B autosampler (Agilent, Waldbronn, Germany) equipped with a 10 µL tapered, fixed needle, PTFE-tipped plunger syringe (23-26s/42, Agilent, Waldbronn, Germany). Calibration of the MS parameters (beam steering, focusing lenses, dynamic range

extension (DRE)) was performed before the analysis of the samples from every experiment. The resolution of the MS was frequently checked and the corresponding parameters (grid-2 voltage and pusher bias) were adjusted to obtain a resolution of ≥ 6000 at m/z 501.97.

Table 17: Constant parameters for GC-EI-MS analysis

	Carrier gas	Helium 5.0
GC	Carrier gas flow	Constant flow at 1 mL min ⁻¹
	Injection pre dwell time	0.1 min (hot needle injection)
EI source	Electron energy	70 eV
	Trap current	200 μ A

4.3 PUA, general methods

4.3.1 Preparation of PUA production potential samples

This method is based on (Wichard *et al.*, 2005b).

Cell concentration

Cells were concentrated from 50 mL to 10 L, depending on the sample density, on a GF/C filter (Glass microfiber, pores ~ 1.2 μ m, Whatmann, via VWR) by filtration under moderate vacuum (~ 500 mBar). The filter was then transferred to the inner surface of a 25 mL glass beaker. The cells were rinsed from the filter with 1 mL of a 25 mM O-(2,3,4,5,6-pentafluorobenzyl)hydroxylamine hydrochloride solution (PFBHA, derivatisation grade $>99\%$, Sigma-Aldrich, or ABCR, Karlsruhe, Germany) in Tris-HCl 100 mM pH 7.2 (Roth). The cell suspension was then transferred to a 4 mL glass vial (Macherey-Nagel, Düren, Germany). Five microlitres of internal standard (benzaldehyde, 1mM in methanol, Sigma-Aldrich) were added and the vial was then closed with a screw cap fitted with butyl-PTFE septum (VWR).

Cell wounding

Two methods, depending on the experiment (see corresponding sections) were used for wounding the cells and initiating the production of PUA.

- Sonicator method: the 4 mL glass vial containing the cells in the derivatisation solution was placed in an ice bath. The sample was then sonicated for 45 s (at 30% power, with pulse cycle of 500 ms ultrasound and 500 ms pause) with a UW 2070 probe attached to a GM 2070 signal

generator (both from Bandelin, Berlin, Germany).

- b) Freeze-and-thaw method: the sample was frozen at -20°C and thawed. This cycle was repeated 3 times.

Once the cells were wounded by one of the two methods described above, the samples were allowed to react for 1 hour at room temperature (RT) and then kept O/N at 4°C . The samples were then stored at -20°C until extraction.

Extraction

Five hundred millilitres of methanol were added to each of the samples while they were still frozen. The samples were then allowed to thaw before addition of 1 mL of hexane. After vortexing for 1 min, 6 drops of sulphuric acid (Rotipuran©, >95%, Roth) were added with a glass Pasteur pipette (fitted with cotton wool to prevent contamination from the pipette ball, Roth). The samples were then again vortexed for 1 min. Phase separation was achieved by centrifugation. To that end, the closed 4 mL vials were placed in 50 mL Falcon tubes and centrifuged 10 min at 1735 g (4000 rpm) at RT (in a Z383K centrifuge, Hermle, Wehingen, Germany). The hexane phase was then carefully transferred into 1.5 mL glass vials (Macherey-Nagel, Düren, Germany). After drying over sodium sulphate (anhydrous Ph.Eur., VWR), the hexane phase was transferred into new 1.5 mL glass vials. The solvent was evaporated under vacuum for ~1 hour, and the samples were redissolved in 100 μL of hexane. After the transfer of the samples into 200 μL glass inserts (Macherey-Nagel, Düren, Germany), the vials were closed with caps fitted with PTFE-butyl-PTFE septa. The samples were then stored at -80°C until analysis by GC-MS (*cf.* 4.3.3).

4.3.2 Preparation of dissolved PUA samples

Solid Phase Extraction (SPE)

Two methods, depending on the experiment (see corresponding sections) were used for SPE extraction of dissolved PUA from the seawater:

- a) C18 method (this is a first version of the SPE extraction): Plankton or culture samples (approximately 1 L) were carefully filtered by vacuum on a ~2 cm thick sea sand bed (Reactolab, Servion, Switzerland), in a Büchner funnel (\varnothing 10 cm), to remove cells. After determination of the exact volume of the filtrate, 1 mL of a 25 mM PFBHA solution in Tris-HCl 100 mM pH 7.2, and 5 μL of internal standard (benzaldehyde, 1 mM in methanol) were added. The solution was then immediately passed through a C18 cartridge (Sep-pak plus, end capped octadecyl sorbent, 360 mg, Waters, Milford, USA) at 250 mL hour^{-1} . The partially derivatised aldehydes were

eluted from the cartridge into 4 mL glass vials using 4 mL methanol containing PFBHA (25 mM).

- b) EASY[®] method (this is the improved version of the SPE extraction): The exact volume (~1 L) of the samples was first determined, then the samples were transferred into 1 L glass bottles. Five microlitres of internal standard (benzaldehyde, 1mM in methanol) were added. EASY[®] cartridges (Chromabond 3 mL, polar modified polystyrene-divinylbenzene copolymer, 200 mg, Macherey-Nagel, Düren, Germany) were slowly loaded with 1 mL of a 25 mM PFBHA solution in Tris-HCl 100 mM pH 7.2. A sand cartridge (empty Chromabond 3 mL cartridge filled with ~3 mL of sea sand [VWR]) was then mounted inline before the EASY cartridge. The sample was passed through the two cartridges, via Teflon tubing, at ~1 L hour⁻¹. After washing with deionised water, the EASY[®] cartridges were air-dried. The partially derivatised aldehydes were then eluted from the EASY[®] cartridges into 4 mL glass vials using 4 mL methanol containing PFBHA (5 mM).

After elution, the eluates were incubated for one hour at RT to ensure complete derivatisation. These samples were then stored at -20°C until extraction.

Extraction

The samples were transferred into 25 mL round-bottom glass flasks. Eight millilitres of hexane and 8 mL of water were added before vortexing for 1 min. Sixty drops of sulphuric acid (Rotipuran©, >95%, Roth) were added with a glass Pasteur pipette (fitted with cotton wool to prevent contamination from the pipette ball, Roth) and the samples were again vortexed for 1 min. The phases were allowed to separate by gravity, and the hexane phases were transferred into 10 mL round-bottom glass flasks. After drying over sodium sulphate (anhydrous Ph.Eur., VWR), the samples were transferred into new 10 mL pointed-bottom flasks and evaporated under vacuum. The PUA-oximes were redissolved in 100 µL of hexane and transferred into glass inserts. The inserts were stored in 1.5 ml vial at -80°C until GC-MS analysis (*cf.* 4.3.3).

4.3.3 Analysis and quantification of PUA samples

Quantification standards

A new set of quantification standards were prepared for each experiment. To that end, 0.1, 0.2, 0.5, 1.0, 5.0, 10.0 or 20.0 nmol of heptadienal (>97%, Sigma-Aldrich), octadienal (96+%, Sigma-Aldrich) and decadienal (85%, Sigma-Aldrich) were added from methanolic 1 mM solutions into 1 mL of a 25 mM PFBHA solution in Tris-HCl 100 mM pH 7.2. After addition of 5 µL of internal

standard (benzaldehyde, 1 mM in methanol), the standard samples were incubated for 1 hour at RT, before being extracted following the same procedure as in 4.3.1.

GC-MS

Samples were run in random order after the quantification standards. The GC-MS parameters for the analysis are summarised in **Table 18**.

Table 18: GC-MS parameters for PUA analysis

	GC		MS
Oven starting temp.	60°C for 2 min	Source temp.	280°C
Oven ramp	To 240°C at 8°C min ⁻¹ , then to 280°C at 15°C min ⁻¹	Transfer line temp.	280°C
Oven final temp.	280°C for 2 min	Scan rate	2 scans s ⁻¹
Injector temp.	280°C	DRE	activated
Injection volume	1 µL		
Injector mode	Splitless for dissolved PUA samples (Purge flow: 20 mL min ⁻¹ for 3 min) Split 1 to 15 for cell samples, depending on the PUA concentrations		

Identification and quantification of PUA

Chromatograms were evaluated with Quanlynx (version 4.1, Waters). Identification of the PUA was based on the retention time compared with standards, on the presence of the molecular ion (m/z 305 for heptadienal, 319 for octadienal, 315 for octatrienal, 347 for decadienal) and of the major fragments ions (m/z 276 for the PUA, 271 for the internal standard, and 181 for all). The quantification was based on the ratio between the fragment m/z 276 of the derivatised PUA and the fragment m/z 271 of the derivatised internal standard (benzaldehyde), if the ions intensities were not saturating the detector. If the ions were saturating the detector, the ratios between the molecular ions of the PUA and the benzaldehyde were used.

4.4 Fatty acids, general method

The transesterification method used here is based on (Lepage and Roy, 1984).

4.4.1 Sample preparation

Cell concentration

Cells from 100 mL to 5 L of cultures or mesocosms samples were concentrated on a GF/C filter (glass microfiber, pores $\sim 1.2 \mu\text{m}$, Whatmann, via VWR) by filtration under moderate vacuum ($\sim 500 \text{ mBar}$). The filter was then transferred on the inner surface of a 25 mL glass beaker. The cells were rinsed from the filter with 1 mL methanol. The cell suspension in methanol was transferred into 4 mL glass vials (Macherey-Nagel, Düren, Germany) and 2 μL of internal standard was added (myristic- d_{27} acid, 10 mg mL^{-1} in methanol, Sigma-Aldrich). The glass vials were closed with caps fitted with PTFE-butyl-PTFE septa. The samples were stored at -80°C until further processing.

Esterification

Samples were cooled to 77 K in a liquid nitrogen bath prior freeze-drying. Five hundred microlitres of methanol:acetyl chloride 9:1 ($>99.0\%$, Sigma-Aldrich) and 300 μL of hexane were added to the freeze-dried samples before tightly closing the vials. Samples were sonicated in an ultrasound bath for 10 min before vortexing for 1 min. Samples were then incubated at 100°C for 10 min and then cooled in an ice bath. Once the samples cooled, 1 mL of deionised water was added and the samples were vortexed for another minute. Phase separation was achieved by centrifugation: the glass vials were placed in 50 mL Falcon tubes and centrifuged 10 min at 1735 g (4000 rpm) at RT (in a Z383K centrifuge, Hermle, Wehingen, Germany). The hexane phase was then carefully transferred into 1.5 mL glass vials (Macherey-Nagel, Düren, Germany). After drying over sodium sulphate (anhydrous Ph.Eur., VWR), the hexane phase was transferred into new 1.5 mL glass vials. The solvent was evaporated under vacuum for ~ 1 hour, and the samples were resuspended in 100 μL of hexane. After the transfer of the samples into 200 μL glass inserts (Macherey-Nagel, Düren, Germany), the vials were closed with caps fitted with PTFE-butyl-PTFE septa. The samples were then stored at -80°C until analyses by GC-MS (*cf.* next section).

4.4.2 Fatty acids samples analysis and quantification

Quantification standards

A new set of quantification standards was prepared for each experiment. A commercially available

mix of fatty acid methyl esters (100 mg mL⁻¹ in methanol, C4-C24 unsaturates, Supelco via Sigma-Aldrich) was used to prepare the quantification standards. To that end, 25, 10 or 5 µL from the stock solution, 25, 10 or 5 µL from a 1/10 dilution of the stock solution, 250, 50, 25 or 5 µL of a 1/1000 dilution of the stock solution were added to 500 µL of methanol:acetyl chloride 9:1. After the addition of 2 µL of internal standard (myristic-d₂₇ acid, 10 mg mL⁻¹ in methanol, Sigma-Aldrich), the standard samples were prepared as described in 4.4.1.

GC-MS

Samples were run in random order after the quantification standards. The GC-MS parameters for the analysis are summarised in **Table 19**.

Table 19: GC-MS parameters for fatty acid analysis

	GC		MS
Oven starting temp.	60°C for 5 min	Source temp.	300°C
Oven ramp	To 300°C at 10°C min ⁻¹	Transfer line temp.	280°C
Oven final temp.	300°C for 1 min	Scan rate	5 scans s ⁻¹
Injector temp.	300°C	DRE	activated
Injection volume	1 µL		
Injector mode	Split 15		

Identification and quantification

Chromatograms were evaluated with Quanlynx (version 4.1, Waters). Quantification was based on the area of the ions m/z 74 and 79 for saturated and unsaturated fatty acid, respectively (Dodds *et al.*, 2005), normalised by the ion m/z 77 of the internal standard. The identification of fatty acids not present in the standards was based on mass spectra and retention times. The quantification of these fatty acids was done using the response factor of the closest standard with the same unsaturation level.

4.5 Metabolomic samples, general method

The preparation and derivatisation of metabolomic samples is described in the SOP found in **Appendix XIII**. Samples were derivatised in batches of 20.

4.5.1 GC-MS

Samples were run in random order. A new deactivated glass liner (4x6.3x78.5 mm inner Ø x outer Ø x length, Agilent, Waldbronn, Germany) was used for every batch of 20 samples. The used liners were shipped to be cleaned and deactivated by CS Chromatography service, Bremen, Germany. The

GC-MS parameters for the analysis are summarised in **Table 20**.

Table 20: GC-MS parameters for metabolomic analyses

	GC		MS
Oven starting temp.	60°C for 1 min	Source temp.	300°C
Oven ramp	To 310°C at 15°C min ⁻¹	Transfer line temp.	280°C
Oven final temp.	310°C for 9.3 min	Scan rate	5 scans s ⁻¹
Injector temp.	300°C	DRE	activated
Injection volume	1 µL		
Injector mode	Splitless to Split 5, depending on the concentrations		

4.5.2 Data processing

Background noise correction

All chromatograms were background-noise corrected with the Component Detection Algorithm (CODA) implemented in Masslynx (version 4.1, Waters). The MCQ index used was 0.8 and the smooth window was 3 scans. The chromatograms were then converted to netCDF files using the Masslynx DataBridge.

Extraction of spectra

Converted spectra were treated in batch jobs in AMDIS (version 2.65, NIST, <http://www.nist.gov/>, 2006). The following parameters were used (**Table 21**):

Table 21: AMDIS parameters

	Parameter	Value
Identification	Minimum match factor	30
	Type of analysis	Simple
Deconvolution	Component width	32
	Omitted m/z	147, 176, 193, 207, 219
	Adjacent peak subtraction	2
	Resolution	Low
	Sensitivity	Medium
	Shape requirement	Low
Library	Target Compounds Library	Golm

* cf. **Table 23**

The CDFs files and the corresponding AMDIS files were fed into MET-IDEA (version 2.03, <http://bioinfo.noble.org/download/>, 2006) with the following parameters (**Table 22**):

Table 22: MET-IDEA parameters

	Parameter	Value
Chromatography	Type	GC
	Average peak width	0.08
	AMDIS transfer	0.5
	Maximum peak width	2
	Peak start/stop slope	1.5
	Adjusted retention time accuracy	0.25
	Peak overload factor	0.9
MS	Type	TOF
	Mass accuracy	0.1
	Mass range	0.3
General	Exclude ion	73, 147, 193, 281, 341, 415
	Lower mass limit	100
	Ions per component	1

The resulting data sets of peak areas were imported into Excel (Office 2007, Microsoft, Redmont, USA). The peaks corresponding to the retention index standards, ribitol and any compound with a retention time lower than 5 min were excluded. Normalisation of the area according the chosen method was performed as follows:

- Sum peak normalisation: each peak area was divided by the sum of all peak areas within one sample.
- Ribitol normalisation: each peak area was divided by the ribitol area. Appropriate normalisation for number of cells or volume filtered was then applied.

The data sets were then exported to *.txt files for CAP analyses.

Canonical analysis of principal coordinate (CAP)

CAP analysis was performed with the software CAP12 (Department of Statistics, University of Auckland, New Zealand, <http://www.stat.auckland.ac.nz/~mja/Programs.htm>, 2004) (Anderson and Willis, 2003) using the following parameters: no transformation, no standardisation, Bray-Curtis dissimilarity for the distance measure, discriminant analysis mode, number of principal coordinates axes chosen by the program, 999 random permutations test.

The resulting CAP axes and sample coordinates were then imported into SigmaPlot (version 11.0, Systat Softwares) for graphing. The variables (corresponding to the peaks) were screened for significant correlation coefficients with the CAP axes. Compounds having such a correlation

coefficient with one of the first two CAP axes were retained as significantly changing compounds. The correlation coefficients were scaled to the CAP coordinate's range (usually 0.5) to generate the vectors corresponding to each significant compound.

Identification of metabolites

The spectrum of each peak retained for the analysis was manually examined and identification was attempted using the software MS search (version 2.0 d, NIST, <http://www.nist.gov/>, 2005). The following libraries were used (**Table 23**):

Table 23: MS spectra libraries

Name	Origin	Version	link	Ref
NIST	NIST	2005		(Ausloos <i>et al.</i> , 1999)
Golm	Golm Metabolome Database, MPI of Molecular Plant	T_MSRI_ID 2004-03-01	http://csbdb.mpimp-golm.mpg.de/csbdb/gmd/msri/gmd	(Wagner <i>et al.</i> , 2003)
MPI	Physiology	Q_MSRI_ID 2004-03-01	msri.html	
Metabo	Own constructed database with unidentified spectra of the different experiments			This work, <i>cf.</i> accompanying CD

A structure was accepted if the reverse match was higher than 800 and if the retention index was close to the index provided in the libraries, or, when a standard was available, by direct comparison of mass spectra and retention indices. The structure was accepted with a tag in cases where the reverse match was lower than 800, but that the retention index and visual inspection of the spectra corresponded to a structure (“?” if the reverse match was between 700 and 800 or “??” if the reverse match was between 500 and 700).

4.6 PUA experiments (chapter 2.1)

4.6.1 North Adriatic Sea sampling (chapter 2.1.1)

2006 Cruise

The cruise in 2006 was conducted in the north Adriatic Sea in March, on the RV Dellaporta. The samples were collected between the 17th and the 20th of March. Seawater was collected from the surface with a PC bucket and kept in PC containers until filtration. Between 6 and 8 L of seawater were filtered through GF/C filters for analysis of the PUA production potentials. These samples were concentrated and the cells wounded with the sonicator method as described in 4.3.1. To

analyse the dissolved PUA two replicates, each consisting of 1 L of seawater, were extracted using the C18 method (*cf.* 4.3.2).

The samples were kept in liquid nitrogen until transported to the Stazione Zoologica Anton Dorn in Naples, Italy. After shipping on dry ice to the laboratory at the EPFL in Lausanne, Switzerland, the PUA production potentials and dissolved PUA samples were extracted as described in 4.3.1 and 4.3.2, respectively, and analysed according 4.3.3.

2008 Cruise

The cruise in 2008 was conducted in the north Adriatic Sea in February, on the RV Urania. The samples were collected between the 15th and the 20th of February. Seawater was collected from the surface and from different depths using Niskin bottles mounted on a rosette. Samples were kept in PC containers until filtration. Between 2 L and 7 L of seawater were filtered through GF/C filters for the determination of PUA production potentials of cells >1.2 µm. For the PUA production potentials of plankton cells with sizes ranging from 0.2 to 1.2 µm, 1 L of water was collected from the GF/C filtration flow through and filtered on 0.2 µm filters (Versapor-200, 47 mm, Pall life science, Port Washington, USA). All the PUA production potential samples were prepared according to the freeze-and-thaw method described in 4.3.1, and stored at -20°C. Extractions and analyses were conducted according 4.3.1 and 4.3.3 in the lab in Jena, Germany.

Dissolved PUA were sampled from 1L at each station as described in 4.3.2, using the EASY method, and stored at -20°C until extracted and analysed according 4.3.2 and 4.3.3 in the lab in Jena, Germany.

Phytoplankton species determination and cells counts for both cruises were performed by M. Bastianini.

The maps in **Figure 4** and **Figure 5** were generated with Ocean Data View (version 4.0.3, Schlitzer, R., <http://odv.awi.de>, 2010).

4.6.2 Culture survey for dissolved PUA (first part of the chapter 2.1.2)

Triplicated 26 L cultures were used for the 30 day survey of the dissolved PUA and PUA production potential of *S. marinoi* RCC75.

Culture preparation

The cultures were prepared starting from three 100 mL stock cultures (density at ~500 000 cells mL⁻¹). After addition of 400 mL of medium, the cultures were kept for two days followed by a

subsequent addition of 1.6 L of medium. After two more days of growth, these cultures were combined to make 6 L of inoculation culture. This culture was divided in three aliquots (2 L) that were used to inoculate 24 L of artificial seawater in the 25 L culture vessel described in 4.1.5, resulting in a density of 10 000 cells mL⁻¹.

Sampling

Approximately 800 mL (for days 1 to 9) or 1L (for days 10 to 26 and day 30) of each of the three 26 L cultures was sampled daily as described in 4.1.5. One millilitre sub samples were used to determine the pH and the cell density by counting (*cf.* 4.1.4).

Dissolved PUA were extracted from day 1 to 26 and on day 30. ~800 mL of each culture was extracted using the C18 method described in 4.3.2. PUA production potentials were analysed from ~200 mL sampled from each culture on days 10 to 26 and day 30 using the sonicator method described in 4.3.1. Samples were kept at -80°C until the end of the experiment. Once all samples were collected, they were extracted (as in 4.3.1 and 4.3.2) and analysed according 4.3.3.

4.6.3 PUA addition to cultures (middle part of the chapter 2.1.2)

Culture preparation

For incubation assays of *S. marinoi* with PUA, 1 L of exponentially growing culture at a density of ~500 000 cells mL⁻¹ was prepared starting from a 100 mL stock (*cf.* 4.1). The culture was diluted to 50 000 cells mL⁻¹ using 9 L artificial seawater and aliquoted as described below.

PUA addition during the exponential and early stationary phase (experiment 1 and 2)

Sixty-three 100 mL aliquots were derived from the 10 L culture (see above). These aliquots were maintained in 250 mL polycarbonate tissue culture flasks (BD Falcon, Franklin Lake, USA) and cultivated under the same conditions as mentioned in 4.1.3. The cell density was estimated every 1-2 days by counting at least 400 living cells (non broken cells that are not coloured by the mortal stain Evans blue and that contain chloroplasts (Gaff and Okong'O-Ogola, 1971; Reynolds *et al.*, 1978)).

Experiment 1: Three sets of additions were performed at day 5 using exponentially growing cultures. In the first set, heptadienal (*2E,4E*-heptadienal, Sigma, Basel, Switzerland) was added to a final concentration of 250 µM, 250 nM, and 250 pM, respectively. In the second set, octadienal (predominantly *2E,4E*-octadienal, Aldrich, Basel, Switzerland) was added to a final concentration of 62 µM, 62 nM and 62 pM, respectively. In the third set a mixture of both PUA was added to final

concentrations of 250 μM / 62 μM , 250 nM / 62 nM, and 250 pM / 62 pM of heptadienal/octadienal, respectively. Each treatment was run in triplicates. The concentrations of methanolic stock solutions were adjusted so that addition of 250 μL of the respective solutions resulted in the desired final PUA concentration. In parallel, we investigated in triplicate solvent controls containing 250 μL of methanol as well as untreated controls.

Experiment 2: Treatments and controls were repeated with previously untreated cultures being in early stationary phase (addition at day 16).

PUA addition during the late stationary phase (experiment 3)

Experiment 3: For a late stationary phase addition of PUA, 42-45 days old 100 ml cultures were divided into two or three replicates. When divided in two, one received a mixture of heptadienal and octadienal resulting in a final concentration of 250 nM and 62 nM of the respective aldehydes. The other aliquot of the culture was kept as a control. When divided in three, one was kept as a control, one received the PUA treatment the same day and the other received the PUA treatment one day later. The cultures chosen for this treatment were either previously untreated (5 replicates), or pre-treated with nM or pM PUA concentrations in early stationary phase (2 replicates of every combination).

Data processing

Growth rates (r) were calculated as $r = \frac{\ln Nt_1 - \ln Nt_0}{\Delta t}$ where Nt_1 and Nt_0 represent the cell density at two different days and Δt represents the number of days between the two cell density determinations. Growth rates were compared before and after treatment using paired t-tests. One-way ANOVA was used to compare the effects of treatment on growth rates between the different treatments and the controls, as well as to test the similarity of all group's growth rates before treatments. These analyses were conducted using the statistical tools provided in Microsoft Excel 2003[®]. A two-way repeated measures analysis of variance (RM-ANOVA) was used to test the effect of the PUA treatment on the late stationary phase. In order to conduct this test, only days where cell density was available for all cultures (days 0, 1, 2, 4, 5, 7, 10, 13, 14 and 31 after treatment) were used. This analysis was conducted with the software GraphPad Prism (version 5.0).

4.6.4 Nutrient effects on PUA production potential (last part of the chapter 2.1.2)

These experiments were conducted on *S. marinoi* strain CCMP 2092 at the Stazione Zoologica

Anton Dorhn and are described in (Ribalet *et al.*, 2009). Briefly, we grew the cells in PC bottles in natural sea water which was amended with f/2 nutrients containing a N:P:Si ratio of 4:1:3 ($\text{NO}_3^- = 145 \mu\text{mol L}^{-1}$, $\text{PO}_4^{3-} = 36 \mu\text{mol L}^{-1}$, $\text{Si(OH)}_4 = 107 \mu\text{mol L}^{-1}$, considered to be N-limited), 80:1:10 ($\text{NO}_3^- = 883 \mu\text{mol L}^{-1}$, $\text{PO}_4^{3-} = 11 \mu\text{mol L}^{-1}$, $\text{Si(OH)}_4 = 107 \mu\text{mol L}^{-1}$, considered to be P-limited) or 24.5:1:1 ($\text{NO}_3^- = 883 \mu\text{mol L}^{-1}$, $\text{PO}_4^{3-} = 36 \mu\text{mol L}^{-1}$, $\text{Si(OH)}_4 = 36 \mu\text{mol L}^{-1}$, considered to be Si-limited). Dilution rate (flow rate divided by culture volume) was controlled by a peristaltic pump to reach 0.90 d^{-1} and 0.28 d^{-1} for the high (control) and low (nutrient limited) flow respectively. Samples were taken 6 h after the onset of the light period in order to avoid interference from circadian variability. Sampling was carried out in technical triplicates and every culture condition was repeated twice using independent cultures. All data are presented as the mean of the two biological replicates and the range associated with the mean. The PUA production potential and fatty acids samples were shipped to Jena, Germany on dry ice and extracted and analysed according 4.3.1 and 4.4 respectively.

4.7 Metabolomic methods development (chapter 2.2)

The grade of the solvent used was:

- methanol (Chromasolv © Plus >99.9%, Sigma-Aldrich)
- acetone (HiPerSolv, VWR)
- chloroform (HiPerSolv, VWR)
- tetrahydrofuran (THF, HiPerSolv, VWR)
- water (Chromasolv[®] Plus, Sigma-Aldrich)
- pyridine (Chromasolv[®] Plus, Sigma-Aldrich)
- ethanol (LiChrosolv[®], Merck)
- acetonitrile (ULC/MS, Biosolve, Valkenswaard, the Netherlands)

4.7.1 Procedures to optimise the extraction mix

Sample preparation

For the testing of the different extraction mixes, 230 mL of a dense *S. marinoi* RCC75 culture was filtered through a GF/C filter and resuspended in 10 mL methanol. Thirty three aliquots of 200 μL of this cell suspension in methanol were prepared in Eppendorf microcentrifuge tubes. Methanol, acetone, acetonitrile, ethanol and chloroform were added according to the proportions of the 11

solvent mixes (**Table 2**) in order to reach a final volume of 1 mL in each sample. Five microliters of internal standard (ribitol, >99%, Sigma-Aldrich, 4 mM in water) was added to each sample. After vortexing for 5 min, the samples were sonicated for 10 min in an ultrasound bath. The samples were then centrifuged at 4°C for 15 min at 30000 g (17000 rpm) in a Z383K centrifuge (Hermle, Wehingen, Germany). Nine hundred fifty microlitres of the supernatant was transferred into a 1.5 ml glass vial and evaporated to dryness under vacuum for ~ 5 hours. The samples were then randomly separated into two batches. The two batches were sequentially derivatised and analysed.

Derivatisation

For each batch, 20 µg of methoxyamine hydrochloride (Sigma-Aldrich) was dissolved in 1 mL of pyridine by sonication for 5 min in an ultrasound bath. Fifty microliters of this solution was added to each sample of a batch and the vials were closed with caps fitted with PTFE-butyl-PTFE septa (VWR). After vortexing for 1 min, the samples were incubated at 60°C for one hour followed by 9 hours at room temperature. Silylation reagent was prepared by adding 40 µL of retention time mix (decane, pentadecane, nonadecane, octacosane, dotriacontane, all at 1 µM and hexatriacontane at 0.5 µM in hexane, all >99%, Sigma-Aldrich) with a glass syringe into 1 mL of N-Methyl-N-trifluoroacetamide (MSTFA, in 1 mL vials, Macherey-Nagel, Düren, German). Fifty microlitres of this silylation reagent was added with a glass syringe into the samples before incubating them for one hour at 40°C. The samples were then transferred into glass inserts and were immediately analysed by GC-MS.

GC-MS

Batches of 20 samples were analysed by GC-MS as described in 4.5.1.

Number of peaks and reproducibility

The chromatograms were analysed with AMDIS and MET-IDEA as described in 4.5.2. The data sets were imported into excel for determination of the reproducibility. The relative standard deviation (standard deviation divided by the average) of each compound was calculated for each triplicated mix. The median of these relative standard deviations was reported in the **Figure 13**.

Relative recovery of different compound classes

Manual evaluation of the chromatograms allowed the identification of 9 amino acids (proline, alanine, glycine, pyroglutamate, glutamine, phenylalanine, ornithine, lysine, and tyrosine), 9 fatty acids and sterols (myristic acid, stearic acid, hexadecatrienoic acid, hexadecatetraenoic acid, oleic

acid, eicosapentaenoic acid, cholesterol, campesterol, and an unidentified sterol) and 9 sugars and related compounds (glucose, glycerol, ribose, arabinose, fucose, erythrose, inositol isomer, xylopyranose, and galactosyl-glycerol). The corresponding compounds in the data set generated by AMDIS and MET-IDEA were identified and their intensities, after normalisation by the ribitol intensity, was used to calculate the relative recovery (intensity reported to the highest intensity) of each of these metabolites. The averages of the relative recoveries were calculated for the 3 groups of compounds.

4.7.2 Procedures to optimise the volume of extraction

Two hundred millilitres of a *S. marinoi* RCC75 culture in exponential phase was filtered through a GF/C filter. The cells were resuspended in 1 mL of extraction mix (methanol:ethanol:chloroform, 2:6:2). Four aliquots of 60 μ L were transferred into Eppendorf microcentrifuge tubes. Extraction mix was added in three of the aliquots to reach final volumes of 120, 180 and 300 μ L. The samples were then extracted and derivatised as described in 4.7.1.

The chromatograms were evaluated manually and the areas of 14 compounds (glucose, proline, alanine, glycine, pyroglutamate, threonic acid, myristic acid, stearic acid, inositol isomer, galactosyl-glycerol, eicosapentaenoic acid, cholesterol, campesterol, and tryptamine) were integrated using Quanlynx (version 4.1, Waters). The area of each compound was reported to the highest area of the same compound and the average of these relative recoveries was calculated.

4.7.3 Procedures to test the different cartridges for solid phase extraction (SPE)

A test of the recovery efficiency of different SPE cartridges, in duplicates, was conducted on the Bond ElutTM PPL (500 mg), Bond ElutTM Carbon (500 mg, Varian, Lake Forest, USA), Chromabond[®] Easy (200 mg), Chromabond[®] C18Hydra (200mg, Macherey-Nagel, Düren, Germany) and Sep-Pak C18 (360 mg, Waters, Manchester, UK). Each cartridge was first conditioned with 10 mL methanol and 10 mL water. PPL cartridges were then mounted in line with Carbon cartridges as recommended by the Varian's development team. Two hundred fifty millilitres of 100 μ M glucose in artificial seawater was then passed through each cartridge. The same procedure was repeated on other cartridges but with the seawater at pH 2 (acidified with HCl). All cartridges were then washed with 5 mL deionised water, dried in air and eluted by gravity with 2.5 mL of methanol followed by 2.5 mL of methanol:THF (1:1). Five microlitres of ribitol (4 nM in water) were added to each eluate. The whole 5 mL eluate of each cartridge was then evaporated to dryness under vacuum in 1.5 mL vials. The samples were then derivatised and analysed by GC-MS as in 4.5. The areas of the fructose and ribitol peaks were then integrated with Quanlynx (version

4.1, Waters). After normalisation of the glucose area by the ribitol area, the recoveries relative to the highest signal were calculated.

Tests were also conducted with diatom culture samples (data not shown, see (Barofsky *et al.*, 2009))

4.7.4 Procedures to optimise the derivatisation time

Sample preparation

Approximately 360 mL of a *S. marinoi* RCC75 culture in exponential phase ($\sim 450 \cdot 10^6$ cells) was filtered through a GF/C filter. The cells were resuspended in 16 mL of extraction mix (methanol:ethanol:chloroform, 2:6:2), vortexed for 5 min, and sonicated for 10 min in an ultrasound bath. Fifteen aliquots of 1 mL were transferred into Eppendorf microcentrifuge tubes. A blank was created at that step by adding 1 mL of extraction mix into a microcentrifuge tube. Five microlitres of ribitol (4 nM in water) were added to every sample before centrifugation at 4°C for 15 min at 30000 g (17000 rpm) in a Z383K centrifuge (Hermle, Wehingen, Germany). Nine hundred fifty microlitres of the supernatant were transferred into a 1.5 mL glass vial and evaporated to dryness under vacuum for ~ 5 hours.

Derivatisation and GC-MS

Methoxymation was achieved as in 4.7.1 but the derivatisation time at RT was extended to 15 hours. Silylation reagent was prepared as in 4.7.1.

Fifty microlitres of the silylation solution was added to each sample just before the incubation. Five samples were incubated for 30, 45, 60, 85 or 110 min at 40°C. The addition of the silylation solution and the starting of the incubation were timed in a way so that each sample could be immediately run on the GC-MS after the incubation at 40°C. The whole derivatisation time series was then repeated twice. The GC-MS parameters were as described in 4.5.1.

Evaluation of the results of the derivatisation time optimisation

The areas of 9 amino acids (proline, alanine, glycine, pyroglutamate, glutamine, phenylalanine, ornithine, lysine, and tyrosine), 9 fatty acids and sterols (myristic acid, stearic acid, hexadecatrienoic acid, hexadecatetraenoic acid, oleic acid, eicosapentaenoic acid, cholesterol, campesterol, and an unidentified sterol), 9 sugars and related compounds (glucose, glycerol, ribose, arabinose, fucose, erythrose, inositol isomer, xylopyranose, and galactosyl-glycerol) and of the internal standard (ribitol) were integrated with Quanlynx (version 4.1, Waters). Relative recoveries

and relative standard deviations of each compound were calculated from the ribitol-normalised areas. The averages of each group were then calculated.

4.7.5 Procedure for tests of the GC liner

Samples

The last replicate of the derivatisation time series of 4.7.4 was used for this test.

GC-MS

A new liner was placed in the GC injector. The samples were then injected repeatedly one after the other. The injections were stopped based on a visual pre-evaluation of the ribitol peak. The areas of the compounds mentioned in 4.7.4 were integrated in Quanlynx (version 4.1, waters).

4.8 Metabolic survey of a *S. marinoi* culture (chapter 2.3)

4.8.1 Culture preparation

S. marinoi G4 cultures were prepared starting from three 100 mL stock cultures (density at $\sim 0.4 \cdot 10^6$ cells mL⁻¹). After addition of 400 mL of medium, the cultures were kept for two days followed by a subsequent addition of 1.5 L medium. After two more days of growth, these cultures were combined to make 6 L of inoculation culture. Five large culture vessels (with 24L of medium, see 4.1.5 for preparation of the culturing bottles) were inoculated with one litre of the inoculation culture each, resulting in $\sim 0.02 \cdot 10^6$ cells mL⁻¹. Another 25 L bottle was prepared with 25 L of medium and used as blank.

Cultures were mixed by continuous air bubbling and were also shaken every morning at 11:00. Culture conditions were as described in 4.1.3 and 4.1.5

4.8.2 Sampling

Basic sampling

Twenty millilitres of each culture was sampled every day as described in 4.1.5. Subsamples were used for chlorophyll a fluorescence (*cf.* 4.8.5) and PSII efficiency (*cf.* 4.8.6) determination. Another subsample of one culture was fixed with one drop of lugol and kept in the dark until cell counting (*cf.* 4.1.4). For nutrient determination (*cf.* 4.8.4), ten millilitres of each sample was passed through a

GF/C filter (20 mm, Whatman) into 15 mL falcon tubes. These samples were used first for pH determination (*cf.* 4.8.3), and then five microlitres of chloroform was added as preservative to these samples prior to freezing at -20°C. Every other day, 1 mL was also collected directly from the culture outlet into autoclaved 1.5 mL Eppendorf microcentrifuge tubes and used for bacterial plating (*cf.* 4.8.7) and diatom regrowth lag determination (*cf.* 4.8.8).

Metabolomic sampling

Sampling for the metabolomic analysis was performed at 11:00, 15:00, 19:00 (one hour before switching to night), 21:00 and the next day at 01:00, 05:00 (one hour before the transition to day), 07:00 and 11:00. The exponential phase sampling was conducted on days 6-7, the stationary phase sampling at day 14-15 and the declining phase sampling at day 23-24. For this later phase, the remaining culture volume only allowed seven sampling points; therefore the last 11:00 sample was not taken. Before each sampling, each culture, including the blank, was shaken. One litre (in exponential phase) or 500 mL (in stationary and declining phase) was collected in 1 L glass bottles, as described in 4.1.5. The bottles were kept in a water bath at ~15°C during the preparation of the samples. The night sampling and sample preparation were performed under extremely dimmed green light to prevent activation of light related processes.

Several subsamples (**Table 24**) were filtered through GF/C filters for determination of PUA production potentials, fatty acid concentrations and metabolic profiles. Due to the low amount of volume available for all sampling, the medium was collected for each of these filtrations and used for the extracellular metabolite profiling.

Table 24: Filtration volumes for metabolomic samples

Phase of growth	PUA production Potential	Volume (mL) filtered for			Total volume used for extracellular metabolite profile
		fatty acids	Intracellular metabolite profile		
Exponential	~250*	250	500	~1000	
Stationary	~100*	150	300	~500	
Declining	100	100	100	~500 [†]	

* Filtration with the remaining volume of the total volume sampled after filtration of the intracellular metabolites and fatty acids samples. [†] filtration through a GF/C in addition to the filtration for the cell samples was performed to obtain this volume

The samples for PUA production potential were prepared and analysed as described in 4.3 with the sonicator method, the fatty acids samples as described in 4.4, and the metabolic profile of intra- and extra-cellular metabolites as described in 4.5.

4.8.3 pH measurements

pH was measured with a HI 1131 electrode (Roth) attached to a C830 pH meter (Consort, Turnhout, Belgium). The samples were acclimated to room temperature prior measurement. The pH meter was calibrated each day before measuring the samples with standard solutions of pH 7.00 \pm 0.02 and pH 4.00 \pm 0.02 (Roth).

4.8.4 Nutrients

Silicate, phosphate and nitrite concentrations were determined by photospectroscopy according to (Parsons *et al.*, 1984), and nitrate according to (Zhang and Fischer, 2006). The volumes were adapted for measuring in 1 cm half micro cuvettes (Roth). Each sample was measured three times on a Specord M82 photospectrophotometer (Carl-Zeiss, Jena, Germany).

4.8.5 Chlorophyll a fluorescence

Two hundred microlitres of each culture was transferred into 10 wells of a 96 well black microplate (Roth). The chlorophyll a fluorescence was measured using a microplate reader (Mithras LB 940, Berthold, Bad Willbad, Germany). The following parameters were used:

- Excitation wavelength: 430 nm
- Emission wavelength: 665 nm
- Counting time: 0.1 s
- Lamp energy: 15000

The microplate with ten replicates of each culture was further used for the PSII efficiency determination

4.8.6 Photosystem II efficiency

The photosynthetic efficiency of photosystem II was determined as $\frac{F_m - F_0}{F_m}$ (Roy and Legendre, 1979). F_0 (initial fluorescence) was determined after incubating the 96 well plate used for chlorophyll a fluorescence determination (4.8.5) in the dark for 30 min at 15°C. The fluorescence was measured using the following parameters:

- Mixing: double orbital shaking for 30 s.
- Excitation wavelength: 430 nm
- Emission wavelength: 665 nm
- Counting time: 0.5 s

- Lamp energy: 15000

F_m (maximal fluorescence) was determined by adding 15 μL of 10 M aqueous 3'-(3,4-dichlorophenyl)-1',1'-dimethylurea (DCMU, 98%, Sigma-Aldrich) and measuring the fluorescence with the same parameters mentioned above, but with a shaking time of 90 s.

4.8.7 Bacterial CFU determination

Subsamples of the samples collected in autoclaved microcentrifuge tubes were diluted (50-10000 fold, by serial dilution in 0.22 μm -filtered artificial seawater) and 100 μL of each dilution was plated on a marine broth plate (marine broth + 2% agar, Roth). The CFU were counted after 2 and 5 days, and colony morphology was inspected visually.

4.8.8 Diatom lag time for regrowth

Subsamples of the samples collected in autoclaved microcentrifuge tubes were diluted in 5 mL of artificial seawater to reach approximately the same level of chlorophyll a fluorescence than the cultures had at day 1. The diluted samples were placed into a 6 well plate (PC, transparent, Roth). The plate was then sealed with a gas permeable plastic foil (Breatheasy, Roth) and kept in the same condition as the culture described in 4.1.3. The fluorescence was measured daily at 11:00 am with the following parameters:

- Mixing: double orbital shaking for 2 s.
- Excitation wavelength: 430 nm
- Emission wavelength: 665 nm
- Counting time: 0.1 s
- Lamp energy: 15000

The lag time was calculated as the period in days before the chlorophyll a fluorescence doubled within one day.

4.9 Mesocosms (chapter 2.4)

Mesocosm settings are described in 2.4 and in (Barofsky *et al.*, 2010). Sampling was performed daily at 9:00 am, and the samples were kept until filtration in PP carboys in a climate chamber which was maintained at the same temperature as the mesocosm. The metabolic profiling of the extracellular metabolites were performed in triplicate from 1 L of seawater, as described in 4.5. The samples were stored at -20°C until the end of the experiment before being transported on ice to the

labs in Jena, Germany. The samples were then stored at -80°C until analysis (approximately one year later). The analysis by GC-MS and the generation of the data sets were made according to chapter 4.5, with the ribitol normalisation.

The cluster analysis was performed with ViDaExpert ((Gorban and Zinovyev, 2001), <http://www.ihes.fr/~zinovyev/vida/vidaexpert.htm>).

Cell counts were determined by H. H. Jakobsen.

4.10 Decadienal treatment of *P. tricornutum* (chapter 2.5)

4.10.1 Culture preparation

Phaeodactylum tricornutum cultures were prepared starting from two 40 mL stock cultures. After addition of 160 mL of medium, the cultures were kept for two days followed by a subsequent addition of 800 ml of medium. After two more days of growth, both cultures were combined to make 3 L of inoculation culture. Six large (10 L) culture vessels (with 9.6 L of medium, see 4.1.5 for preparation of the culturing bottles) were inoculated with 400 mL of the inoculation culture each. Cultures were mixed by bubbling and shaking every morning at 9:00. Ten millilitre samples were taken every day for cell density determination.

4.10.2 Decadienal treatment

On the third day of the experiment, 1.5 L was sampled at 9:00 am from every culture as described in 4.1.5. Ten millilitres of methanolic *E2,E4*-decadienal (0.4 mg mL^{-1} , 85%, Sigma-Aldrich) was then added to three of the six cultures. Ten millilitres of methanol was added to the three other cultures (controls). Sampling of 1.5 L was performed again after 6, 24, and 48 hours. After each sampling, 250 mL was filtered for intracellular metabolic profiling. These samples were filtered, extracted, and analysed as described in 4.5. The extracellular metabolite profiles were obtained according to 4.5 by filtering 750 mL of the samples. For the 3 cultures treated with decadienal and for one control culture, 500 mL was used for determination of dissolved PUA using the EASY method as described in 4.3.

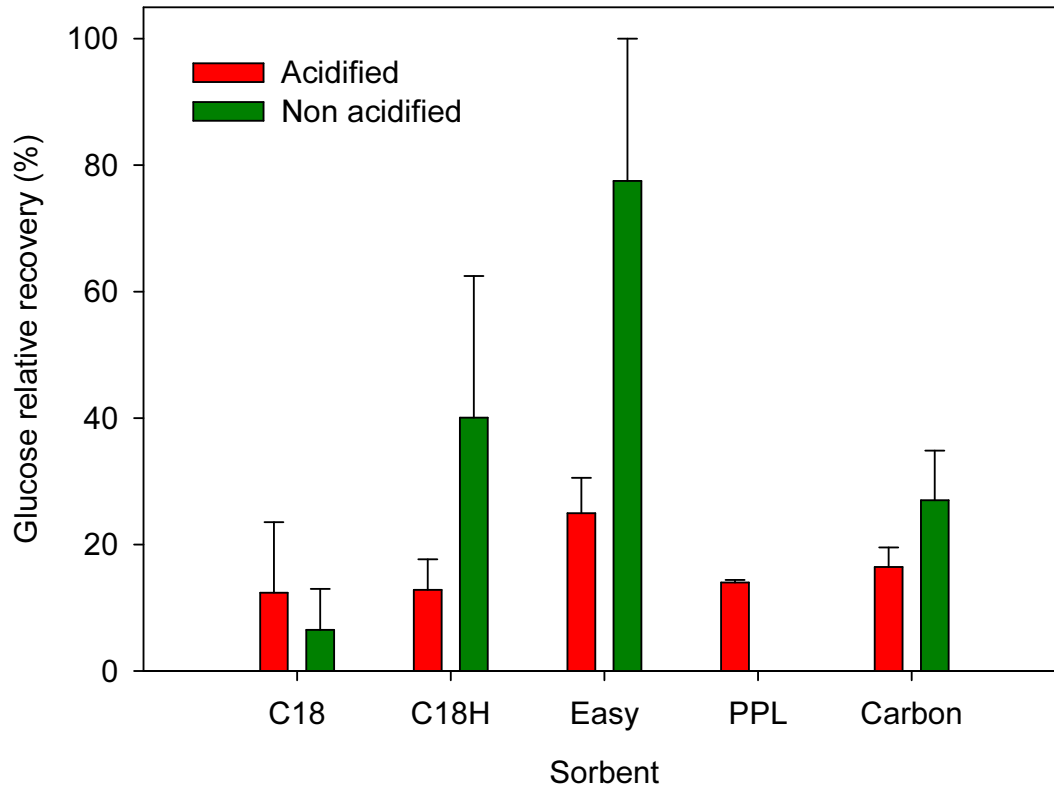
The metabolic profile datasets were generated according 4.5, using the sum normalisation.

4.11 Statistical analysis

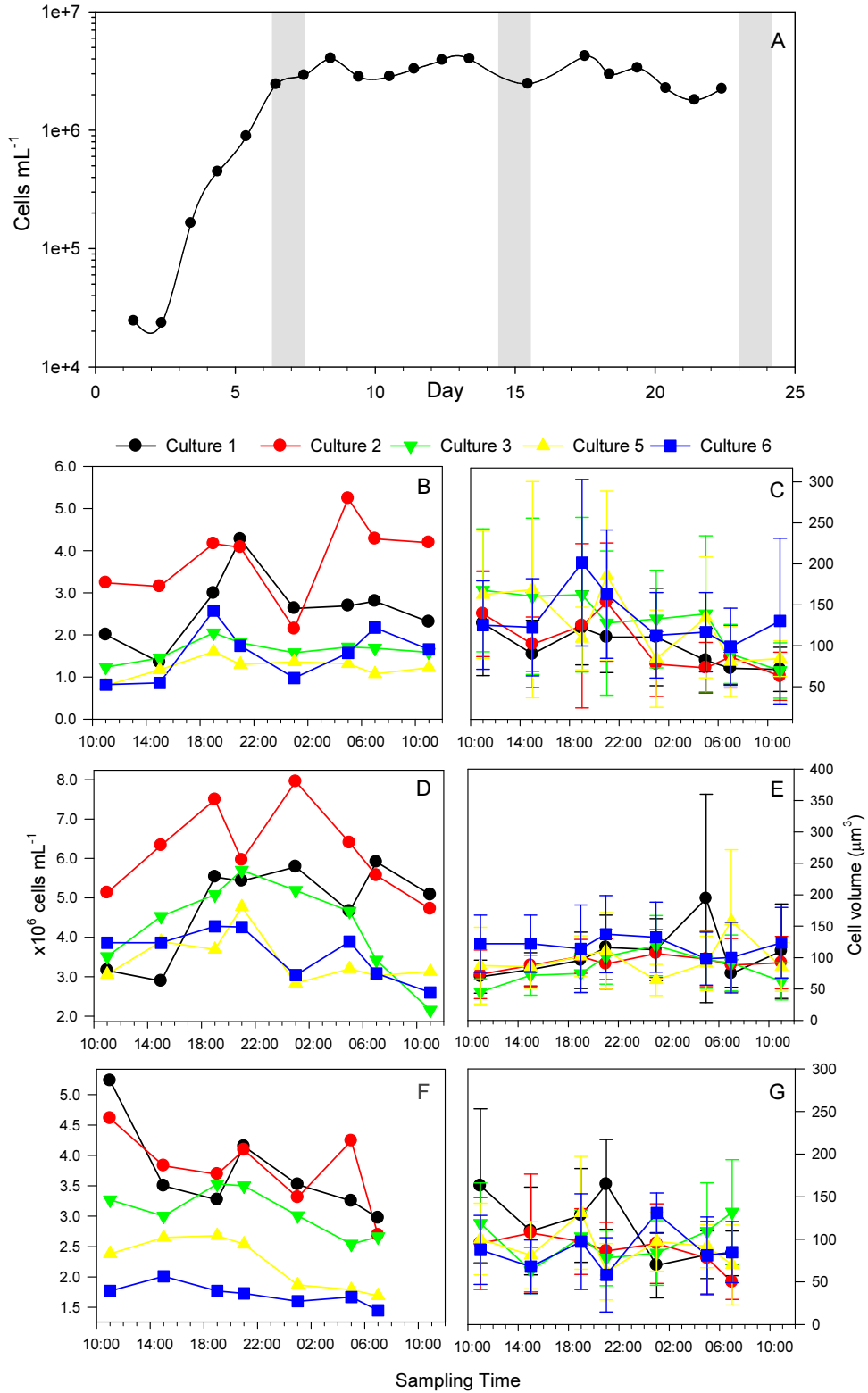
Unless otherwise mentioned, all statistical analyses were performed in SigmaPlot (version 11.0, Systat Softwares)

Appendices

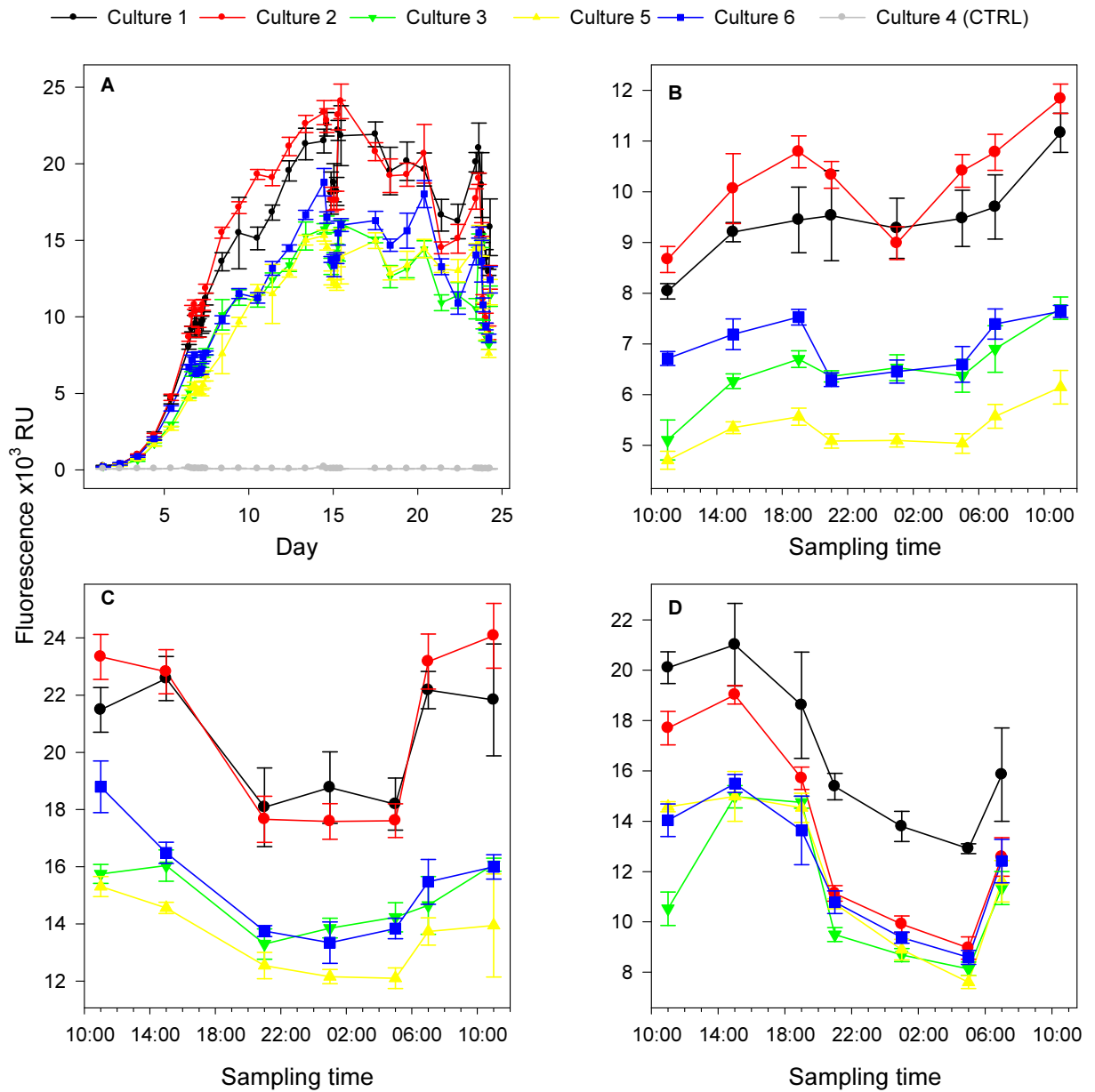
Appendix I: Efficiency of different SPE sorbents in recovering glucose from seawater. In red, the seawater pH was adjusted to 2 before filtration. In green, the pH was not modified (pH ~7.5). Values are relative recovery reported to the highest glucose peak area. n = 2, the average is displayed \pm range.



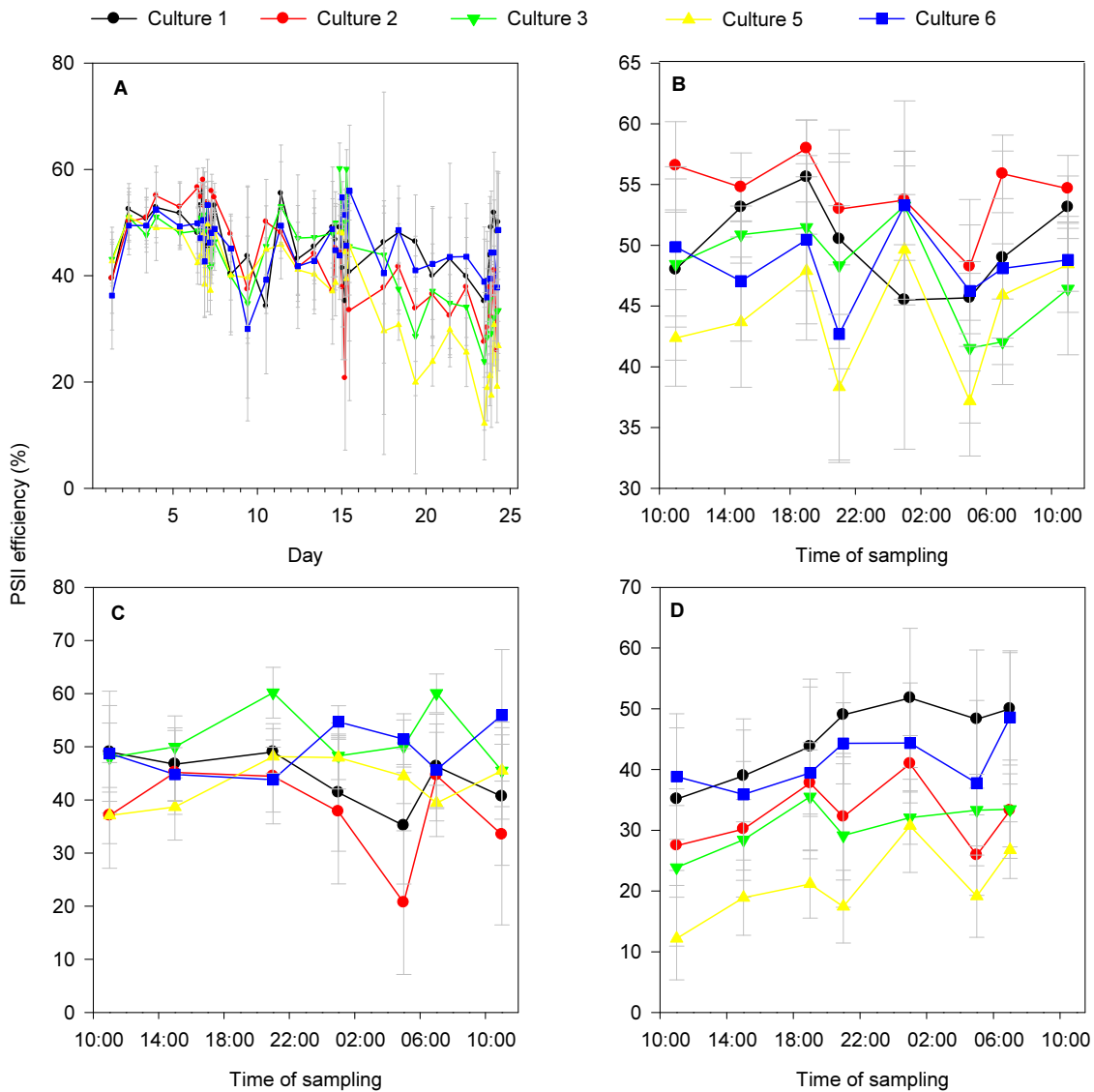
Appendix II: Cell density and volume in *S. marinoi* G4 cultures. **A**, daily cell counts of culture 1. The metabolic sampling periods are indicated by gray bars **B**, **D** & **F**, cell density at sampling point in exponential, stationary and declining phase respectively. **C**, **E** & **G**, Estimation of the cell volume at sampling point in exponential, stationary and declining phase, respectively.



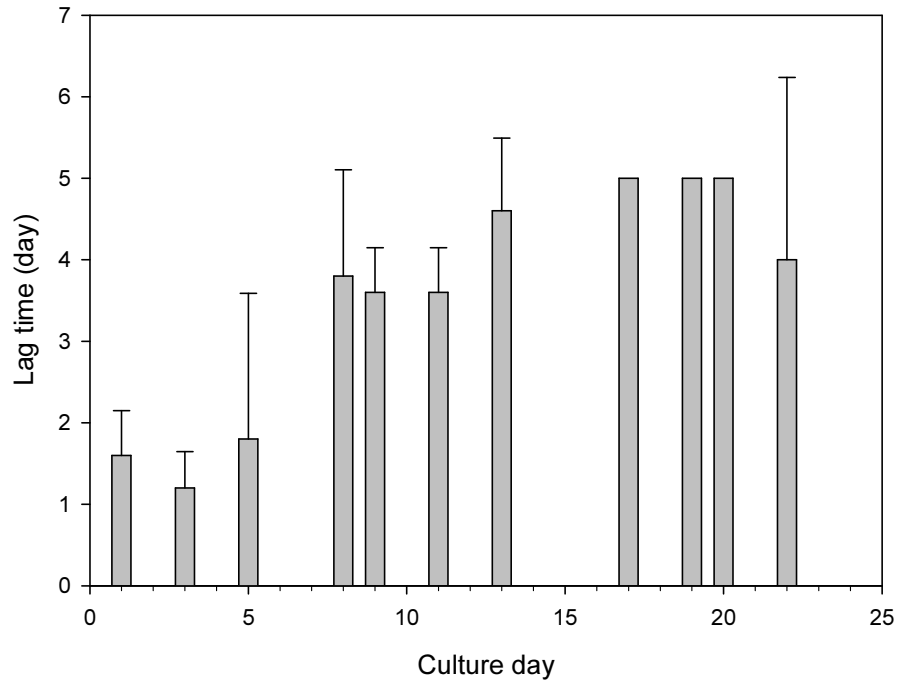
Appendix III: Fluorescence (RU: relative units) of *S. marinoi* G4 cultures. **A**, all sampling time points. **B**, **C** & **D**, details for the 24 hour sampling in exponential, stationary and declining phase respectively. Values are average of 10 technical replicates \pm standard deviation.



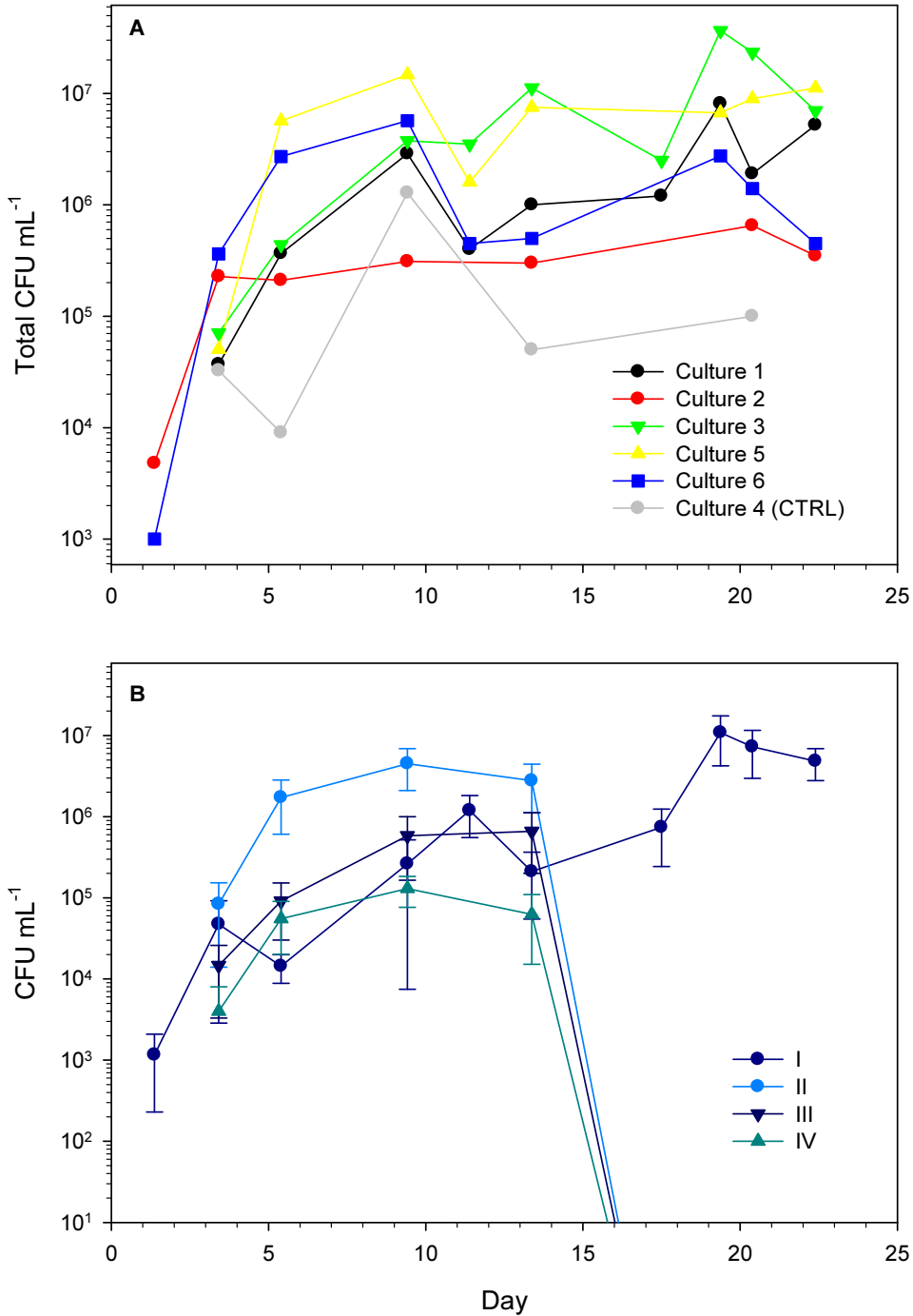
Appendix IV: Photosystem II efficiency, estimated by $(F_m - F_0) \cdot F_m^{-1}$, in *S. marinoi* G4 culture. **A**, sampling time over the 25 days of culture. **B**, **C** & **D**, details of the sampling time over 24 hours in exponential, stationary and declining phase respectively. Values are average of 10 technical replicates \pm standard deviation.



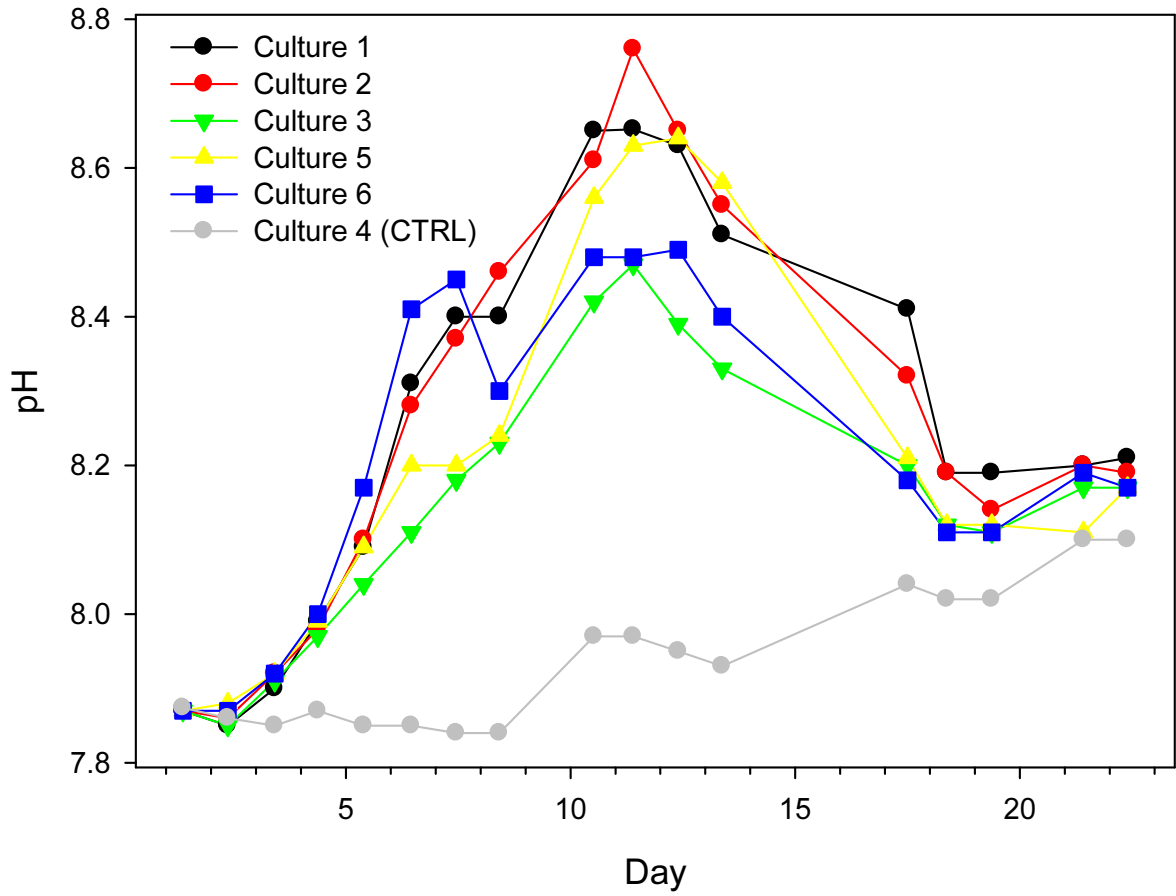
Appendix V: Lag time for regrowth of *S. marinoi* G4 cultures. In abscissa, the day of culturing when a cell sample is placed in new medium. In ordinate, the time necessary for the cells to restart to double each day. Values are average of the 5 cultures \pm standard deviation.



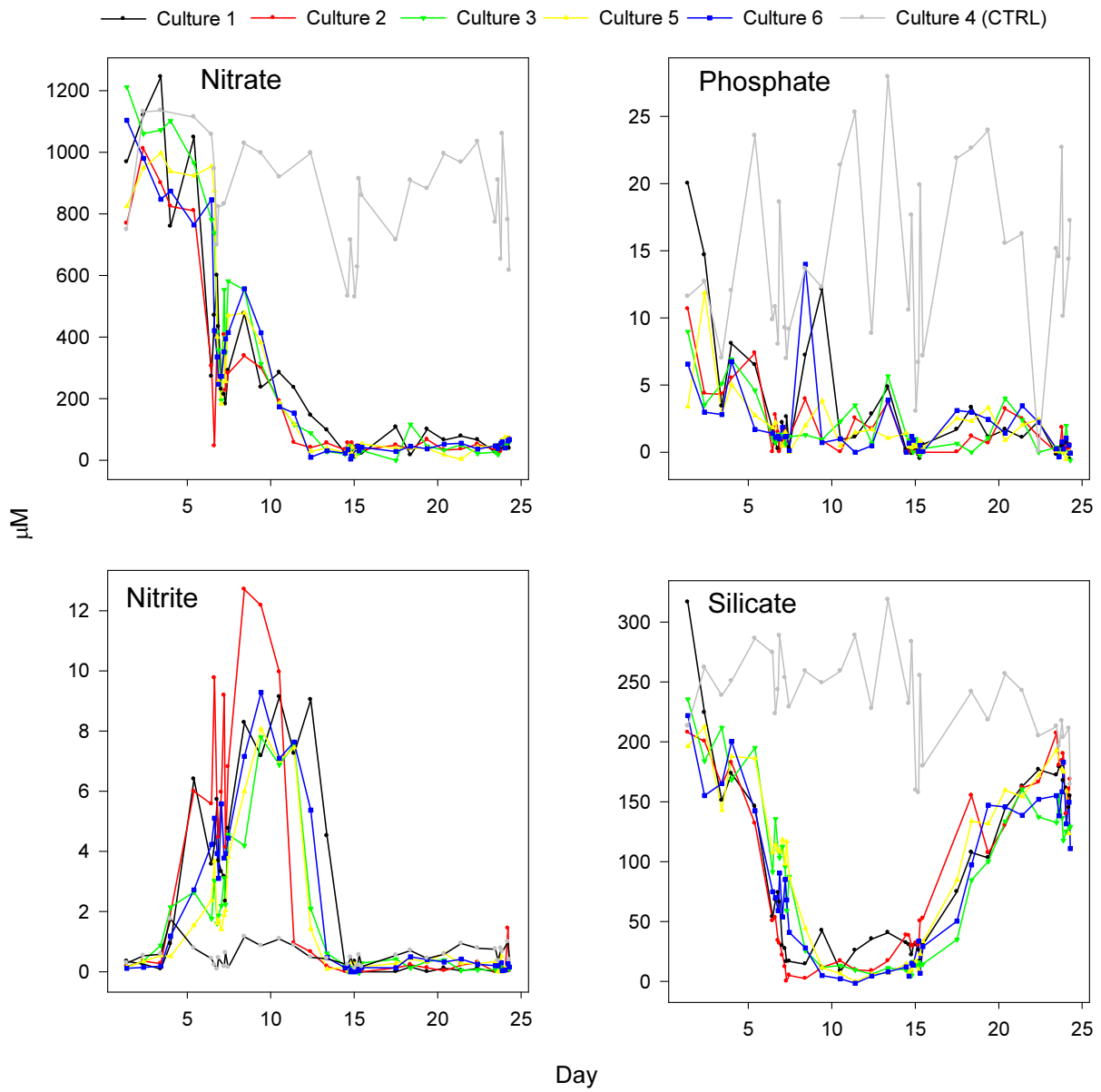
Appendix VI: Bacteria density in *S. marinoi* G4 culture, estimated as CFU. **A**, total CFU in each culture in function of time. **B**, CFU of colonies 4 major phenotypes. Values are average of the CFU for each type in all 5 cultures, except the blank, \pm standard deviations. Note the logarithmic scale.



Appendix VII: pH of *S. marinoi* G4 cultures.



Appendix VIII: Nutrient concentration in *S. marinoi* G4 cultures. Note the different scales.



Appendix IX: *S. marinoi* G4 culture cell metabolites identified by CAP.

n ^{o1}	RT ²	model ion ³	CAP hit ⁴	Identification	R ⁵ match	Library ⁶	Class ⁷
1	6.19	116.1	I_Eg_	Alanine *	806	NIST	aa
2	6.53	158.1	I_Dg_Ejn_	?			?
3	6.55	101	I_Eg_	?			?
5	6.71	174.1	I_Eg_	?			?
6	6.93	129	I_Dg_	?			?
7	7.03	132.1	Ejn_	?			?
9	7.33	144.1	I_Ejn_	Valine *	778	Golm	aa
10	7.59	117.1	I_Eg_Dg_	Diethylenglycol	854	NIST	Other
11	7.83	174.1	Ejn_	Ethanolamine	844	Golm	Other
12	7.86	158.1	I_Eg_Ejn_	Isoleucine?	730	Golm	aa
14	7.89	103	I_	Glycerol	856	MPL	Other
17	8.06	158.1	I_Eg_Ejn_	Isoleucine	870	Golm	aa
18	8.10	142.1	I_Eg_Ejn_	Proline*	820	Golm	aa
19	8.21	174.1	I_Eg_	Glycine*	861	NIST	aa
21	8.22	113.1	I_	?			?
23	8.35	196.1	I_Eg_Dg_	?			?
24	8.45	184	Eg_Ejn_	?			?
24	8.45	184	Eg_Ejn_	?			?
25	8.70	199.1	I_	3-octenoic acid??	624	NIST	FA
26	8.71	204.1	I_Eg_	Serine*	804	Own	aa
27	8.72	156.1	I_Eg_	Pyroglutamic acid?	740	Golm	aa
28	8.94	218.1	I_Eg_	Threonin?	716	Golm	aa
29	9.16	221.1	I_	?			?
30	9.18	189.1	I_	?			?
31	9.24	189.1	I_	?			?
33	9.56	350.1	I_	?			?
36	10.07	146.1	I_Eg_Dg_Ejn_	Hydroxy-proline	880	NIST	aa
38	10.16	174.1	I_	N-acetyl-glutamic acid?	792	Golm	aa
40	10.36	120.1	I_	Phenylalanine?	732	NIST	aa
41	10.40	205.1	I_Dg_Ejn_	Threonic acid	864	NIST	aa
43	10.57	217.1	I_	Pentafuranose	812	NIST	Sugar
44	10.68	217.1	I_	Pentafuranose			Sugar
45	10.71	239.1	I_	Trishydroxybenzen	814	Golm	Other
46	10.73	217.1	I_	Pentafuranose	812	NIST	Sugar
47	10.84	217.1	I_Dg_	Pentafuranose			Sugar
50	10.97	174.1	I_Dg_	?			?
51	11.10	174.1	Eg_Ejn_	?			?
57	11.55	123.1	I_Eg_	?			?
60	11.78	174.1	I_Eg_Dg_	Putrescine*	869	NIST	Other
61	11.88	140.1	I_	?			?
62	12.03	103.1	I_Ejn_	?			?
62	12.03	103.1	I_Ejn_	?			?
65	12.17	302.1	I_	?			?
68	12.38	218.1	I_	Hexofuranose?	691	NIST	Sugar
69	12.41	174.1	I_	?			?

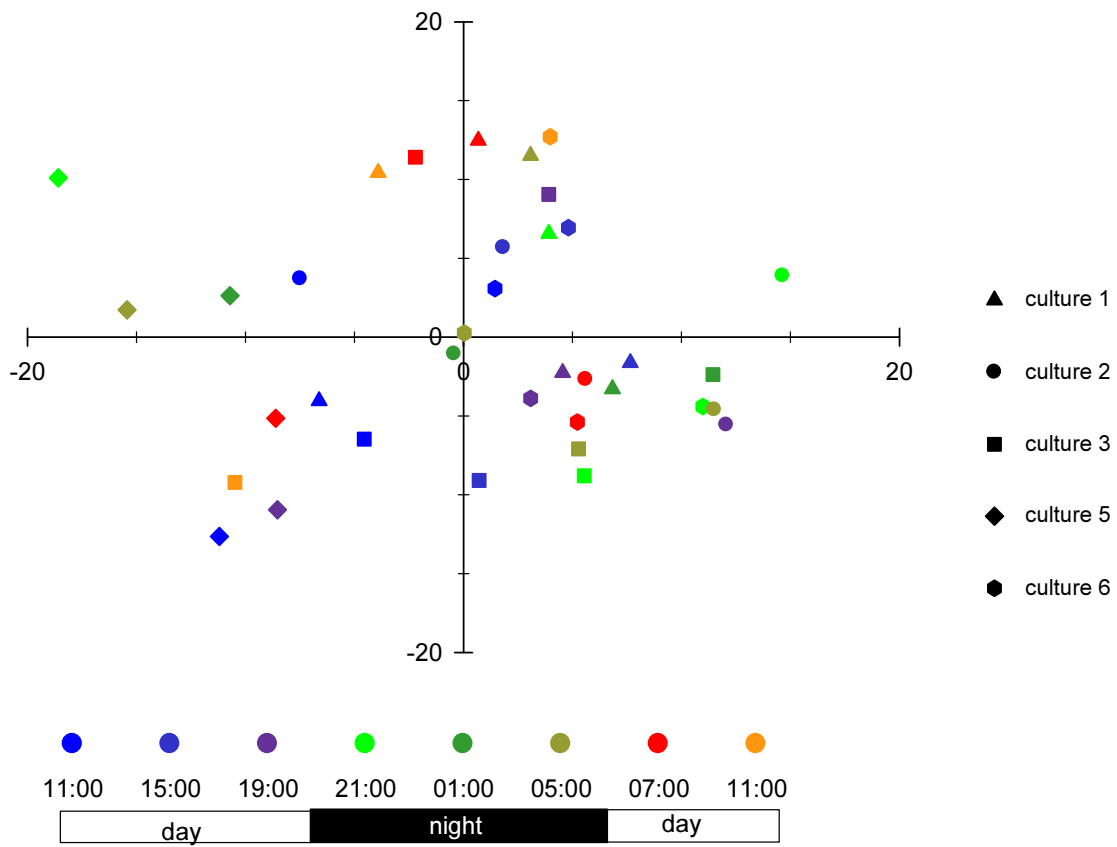
Appendices

n ^{o1}	RT ²	model ion ³	CAP hit ⁴	Identification	R ⁵ match	Library ⁶	Class ⁷
71	12.47	123.1	I_Dg_	3,7,11,15-tetramethyl-2-hexadecen-1-ol?	780	NIST	Terpene
72	12.52	117	Dg_	Tetradecanoic acid	731	NIST	FA
73	12.57	204.1	Eg_	Hexofuranose?	721	NIST	Sugar
74	12.64	123.1	I_Dg_	3,7,11,15-tetramethyl-2-hexadecen-1-ol?	841	NIST	Terpene
77	12.77	123.1	I_Dg_	3,7,11,15-tetramethyl-2-hexadecen-1-ol?	762	NIST	Terpene
78	12.80	204.1	Eg_	Hexopyranose??	637	Golm	Sugar
79	12.81	117		Unidentified fatty acid			FA
85	13.00	174.1	I_	?			?
87	13.03	103	I_	Glucose*	947	MPL	Sugar
91	13.10	126	I_Ejn_	?			?
94	13.20	117	Eg_	Pentadecanoic acid?	700	NIST	FA
96	13.27	152.9	I_	?			?
98	13.40	217.1		Hexose?			Sugar
99	13.42	215.2	I_	?			?
100	13.45	333.1	I_	Hexonic acid	806	Golm	Other
103	13.52	101.1	I_Dg_	Inositol isomer	703	NIST	Sugar alcohol
104	13.59	105.1	I_	Unidentified fatty acid	752	NIST	FA
105	13.61	234.2	I_	Hexadecenoic acid*	826	Golm	FA
106	13.63	122.1	I_	Hexadecatrienoic acid(HDTRI)	822	Golm	FA
107	13.72	117	I_Eg_Dg_	Hexadecenoic acid?	762	Golm	FA
109	13.74	309.2	I_Dg_	Hexadecadienoic acid?	740	NIST	FA
110	13.77	231.1	Dg_	?			?
112	13.79	305	I_Eg_	Inositol isomer	839	MPL	Sugar alcohol
115	13.81	217.1	I_Eg_	Inositol isomer	834	NIST	Sugar alcohol
116	13.84	117	I_	Hexadecanoic acid	859	NIST	FA
117	13.95	108.1	I_Eg_	Hexadecatetraenoic acid?			FA
118	13.98	285.3	Eg_Ejn_	2,5-Furandicarboxylic acid?	736	NIST	Other
119	14.07	204.1	I_Eg_Ejn_	Hexose	850	NIST	Sugar
120	14.15	217.1	I_	Hexose?	709	NIST	Sugar
121	14.22	217.1	I_Eg_Ejn_	Inositol isomer	925	MPL	Sugar alcohol
123	14.64	143.1	I_Dg_	Oxo-terpen	801	NIST	Other
128	14.76	148	I_	Unidentified sugar			Sugar
129	14.78	167	I_Dg_	?			?
131	14.85	329.2	I_	?			?
132	14.88	197.1	I_	Linoleic acid*	768	NIST	FA
138	15.51	204	I_	2-GalactosylGlycerol	896	NIST	Cplx-Sugar
141	15.74	129.1	I_	Myristic-glycerol?	751	NIST	FA
142	15.85	106.1	I_Dg_	EPA	834	NIST	FA
145	16.61	103.1	I_	?			?
146	16.68	130	I_Dg_	C16:1-glycerol??	680	NIST	FA
147	16.69	103	Dg_	?			?
150	16.77	129.1	I_Eg_	C16:2-glycerol?			FA
151	16.87	129.1	I_Eg_Dg_	C16:1-glycerol?			FA
158	17.78	189.1	Ejn_	Maltose *	883	MPL	Sugar
164	17.90	271.1		Disaccharide	859	MPL	Sugar
165	17.96	204.1	I_Ejn_	Disaccharide	846	MPL	Sugar
166	18.00	311.3	I_Eg_Dg_	?			?
168	18.09	145.1	I_Dg_	Sterol?			Sterol
169	18.39	103.1	I_	?			?
171	18.83	353.3	I_	Cholesterylpelargonate ?	863	NIST	Sterol
172	20.13	204.1	I_	Digalactosylglycerol?	735	Golm	Cplx-Sugar
174	20.44	129.1	I_	Cholesterol	878	NIST	Sterol
176	20.72	113.1	Ejn_	?			?
176	20.72	113.1	Ejn_	?			?
178	21.28	129.1	I_Ejn_	Sterol			Sterol
179	21.34	382.4		Campesterol??	635	Golm	Sterol

n ^{o1}	RT ²	model ion ³	CAP hit ⁴	Identification	R ⁵ match	Library ⁶	Class ⁷
183	24.03	204.1	I_Dg_Ejn_	?			?
184	24.15	204.1	I_Dg_Ejn_	Trisaccharide	824	NIST	Sugar
185	24.34	204.1	I_Dg_Ejn_	Trisaccharide			Sugar
186	24.46	204.1	I_Ejn_	Trisaccharide?	797	Golm	Sugar
188	25.58	204.1	I_	Trisaccharide			Sugar

¹ Metabolite identification number. ² retention time (min). ³ Ion chosen by MET-IDEA to quantify the metabolite intensity. ⁴ CAP analysis that showed a significant level for the metabolite, I: CAP interphase, E, D: CAP intraphase in exponential and declining phase. Jn: CAP intraphase with day and night sampling as groups, g, CAP intraphase with every sampling time as a group. ⁵ reverse match score of the library identification, if lower than 800 and no standard available, the metabolite identification is tagged with a "?", and "???" if the score is lower than 700. ⁶ cf. Table 23. ⁷ metabolite class, aa: amino acids, FA: fatty acid-related, Cplx-sugar: complex sugars. * identification confirmed by comparison with a standard.

Appendix X: Principal Coordinate Analysis of the *S. marinoi* G4 cell metabolites, in stationary phase. In abscissa the first coordinate axis, in ordinate the second coordinate axis.



Appendix XI: Compounds found in the culture medium of *S. marinoi* G4

N ^{o1}	RT ²	model ion ³	in cells? ⁴	Metabolite	R ⁵ match	Library ⁶
86	8.31	196.1	-	-		
97	8.65	199.1	25	-		
127	9.67	231.1	-	-		
132	9.84	224.1	-	3 or 4 hydroxybenzoic acid?	682	NIST
141	10.12	184.1	-	-		
165	10.85	217.1	47	Pentafuranose?	635	NIST
168	10.92	255.2	-	-		
178	11.29	275.2	-	-		
190	11.67	357.2	-	-		
195	11.83	271.2	-	-		
196	11.86	157.1	-	-		
204	12.15	263.2	-	-		
205	12.19	253.1	-	-		
209	12.32	294.2	-	-		
214	12.44	263.2	-	-		
215	12.46	157.1	-	-		
218	12.54	285.2	72	Tetradecanoic acid*	808	NIST
226	12.78	197.2	-	-		
229	12.94	199.2	-	Hexose	722	NIST
230	12.98	319.2	103	Glucose*	710	Golm
231	13.00	307.2	-	-		
233	13.07	197.2	-	-		
243	13.44	211.2	-	FA?		
251	13.73	311.2	107	Hexadecenoic acid	792	Golm
254	13.87	335.2	117	Hexadecanoic acid*	538	NIST
255	13.90	293.2	-	-		
259	14.08	225.2	-	-		
262	14.19	346.3	-	-		
264	14.34	173.1	-	-		
275	14.87	329.2	131	-		
278	14.99	146.1	-	-		
281	15.18	168.1	-	-		
285	15.40	200.1	-	-		
286	15.43	145.1	-	-		
287	15.55	204.1	138	Galactosyl-Glycerol?	785	NIST
288	15.61	401.3	-	-		
291	15.71	230.1	-	-		
304	16.56	225.1	-	-		
317	17.92	361.2	164	Trisaccharide?	723	MPI
329	19.50	204.1	-	Trisaccharide?	712	Golm

¹ Metabolite identification number. ² retention time. ³ ion chosen by MET-IDEA to quantify the metabolite intensity, ⁴ indicates the identification number of the metabolites in the cell analysis, if found. ⁵ reverse match score of the library identification, if lower than 800 and no standard is available, the metabolite identification is tagged with a "?" ⁶ cf. Table 23. *, identification confirmed by comparison with a standard.

Appendix XII: Metabolites found in the seawater of the mesocosms.

n ^{o1}	RT ²	model ion ³	Identification	R ⁴ match	Library ⁵
52	228.1	6.684	-	-	
53	129	6.724	-	-	
56	169.1	6.841	-	-	
60	131.1	6.969	-	-	
75	299.1	7.538	Phosphate??	791	NIST
101	191.1	8.585	-	-	
115	205.1	9.072	Tetrose?	820	Golm
123	181.1	9.434	-	-	
124	209.1	9.464	Hydroxybenzoic acid	833	NIST
129	232.1	9.631	Aspartic acid*	803	Golm
134	209.1	9.796	-	-	
136	181.1	9.858	-	-	
141	131.1	10.01	-	-	
143	131.1	10.05	-	-	
145	217	10.13	Pentafuranose	823	Metabo
147	131.1	10.18	-	-	
148	217.1	10.20	Pentafuranose?	777	NIST
149	217	10.23	Pentafuranose	829	Metabo
151	217.1	10.29	Pentafuranose?	760	NIST
155	217	10.42	Pentafuranose	829	Metabo
162	217.1	10.65	Pentafuranose?	722	NIST
167	217.1	10.76	Pentose	850	MPI
168	307.2	10.77	Pentose	850	MPI
180	228.1	11.37	-	-	
185	131.1	11.55	Sugar alcohol?	735	Golm
187	131.1	11.63	Desoxyhexose??	565	Golm
195	138.1	11.91	-	-	
200	123.1	12.07	Terpen??	-	
202	285.2	12.12	Tetradecanoic acid*	835	Golm
209	273.1	12.33	-	-	
213	318.9	12.47	Glucose*	940	MPI
214	273.1	12.55	-	-	
218	382.2	12.64	-	-	
222	382.2	12.72	-	-	
225	257.1	12.83	-	-	
226	301.1	12.87	-	-	
229	382.2	12.97	-	-	
230	131.1	13.02	-	-	
232	351.2	13.10	-	-	
235	131.1	13.19	Hexadecadienoic acid?	-	
237	161.1	13.27	-	-	
238	312.3	13.31	Hexadecenoic acid?	771	NIST
240	318.1	13.36	Inositol isomer?	736	MPI
242	311.2	13.38	Hexadecenoic acid*	-	
246	288.2	13.61	-	-	
248	225.2	13.66	-	-	
261	343.1	14.14	Hydroxy-octadecanoic acid??	-	
266	143.1	14.31	-	-	
267	319.2	14.32	Skel-cell 128	828	Metabo
269	131.1	14.34	C20:x??	-	
273	329.2	14.45	Skel-cell 131?	736	Metabo
279	131.1	14.62	-	-	
289	204.1	15.05	Galactosyl glycerol	888	Metabo
291	204.1	15.15	Galactinol??	-	
296	204.1	15.40	Disaccharide?	-	
301	485.3	15.68	Inositolphosphate??	657	NIST
311	225.2	16.14	-	-	

Appendices

n ^o 1	RT ²	model ion ³	Identification	R ⁴ match	Library ⁵
319	204.2	16.42	-	-	
320	369.5	16.46	C20:0??	575	NIST
326	445.5	16.61	Hexosephosphate?	-	
327	161.1	16.75	-	-	
329	131	16.77	-	-	
336	464.3	16.99	-	-	
343	131.1	17.22	-	-	
345	204.1	17.27	-	-	
346	204	17.31	Disaccharide	955	MPI
349	395.5	17.38	Sugar alcohol??	-	
353	361	17.49	Disaccharide?	-	
395	204	19.46	Disaccharide	845	NIST
401	129.1	20.49	Sterol??	637	Metabo
413	204.1	21.17	Saccharide	-	
419	204.1	21.56	Saccharide	-	
421	204.1	21.81	Saccharide	-	
429	204.1	23.64	Trisaccharide	-	
432	205	23.71	Trisaccharide	-	
444	361.2	24.11	Trisaccharide	-	
446	204.1	24.17	Trisaccharide	-	
447	221.1	24.18	-	-	
449	361.2	24.25	-	-	

¹ Metabolite identification number. ² retention time (min). ³ Ion chosen by MET-IDEA to quantify the metabolite intensity, ⁴ reverse match score of the library identification, if lower than 800 and no standard is available, the metabolite identification is tagged with a "?", and "???" if the score is lower than 700. ⁵, cf. Table 23. ⁷* identification confirmed by comparison with a standard.

Appendix XIII: Diatom metabolomic SOP

FSU / IAAC LS f. instrumentelle Analytik	SOP Standard Operating Procedure	
Date: 02.07.2009	Met.Prof.Derivatisation	
Issued: 02.07.2009 Valid from: 02.07.2009	Created by: Charles Vidoudez	Validity Area: FSU / IAAC -LS f. instrumentelle Analytik -
Responsible: Charles Vidoudez	This SOP supersedes: none	
Extraction and Derivatisation of diatom samples for intra- and extra-cellular metabolomic profiling		
<ol style="list-style-type: none"> 1. References: Vidoudez, in preparation 2. Starting material: <ol style="list-style-type: none"> a. Diatom culture 3. Equipment: <ol style="list-style-type: none"> a. Eppendorf Pipettes, 1000, 200, 20 and 10 or 5, recently checked and calibrated. b. Eppendorf tips, blue, yellow and white, only manipulated with gloves. c. Eppendorf centrifuge tube, 1.5 mL, PCR clean grade or higher. d. Glass syringe, 100 µL, Hamilton, Bonaduz, Switzerland. e. Centrifuge for centrifuge tubes, with temperature control. f. Vacuum evaporation facility and vacuum pump. g. Heat block. h. 1 L glass bottle. i. Teflon tubing, Ø 0.8 mm. 4. Chemicals and consumables: <ol style="list-style-type: none"> a. Methanol, Chromasolv[®] Plus, Sigma-Aldrich, Munich, Germany. b. Ethanol, LiChrosolv[®], Merck, Darmstadt, Germany. c. Chloroform, HiPerSolv, VWR, Dresden, Germany. d. Water, Chromasolv[®] Plus, Sigma-Aldrich. e. Tetrahydrofuran (THF), HiPerSolv, VWR. f. N-Methyl-N-trifluoroacetamide (MSTFA), in 1 mL vials, Macherey-Nagel, Düren, Germany. g. Pyridine, Chromasolv[®] Plus, Sigma-Aldrich. h. Methoxyamine hydrochloride, Sigma-Aldrich. i. Ribitol, >99%, Sigma-Aldrich, 4 mM in water. j. RI mix: decane, pentadecane, nonadecane, octacosane, dotriacontane all 1 mM and hexatriacontane 0.5 mM in hexane (all >99%, Sigma-Aldrich). k. Extraction mix: Methanol:Ethanol:Chloroform mix, 2:6:2, freshly prepared. l. Sand, sulphuric acid-washed, VWR. m. EASY Chromabond cartridge, 3mL, 360 mg, Macherey-Nagel. n. Polycarbonate syringe, 5 mL, B.Braun, Berlin, Germany. o. Empty Chromabond cartridge, 3mL, Macherey-Nagel. p. 1.5 mL (N8) glass vials, Macherey-Nagel. q. 4 mL (N13) glass vials, Macherey-Nagel. r. 200 µL glass inserts, Macherey-Nagel. s. PTFE-butyl-PTFE septa for 1.5 mL glass vials, VWR. t. PTFE-butyl septa for 4 mL glass vials, VWR. 5. Procedure for intra-cellular metabolite sample preparation: <ol style="list-style-type: none"> a. Concentrate a determined amount of cells on a GF/C filter under reduced vacuum (~400 mBar). b. Immediately transfer the filter on the inner surface of a 25 mL glass beaker. c. Resuspend the cells in 1 mL of extraction mix and transfer in an eppendorf centrifuge tube. d. Vortex 10 sec. e. Add 5 µL of the ribitol solution (20 nmol). f. The sample can be stored then at -20°C for short period and -80°C for longer period. 		

FSU / IAAC LS f. instrumentelle Analytik	SOP Standard Operating Procedure	
Date: 02.07.2009	Met.Prof.Derivatisation	
<p>g. Vortex.</p> <p>h. Transfer the equivalent of $\sim 50 \cdot 10^6$ cells, if available, into a new eppendorf tube.</p> <p>i. Adjust the volume with the extraction mix to reach a equivalent to a maximum cell density of $\sim 0.5 \cdot 10^6$ cells μL^{-1}.</p> <p>j. Place the samples in an ultrasound bath for 10 min.</p> <p>k. Centrifuge the samples at 30000 g (17000 rpm) at 4°C for 15 min.</p> <p>l. Transfer the supernatant into a 1.5 mL glass vial, sealable with PTFE-butyl-PTFE septa.</p> <p>m. Evaporate to dryness under vacuum for ~ 5 hours, and vent the vacuum dryer with dry air.</p> <p>n. Samples are ready for derivatisation.</p> <p>6. Procedure for extra-cellular metabolite sample preparation</p> <p>a. Push with a syringe 4 mL methanol an EASY cartridge.</p> <p>b. Wash with 4 mL water.</p> <p>c. Fill an empty Chromabond cartridge with ~ 3 g of sand and connect in line with a preconditionated Easy cartridge. The sand cartridge will filter out the cells.</p> <p>d. Connect ~ 30 cm of Teflon tubing in line with the sand cartridge to form a Teflon-tubing-sand-cartridge-EASY filtration unit.</p> <p>e. Place the Teflon tubing end of the filtration unit in a 1 L glass bottle.</p> <p>f. Pour a determined volume (usually 1 L) of sample in the glass bottle.</p> <p>g. Start filtration by connecting the EASY-end of the filtration unit to a vacuum pump.</p> <p>h. Pass the sample through the column at a rate of ~ 1 L hour^{-1}.</p> <p>i. Disconnect the EASY from the filtration unit and wash with 4 mL of water (Chromasolv).</p> <p>j. Air dry the EASY cartridge.</p> <p>k. Elute the metabolites by gravity with 2 mL of methanol in a 4 mL glass vial</p> <p>l. Elute the metabolites by gravity with 2 mL of methanol:THF 1:1 in the same vial.</p> <p>m. Add 5 μL of ribitol internal standard solution.</p> <p>n. Close the vials with caps fitted with PTFE-butyl septa.</p> <p>o. Samples can be stored at -80°C at that step.</p> <p>p. Transfer 1.5 mL of sample into a 1.5 mL glass vial</p> <p>q. Evaporate to dryness under vacuum for ~ 10 hours, and vent the vacuum dryer with dry air.</p> <p>r. Samples are ready for derivatisation.</p> <p>7. Derivatisation</p> <p>a. Prepare methoxymation solution by adding 20 mg of methoxyamine in 1 mL of pyridine and ensure complete dissolution by sonicating 5 min in an ultrasound bath.</p> <p>b. Add 50 μL of methoxymation solution to a maximum of 20 dry samples.</p> <p>c. Vortex 1 min.</p> <p>d. Incubate at 60°C for 1 hour.</p> <p>e. Incubate at room temperature for 9 hours.</p> <p>f. Prepare the silylation solution by adding with a glass syringe 40 μL of the RI mix into a new 1 mL vial of MSTFA.</p> <p>g. Add 50 μL of silylation solution to the samples with a glass syringe (in batch not bigger than 20 samples)</p> <p>h. Incubate at 40°C for one hour.</p> <p>i. Transfer the samples into glass inserts and close the vials.</p> <p>j. Analyse the batch of samples immediately.</p>		

Bibliography

- Ackman, R.G., Jangaard, P.M., Hoyle, R.J. and Brockerhoff, H. (1964) Origin of marine fatty acids .1. Analyses of the fatty acids produced by the diatom *Skeletonema costatum*. *Journal of the Fisheries Research Board of Canada*, **21**, 747-756.
- Adolph, S., Bach, S., Blondel, M., Cuffe, A., Moreau, M., Pohnert, G., Poulet, S.A., Wichard, T. and Zuccaro, A. (2004) Cytotoxicity of diatom-derived oxylipins in organisms belonging to different phyla. *Journal of Experimental Biology*, **207**, 2935-2946.
- Alderkamp, A.-C., Buma, A. and van Rijssel, M. (2007) The carbohydrates of *Phaeocystis* and their degradation in the microbial food web. *Biogeochemistry*, **83**, 99-118.
- Allen, A.E., LaRoche, J., Maheswari, U., Lommer, M., Schauer, N., Lopez, P.J., Finazzi, G., Fernie, A.R. and Bowler, C. (2008) Whole-cell response of the pennate diatom *Phaeodactylum tricoratum* to iron starvation. *Proceedings of the National Academy of Sciences*, **105**, 10438-10443.
- Amsler, C.D. and Fairhead, V.A. (2005) Defensive and sensory chemical ecology of brown algae. *Advances in botanical research*, **43**, 1-91.
- Anderson, M.J. (2001) Permutation tests for univariate or multivariate analysis of variance and regression. *Canadian Journal of Fisheries and Aquatic Sciences*, **58**, 626-639.
- Anderson, M.J. and Willis, T.J. (2003) Canonical analysis of principal coordinates: A useful method of constrained ordination for ecology. *Ecology*, **84**, 511-525.
- Armbrust, E.V. (2009) The life of diatoms in the world's oceans. *Nature*, **459**, 185-192.
- Ausloos, P., Clifton, C.L., Lias, S.G., Mikaya, A.I., Stein, S.E., Tchekhovskoi, D.V., Sparkman, O.D., Zaikin, V. and Zhu, D. (1999) The critical evaluation of a comprehensive mass spectral library. *Journal of the American Society for Mass Spectrometry*, **10**, 287-299.
- Ballestar, E., Abad, C.n. and Franco, L. (1996) Core histones are glutaminyl substrates for tissue transglutaminase. *Journal of Biological Chemistry*, **271**, 18817-18824.
- Barofsky, A. and Pohnert, G. (2007) Biosynthesis of polyunsaturated short chain aldehydes in the diatom *Thalassiosira rotula*. *Organic Letters*, **9**, 1017-1020.
- Barofsky, A., Vidoudez, C. and Pohnert, G. (2009) Metabolic profiling reveals growth stage variability in diatom exudates. *Limnology and Oceanography-Methods*, **7**, 382-390.
- Barofsky, A., Simonelli, P., Vidoudez, C., Troedsson, C., Nejstgaard, J.C., Jakobsen, H.H. and Pohnert, G. (2010) Growth phase of the diatom *Skeletonema marinoi* influences the metabolic profile of the cells and the selective feeding of the copepod *Calanus* spp. *Journal of Plankton Research*, **32**, 263-272.
- Beardall, J., Mukerji, D., Glover, H.E. and Morris, I. (1976) Path of carbon in photosynthesis by marine phytoplankton. *Journal of Phycology*, **12**, 409-417.
- Bekker, A., Holland, H.D., Wang, P.L., Rumble, D., Stein, H.J., Hannah, J.L., Coetzee, L.L. and Beukes, N.J. (2004) Dating the rise of atmospheric oxygen. *Nature*, **427**, 117-120.
- Ben-Amotz, A. and Avron, M. (1983) Accumulation of metabolites by halotolerant algae and its industrial potential. *Annual Reviews in Microbiology*, **37**, 95-119.
- Berge, J.-P., Gouygou, J.-P., Dubacq, J.-P. and Durand, P. (1995) Reassessment of lipid composition of the diatom, *Skeletonema costatum*. *Phytochemistry*, **39**, 1017-1021.
- Bidle, K.D. and Falkowski, P.G. (2004) Cell death in planktonic, photosynthetic microorganisms. *Nature Review Microbiology*, **2**, 643-655.

- Bisignano, G., Lagana, M.G., Trombetta, D., Arena, S., Nostro, A., Uccella, N., Mazzanti, G. and Saija, A. (2001) In vitro antibacterial activity of some aliphatic aldehydes from *Olea europaea* L. *Fems Microbiology Letters*, **201**, 117-117.
- Blanchemain, A. and Grizeau, D. (1996) Eicosapentaenoic acid content of *Skeletonema costatum* as a function of growth and irradiance; relation with chlorophyll a content and photosynthetic capacity. *Journal of Experimental Marine Biology and Ecology*, **196**, 177-188.
- Bowler, C., Vardi, A. and Allen, A.E. (2010) Oceanographic and biogeochemical insights from diatom genomes. *Annual Review of Marine Science*, **2**, 333-365.
- Broeckling, C.D., Reddy, I.R., Duran, A.L., Zhao, X.C. and Sumner, L.W. (2006) MET-IDEA: Data extraction tool for mass spectrometry-based metabolomics. *Analytical Chemistry*, **78**, 4334-4341.
- Brown, K.L., Twing, K.I. and Robertson, D.L. (2009) Unraveling the regulation of nitrogen assimilation in the marine diatom *Thalassiosira pseudonana* (Bacillariophyceae): diurnal variations in transcript levels for five genes involved in nitrogen assimilation. *Journal of Phycology*, **45**, 413-426.
- Buttino, I., Miralto, A., Ianora, A., Romano, G. and Poulet, S.A. (1999) Water-soluble extracts of the diatom *Thalassiosira rotula* induce aberrations in embryonic tubulin organisation of the sea urchin *Paracentrotus lividus*. *Marine Biology*, **134**, 147-154.
- Buttino, I., De Rosa, G., Carotenuto, Y., Mazzella, M., Ianora, A., Esposito, F., Vitiello, V., Quaglia, F., La Rotonda, M.I. and Miralto, A. (2008) Aldehyde-encapsulating liposomes impair marine grazer survivorship. *Journal of Experimental Biology*, **211**, 1426-1433.
- Carvalho, V.M., Asahara, F., Di Mascio, P., Campos, I.P.D., Cadet, J. and Medeiros, M.H.G. (2000) Novel 1,N-6-etheno-2'-deoxyadenosine adducts from lipid peroxidation products. *Chemical Research in Toxicology*, **13**, 397-405.
- Casotti, R., Mazza, S., Brunet, C., Vantrepotte, V., Ianora, A. and Miralto, A. (2005) Growth inhibition and toxicity of the diatom aldehyde 2-trans, 4-trans-decadienal on *Thalassiosira weissflogii* (Bacillariophyceae). *Journal of Phycology*, **41**, 7-20.
- Cloern, J.E., Cole, B.E., Wong, R.L.J. and Alpine, A.E. (1985) Temporal dynamics of estuarine phytoplankton: A case study of San Francisco Bay. *Hydrobiologia*, **129**, 153-176.
- Collos, Y. (1986) Time-lag algal growth dynamics: biological constraints on primary production in aquatic environments. *Marine Ecology Progress Series*, **33**, 193-206.
- Cutignano, A., d'Ippolito, G., Romano, G., Lamari, N., Cimino, G., Febbraio, F. and Fontana, A. (2006) Chloroplastic glycolipids fuel aldehyde biosynthesis in the marine diatom *Thalassiosira rotula*. *Chembiochem*, **7**, 450-456.
- d'Ippolito, G., Romano, G., Caruso, T., Spinella, A., Cimino, G. and Fontana, A. (2003) Production of octadienal in the marine diatom *Skeletonema costatum*. *Organic Letters*, **5**, 885-887.
- d'Ippolito, G., Tucci, S., Cutignano, A., Romano, G., Cimino, G., Miralto, A. and Fontana, A. (2004) The role of complex lipids in the synthesis of bioactive aldehydes of the marine diatom *Skeletonema costatum*. *Biochimica et Biophysica Acta (BBA) - Molecular and Cell Biology of Lipids*, **1686**, 100-107.
- d'Ippolito, G., Cutignano, A., Tucci, S., Romano, G., Cimino, G. and Fontana, A. (2006) Biosynthetic intermediates and stereochemical aspects of aldehyde biosynthesis in the marine diatom *Thalassiosira rotula*. *Phytochemistry*, **67**, 314-322.
- Desbois, A.P., Mearns-Spragg, A. and Smith, V.J. (2009) A fatty acid from the diatom *Phaeodactylum tricorutum* is antibacterial against diverse bacteria including multi-resistant *Staphylococcus aureus* (MRSA). *Marine Biotechnology*, **11**, 45-52.
- Dickson, D.M.J. and Kirst, G.O. (1987) Osmotic adjustment in marine eukaryotic algae: the role of inorganic ions, quaternary ammonium, tertiary sulphonium and carbohydrate solutes. I. Diatoms and a rhodophyte. *New Phytologist*, **106**, 645-655.
- Dodds, E.D., McCoy, M.R., Rea, L.D. and Kennish, J.M. (2005) Gas chromatographic quantification of fatty acid

- methyl esters: flame ionization detection vs. electron impact mass spectrometry. *Lipids*, **40**, 419-428.
- Dutz, J., Koski, M. and Jonasdottir, S.H. (2008) Copepod reproduction is unaffected by diatom aldehydes or lipid composition. *Limnology and Oceanography*, **53**, 225-235.
- Eppley, R.W. and Renger, E.H. (1974) Nitrogen assimilation of an oceanic diatom in nitrogen-limited continuous culture. *Journal of Phycology*, **10**, 23.
- Fiehn, O., Kopka, J., Trethewey, R.N. and Willmitzer, L. (2000) Identification of uncommon plant metabolites based on calculation of elemental compositions using gas chromatography and quadrupole mass spectrometry. *Analytical Chemistry*, **72**, 3573-3580.
- Fiehn, O., Wohlgemuth, G. and Scholz, M. (2005) Setup and annotation of metabolomic experiments by integrating biological and mass spectrometric metadata. *Proc Lect Notes Bioinformatics*, **3615**, 224-239.
- Fiehn, O., Robertson, D., Griffin, J., van der Werf, M., Nikolau, B., Morrison, N., Sumner, L., Goodacre, R., Hardy, N., Taylor, C., Fostel, J., Kristal, B., Kaddurah-Daouk, R., Mendes, P., van Ommen, B., Lindon, J. and Sansone, S.-A. (2007a) The metabolomics standards initiative (MSI). *Metabolomics*, **3**, 175-178.
- Fiehn, O., Sumner, L., Rhee, S., Ward, J., Dickerson, J., Lange, B., Lane, G., Roessner, U., Last, R. and Nikolau, B. (2007b) Minimum reporting standards for plant biology context information in metabolomic studies. *Metabolomics*, **3**, 195-201.
- Fiehn, O. (2008) Extending the breadth of metabolite profiling by gas chromatography coupled to mass spectrometry. *Trends in Analytical Chemistry*, **27**, 261-269.
- Fiehn, O., Wohlgemuth, G., Scholz, M., Kind, T., Lee, D.Y., Lu, Y., Moon, S. and Nikolau, B. (2008) Quality control for plant metabolomics: reporting MSI-compliant studies. *Plant Journal*, **53**, 691.
- Field, C.B., Behrenfeld, M.J., Randerson, J.T. and Falkowski, P. (1998) Primary production of the biosphere: integrating terrestrial and oceanic components. *Science*, **281**, 237-240.
- Flynn, K.J. and Irigoien, X. (2009) Aldehyde-induced insidious effects cannot be considered as a diatom defence mechanism against copepods. *Marine Ecology-Progress Series*, **377**, 79-89.
- Fontana, A., d'Ippolito, G., Cutignano, A., Miralto, A., Ianora, A., Romano, G. and Cimino, G. (2007) Chemistry of oxylipin pathways in marine diatoms. *Pure and Applied Chemistry*, **79**, 481-490.
- Fuqua, W.C., Winans, S.C. and Greenberg, E.P. (1994) Quorum sensing in bacteria: the LuxR-LuxI family of cell density-responsive transcriptional regulators. *Journal of bacteriology*, **176**, 269-275.
- Gaff, D.F. and Okong'O-Ogola, O. (1971) The use of non-permeating pigments for testing the survival of cells. *Journal of Experimental Botany*, **22**, 756-758.
- Goodacre, R., Broadhurst, D., Smilde, A., Kristal, B., Baker, J., Beger, R., Bessant, C., Connor, S., Capuani, G., Craig, A., Ebbels, T., Kell, D., Manetti, C., Newton, J., Paternostro, G., Somorjai, R., Sjöström, M., Trygg, J. and Wulfert, F. (2007a) Proposed minimum reporting standards for data analysis in metabolomics. *Metabolomics*, **3**, 231-241.
- Goodacre, R., Roberts, L., Ellis, D.I., Thorogood, D., Reader, S.M., Ougham, H. and King, I. (2007b) From phenotype to genotype: whole tissue profiling for plant breeding. *Metabolomics*, **3**, 489-501.
- Gross, E.M. (2003) Allelopathy of aquatic autotrophs. *Critical Reviews in Plant Sciences*, **22**, 313-339.
- Grossart, H.P., Levold, F., Allgaier, M., Simon, M. and Brinkhoff, T. (2005) Marine diatom species harbour distinct bacterial communities. *Environmental Microbiology*, **7**, 860-873.
- Grossart, H.P. and Simon, M. (2007) Interactions of planktonic algae and bacteria: effects on algal growth and organic matter dynamics. *Aquatic Microbial Ecology*, **47**, 163.
- Gullberg, J., Jonsson, P., Nordström, A., Sjöström, M. and Moritz, T. (2004) Design of experiments: an efficient strategy to identify factors influencing extraction and derivatization of *Arabidopsis thaliana* samples in metabolomic studies with gas chromatography/mass spectrometry. *Analytical Biochemistry*, **331**, 283-295.

- Halsband-Lenk, C., Pierson, J.J. and Leising, A.W. (2005) Reproduction of *Pseudocalanus newmani* (Copepoda : Calanoida) is deleteriously affected by diatom blooms - A field study. *Progress In Oceanography*, **67**, 332-348.
- Hamm, C.E., Merkel, R., Springer, O., Jurkojc, P., Maier, C., Prechtel, K. and Smetacek, V. (2003) Architecture and material properties of diatom shells provide effective mechanical protection. *Nature*, **421**, 841-843.
- Hansen, E., Ernstsens, A. and Eilertsen, H.C. (2004) Isolation and characterisation of a cytotoxic polyunsaturated aldehyde from the marine phytoplankton *Phaeocystis pouchetii* (Hariot) Lagerheim. *Toxicology*, **199**, 207-217.
- Hansen, E. and Eilertsen, H.C. (2007) Do the polyunsaturated aldehydes produced by *Phaeocystis pouchetii* (Hariot) Lagerheim influence diatom growth during the spring bloom in Northern Norway? *Journal of Plankton Research*, **29**, 87-96.
- Harrison, P.J., Conway, H.L., Holmes, R.W. and Davis, C.O. (1977) Marine diatoms grown in chemostats under silicate or ammonium limitation. III. Cellular chemical composition and morphology of *Chaetoceros debilis*, *Skeletonema costatum*, and *Thalassiosira gravida*. *Marine Biology*, **43**, 19-31.
- Hinga, K.R. (2002) Effects of pH on coastal marine phytoplankton. *Marine Ecology Progress Series*, **238**, 281-300.
- Horner, R.A., Postel, J.R., Halsband-Lenk, C., Pierson, J.J., Pohnert, G. and Wichard, T. (2005) Winter-spring phytoplankton blooms in Dabob Bay, Washington. *Progress In Oceanography*, **67**, 286-313.
- Ianora, A., Miralto, A., Poulet, S.A., Carotenuto, Y., Buttino, I., Romano, G., Casotti, R., Pohnert, G., Wichard, T., Colucci-D'Amato, L., Terrazzano, G. and Smetacek, V. (2004) Aldehyde suppression of copepod recruitment in blooms of a ubiquitous planktonic diatom. *Nature*, **429**, 403-407.
- Ianora, A., Boersma, M., Casotti, R., Fontana, A., Harder, J., Hoffmann, F., Pavia, H., Potin, P., Poulet, S. and Toth, G. (2006) New trends in marine chemical ecology. *Estuaries and Coasts*, **29**, 531-551.
- Ianora, A., Casotti, R., Bastianini, M., Brunet, C., d'Ippolito, G., Acri, F., Fontana, A., Cutignano, A., Turner, J.T. and Miralto, A. (2008) Low reproductive success for copepods during a bloom of the non-aldehyde-producing diatom *Cerataulina pelagica* in the North Adriatic Sea. *Marine Ecology-an Evolutionary Perspective*, **29**, 399-410.
- Imada, N., Kobayashi, K., Isomura, K., Saito, H., Kimura, S., Tahara, K. and Oshima, Y. (1992) Isolation and identification of an autoinhibitor produced by *Skeletonema costatum*. *Nippon Suisan Gakkaishi*, **58**, 1687-1692.
- Jansen, J.J., Smit, S., Hoefsloot, H.C.J. and Smilde, A.K. (2009) The photographer and the greenhouse: how to analyse plant metabolomics data. *Phytochemical Analysis*, **21**, 48-60.
- Jiye, A., Trygg, J., Gullberg, J., Johansson, A.I., Jonsson, P., Antti, H., Marklund, S.L. and Moritz, T. (2005) Extraction and GC/MS analysis of the human blood plasma metabolome. *Analytical Chemistry*, **77**, 8086-8094.
- Kanani, H.H. and Klapa, M.I. (2007) Data correction strategy for metabolomics analysis using gas chromatography-mass spectrometry. *Metabolic Engineering*, **9**, 39-51.
- Kolber, Z., Zehr, J. and Falkowski, P. (1988) Effects of growth irradiance and nitrogen limitation on photosynthetic energy conversion in photosystem II. *Plant Physiology*, **88**, 923-929.
- Kooistra, W.H.C.F., Sarno, D., Balzano, S., Gu, H., Andersen, R.A. and Zingone, A. (2008) Global diversity and biogeography of *Skeletonema* species (Bacillariophyta). *Protist*, **159**, 177-193.
- Kopka, J., Fernie, A., Weckwerth, W., Gibon, Y. and Stitt, M. (2004) Metabolite profiling in plant biology: platforms and destinations. *Genome Biology*, **5**, 109.
- Krell, A., Funck, D., Plettner, I., John, U. and Dieckmann, G. (2007) Regulation of proline metabolism under salt stress in the psychrophilic diatom *Fragilariopsis cylindrus* (Bacillariophyceae). *Journal of Phycology*, **43**, 753-762.
- Kröger, N., Deutzmann, R., Bergsdorf, C. and Sumper, M. (2000) Species-specific polyamines from diatoms control silica morphology. *Proceedings of the National Academy of Sciences of the United States of America*, **97**, 14133-14138.

Bibliography

- Lee, D. and Fiehn, O. (2008) High quality metabolomic data for *Chlamydomonas reinhardtii*. *Plant Methods*, **4**, 7.
- Leflaive, J. and Ten-Hage, L. (2009) Chemical interactions in diatoms: role of polyunsaturated aldehydes and precursors. *New Phytologist*, **184**, 794-805.
- Legrand, C., Rengefors, K., Fistarol, G.O. and Graneli, E. (2003) Allelopathy in phytoplankton - biochemical, ecological and evolutionary aspects. *Phycologia*, **42**, 406-419.
- Lepage, G. and Roy, C.C. (1984) Improved recovery of fatty acid through direct transesterification without prior extraction or purification. *Journal of Lipid Research*, **25**, 1391-1396.
- Lewis, J., Harris, A.S.D., Jones, K.J. and Edmonds, R.L. (1999) Long-term survival of marine planktonic diatoms and dinoflagellates in stored sediment samples. *Journal of Plankton Research*, **21**, 343-354.
- Lisec, J., Schauer, N., Kopka, J., Willmitzer, L. and Fernie, A.R. (2006) Gas chromatography mass spectrometry-based metabolite profiling in plants. *Nature Protocols*, **1**, 387-396.
- Liu, M.S. and Hellebust, J.A. (1976) Regulation of proline metabolism in the marine centric diatom *Cyclotella cryptica*. *Canadian Journal of Botany*, **54**, 949-959.
- Long, R.A. and Azam, F. (2001) Antagonistic interactions among marine pelagic bacteria. *Applied and Environmental Microbiology*, **67**, 4975-4983.
- Lund, J.W.G., Kipling, C. and LeCren, E.D. (1958) The inverted microscope method of estimating algal numbers and the statistical basis of estimations of counting. *Hydrobiologia*, **11**, 143-170.
- Maheswari, U., Montsant, A., Goll, J., Krishnasamy, S., Rajyashri, K.R., Patell, V.M. and Bowler, C. (2005) The diatom EST database. *Nucleic Acids Research*, **33**, D344-D347.
- Maier, I. and Calenberg, M. (1994) Effect of extracellular Ca²⁺ and Ca²⁺-antagonists on the movement and chemoorientation of male gametes of *Ectocarpus siliculosus* (Phaeophyceae). *Botanica Acta*, **107**, 451-460.
- Matsubara, T., Nagasoe, S., Yamasaki, Y., Shikata, T., Shimasaki, Y., Oshima, Y. and Honjo, T. (2008) Inhibitory effects of centric diatoms on the growth of the dinoflagellate *Akashiwo sanguinea*. *Nippon Suisan Gakkaishi*, **74**, 598-606.
- McQuoid, M.R. and Hobson, L.A. (1996) Diatom resting stages. *Journal of Phycology*, **32**, 889-902.
- McQuoid, M.R. (2002) Pelagic and benthic environmental controls on the spatial distribution of a viable diatom propagule bank on the Swedish west coast. *Journal of Phycology*, **38**, 881-893.
- Miralto, A., Barone, G., Romano, G., Poulet, S.A., Ianora, A., Russo, G.L., Buttino, I., Mazzarella, G., Laabir, M., Cabrini, M. and Giacobbe, M.G. (1999) The insidious effect of diatoms on copepod reproduction. *Nature*, **402**, 173-176.
- Montsant, A., Allen, A.E., Coesel, S., Martino, A.D., Falciatore, A., Mangogna, M., Siaut, M., Heijde, M., Jabbari, K., Maheswari, U., Rayko, E., Vardi, A., Apt, K.E., Berges, J.A., Chiovitti, A., Davis, A.K., Thamatrakoln, K., Hadi, M.Z., Lane, T.W., Lippmeier, J.C., Martinez, D., Parker, M.S., Pazour, G.J., Saito, M.A., Rokhsar, D.S., Armbrust, E.V. and Bowler, C. (2007) Identification and comparative genomic analysis of signaling and regulatory components in the diatom *Thalassiosira pseudonana*. *Journal of Phycology*, **43**, 585-604.
- Moore, L.R., Rocap, G. and Chisholm, S.W. (1998) Physiology and molecular phylogeny of coexisting *Prochlorococcus* ecotypes. *Nature*, **393**, 464-467.
- Morrison, N., Bearden, D., Bundy, J., Collette, T., Currie, F., Davey, M., Haigh, N., Hancock, D., Jones, O., Rochfort, S., Sansone, S.-A., Štys, D., Teng, Q., Field, D. and Viant, M. (2007) Standard reporting requirements for biological samples in metabolomics experiments: environmental context. *Metabolomics*, **3**, 203-210.
- Mortainbertrand, A., Descolasgros, C. and Jupin, H. (1987a) Stimulating effect of light-to-dark transitions on carbon assimilation by a marine diatom. *Journal of Experimental Marine Biology and Ecology*, **112**, 11-26.
- Mortainbertrand, A., Descolasgros, C. and Jupin, H. (1987b) Short-term C-14 incorporation in *Skeletonema costatum* (Greville) Cleve (Bacillariophyceae) as a function of light regime. *Phycologia*, **26**, 262-269.

- Myklestad, S. and Haug, A. (1972) Production of carbohydrates by the marine diatom *Chaetoceros affinis* var. *willei* (Gran) Hustedt. I. Effect of the concentration of nutrients in the culture medium. *Journal of Experimental Marine Biology and Ecology*, **9**, 125-136.
- Myklestad, S., Haug, A. and Larsen, B. (1972) Production of carbohydrates by the marine diatom *Chaetoceros affinis* var. *willei* (Gran) Hustedt. II. Preliminary investigation of the extracellular polysaccharide. *Journal of Experimental Marine Biology and Ecology*, **9**, 137-144.
- Myklestad, S., Holmhansen, O., Varum, K.M. and Volcani, B.E. (1989) Rate of release of extracellular amino-acids and carbohydrates from the marine diatom *Chaetoceros affinis*. *Journal of Plankton Research*, **11**, 763-773.
- Nelson, D.M., Treguer, P., Brzezinski, M.A., Leynaert, A. and Queguiner, B. (1995) Production and dissolution of biogenic silica in the ocean - Revised global estimates, comparison with regional data and relationship to biogenic sedimentation. *Global Biogeochemical Cycles*, **9**, 359-372.
- Noureddine Yassaa, A., Ilka Peeken, C., Eckart Zöllner, C., Katrin Bluhm, C., Steve Arnold, E., Dominick Spracklen, E. and Jonathan Williams, A. (2008) Evidence for marine production of monoterpenes. *Environmental Chemistry*, **5**, 391-401.
- Oliver, S.G., Winson, M.K., Kell, D.B. and Baganz, F. (1998) Systematic functional analysis of the yeast genome. *Trends in Biotechnology*, **16**, 373-378.
- Owens, T.G., Falkowski, P.G. and Whitedge, T.E. (1980) Diel periodicity in cellular chlorophyll content in marine diatoms. *Marine Biology*, **59**, 71-77.
- Paschalidis, K.A. and Roubelakis-Angelakis, K.A. (2005) Spatial and temporal distribution of polyamine levels and polyamine anabolism in different organs/tissues of the tobacco plant. Correlations with age, cell division/expansion, and differentiation. *Plant Physiology*, **138**, 142-152.
- Paul, C., Barofsky, A., Vidoudez, C. and Pohnert, G. (2009) Diatom exudates influence metabolism and cell growth of co-cultured diatom species. *Marine Ecology-Progress Series*, **389**, 61-70.
- Pohnert, G. (2000) Wound-activated chemical defense in unicellular planktonic algae. *Angewandte Chemie*, **39**, 4352-4354.
- Pohnert, G. (2002) Phospholipase A₂ activity triggers the wound-activated chemical defense in the diatom *Thalassiosira rotula*. *Plant Physiology*, **129**, 103-111.
- Pohnert, G., Adolph, S. and Wichard, T. (2004) Short synthesis of labeled and unlabeled 6Z,9Z,12Z,15-hexadecatetraenoic acid as metabolic probes for biosynthetic studies on diatoms. *Chemistry and Physics of Lipids*, **131**, 159-166.
- Pohnert, G., Steinke, M. and Tollrian, R. (2007) Chemical cues, defence metabolites and the shaping of pelagic interspecific interactions. *Trends in Ecology & Evolution*, **22**, 198-204.
- Pohnert, G. (2010) Chemical noise in the silent ocean. *Journal of Plankton Research*, **32**, 141-144.
- Poulet, S.A., Escribano, R., Hidalgo, P., Cueff, A., Wichard, T., Aguilera, V., Vargas, C.A. and Pohnert, G. (2007) Collapse of *Calanus chilensis* reproduction in a marine environment with high diatom concentration. *Journal of Experimental Marine Biology and Ecology*, **352**, 187-199.
- Prince, E.K., Myers, T.L. and Kubanek, J. (2008) Effects of harmful algal blooms on competitors: Allelopathic mechanisms of the red tide dinoflagellate *Karenia brevis*. *Limnology and Oceanography*, **53**, 531-541.
- Puskaric, S. and Mortain-Bertrand, A. (2003) Physiology of diatom *Skeletonema costatum* (Grev.) Cleve photosynthetic extracellular release: evidence for a novel coupling between marine bacteria and phytoplankton. *Journal of Plankton Research*, **25**, 1227-1235.
- Reynolds, A., Mackiernan, G. and Van Valkenburg, S. (1978) Vital and mortal staining of algae in the presence of chlorine-produced oxidants. *Estuaries and Coasts*, **1**, 192-196.
- Ribalet, F., Berges, J.A., Ianora, A. and Casotti, R. (2007a) Growth inhibition of cultured marine phytoplankton by

- toxic algal-derived polyunsaturated aldehydes. *Aquatic Toxicology*, **85**, 219-227.
- Ribalet, F., Wichard, T., Pohnert, G., Ianora, A., Miralto, A. and Casotti, R. (2007b) Age and nutrient limitation enhance polyunsaturated aldehyde production in marine diatoms. *Phytochemistry*, **68**, 2059-2067.
- Ribalet, F., Intertaglia, L., Lebaron, P. and Casotti, R. (2008) Differential effect of three polyunsaturated aldehydes on marine bacterial isolates. *Aquatic Toxicology*, **86**, 249-255.
- Ribalet, F., Vidoudez, C., Cassin, D., Pohnert, G., Ianora, A., Miralto, A. and Casotti, R. (2009) High plasticity in the production of diatom-derived polyunsaturated aldehydes under nutrient limitation: Physiological and ecological implications. *Protist*, **160**, 444-451.
- Rice, E. (1979) Allelopathy—An update. *The Botanical Review*, **45**, 15-109.
- Roessner, U., Luedemann, A., Brust, D., Fiehn, O., Linke, T., Willmitzer, L. and Fernie, A.R. (2001) Metabolic profiling allows comprehensive phenotyping of genetically or environmentally modified plant systems. *Plant Cell*, **13**, 11-29.
- Roubeix, V., Becquevort, S. and Lancelot, C. (2008) Influence of bacteria and salinity on diatom biogenic silica dissolution in estuarine systems. *Biogeochemistry*, **88**, 47-62.
- Rowland, S.J., Allard, W.G., Belt, S.T., Massé, G., Robert, J.M., Blackburn, S., Frampton, D., Revill, A.T. and Volkman, J.K. (2001) Factors influencing the distributions of polyunsaturated terpenoids in the diatom, *Rhizosolenia setigera*. *Phytochemistry*, **58**, 717-728.
- Roy, S. and Legendre, L. (1979) DCMU-enhanced fluorescence as an index of photosynthetic activity in phytoplankton. *Marine Biology*, **55**, 93-101.
- Sarno, D., Kooistra, W.H.C.F., Medlin, L.K., Percopo, I. and Zingone, A. (2005) Diversity in the genus *Skeletonema* (Bacillariophyceae). II. An assessment of the taxonomy of *S. costatum*-like species with the description of four new species. *Journal of Phycology*, **41**, 151-176.
- Sarthou, G., Timmermans, K.R., Blain, S. and Tréguer, P. (2005) Growth physiology and fate of diatoms in the ocean: a review. *Journal of Sea Research*, **53**, 25-42.
- Serra, J.L., Llana, M.J. and Cadenas, E. (1978) Nitrate Utilization by the Diatom *Skeletonema costatum*: I. Kinetics of Nitrate Uptake. *Plant Physiology*, **62**, 987-990.
- Sfichi-Duke, L., Ioannidis, N. and Kotzabasis, K. (2008) Fast and reversible response of thylakoid-associated polyamines during and after UV-B stress: a comparative study of the wild type and a mutant lacking chlorophyll b of unicellular green alga *Scenedesmus obliquus*. *Planta*, **228**, 341-353.
- Sharp, J.H. (1977) Excretion of organic matter by marine phytoplankton: do healthy cells do it? *Limnology and Oceanography*, **22**, 381-399.
- Sims, P.A., Mann, D.G. and Medlin, L.K. (2006) Evolution of the diatoms: insights from fossil, biological and molecular data. *Phycologia*, **45**, 361-402.
- Smetacek, V. and Cloern, J.E. (2008) OCEANS: On Phytoplankton Trends. *Science*, **319**, 1346-1348.
- Staples, C.A., Williams, J.B., Craig, G.R. and Roberts, K.M. (2001) Fate, effects and potential environmental risks of ethylene glycol: a review. *Chemosphere*, **43**, 377-383.
- Stein, S.E. (1999) An integrated method for spectrum extraction and compound identification from gas chromatography/mass spectrometry data. *Journal of the American Society for Mass Spectrometry*, **10**, 770-781.
- Sumner, L., Amberg, A., Barrett, D., Beale, M., Beger, R., Daykin, C., Fan, T., Fiehn, O., Goodacre, R., Griffin, J., Hankemeier, T., Hardy, N., Harnly, J., Higashi, R., Kopka, J., Lane, A., Lindon, J., Marriott, P., Nicholls, A., Reilly, M., Thaden, J. and Viant, M. (2007) Proposed minimum reporting standards for chemical analysis. *Metabolomics*, **3**, 211-221.
- Taylor, R.L., Caldwell, G.S., Dunstan, H.J. and Bentley, M.G. (2007) Short-term impacts of polyunsaturated aldehyde-producing diatoms on the harpacticoid copepod, *Tisbe holothuriae*. *Journal of Experimental Marine Biology and*

Ecology, **341**, 60-69.

- Taylor, R.L., Abrahamsson, K., Godhe, A. and Wangberg, S.A. (2009) Seasonal variability in polyunsaturated aldehyde production potential among strains of *Skeletonema Marinoi* (Bacillariophyceae). *Journal of Phycology*, **45**, 46-53.
- Terekhova, V.E., Aizdaicher, N.A., Buzoleva, L.S. and Somov, G.P. (2009) Influence of extrametabolites of marine microalgae on the reproduction of the bacterium *Listeria monocytogenes*. *Russian Journal of Marine Biology*, **35**, 355-358.
- van der Werf, M., Takors, R., Smedsgaard, J., Nielsen, J., Ferenci, T., Portais, J., Wittmann, C., Hooks, M., Tomassini, A., Oldiges, M., Fostel, J. and Sauer, U. (2007) Standard reporting requirements for biological samples in metabolomics experiments: microbial and in vitro biology experiments. *Metabolomics*, **3**, 189-194.
- Vardi, A., Formiggini, F., Casotti, R., Martino, A.D., Ribalet, F., Miralto, A. and Bowler, C. (2006) A stress surveillance system based on calcium and nitric oxide in marine diatoms. *PLoS Biology*, **4**, e60.
- Vargas, C.A., Escribano, R. and Poulet, S. (2006) Phytoplankton food quality determines time windows for successful zooplankton reproductive pulses. *Ecology*, **87**, 2992-2999.
- Veldhuis, M.J.W., Kraay, G.W. and Timmermans, K.R. (2001) Cell death in phytoplankton: correlation between changes in membrane permeability, photosynthetic activity, pigmentation and growth. *European Journal of Phycology*, **36**, 167-177.
- Villas-Boas, S.G., Hojer-Pedersen, J., Akesson, M., Smedsgaard, J. and Nielsen, J. (2005) Global metabolite analysis of yeast: evaluation of sample preparation methods. *Yeast*, **22**, 1155-1169.
- Volkman, J.K., Jeffrey, S.W., Nichols, P.D., Rogers, G.I. and Garland, C.D. (1989) Fatty acid and lipid composition of 10 species of microalgae used in mariculture. *Journal of Experimental Marine Biology and Ecology*, **128**, 219-240.
- Wagner, C., Sefkow, M. and Kopka, J. (2003) Construction and application of a mass spectral and retention time index database generated from plant GC/EI-TOF-MS metabolite profiles. *Phytochemistry*, **62**, 887-900.
- Watson, S.B. (2003) Cyanobacterial and eukaryotic algal odour compounds: signals or by-products? A review of their biological activity. *Phycologia*, **42**, 332-350.
- Wells, M.L., Trick, C.G., Cochlan, W.P., Hughes, M.P. and Trainer, V.L. (2005) Domoic acid: the synergy of iron, copper, and the toxicity of diatoms. *Limnology and Oceanography*, **50**, 1908-1917.
- Wendel, T. and Juttner, F. (1996) Lipxygenase-mediated formation of hydrocarbons and unsaturated aldehydes in freshwater diatoms. *Phytochemistry*, **41**, 1445-1449.
- Wichard, T., Poulet, S.A., Halsband-Lenk, C., Albaina, A., Harris, R., Liu, D. and Pohnert, G. (2005a) Survey of the chemical defence potential of diatoms: screening of fifty species for alpha, beta, gamma, delta-unsaturated aldehydes. *Journal of Chemical Ecology*, **31**, 949-958.
- Wichard, T., Poulet, S.A. and Pohnert, G. (2005b) Determination and quantification of [alpha],[beta],[gamma],[delta]-unsaturated aldehydes as pentafluorobenzyl-oxime derivatives in diatom cultures and natural phytoplankton populations: application in marine field studies. *Journal of Chromatography B*, **814**, 155-161.
- Wichard, T., Poulet, S.A., Boulesteix, A.-L., Ledoux, J.B., Lebreton, B., Marchetti, J. and Pohnert, G. (2008) Influence of diatoms on copepod reproduction. II. Uncorrelated effects of diatom-derived [alpha],[beta],[gamma],[delta]-unsaturated aldehydes and polyunsaturated fatty acids on *Calanus helgolandicus* in the field. *Progress In Oceanography*, **77**, 30-44.
- Williams, P., Winzer, K., Chan, W.C. and Cámara, M. (2007) Look who's talking: communication and quorum sensing in the bacterial world. *Philosophical Transactions of the Royal Society B: Biological Sciences*, **362**, 1119.
- Winder, C.L., Dunn, W.B., Schuler, S., Broadhurst, D., Jarvis, R., Stephens, G.M. and Goodacre, R. (2008) Global metabolic profiling of *Escherichia coli* cultures: an evaluation of methods for quenching and extraction of intracellular metabolites. *Analytical Chemistry*, **80**, 2939-2948.

Bibliography

- Yamasaki, Y., Nagasoe, S., Matsubara, T., Shikata, T., Shimasaki, Y., Oshima, Y. and Honjo, T. (2007) Allelopathic interactions between the bacillariophyte *Skeletonema costatum* and the raphidophyte *Heterosigma akashiwo*. *Marine Ecology-Progress Series*, **339**, 83-92.
- Zhang, J.Z. and Fischer, C.J. (2006) A simplified resorcinol method for direct spectrophotometric determination of nitrate in seawater. *Marine Chemistry*, **99**, 220-226.

Curriculum Vitae

Charles Vidoudez

charlesvidoudez@yahoo.fr

Nationality: Swiss

Birth date: 22 January 1982

Education

2006-2010: PhD in chemical ecology in the bioorganic analytic group of Prof. Dr. Pohnert, University of Jena, Germany.

Thesis: Diatoms metabolomics

2000-2005: Study and Diploma in Biology (equivalent to Ms.), Department of Plant and Molecular Biology, University of Lausanne, Switzerland

Specialisations: Plant Biochemistry, Plant Biotechnology, Genetic Signalling.

Thesis: Discovery and characterisation of a new class of acetyl-CoA isomerases in *Arabidopsis thaliana*

1997-2000: Baccalauréat and Maturité Fédérale, section Latin-Grec-Sciences, Gymnase Auguste-Piccard, Lausanne, Switzerland

Experience

Practical course supervisor 2008-2010, Friedrich Schiller University (DE). Course: Gel electrophoresis.

Diploma student supervisor, 2008

Semester student supervisor, 2007

Research assistant, 2005, Department of Plant and molecular Biology, University of Lausanne (CH)

Research experience and techniques

GC-MS, UPLC-MS, Solid phase extraction, Metabolomics, Bioinformatics, Molecular biology.
Extensive knowledge of Excel, SigmaPlot, and AMDIS.

Field experience

Cruises: March 2006, Adriatic Sea on the RSV Dellaporta
February 2008, Adriatic Sea on the RSV Urania.

Mesocosms: 2007, preliminary study with 3 mesocosms, Bergen, Norway
2008, metabolic profiling of 6 mesocosms, Bergen, Norway

Skills and qualifications

Language: French (mother language), English (fluent), German (proficient)

Informatics: Java programming (basic knowledge).

Charles Vidoudez

Selbständigkeitserklärung

Ich erkläre, dass ich die vorliegende Arbeit selbständig und unter Verwendung der angegebenen Hilfsmittel, persönlichen Mitteilungen und Quellen angefertigt habe.

Jena, den 27/04/2010

Charles Vidoudez